AIRBUS

2, Rond point Dewoitine
31703 Blagnac Cedex
France

FROM: Airport Operations
DATE: January 2005
ISSUE: Issue 1.0

Subject: A380 Pavement Experimental Programme (PEP) – Rigid brochure

Objective:

The A380 PEP, including flexible and rigid phases, was launched in June 1998 with the aim of studying the impact on pavements using aircraft of large capacity such as the A380. Both phases consist in simulating aircraft coverages on an airport runway using a vehicle simulator able to reproduce various types of aircraft bogies such as A340, A380, B747, B777 or MD11. The variable parameters were mainly the load applied (individual wheel loads, tires pressure), the geometrical configuration of the landing gears (track, base, type of bogie) under a given thermal load (for rigid pavement). Up to 22 wheels could be individually loaded up to 32 t.
The first phase, dedicated to flexible tests, consisted in designing and testing a pavement with varying instrumented surfaces of bituminous materials. Results gave place to a previous brochure (October 2001). See A380 Pavement Experimental Programme (PEP) – Flexible brochure.
The present phase involves with rigid pavements. The aims of the rigid phase are, first, to obtain a set of data to improve pavements knowledge and secondly to correlate mathematical models using finite element method.
These models would supersede the ACN / PCN method and obtain a much more reliable classification of aircrafts and pavements which would be aligned with the latest pavement design procedures.

For any question, please contact airport operations department
airport.compatibility@airbus.com

Related documents: A380 Pavement Experimental Programme (PEP) – Flexible brochure

AIRBUS / LCPC / STBA

A380 PAVEMENT EXPERIMENTAL PROGRAMME

RIGID PHASE

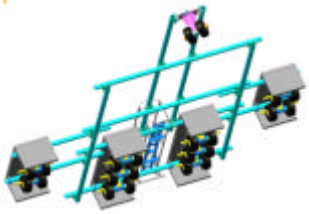

AIRBUS

AIRBUS, Programme A380
Toulouse, France – January.2005

CONTENTS

FIGURES TABLE

GLOSSARY OF ABREVIATIONS USED

ACN / PCN	:	aircraft classification number / pavement classification number
ACNSG	:	aircraft classification number study group
BLG	:	body landing gear
BPOA	:	béton, précontraintes et ouvrages d'art
CCTP	:	cahier des clauses techniques particulières
CG	:	center of gravity
DGAC	:	direction générale de l'aviation civile
HUGA	:	humidified untreated graded aggregate
ICAO	:	international civil aviation organisation
LCPC	:	laboratoire central des ponts et chaussées
LRE	:	laboratoire régional de l'équipement
LVDT	:	Linear Variable Differential Transformer
NLA	:	new large aircraft
MTOW	:	maximum take off weight
PEP	:	pavement experimental programme
STBA	:	service technique des bases aériennes
WLG	:	wing landing gear

INTRODUCTION

➢ General context

In the context of the new large airplane (NLA), AIRBUS proposes the A380 programme, an aircraft whose mission is to transport 555 passengers over 7920 nm.
The aircraft sets the standard for new code F airports (80m wing span, Landing Gear (L/G) overall track >14m) and will feature 20 or 22 Main Landing Gear wheels for maximum take off weight (MTOW) ranging from 560 T to 600 T with potential development beyond 650 T.

This work, the A380 Pavement Experimental Programme (A380 PEP) rigid phase, deals with rigid pavement compatibility under high aeronautical loads. In fact, problems occurs because the current "aircraft classification number / pavement classification number" ACN/PCN method seems to have reached its limit of reliability with 6 wheels bogie loads. So a group of pavement designers felt the need for a research programme aiming at defining more accurate pavement design methods. The group consisted of:

- The pavement designers from Airport and Airforce Bases Engineering Department (DGAC-STBA), ICAO ACNSG European member,
- The pavement structure and materials experts (French Laboratory for Civil Engineering – LCPC),
- The European aircraft manufacturer AIRBUS.

➢ Objectives

The A380 PEP, including flexible and rigid phases, was launched in June 1998 with the aim of studying the impact on pavements, of using aircraft of large capacity such as the A380. Both phases consist in simulating aircrafts passages on a airport runway using a vehicle simulator able to reproduce various types of aircraft bogies such as A340, A380, B747, B777 or MD11. The variable parameters were mainly the load applied (load at wheel, tires pressure), the geometrical configuration of the landing gears (track, base, type of bogie) under a given thermal load. Up to 22 wheels could be individually loaded up to 32 tons.
The first stage, devoted to flexible tests, consisted in designing and testing a pavement with varying instrumented surfaces of bituminous materials. Results gave place to a conference and a previous brochure (October 2001).
The present phase deals with rigid pavements. The aims of the rigid phase are, firstly, to obtain a set of data to improve pavements knowledge and secondly to correlate mathematical models using finite element method. These models would supersede the ACN / PCN method and obtain a much more reliable classification of aircrafts and pavements.

➢ Report content, future results

This brochure presents the rigid phase of the PEP, which took place from June 2002 to October 2003 on a taxiway zone reserved by AIRBUS France. As for the flexible phase, the rigid phase includes a static and a fatigue campaign. Many complementary tests and a post investigation are also realized.
The first part of the document is devoted to the presentation of the experimental runway. After a brief description of the site, the pavement foundation and design are studied. Then we show some descriptions of the works during the construction of the runway.

The second section presents the instrumentation used during the rigid pavement experimentation. The principles of the expected measurement are recalled. Then the types of sensors, the experimental device and the method used for the data acquisition are described.
The static tests are exposed in the third part. The tested configurations, the load passages and the main trajectories are detailed.
Finally the main results and a first analysis are carried out in the last part of the present brochure.

I. EXPERIMENTAL RUNWAY PRESENTATION

Many parameters are to be taken into account when designing cement concrete aeronautical pavements:

- subgrade,
- type of foundation,
- size of the slabs,
- dowelling or not,
- environment (temperature, etc.).

Many of these parameters can vary over time. As the life of a rigid pavement is at least twenty years, the "world-wide population" of cement concrete pavements is fairly heterogeneous and various techniques coexist. So it is therefore not easy to select a typical structure. The test runway must therefore include several zones using various techniques to evaluate their behaviours under aeronautical loads.

I.1 Site description

Logically following the flexible pavement tests, the rigid PEP is based on the same assumptions, that is full scale and "open air" tests under environmental conditions (especially thermal and hygrometric) representative of operational conditions.

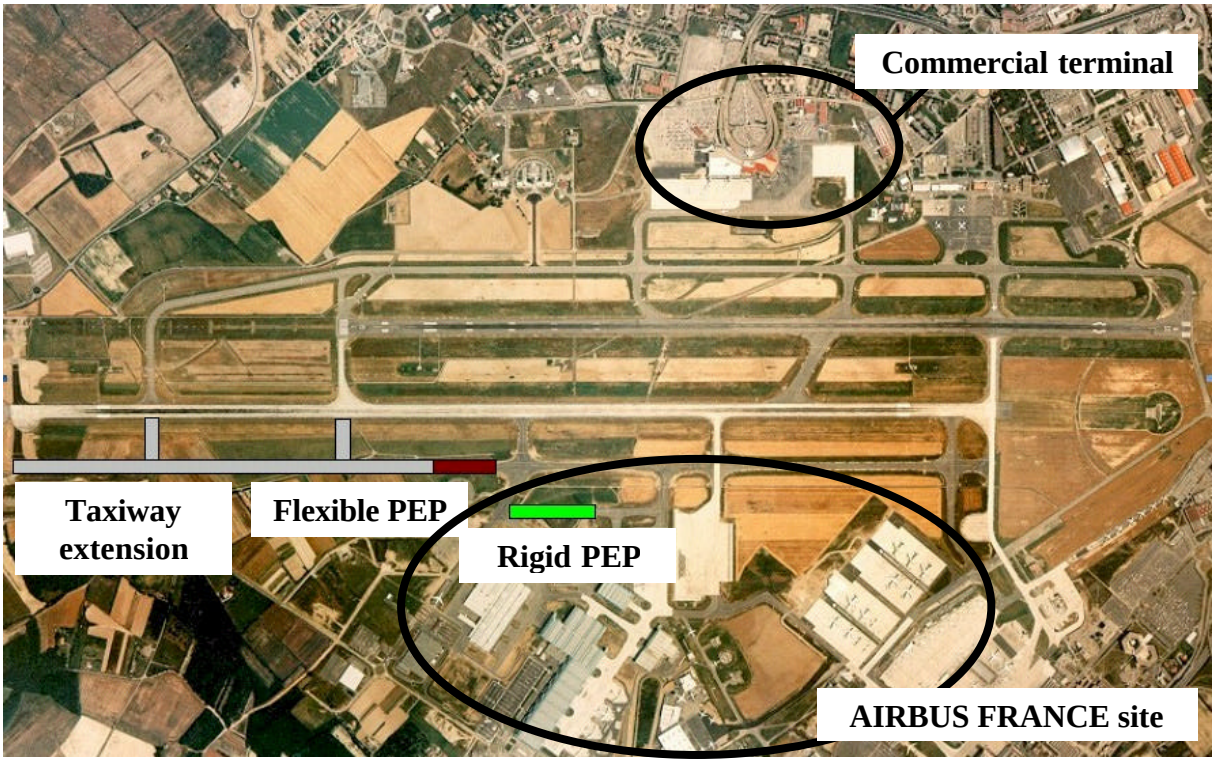

Figure I-1 : The Toulouse-Blagnac site.

The site selected for the flexible PEP was located in the extension of taxiway B20 at the Toulouse Blagnac airport. This site incurred a certain number of constraints during the flexible runway tests especially utilisation restrictions under low visibility procedures conditions. The main negative point remains however the premature interruption of the fatigue campaign to hand over

the zone to the airport manager in order to extend this taxiway. That is why the site chosen for the rigid PEP is located within the AIRBUS France site away from all aeronautical constraints and independent of the airport development scheme. The fatigue test phase will therefore not be interrupted. The selected site provides a surface area of around 250 m x 100 m. Lastly, the test runway must be constructed according to techniques used traditionally for cement concrete pavements (mainly use of slip-form; all manual construction is to be prohibited). The selected slab pattern must not create constraints making the sections unrepresentative of the operational pavements.

I.2 Pavement foundation

I.2.1 Subgrade

The dimensioning problem of the test runway is quite different from conventional dimensioning. The aim is here to construct a pavement representative of real runways, representative of the types of subgrade considered by the ACN / PCN method, from very low to very high strength. Indeed, rigid pavements are in general advantageous on low bearing capacity subgrades; most of the reference platforms for the A380 are thus listed in classes B and C.
The underlying hypothesis was to retain a typical foundation commonly used today:

- 15 cm of lean concrete
- 25 cm of humidified untreated graded aggregate (HUGA)

Knowing the K_0 modulus of the subgrade and considering the equivalent thickness of 47.5 cm given by the selected foundation, it is possible to determine the K_C modulus what give the pavement class in the sense used by ACN / PCN method. So by using the modulus correction curve in reverse, we can determine the K_0 modulus from the K_C modulus. With K_C modulus, we can also directly calculate the thickness of concrete slab.
Thus, by choosing to construct a class C experimental pavement with therefore a representative modulus K_C = 40 MN/m^3, the corrected modulus K_0 of the subgrade is therefore well below 20 MN/m^3 (between 5 and 10), which represents a very poor subgrade and especially difficult (or even impossible) to reconstruct. Also, compacting a foundation course of 25 cm of HUGA on such a subgrade is quite impossible.
This also means that with the foundation courses used at present, the provided protection and the modulus correction are such that the pavement cannot be placed in class D (the only airport of the A380 target airports in this class is the Djakarta airport which corresponds in fact to a runway constructed "on piles"…). Most of the runways classed as R/D in the sense used by the ACN / PCN method have in fact very weak foundations (or even no foundation at all) – see Annexe 1.
The weakest category of experimental sections has been chosen so that the base ground will be "reconstructable". The limit of categories B and C has been chosen, this means K_C = 60 MN/m^3 and K_0 = 25 MN/m^3 (corresponding to a CBR = 3 which had already been difficult to reconstruct for the flexible PEP). The second chosen category corresponds to the limit of categories A and B, i.e. K_C = 120 MN/m^3 and K_0 = 80 MN/m^3.

I.2.1.1 Experimental check

As obtaining K_C is important for the classification of the structures, it is decided to do an experimental check on the theoretical correction of modulus K_C given by the foundation course. As a Westergaard plate test has no significance on the lean concrete, modulus K'_C on the HUGA course is submitted to a check and validation:

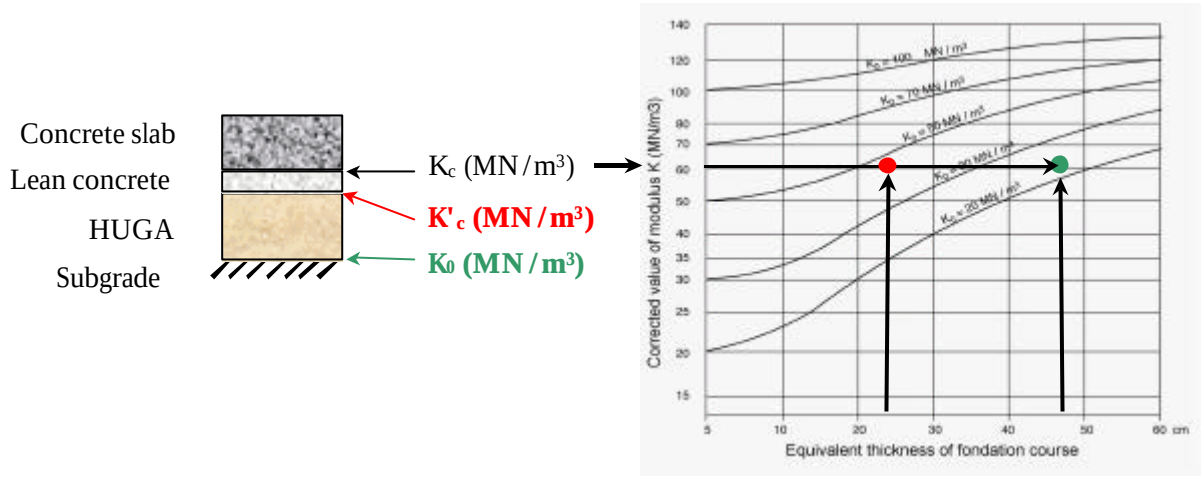

Figure I-2 : STBA design method – correction of K_C modulus.

I.2.1.2 Subgrades

The theoretical values (correction of 47.5 cm equivalent for K_0 and correction of 22.5 cm equivalent for K'_C) are:

Table I-1 : Subgrade characteristics.

Subgrade N°.1	Subgrade N°.2
K_C = 60 MN/m³ K'_C = 45 MN/m³ K_O = 25 MN/m³	K_C = 120 MN/m³ K'_C = 100 MN/m³ K_O = 80 MN/m³

Experimental test plates are made on reconstructed subgrades to adjust the HUGA thickness in order to measure on this course the values given by theory. The results are as follows:

Table I-2 : HUGA thicknesses.

	Subgrade N°.1	Subgrade N°.2
Target K'_C	45 MN/m³	100 MN/m³
Theoretical thickness	25 cm	25 cm
Thickness required	43 cm	30 cm

I.2.1.3 Conclusions

The overthickness to be used in relation to theory can have two explanations: either the correction curves are inaccurate or, more probably, (this seems to be confirmed by the flexible PEP cyclic loaded triaxial tests) the quality of the HUGA used is fairly poor which would mean that its equivalence coefficient is lower than 1. In theory, it is equal to 25/43 and 25/30. The difference between the HUGA equivalence coefficient on the two subgrades can be explained by approaching road pavement modeling techniques where the modulus of the HUGA courses is fixed proportionally to the one of the subgrade.

I.2.2 Subbase

I.2.2.1 HUGA

It consists of a humidified untreated graded aggregate (HUGA) 0/20 type B2, manufactured by mixing various size fractions in a level 2 plant as defined by standard NF P 98 115. It must be in compliance with the standard NF P 98 129 and is reconstructed from at least two separate size fractions in compliance with standard XP P 18 540.

I.2.2.1.1 Intrinsic characteristics

The aggregate must be at least category D.

I.2.2.1.2 Manufacturing characteristics

The aggregates must be at least category III.
The sands must be at least category "b".

I.2.2.1.3 Additional characteristics

- Graduation

The composition and the characteristics of HUGA 0/20 type B2 will be determined according to the methodology given in standard NF P 98 125

- Angularity

The crushing ratio Ic will be greater than or equal to 60%.

- Frost sensitivity

The aggregate must be classed SGn as per standard NFP 98 080-1, the aggregates must be insensitive to frost G < 25% as per P 18 593).

I.2.2.2 Lean concrete

The average strength of the concrete is measured in compression at 28 days on 16 mm diameter and 32 cm high test specimens. Taking the normal manufacturing scatter into account, the concrete will be in class 2 (NF P 98 170) i.e. an average strength greater than 20 MPa (mean strength as determined by splitting tests: 1.7 MPa). The minimum cement content required is 160 kg/m^3 of concrete.
The characteristics required for the aggregates comprising the lean concrete (and the surface concrete) are as follows:

I.2.2.2.1 Intrinsic characteristics

- The aggregates of grain size 5/20 and 20/40 used for the surface and the foundation concrete must belong to category "D" defined by standard XP P 18 540 in compliance with standard NF P 98 170.

  CPA = 0.40 (for **surface** concrete).

- Concerning sand 0/5

  Sand friability: FSb for **foundation** concrete.

  Sand friability: FSa for **surface** concrete.

  Sand water absorption coefficient: $V_{SS} \leq 5$ for the **foundation** concrete

  Sand water absorption coefficient: $V_{SS} \leq 2.5$ for the **surface** concrete (*Applicable when it has been demonstrated that the concrete is free from risks of bleeding. If no test has been conducted, we will specify that the water absorption coefficient is £ 2.5*)

- Total sulphur content

  S_B for the **foundation** concrete.

  S_A for the **surface** concrete.

I.2.2.2.2 Manufacturing characteristics

- The aggregates must belong to category "III" defined by standard XP P 18 540 in compliance with standard NF P 98 170.
- The sand 0/5 must belong to category "a1" defined by standard XP P 18 540 in compliance with standard NF P 98 170.
- The fillers, used as granulometric corrector must meet the specifications given in standard XP P 18 540.

I.2.2.2.3 Formulation of the cement

The cement entering into the composition of the concretes intended to manufacture the lean concrete foundation course and the concrete slabs must be at least of Portland CPA-CEM I 32.5 or CPJ-CEM II (A or B) 32.5 type.
The suitability tests led to the choice of the following formulation for the lean concrete (Quantities per cubic metre of concrete):

Table I-3 :Formulation of the lean concrete cement.

Cement CPJ CEM II/A-LL 52.5 N CE CP2 NF	200 kg
Aggregates 5/12.5	435 kg
Aggregates 10/20	690 kg
Sand 0/4	875 kg
Water	150 l
Air-entraining agent AER Sika	0.06%
Plasticiser 22S Sika	0.6%

I.2.2.2.4 Joint characteristics

Special care is brought to the positioning of the longitudinal lean concrete joint. Indeed, it is very important that no superimposition between the lean concrete and surface concrete construction joints occurred (for more details on surface joint see § I.3.2.3). The chosen solution allows a minimum distance of 50 cm to be obtained between the lean concrete and surface concrete longitudinal joints.

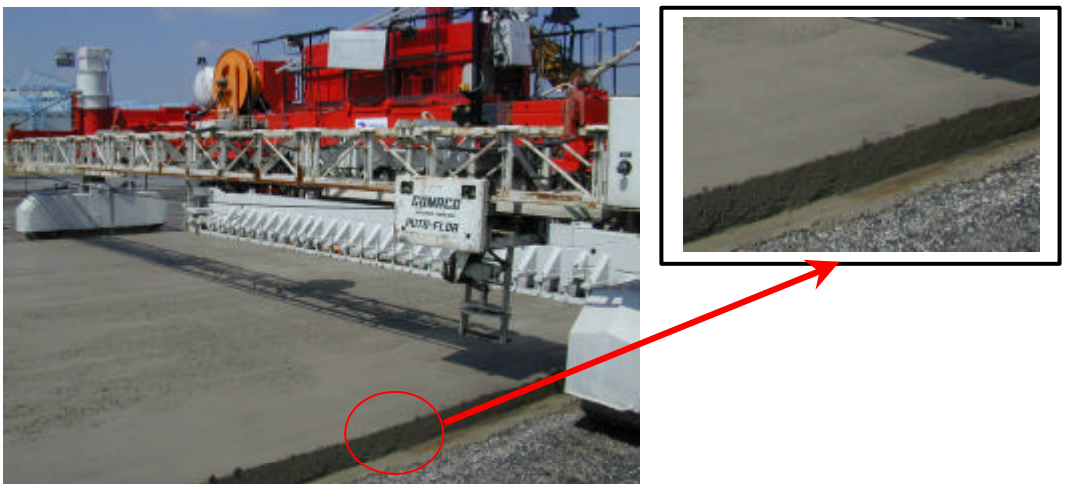

Figure I-3 : lean concrete longitudinal joint.

The lean concrete surface is realised by seven strips (6 and 9m width) which are obtained by a single slip-form pass (around 250 ml each). No transverse joints are created by sawing, so natural cracking appeared during drying. The longitudinal construction joints have no load transfer systems of tongue-groove type or other. The edges are smooth, like shown in Figure I-3.

I.3 Pavement design

I.3.1 Thickness calculation

Knowing K_C modulus, allowed flexural strength stress of concrete and designing traffic, we can calculate with the French rigid airfield pavement design method the thickness of concrete slabs.
Three structures are to be dimensioned:

- Dowelled structure (σ_a = 6/1.8 = 3.33 Mpa) on subgrade n°.1 (K_C = 60 MN/m^3)
- Undowelled structure (σ_a = 6/2.6 = 2.22 Mpa) on subgrade n°.1 (K_C = 60 MN/m^3)
- Undowelled structure (σ_a = 6/2.6 = 2.22 Mpa) on subgrade n°.2 (K_C = 120 MN/m^3)

The dual constraint is here as follows:
- on one hand, designing a pavement allowing, during the static tests, in situ measurement by means of instrumentation of displacement and strain values sufficiently high to be representative (low thickness preferable),
- on the other hand, considering that the pavement should not fracture during the static tests and not fracture at a too early stage during the fatigue tests (high thickness preferable).
Finally, the dimensioning is done on the basis of 10,000 movements of B747-400 at maximum weight (395.9 T), taking into account the current fatigue law of the French design method. The load weighting coefficient retained is 1.

Table I-4 : Thicknesses of concrete layers.

	Subgrade N°.1 K_C = 60 MN/m^3		Subgrade N°.2 K_C = 120 MN/m^3
	With dowels	*Without dowels*	*Without dowels*
Slab thickness	30.1 cm *rounded off to 31 cm*	41.2 cm *rounded off to 42 cm*	36.2 cm *rounded off to 37 cm*

The following table presents the pavements life sensitivity due to a slight variation in thickness. The number of allowable movements are calculated with the current fatigue law of the French design method for a B747-400 on subgrade n°1 with dowelled slabs.
The table below gives the theoretical number of allowable movements of the main aircraft loading the test runway either during the static tests or during the fatigue tests. This permits to "visualize" the fracture risks for different kinds of aircraft:

Table I-5 : Number of allowable movements.

		Subgrade N°.1 K_C = 60 MN/m³		Subgrade N°.2 K_C = 120 MN/m³
		With dowels	*Without dowels*	*Without dowels*
Theoretical number of allowable movements	B 747-400	*» 17,000*	*» 13,500*	*» 14,250*
	A 380-800 WLG	*» 15,500*	*» 12,000*	*» 12,800*
	A 380-800 BLG	*» 9,700*	*» 3,800*	*» 8,900*
	A 380-800F WLG	*» 7,400*	*» 5,700*	*» 6,000*
	A 380-800F BLG	*» 4,500*	*» 1,500*	*» 4,000*
	B 777- 300	*» 8,700*	*» 3,700*	*» 8,100*
	B 777 -300ER	*» 1,500*	*» 600*	*» 1,400*

Finally, the final configuration of the test runway is as follows:

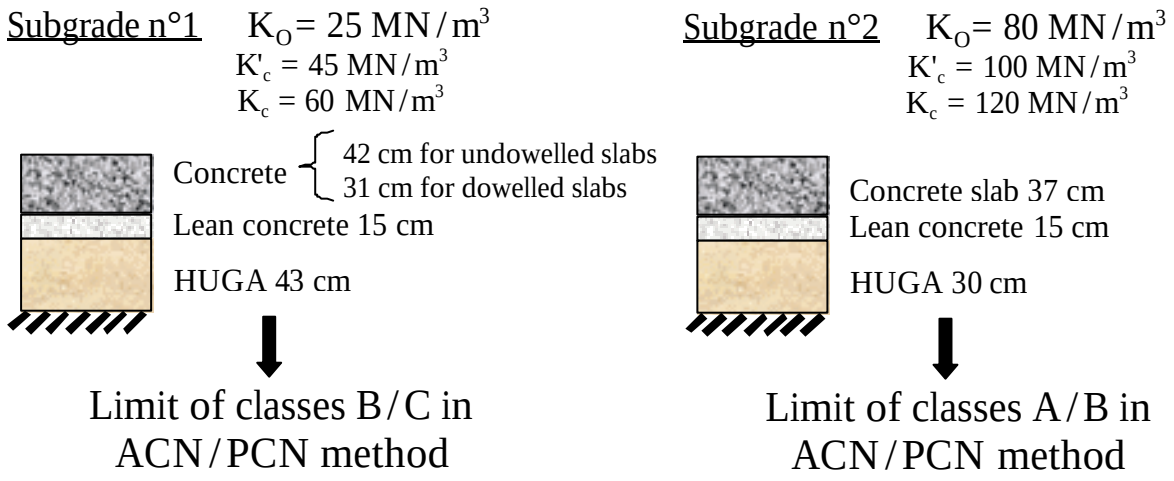

Figure I-4 : Cross sections of pavement.

I.3.2 Slabs arrangement

I.3.2.1 Preliminary remarks

The test runway must allow both static tests and fatigue tests to be conducted. In the same way as for the flexible campaign, the fatigue tests will consist in comparing different aircrafts. So choices of slabs pattern induce many consequences.

Firstly, the independency of the bogies will require at least one complete slab between each trajectory of the tested bogies (During fatigue tests, two bogies of two different aircrafts must never run on the same slab). Already at this stage, this parameter and the geometrical limits of the simulator exclude the possibility of testing four different bogies as for the flexible tests. The fatigue campaign is devised considering the hypothesis of an hybrid simulator configuration combining the main landing gear of the B 777-300ER and 3/4 of the A380-800F landing gear.

The second problem concerns the choice of the critical trajectory for the fatigue campaign. This trajectory varies according to the climatic conditions and, in particular, the thermal gradient in concrete slab. A longitudinal trajectory at slab edge will be penalizing for negative gradients

(convex curvature of slab, raised corners), whereas a longitudinal trajectory in the centre of the slab will be penalising for positive gradients (concave curvature of slab) as shown in Figure I-5:

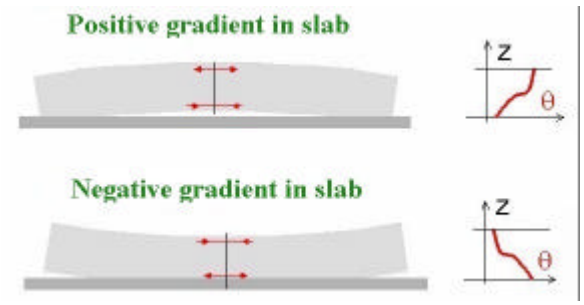

Figure I-5 : positive and negative gradient in slab.

The conventional pathology of cement concrete aeronautical pavements consists mainly of corner breaks for negative gradient and also cracks in the centre of the slab for positive gradient. To best estimate life of a given section, several trajectories must be tested at the same time, i.e. at constant gradient. This presents the advantage of not having to make a preliminary choice for the critical trajectory.
On account of the many parameters and the fact that the fatigue of section can only be observed over a minimum of four slabs (longitudinally), we can see that it is impossible to study all parameters one by one (for example, for a given subgrade and slab size, we study the influence of the dowelling on two sections for the fatigue approach… then, we modify subgrade, etc.). The test runway must at least allow a comparison by crossed parameters.

I.3.2.2 Slabs width and length

Commonly, dimensions of aeronautical slabs are varying between 4 and 7.5m. Thus, the trend has been to move away from the short undowelled slabs used in the '60's (Californian technique) to the larger slabs used today with dowelling according to the areas (gates, runways, taxiways, holding areas, etc.). Short slabs present the advantage of being less sensitive to thermal fluctuations, but need more maintenance.
So it seems to be interesting to take into account two dimensions of square slabs: 5m and 7.5m. This leads to many configurations considering the dimensions slabs, the subgrade or even the kind of joints.

I.3.2.3 Slabs junction

Usually the concrete pavement are classified according to the localization and the treatment of the discontinuities due to concrete shrinkage. In order to be the most representative of existing structures, it is decided to construct dowelled and undowelled slabs (Figure I-6). Placed at semi-height of slabs, the dowels permit to improve joints behavior and load transfer at joint. Note that the dowelling technique is often used for large airplanes traffics.
So the runway will be composed of:

- Short square undowelled slabs (5m)
- Square undowelled slabs (7.5m)
- Square dowelled slabs (7.5m)

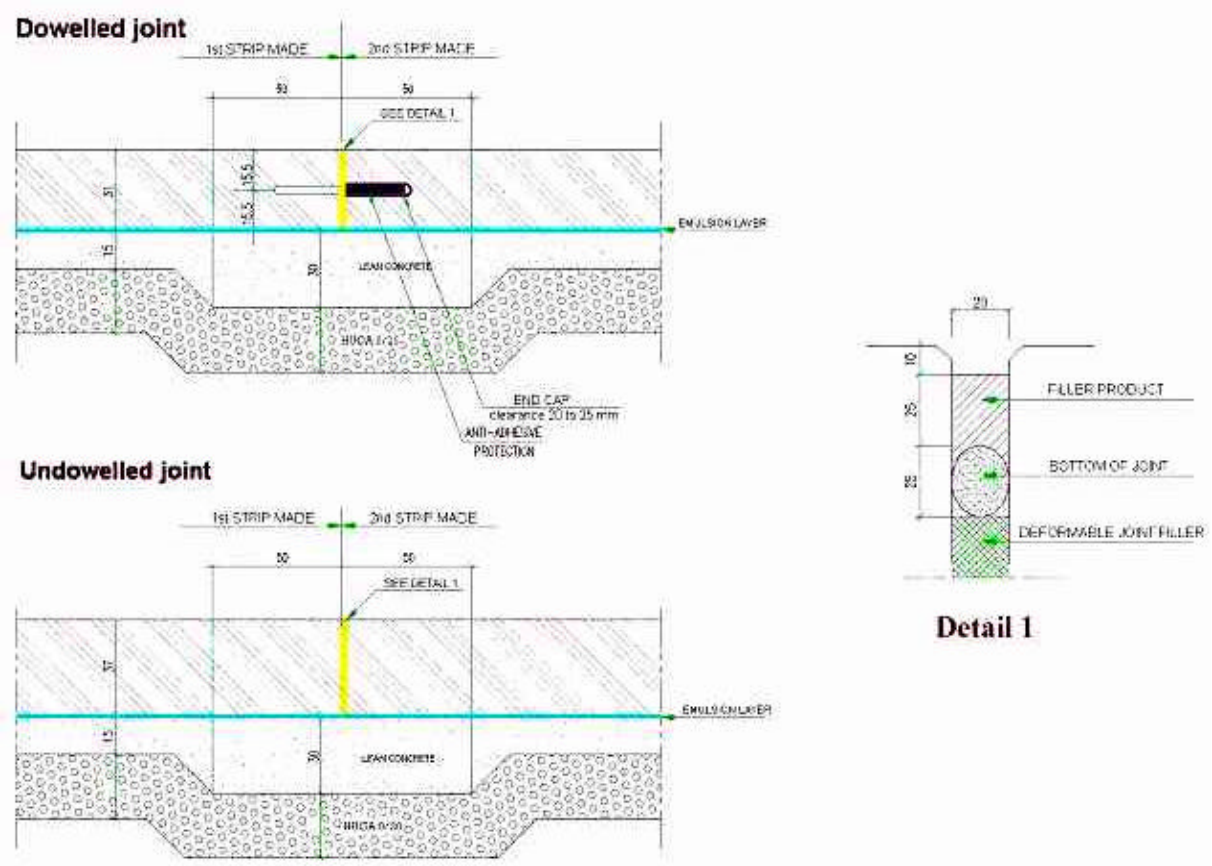

Figure I-6 : Cross section of contraction joints.

Dowels supports (Figure I-7) and dowels are in compliance with standard NF P 98 170 and standards of subseries NF P A 35-015. The dowels are smooth and straight, of grade at least equal to FE 240, 40 mm in diameter and 50 cm long. These are coated with a thin film of a product preventing adhesion to the concrete (completely for dowels placed on baskets, on the unsealed part for dowels installed by drilling). Also, a metal or plastic cap is placed on the end of the expansion joint dowels on coated side. The selected dowel spacing is 40 cm.

Figure I-7 : Dowels on basket / Concreting.

I.3.2.4 Joints characteristics

I.3.2.4.1 Expansion joint

Because of the presence of offsets, the slip-form paver can not cast concrete form one side to another. So the installation plane has been divided into "straight sections". Each installation section is then separated by an expansion joint (Figure I-8). The table I-6 presents the installation date of concrete strips.

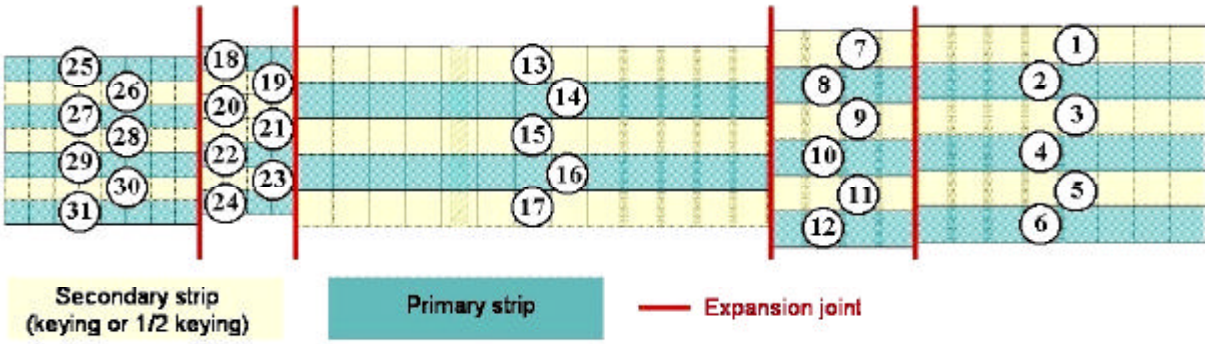

Figure I-8 : Expansion joints and concrete strips.

Table I-6 : Installation date of concrete strips.

1	*28/09*	**7**	*03/10*	**13**	*01/10*	**18**	*14/09*	**25**	*18/09*
2	*21/09*	**8**	*13/09*	**14**	*16/09*	**19**	*24/09*	**26**	*21/09*
3	*03/10*	**9**	*02/10*	**15**	*02/10*	**20**	*29/09*	**27**	*18/09*
4	*27/09*	**10**	*13/09*	**16**	*20/10*	**21**	*24/09*	**28**	*24/09*
5	*04/10*	**11**	*03/10*	**17**	*25/09*	**22**	*14/09*	**29**	*19/09*
6	*27/09*	**12**	*13/09*			**23**	*24/09*	**30**	*24/09*
						24	*17/09*	**31**	*20/09*

I.3.2.4.2 Transition joints

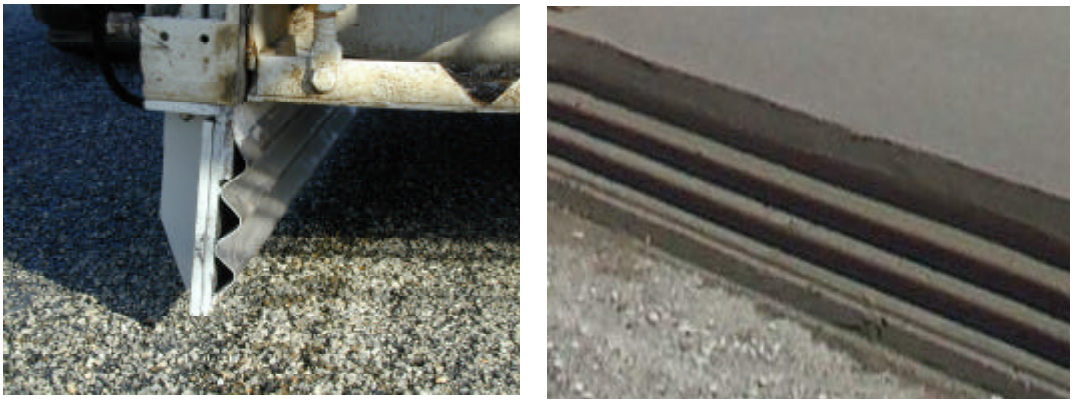

Figure I-9 : Corrugated profile at transition joint.

The transition joints are ensured by corrugated profiles (Figure I-9) chosen to ensure load transfer. The selected profile, in terms of wave geometry, is the same for the three slab

thicknesses. This permits to simplify the placing of the concrete because only one wave has to be constructed. Even if general practice recommends to select three different profiles, the load transfer is still well assured. The corrugated profile is placed directly on the slip-form placer.

I.3.2.4.3 Contraction joints

There are two types of contraction joints, depending on the presence of dowels (Figure I-10).

Figure I-10 : Contraction joints.

Because of the low length of certain sections (for example strips 18 to 24), shrinkage cracks may not appeared at the joints but over the complete length. To avoid this phenomenon, the depth of the saw mark is fixed to 1/3 of the slab thickness, instead of the standard recommendation of 1/4. The joint sealing is realised with a silicon joint filler.

I.3.3 Pavement materials

The surface layer is made of cement concrete. The mean strength of the concrete at 28 days is determined by splitting tests on 16 cm diameter and 32 cm high test specimens. Taking the normal manufacturing scatter expected on the site into account, the concrete will be class 6 (NF P 98 170), i.e. a mean strength determined by splitting tests greater than 3.3 MPa (corresponding to a bending tensile strength of 6 MPa; value used for designing). The minimum content required for the cement is 330 kg/m^3 of concrete. The ratio water / cement $\frac{W}{C}$ must be ≤ 0.45.

The range of fluctuation of the consistency at placement location is 3 cm and occluded air content in compliance with standard NF P 98 170.

I.3.3.1 Material characteristics

Recommendations are the same as the ones for the materials comprising the lean concrete (see § I.2.2.2).

I.3.3.2 Formulation of cement

The suitability tests led to the choice of the following formulation for surface concrete (Quantities per cubic meter of concrete):

Table I-7 : Formulation of the pavement cement.

Cement CPJ CEM II/A-LL 52.5 N CE CP2 NF	335 kg
Aggregates 5/12.5	360 kg
Aggregates 10/20	400 kg
Sand 0/4	775 kg
Water	150 l
Air-entraining agent AER Sika	0.08%
Plasticiser 22S Sika	0.5%

I.3.3.3 Surface treatment; cure product

Trowelling is done automatically by the slip-form. The surface of the hydraulic concrete foundation course must be free from irregularities liable to cause mechanical bonds between the two courses. To limit this phenomenon, an emulsion layer is placed on the lean concrete. No other surface treatment than the wet burlap brush finish is applied to the surface course (Figure I-11 (a)).

(a) (b)

Figure I-11 : (a) Burlap brush / (b) Cure product.

The concrete must be protected against all excessive evaporation by continuous and uniform spraying of a cure product (SIKA ANTISOL XC42 (content ≥ 80 g / m²)). This operation is done at most half an hour after the surface concrete treatment to comprise an impervious surface film (Figure I-11 (b)). Note that this product is also applied to the lean concrete foundation course and to the edges of concrete slabs.

I.3.4 Runway configuration

Finally considering the previous description, we obtain the following runway, which can be decomposed into three main parts:

- A centre portion dedicated to the static tests. The dowelling, slab size and subgrade parameters are studied by comparing test sections two by two. These slabs are aligned

along a common joint (reference joint). In this way, one simulator trajectory allows the responses of various slabs to this loading to be compared under identical conditions (especially thermal).

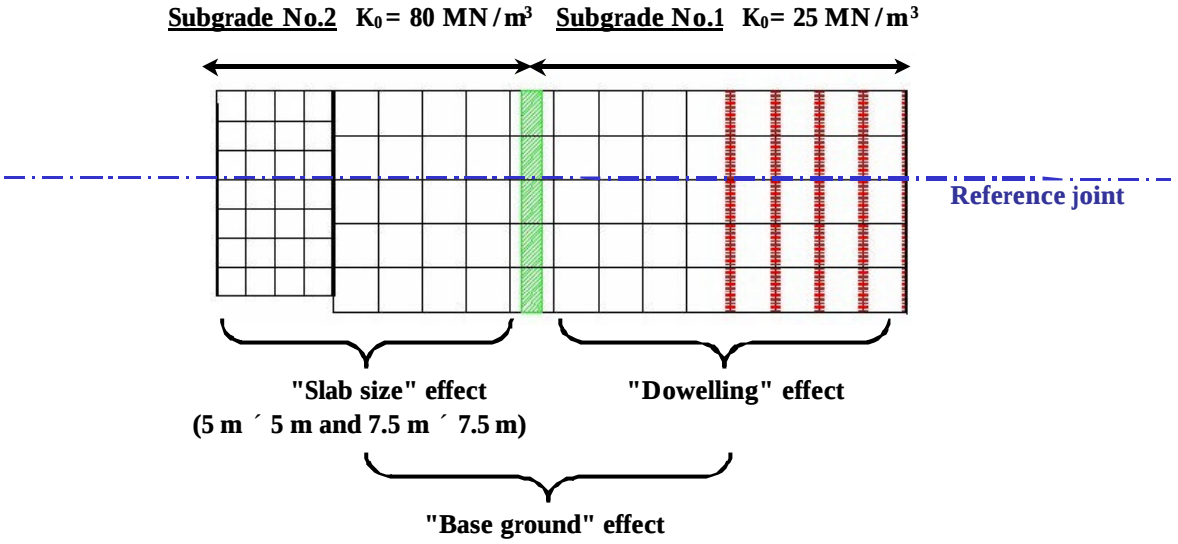

Figure I-12 : Runway static tests parts.

- Two portions at each end dedicated to the fatigue tests. Added sections present offsets. Thus, one simulator trajectory (defined in paragraph III.2) will load a structurally identical section both at the joint edge and in the centre of the slab.

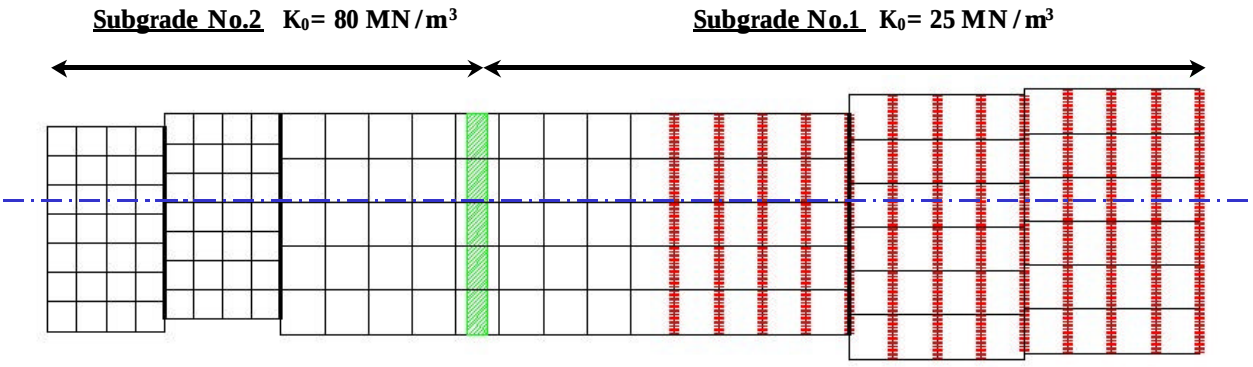

Figure I-13 : Runway fatigue tests parts.

- Two additional sections used to store the simulator have been added at the ends.

I.4 Construction

I.4.1 Description of works

I.4.1.1 Specific provisions

As for the flexible PEP, the geometrical specifications for the test runway are in compliance with ICAO recommendations.

I.4.1.1.1 Slope

In order to facilitate the running of the simulator, a null longitudinal slope is selected for all test sections. The selected transverse slope is a single slope profile of 0.5%.

I.4.1.1.2 Geomembrane and geotextile fabric

A tight polypropylene geomembrane of 1.5 mm thickness is placed on the bottom and on the sides of the excavation to avoid any infiltration of water modifying the water content of the reconstructed subgrades during the tests. This technique is the same as the one used for retention ponds. The membrane is then extended over 8.5 metres at the top (Figure I-14) of the HUGA so as to be under the surface concrete and the lean concrete courses to avoid any infiltration via the top (especially via the uncoated shoulders).

Figure I-14 : View of the geomembrane (extended over HUGA).

A shear failure resistant geotextile fabric was placed on subgrade N°.1 (K_0 = 25 MN/m^3) to facilitate the placing of the HUGA course (levelling and especially compacting). The mechanical characteristics of the geotextile are:

- Resistance to punching ≥ 1.5 kN in compliance with standart NF G 38019,
- Tensile strength ≥ 15 kN/m in compliance with standart NF EN ISO 10 319,
- Maximum tensile strain ≥ 50 % in compliance with standart NF EN ISO 10 319.

Indeed, a foundation course is generally not placed on a base with such a low bearing capacity and is therefore usually treated with lime. The experimental character of the site and the need to obtain a pavement corresponding to the required ACN/PCN classification requires this specific construction arrangement.

I.4.1.2 Earthworks

The earthwork is done in August and September 2000 by the STBA team. This consists of the excavation work (around 50,000m^3 / Figure I-15) and the sorting of the site material to facilitate the subgrade reconstruction operations. In October 2000, the geomembrane is installed by EUROVIA.

Figure I-15 : Earthworks

I.4.1.3 Reconstitution of subgrades

The reconstruction of the subgrades is a delicate phase. In the same way as for the flexible PEP, the principle selected is to excavate to a depth of 2.82 metres in relation to the proposed grade. On account of the various thicknesses of concrete slabs and HUGA, the thickness of the reconstructed subgrade varies according to the test sections. The excavated material from this earthwork is sorted and stored on site. The site materials rang (according to GTR classification) from type A2 (clay) to type C1B5 (clayed gravel). The recommendations given in the Detailed Specifications (CCTP) concerning the targets to be reached in terms of bearing capacity on reconstructed subgrades are:

Table I-8 : Subgrades characteristics.

	K_0 modulus (MN/m^3)	Classification	Water content
Subgrade N°.1	K_0 = 25 EV2 = 20 MPa +/- *5 MPa* *(for 100% of the values)*	80% of C1B5 20% of A2	11.8 to 12.7%
Subgrade N°.2	K_0 = 80 EV2 = 70 MPa +/- *5 MPa* *(for 95% of the values)*	60% of C1B5 40% of D3	8 to 9.1%

Remarks concerning subgrade N°.1:

- *EV2 test is more commonly used to check road earthworks than the Westergaard test.*
- *The initial tolerance of +/- 3 Mpa for 95% of the values is modified. It turned out to be too severe and extremely difficult to reach.*

Remarks concerning subgrade N°.2:

- *Aggregate 0/80: material not available on the site which had to be imported.*

Very accurate specifications are imposed concerning the placement of the subgrades, especially concerning the slopes to be observed corresponding to a minimum camber of 2° (final profile with a unique slope of 0.5° being done therefore on the last reconstructed subgrade layer). This is done to avoid, as far as possible, the presence of stagnant water in the centre of the zone in case of adverse weather conditions (on account of the profile, the running waters are preferably directed to the two sides of the ditch). Self-priming pumps then evacuated the drained water to

the edges of the ditch. Then, after each rainy period, the company has to evacuate and replace the impregnated materials.

Figure I-16 : Cross sections during subgrade reconstruction.

Until the end of December 2000, the subgrade reconstruction work go off more or less normally. The four following months (up to start of May 2001) are marked by very bad weather conditions making the continuation of the work absolutely impossible. It even requires to remake works already done, the subgrades being completely drenched throughout the complete depth (Figure I-17).

Figure I-17 : Drenched soils.

A new start of the job consists of:

- Removing the materials put into place up to grade +20 cm in relation to the subgrade (we cannot go beyond this level without risk of tearing the geomembrane),
- Spreading of lime 10 kg/m² and resumption of subgrade reconstruction. This means that for this subgrade, height of reconstructed subgrade is 1.7 to 1.8 m (instead of the 2 metres planned for a single slab thickness of 0.37 m) resting on a relatively rigid horizon (lime bed), then 20 cm of drenched soils and lastly the subgrade. The 20 cm of drenched soils should pose no pavement structure behaviour problems. The lime bed after absorption of the surrounding water and after "setting" should create a sufficiently rigid layer to "mask" this weakness of the base ground. The real height of the reconstructed

subgrade should be taken into account, especially for the theoretical modelling of the pavement structures.

I.4.1.4 Reconstruction of subbase / HUGA

Because of the damage locally done by the water, , isolated reworks concerning the HUGA placing are required to obtain the specified bearing capacities. The failed areas are replaced according to the following methodology:

- Opening of the area and airing of the soil,
- Drying,
- Compacting of the soil,
- Check of soil bearing capacities,
- Placing and compacting of HUGA,
- Closing by a coating and check of bearing capacities on HUGA.

Note that the measurement on the HUGA are done three days after placing to take bleeding into account.

I.4.1.4.1 Lean concrete

The work concerning the placing of the lean concrete is done in August, September and October 2001 by the company Eurovia-Béton. The main difficulty is substantial cracking of the lean concrete. As given in the specifications, the lean concrete course is not sawn transversely, so that the shrinkage cracking occurred "naturally" as shown Figure I-18.

Figure I-18 : Cracking of the lean concrete.

Moreover lean concrete cracks are observed and noticed as follows :

Figure I-19 : Cracks recording.

These cracks are normally not troublesome. However, we have to be careful if a crack appeared under an instrumented slab and, moreover, in particular in subgrade N°.1. The opening of certain cracks is very significant, sometimes reached more than 0.5 cm (Figure I-20). This phenomenon can be explained by the combined effects of the weakness of the base ground and the passing of the mixers truck, even lightened.

Figure I-20 : Width of a lean concrete crack.

The major problem appears the day after the pouring of the first three surface concrete strips (strips 8, 10 and 12 poured on 13/09/2001). A crack appears in the surface concrete slab at the location of the lean concrete crack. This crack is surely initiated in the fresh concrete of the surface slab by the opening/closing of a lean concrete crack due to the day/night temperature variations (an opening difference of several millimetres was recorded). To prevent this phenomenon from reoccuring, it is decided :

- To stop the growth of the existing cracks in the lean concrete by core drilling,
- To bridge the lean concrete cracks with a geotextile fabric impregnated with asphalt (with the aim of preventing the initiation of cracks in the fresh surface concrete during opening / closing of cracks in the lean concrete).

Also, in order to avoid the occurrence of new shrinkage cracks in the foundation of a future instrumented slab, preventive transverse saw marks are made on either side of the instrumented slabs, except in cases where shrinkage cracks already existed (Figure I-21).

Figure I-21 :Prevention of the cracks in lean concrete.

I.4.1.4.2 Surface course

The cement concrete is placed by the slip-form placer. It will be important, especially for the modelling phase, to notice that the edges of the slab are not exactly vertical. Figure I-22 presents a vertical offset of 3.5 to 4 cm.

Non-vertical edge

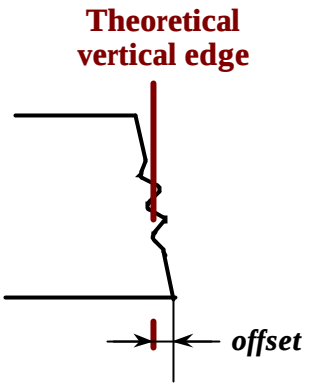

Figure I-22 :Offset due to the slip-form placer.

The level differences due to the slab thickness variations are made with a transition zone over a length of 3 meters, as shown in Figure I-23.

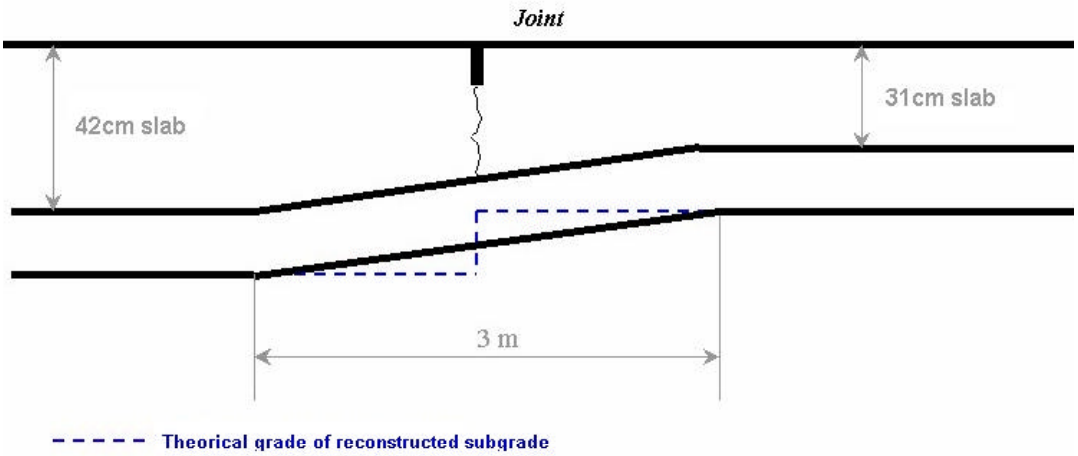

Figure I-23 :Slabs thickness variations.

To avoid anarchic cracks during shrinkage, the slabs are sawn to a depth of around one third of the thickness (cf. § I.3.2.4.3). Nevertheless, late sawing led to a shrinkage crack in slab N°.133 (Figure I-24). This crack is dowelled to block the opening movements of this joint and also to avoid any initiation of cracks in the adjacent fresh concrete strips.
The opening of the shrinkage cracks at the joint saw marks is carefully observed during the whole phase of instrumentation, this means between 2 and 4 weeks considering the place. The transverse shrinkage joints in the 7.5 m slabs open faster than those in the 5 m slabs.

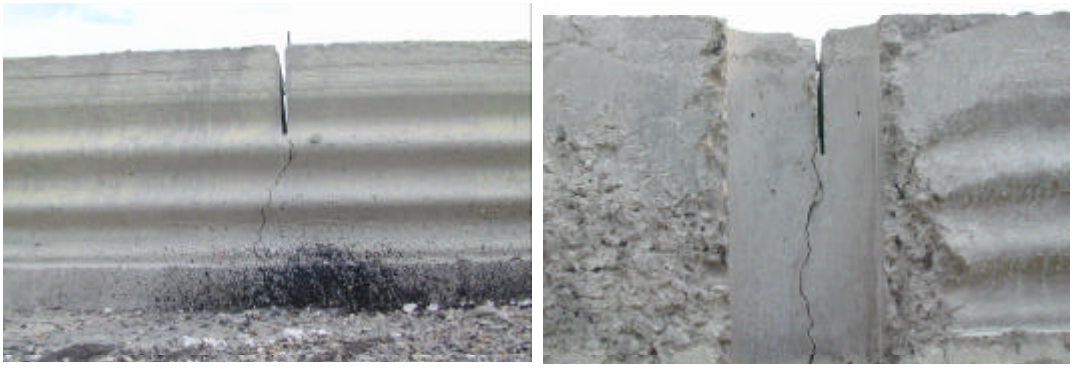

Figure I-24 : Shrinkage cracks under sawn transverse joints.

Figure I-25: Shrinkage crack of slab N° 133 before and after dowelling.

I.4.2 Acceptance of works

On account of the experimental character of this program, utmost care is reserved to the inspection. Contractually, companies has to do their own inspections and the Toulouse Laboratoire Régional de l'Équipement (LRE) ensures the external inspections.

I.4.2.1 Bearing capacities of base grounds

I.4.2.1.1 Subgrade

The results for both subgrades in terms of bearing capacity are:

Table I-9 : Plates test results.

Subgrade N°.1	$K'_C = 45\ MN/m^3$
Subgrade N°.2	$K'_C = 100\ MN/m^3$

Many points are tested on the two subgrades. The recommendations given in the special technical conditions of contract are consigned Table I-10.

Table I-10 : Recommandations on subgrades.

Subgrade N°.1	K_0 = 25 MN/m^3 i.e. EV2 = 20 MPa *+/- 5 MPa (for 100% of the values)*
Subgrade N°.2	K_0 = 80 MN/m^3 i.e. EV2 = 70 MPa *+/- 5 MPa (for 95% of the values)*

The modulus values given in Figure I-26 correspond to a restitution coefficient on dynaplaque test (impulse generator applying loading to the ground developed by LCPC) for subgrade N°.1 and to an EV2 test for subgrade N°.2.

Figure I-26 : Results of tests on subgrades.

I.4.2.1.2 Untreated graded aggregate test sheet

Table I-11 : Reception Dynaplaque tests results.

RIGID EXPERIMENTAL PAVEMENT A380

RECEPTION WITH THE DYNAPLAQUE OF THE BOARD 20 Mpa ± 5
BEFORE MAKING USE OF THE GNT 0/20

Tracks \ Strip	1	2	3	4	5	6	7	8	9	10	11	Hangars
P105	20	18	17	22	20	17	22	18	20	18	20	
P110	22	20	24	24	18	24	25	21	22	18	16	
P120	18	22	21	15	18	23	16	19	20	16	16	
P130	17	25	16	20	16	21	16	25	24	17	17	
P140	18	17	22	17	20	25	25	20	22	16	25	
P150	23	20	17	15	24	21	18	25	25	24	20	
P160	17	16	15	18	18	22	25	22	22	25	16	
P170	17	17	17	16	20	22	20	16	19	20	18	
P180	22	24	17	15	23	21	16	17	22	18	15	
P190	23	22	21	19	24	23	17	19	23	20	19	
P200	18	19	25	18	25	16	25	18	16	16	17	
P210	22	25	18	16	18	16	20	19	21	15	16	

Average		**19,69**
Standard deviation		**3,106**

I.4.2.2 Concrete checking

I.4.2.2.1 Modes of inspection

The external inspection is entrusted to the BPOA technical unit of the Toulouse LRE. Several inspections are conducted, including:

- Inspection and check of the concrete plant settings,
- Foundation and surface concrete manufacturing suitability tests:
  - -3 samples for particle size analyses and cleanliness tests,
  - -sample of cement for mechanical tests at 28 days,
  - -2 samples of 6 test specimens for mechanical compression and splitting strength tests at 7 and 28 days,
- Monitoring of manufacture and use of foundation cement:
  - -compression tests of concrete at 7, 14 and 28 days,

- Checks of concrete plant settings before concreting of surface course,
- Monitoring of manufacture and placement of surface concrete:
  -compression tests of concrete at 7, 14 and 28 days,
  -sampling during the concrete casting of each strip
  -additional sampling in the instrumented slabs.

I.4.2.2.2 Compression test

To obtain input data for modelling, tests to determine the modulus of elasticity of the surface concrete are conducted at various deadlines (7, 28 and 90 days).
A mechanical compression strength measurement is made before the modulus of elasticity test. This allows to determine the load variation range to be taken into account for the modulus of elasticity tests. This variation range is 30% of the breaking load. Each loading cycle is performed by 20 kN steps up to 200 kN. The test is repeated three times rotating the test specimen through 120° around its symmetry axis. After surfacing of the two faces of the test specimen, three 60 mm long strain gauges are bonded lengthwise on three generatrices of the cylindrical test specimen spaced of 120°.
In the elastic range, the longitudinal strain is proportional to the stress applied. The proportionality factor 1/E is the inverse of the modulus of elasticity or Young's modulus.
The results concerning the future instrumented slabs are consigned in Table I-12. Figure I-27 shows the results of determining modulus of elasticity at 28 days on slab N°.108.

Table I-12 : Results for compression tests.

		Date	Weight (kg)	Density	Characteristic strength (MPa)	Elasticy modulus (Gpa)
Slab 45	***7 days***	26/09/01	15.48	2.45	35.3	33.5
	28 days	17/10/01	15.36	2.45	43.6	34.2
	90 days	18/12/01	15.52	2.46	45.5	35.2
Slab 68	***12 days***	08/10/01	15.43	2.42	40.9	32.9
	28 days	24/10/01	15.47	2.42	44.1	34
	91 days	26/12/01	15.38	2.42	49.4	35.5
Slab 93	***12 days***	08/10/01	15.55	2.422	41.8	31.9
	28 days	24/10/01	15.48	2.43	47.1	33.2
	91 days	26/12/01	15.26	2.42	51.2	34.5
Slab 108	***12 days***	08/10/01	15.39	2.41	38.7	28.9
	28 days	24/10/01	15.34	2.42	44.0	31.2
	91 days	26/12/01	15.17	2.42	46.6	31.7

Figure I-27 : modulus of elasticity for slab N°.108.

I.4.2.2.3 Splitting test

The measurement are done on slender test samples of slenderness ratio 2, dimensions as per standart NF P 18-400.

The Table I-13 shows an example of surface concrete mechanical strength inspection results for splitting tests. The specimen is taken on slab N°.2 the 24/09/2001 at 11h40.

Table I-13 : Splitting tests results.

	Date	**Strength (MPa)**	**Test specimen N°.**	**Strength (MPa)**	**Weight (kg)**	**Density**
7 days	01/10/01	3.5	1	3.8	15.560	2.401
			2	3.7	15.500	2.407
			3	3.2	15.620	2.425
14 days	08/10/01	3.8	1	3.9	15.540	2.406
			2	3.6	15.570	2.418
			3	3.9	15.550	2.422
28 days	22/10/01	3.8	1	4.0	15.630	2.420
			2	4.0	15.590	2.428
			3	3.4	15.510	2.416

II. INSTRUMENTATION

II.1 Principles

A fundamental principle for the test runway design stage is to align four instrumented slabs so that they would be loaded in the same way when passing the simulator. This allows acquisition of data in the same thermal gradient conditions which will facilitate the comparison of the reactions of the various types of slabs. The instrumentation has to achieve the following aims:

- knowledge of the strains (loaded slab and adjacent slabs),
- knowledge of the vertical relative and absolute displacements (loaded slab and adjacent slabs),
- knowledge of the longitudinal displacements (loaded slab and adjacent slabs),
- knowledge of the stresses in a slab (mainly at the base) during the loading tests,
- knowledge of the temperature field in a slab (to evaluate the effect of thermal gradients by measuring the displacements of the surface concrete slab in relation to its base ground),
- evaluation of the load transfer between slabs (possible with the displacements fields).

As the number of acquisition channels is obviously limited, the transducers and gauges are placed at the most relevant zones of the slabs (corner, longitudinal and transverse edge, centre, etc.).
Note also that the instrumentation must not place specific constraints on the techniques or on the concrete placement equipment.

II.2 Types of sensors

II.2.1.1 Strain sensors

The aim is here to measure the strain at the bottom of a slab. The chosen sensors are strain gauges installed on a steel rod clamped via a support on the lean concrete (Figure II-1 (a)). The sensor rod is placed 4 cm from the lean concrete to allow the concrete (granulometry 0/20 mm) to pass under. The sensors require a concreting resistance test, especially to internal vibrations. These sensors, manufactured by the Bordeaux LRE, use the complete bridge principle. Strain gauges are also directly bonded at the top of the lean concrete (Figure II-1 (b)), using the 1/4 bridge principle. The average gauge factor is 300 µstrain/mV/V.

(a) (b)

Figure II-1 : (a) sensor and support / (b) strain gauge.

II.2.1.2 Horizontal displacement gages

LVDT sensors (*Linear Variable Differential Transformer*) are chosen for displacement measurement The amplitude of the sensors used (made by HBM, Figure II-2) for the horizontal displacement (**H: *horizontal***) measurement is +/- 5mm. The installation is based on the 1/2 bridge principle. The average sensitivity is 9.99 mm/mV/V.

Figure II-2 : HBM LVDT sensor.

II.2.1.3 Vertical displacement gauges

Solartron LVDT sensors are used for vertical displacement measurement. Their amplitude is +/- 10 mm. The installation used the 1/2 bridge principle. The average sensitivity is 33.39 mm/mV/V. Many sensors are installed on a frame.

Figure II-3 : Solartron LVDT sensors on their frame.

A system, interdependent of a plate (Figure II-4 (a)), is embedded in the lean concrete and fixed to a rod anchored 7 m deep (Figure II-4 (b)).

(a) (b)

Figure II-4 : (a) Frame attachment plate / (b) Reference rod.

A first sensor (**VA: *absolute vertical***) measures the vertical displacements of the frame (and therefore the lean concrete) in relation to the reference fixed at -7 metres. Then, from one to four sensors (**VR: *relative vertical***) according to the positioning of the system in relation to the slab measure the vertical displacements of the instrumented slab (and of the adjacent slabs) in relation to the frame. The following figure, Figure II-5, represents a cross section of an instrumented frame with horizontal and vertical LVDT sensors placed "in situ".

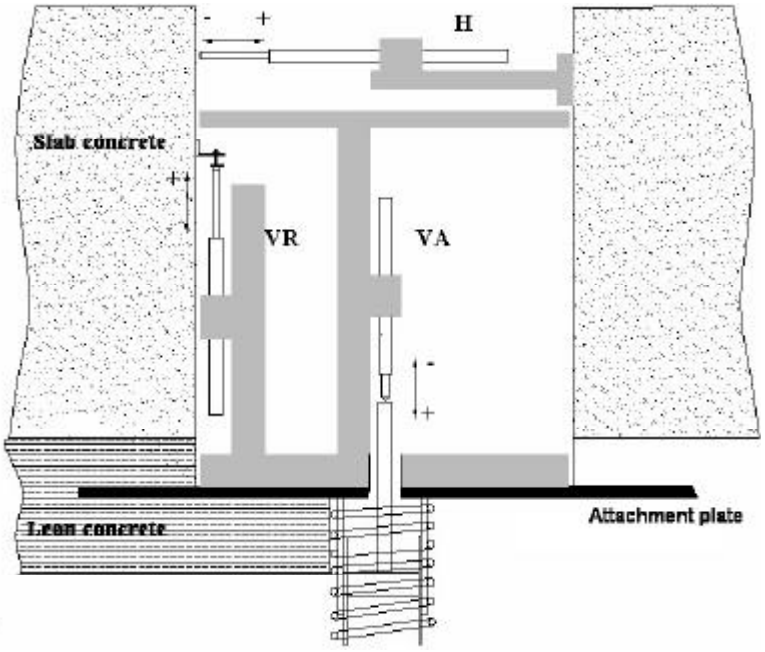

Figure II-5 : scheme of an instrumented frame.

II.2.1.4 Temperature sensors

On account of the importance of the temperature effect on slab movements, many gauges are installed to monitor profile temperatures in the pavement. The temperature gauges used are Pt 100s (accuracy: 0.01°C) as shown in Figure II-6, calibrated after 24 hours of immersion.

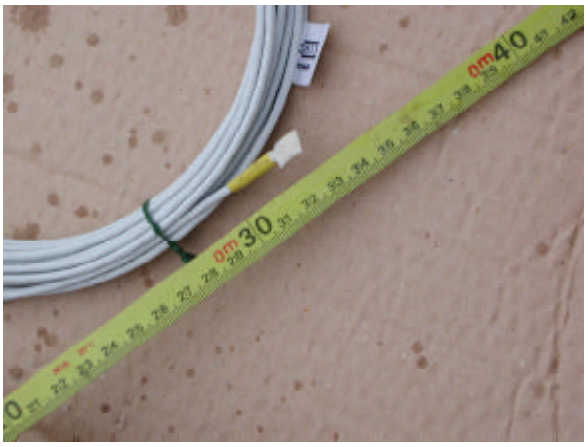

Figure II-6 : Pt 100 gauge.

To ensure redundancy of measures, two profiles are installed. The profile was reconstructed in a concrete core sample (Figure II-7) then sealed with mortar in a test runway core drilling. The depth of each gauge is noticed on the right side of the figure.

Figure II-7 : Instrumented core sample.

Several problems occurred with the resistance of the gauges over time during the tests. This requires the replacement of one core sample, first of all by an identical core sample, then by a core sample with another type of Pt 100 gauge.

II.3 Experimental device

II.3.1 Installation of the sensors

II.3.1.1 Strain gauges

The positions of the sensors are precisely measured on the lean concrete slab (Figure II-8 (a)). Before passing the slip-form paver (Figure II-8 (b)), fresh concrete is placed by shovel over the sensors and vibrated to ensure a correct homogeneity.

(a) (b)

Figure II-8 : (a) place of the sensors / (b) concrete casting.

II.3.1.2 Displacement gauges

The installation has to be very accurate because of the need of alignment of the frame, the plate and reference rod. The installation principle chosen is described in the following procedure.

II.3.1.2.1 Installation of the reference

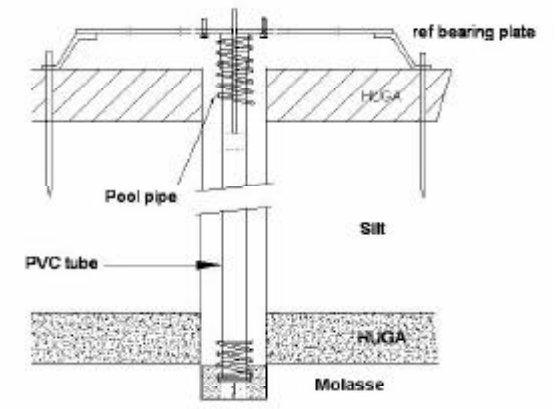

Figure II-9 : Scheme of the placing of the rod reference.

- Extraction of 140 mm Ø of materials (HUGA, silt, natural gravel) with drill. Use of a recoverable 140 mm Ø temporary protection tube placed on the top of the molasse to prevent water from natural gravel under the added silt from entering. The casing is rotated down without water nor air to preserve the environment.

- Drilling of the compact molasse by around 0.5 m by a triple cutter passed inside the casing.
- Installation of the absolute reference inside the tubing. This consists of a PVC tube covered by a swimming pool tube protecting the PVC from all constraints due to the subgrade. The lower part consists of a part bonded to the end of the tube. The upper part will accommodate the bearing plate which will be embedded in the lean concrete.
- Injection of a sealing coat at the bottom by gravity with a plunger tube. An appropriate grout is placed between the assembly and the tubing with the same protocol as for the sealing.
- Raising of the tubing by 1 m lengths topping up grout up to HUGA level.
- Placing of the bearing plate on the HUGA (height 5 cm). The geometrical coordinates are taken by a triangulation system. Plate setting will be done with a level, in 4 directions, before welding the assembly to the stakes inserted about 1 m into the material.

II.3.1.2.2 Casting of the lean concrete

To obtain something right round, a formwork case is attached to the bearing plate and filled up with sand. For placement reasons, the height is 5 cm lower than the lean concrete thickness required. The extra concrete above the case is removed manually after pouring the lean concrete.

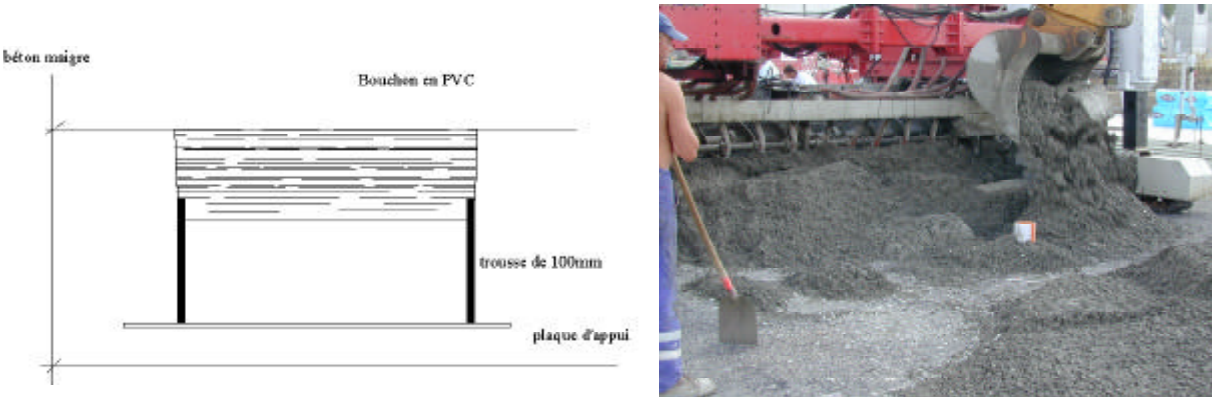

Figure II-10 :Casting of the lean concrete.

II.3.1.2.3 Casting of the slab concrete

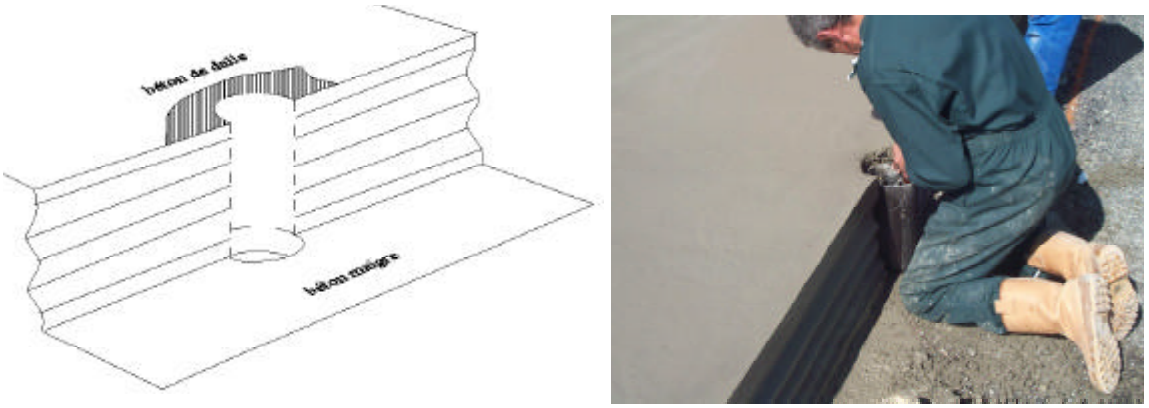

Figure II-11 : Construction joint case installation.

The height of the formwork case is 5 cm lower than the surface course. The same principle as for the lean concrete is used for the holes located in the centre of the instrumented slabs. For those which are in the construction joint, a manual rework is required and the cases are installed after the passage of the slip-form paver. The holes of the horizontal sensors are core drilled to 140 mm Ø to a depth of 110 mm. The cables pass below the bottom of the joint protected by a braid which must resist a temperature of around 160°.

II.3.2 Plan of the instrumented slabs

II.3.2.1 Instrumented slabs on the runway

Four slabs are instrumented on the experimental runway. These slabs are aligned along a common joint so as to compare their response under the same conditions (trajectory, loading, thermal…).
In order to test the sensitivity of the different studying parameters (slab dimensions, subgrade, dowels or not), each instrumented slab has to be "distinctive". Figure II-12 represents the distribution of the instrumented slabs on the experimental runway.

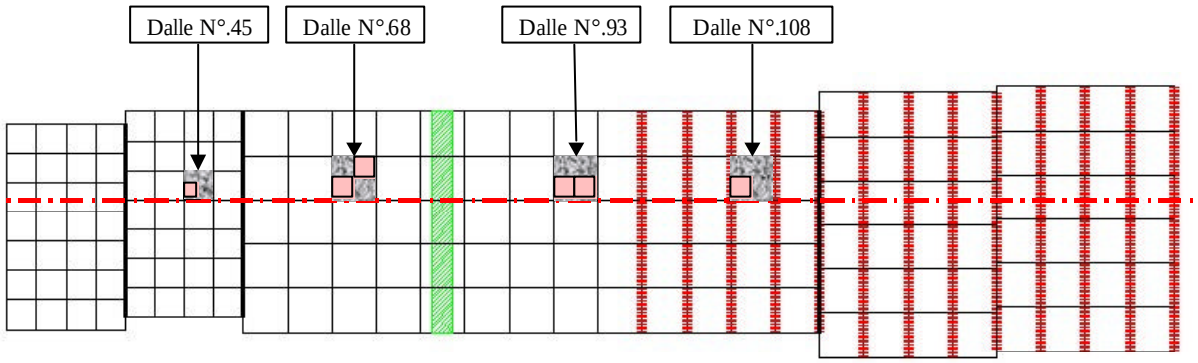

Figure II-12 : Distribution of instrumented slabs.

Let's describe now how the sensors are localized on each slabs. The following notations are used on the figures:

- VA means "vertical absolute"
- VR means "vertical relative"
- H means "horizontal"

II.3.2.2 Slab N°.45

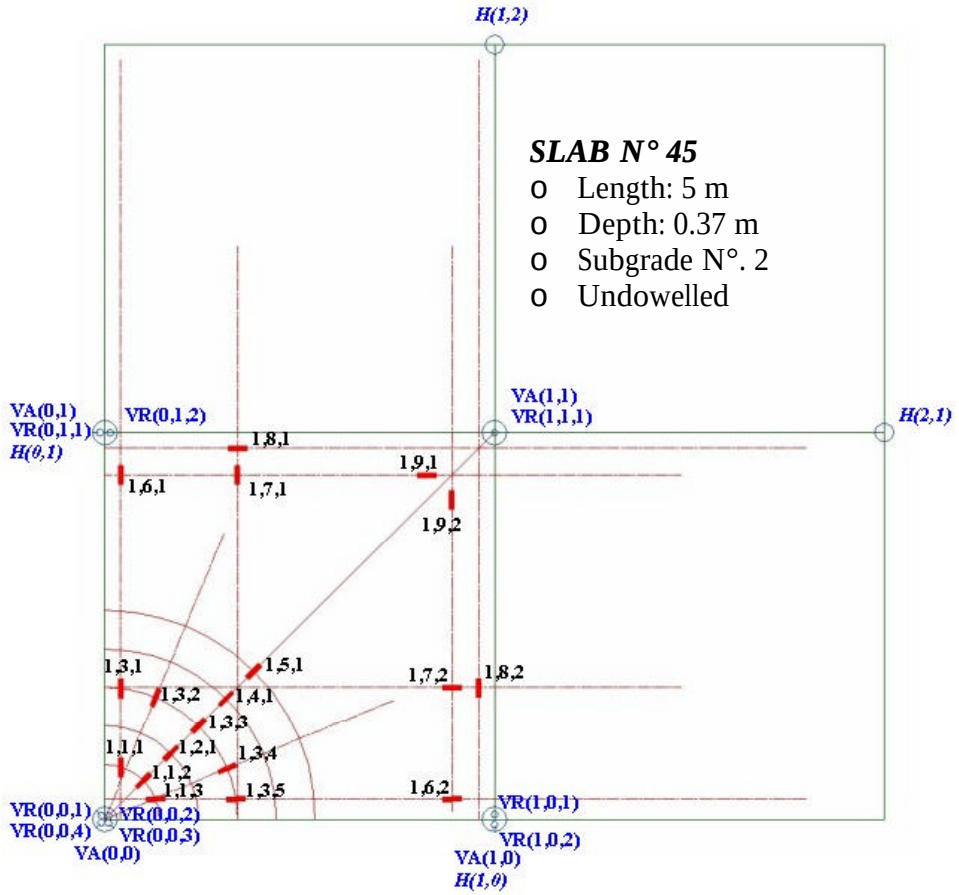

Figure II-13 Slab N°. 45.

The following figure present a detailed cartography of the strain gauges.

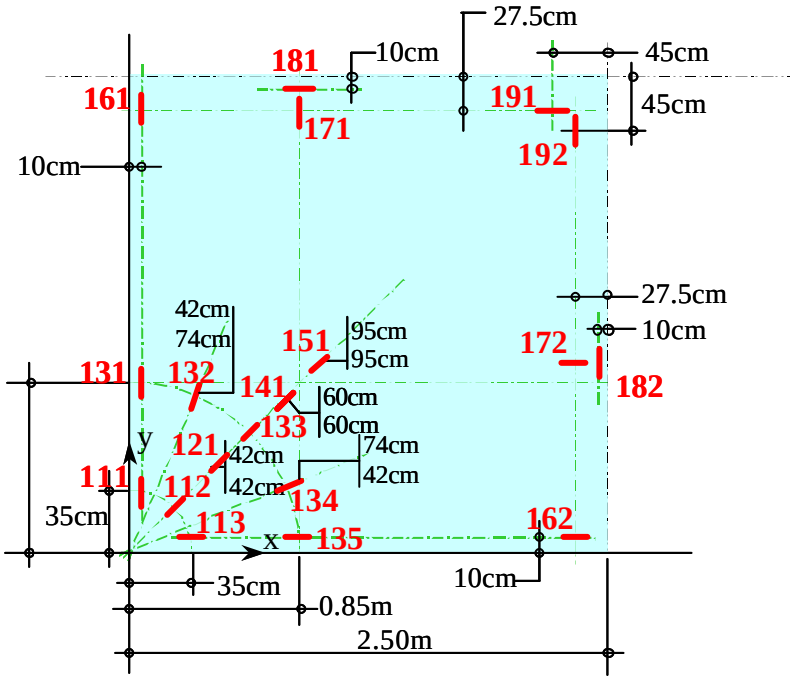

Figure II-14 Slab N°. 45 _ details.

II.3.2.3 Slab N°.68

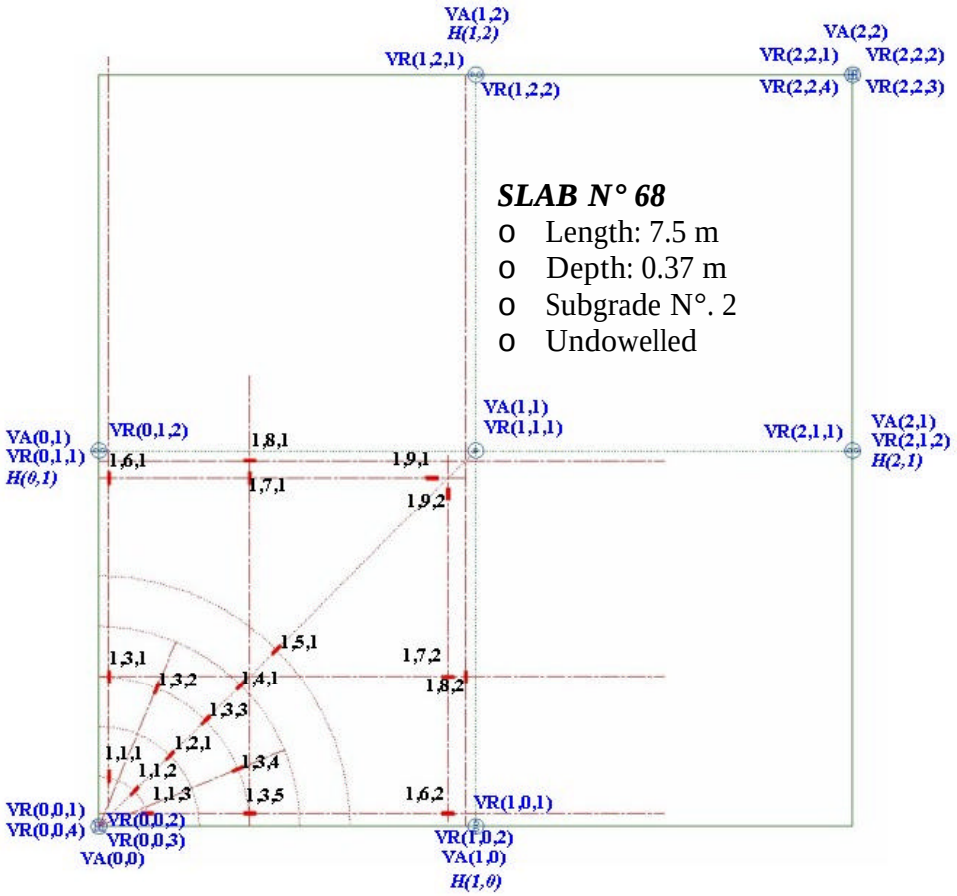

Figure II-15 : Slab N°. 68.

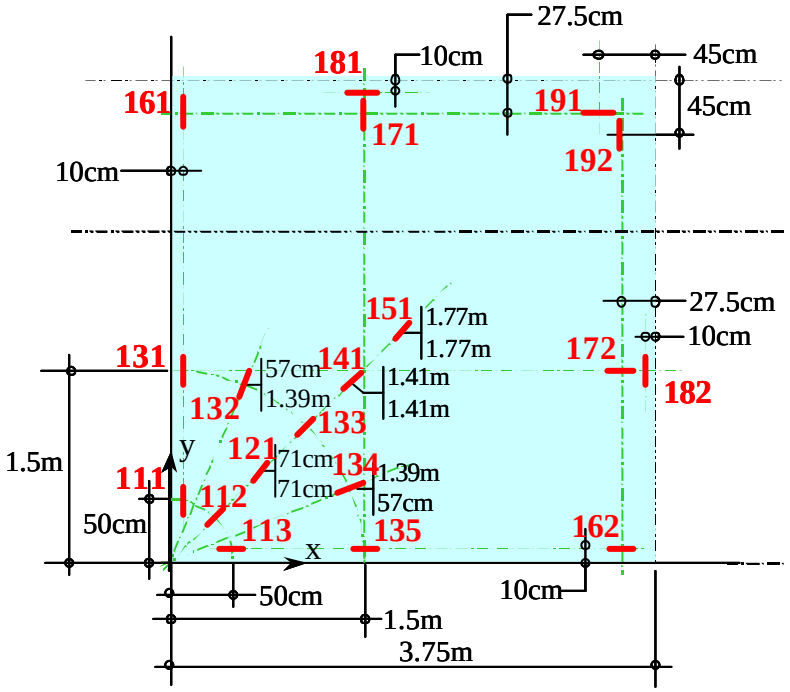

Figure II-16 : Slab N°. 68 _ details.

II.3.2.4 Slab N°.93

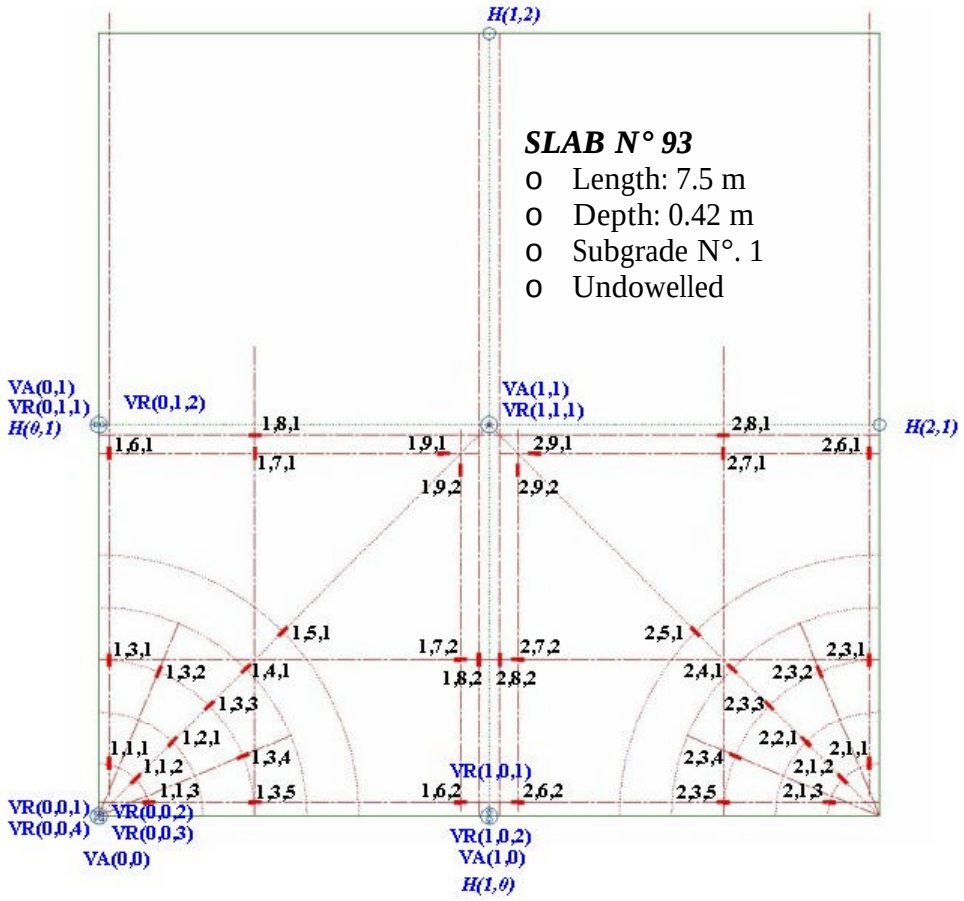

Figure II-17 : Slab N°. 93.

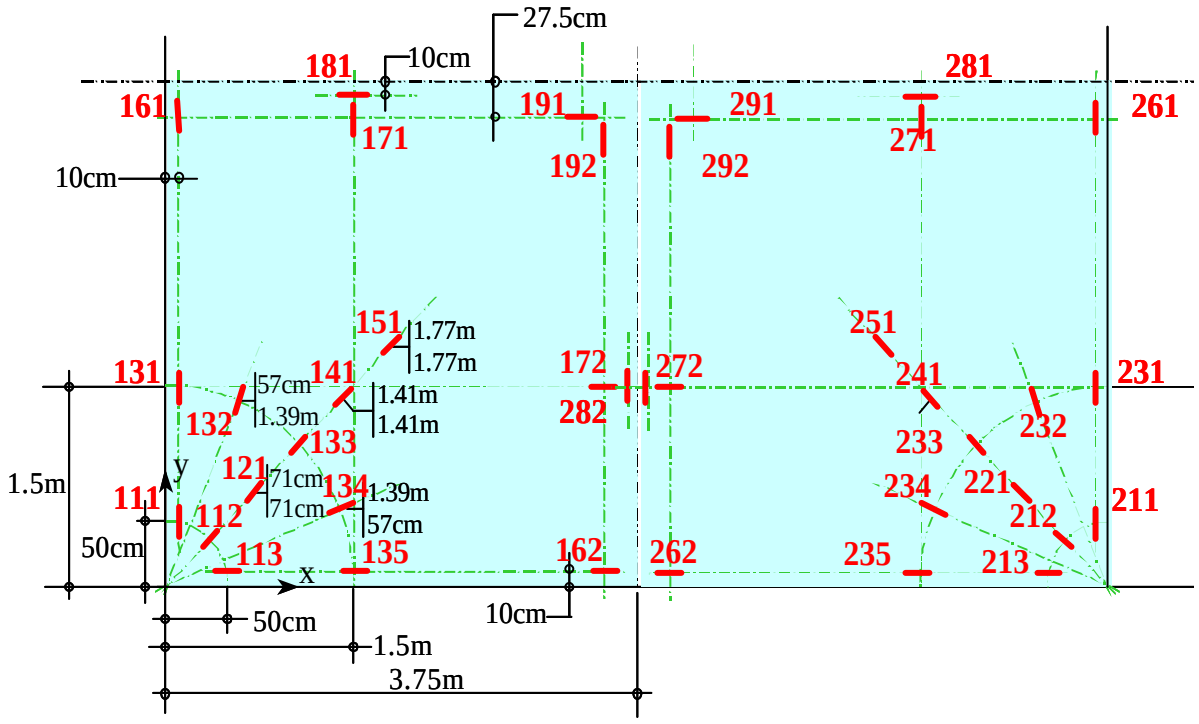

Figure II-18 : Slab N°. 93 _ details.

II.3.2.5 Slab N°.108

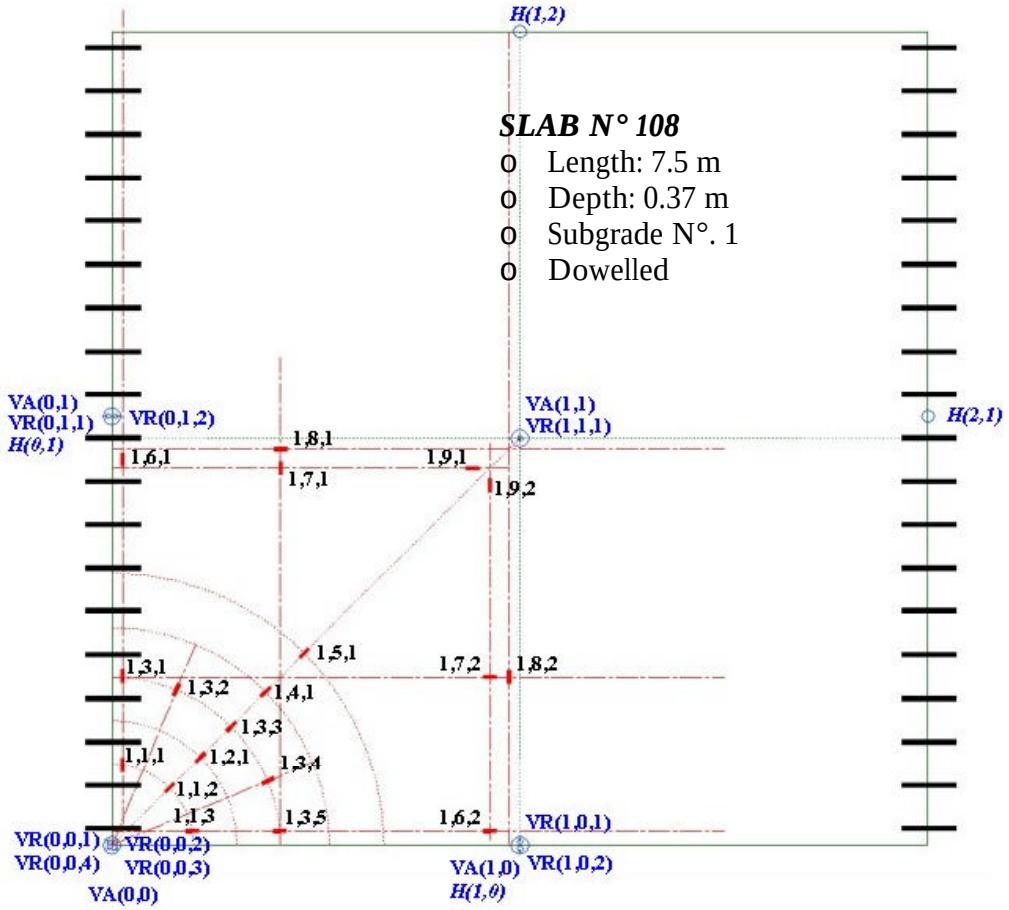

Figure II-19 : Slab N°. 108.

The localization of the strain gauges are the same than for the slab n° 68.

II.3.3 Acquisition system

II.3.3.1 Wiring

The instrumentation wiring may induces a possibility that the presence of cables in the concrete could lead to the initiation of cracks. A data collection system through conduits installed in the HUGA is chosen. This requires accurate topographical identification to find the conduits after the casting of the lean concrete. To limit the number of conduits, the cables from the strain gauges were grouped into data collector conduits thanks to grooves made in the surface of the lean concrete (Figure II-20). At the edge of the pavement, the conduits are grouped at five inspection holes for routing to the measurement bungalow.
For the horizontal LVDT sensors, the cable is routed to the nearest conduit along the joints (Figure II-21). This requires the installation of flexible material layers sufficiently slack (especially at slab corners) to avoid all rupture due to the movement of the slabs.

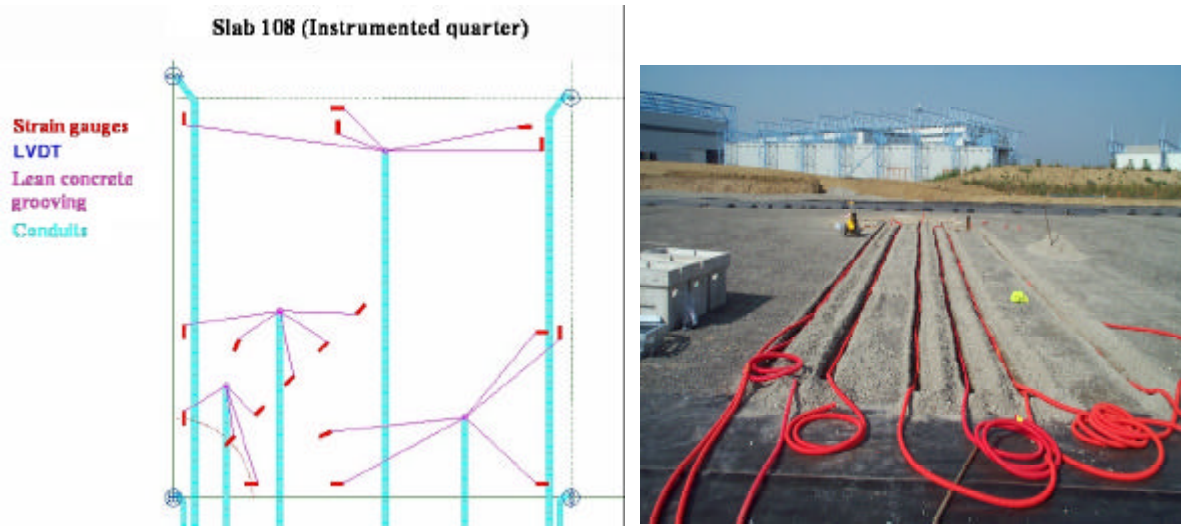

Figure II-20 : Slab wiring.

Figure II-21 : Passing cable in a saw joint.

II.3.3.2 Acquisition unit

Figure II-22 : Acquisition unit, MGCPlus & Spiders.

The acquisition unit corresponds to the general instrumentation context. The responses of the four instrumented slabs sensors of under a same load on the test runway have to be monitoring. It is decided that all instrumentation would be managed by a single acquisition unit (except for temperature data) for the following reasons:

- to facilitate analysis and avoid possible file concatenation errors,
- to allow tests to be conducted by a single operator.

Different hardware are used (Figure II-22):

- 1 MGCPlus unit (associated cards) with a maximum capacity of 128 channels (16 8-channel cards), connected to the acquisition PC by an Ethernet link and including all strain sensors.
- 10 Spiders with a capacity of 8 channels maximum:
    - 8 Spiders with a master spider connected to the acquisition PC parallel port including all vertical LVDT sensors,
    - 2 Spiders with a master spider attached to the acquisition PC RS232 ports including all horizontal LVDT sensors.

This relative heterogeneity is explained by the choice of a single acquisition unit and also by the limits of the equipment (128 channels maximum for the MGCPlus unit, 8 spiders maximum in parallel, etc..). The acquisition unit is controlled by Catman V3.0 Release4 software.

II.3.3.3 Acquisition procedure

The acquisition methods differ according to the measurements are carried out.

II.3.3.3.1 Quasi-static tests

The quasi-static tests are done as follows:

- Triggering of acquisition after calibration of the sensors at start of simulator or truck runover,
- Acquisition frequencies:
    - 50 Hz for the strain gauges and vertical LVDTs
    - 10 Hz for the horizontal LVDTs (frequency reduced due to the transmission speed limits of the RS232 link),
- Stop and saving acquisitions.

II.3.3.3.2 Slow tests

These are made during nights, weekends and outside quasi-static test periods. The procedure is described below:

- Triggering of acquisitions,
- Acquisition frequencies: one acquisition every 5 minutes,
- Stop and saving acquisition.

II.3.3.3.3 Data processing

A Bessel type filter with the following frequencies is used by the Catman software:

- MGCPlus: 1 Hz,
- Parallel port Spiders: 1 Hz,
- RS232 port Spiders : 1Hz.

A display allows signal waveforms to be checked in real time:

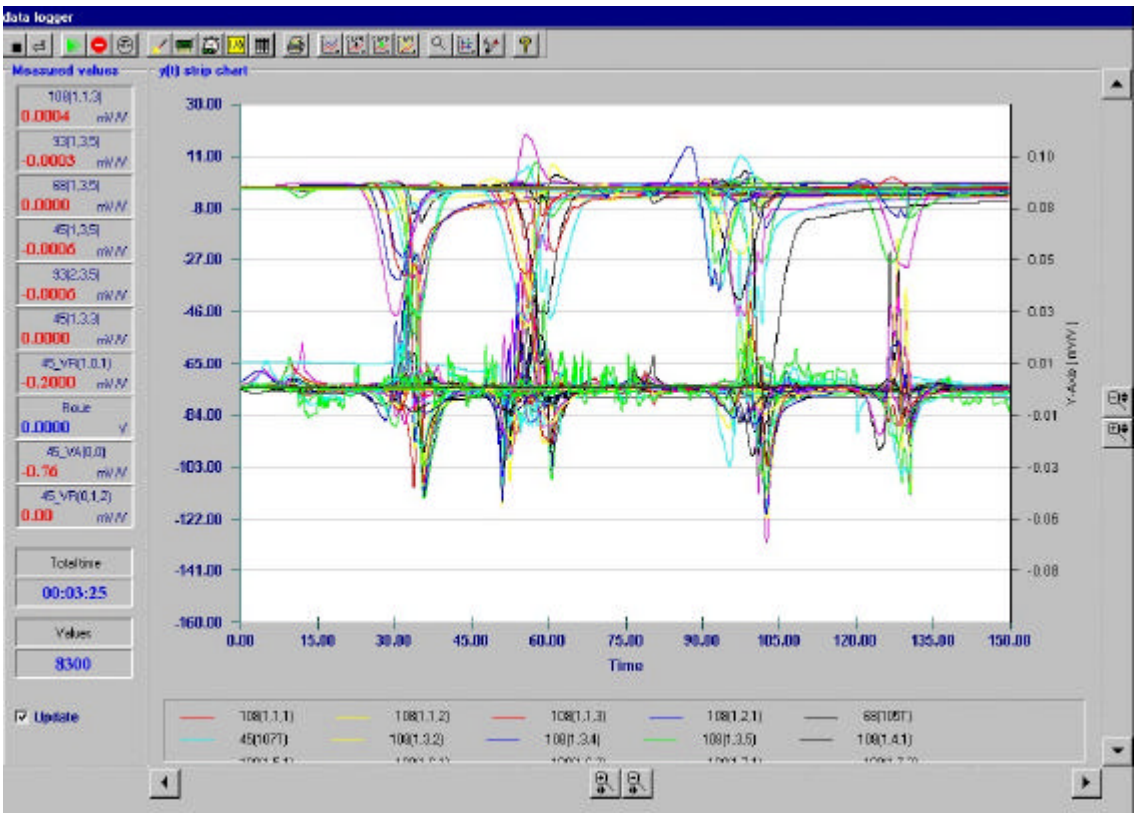

Figure II-23 : Acquisition signal waveforms.

II.3.3.4 Temperature acquisition

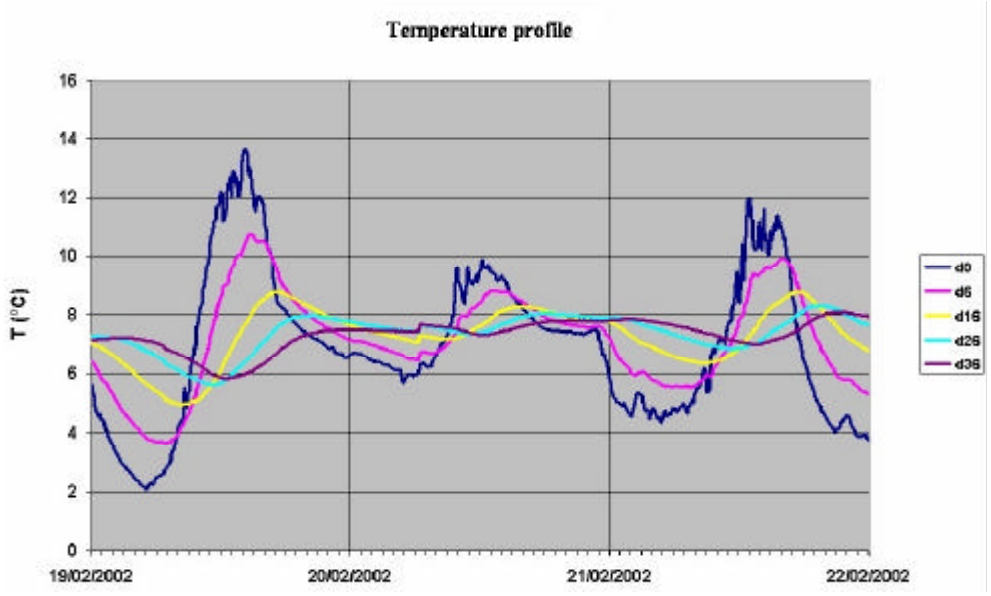

Figure II-24 : Temperature profile (19,20 & 21/02/2002).

Temperatures are monitored by a DataTaker unit connected to a standalone PC These are recorded 24 hours-a-day, every quarter of an hour until 15 February 2002 8h50 and, every five minutes after. Figure II-24 represents an example of temperature profile for three days of February 2002. To control the temperature gradient in real time, a temperature profile display and gradient calculation software package was developed by the Aéroport de Paris, like shown Figure II-25.

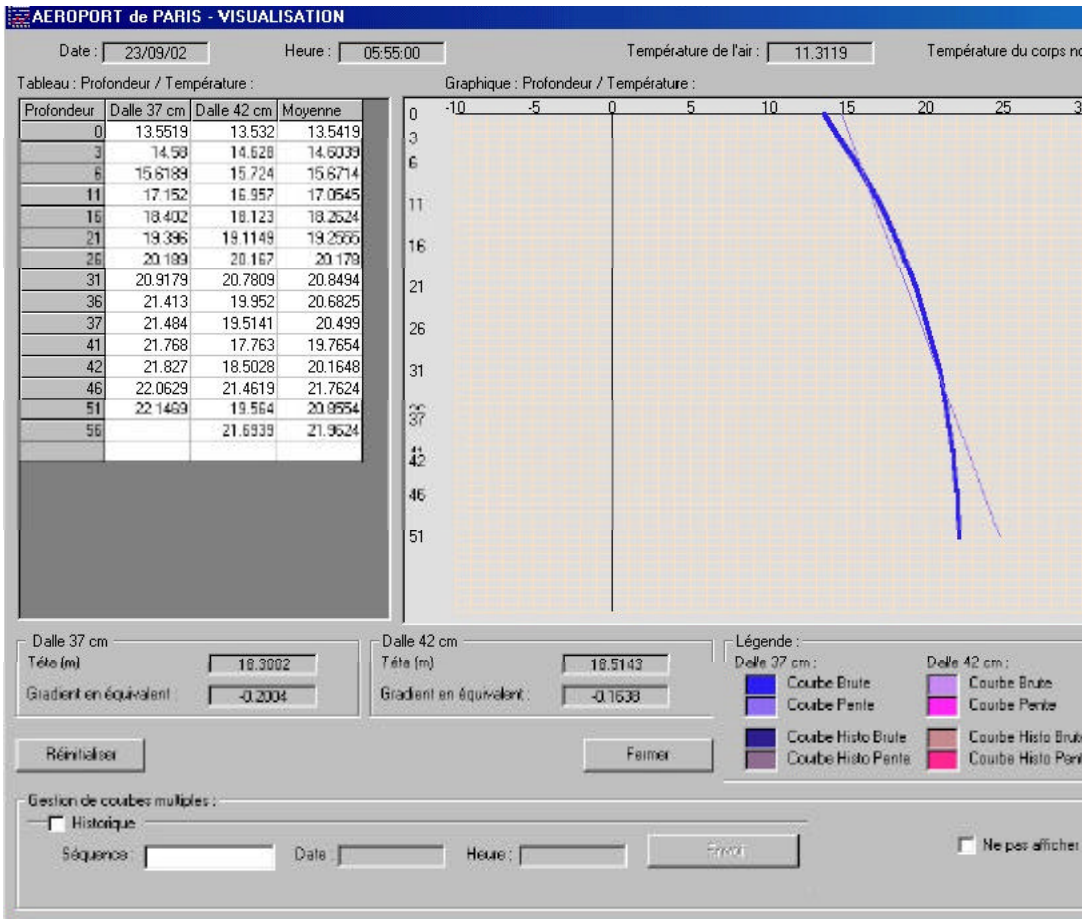

Figure II-25 : Temperature acquisition software.

II.3.4 Database

The files are saved in ASCII format for direct use with Excel software. This leads to long recording times (when compared with a binary save which is instantaneous). For instance, for a complete passage of the simulator over the four instrumented slabs at a speed of around 2 to 3 km/h, the acquisition time is approximately 3 to 4 minutes and save time is in the order of 3 to 4 minutes too. The data file size is between 10 and 14 Mbytes. Note that the file times are expressed in Universal Time (UT).

The output file includes all sensors as shown in Figure II-26:

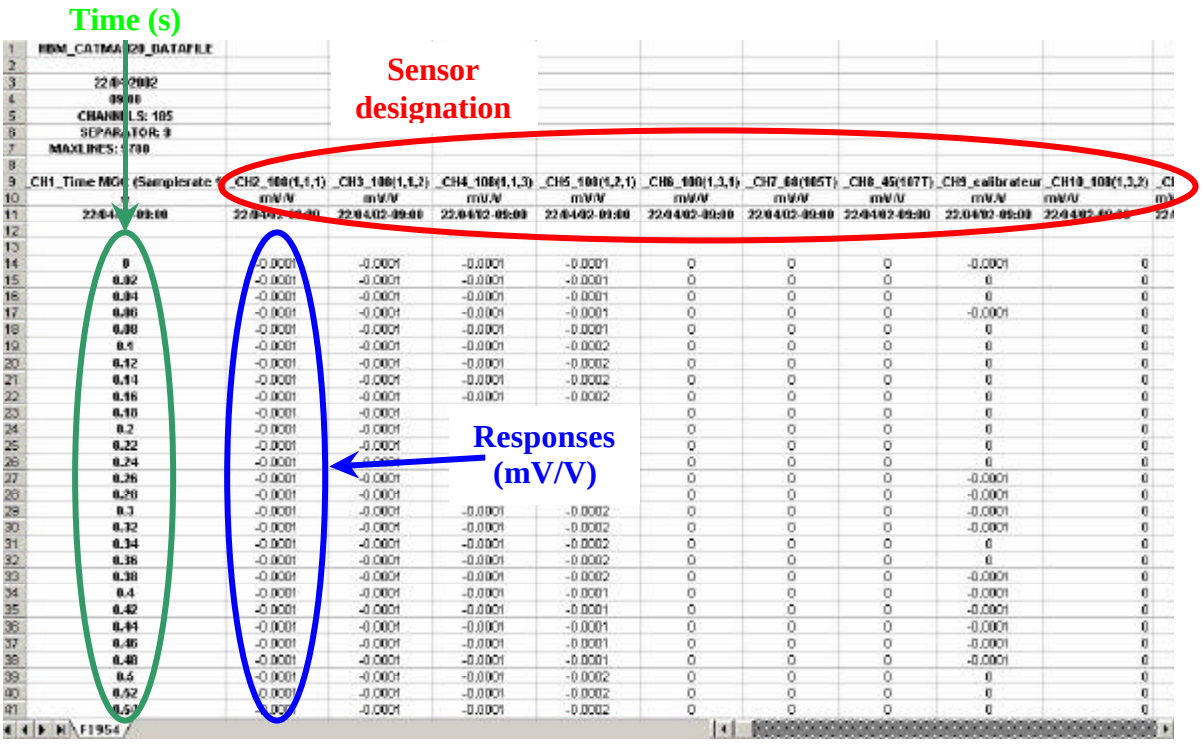

Figure II-26 : Example of an output file.

III. QUASI-STATIC TESTS

The main aim of the quasi-static tests is to improve the understanding of the stresses generated to a cement concrete pavement by aeronautical loads. The study has to underscore the influence of the loading parameters (thermal and mechanical) and of the pavement design parameters.
The static test principle consists in varying the load parameters one by one. These parameters are mainly the applied load per wheel load tyre pressure, the geometrical configuration of the landing gears (track, base, type of bogie) under a given thermal load. These results are to be related with the parameters of the pavement used (dowelled, slab dimensions, type of foundation, base ground, etc).

III.1 Tested configurations

III.1.1Principles of the different configurations

Different configurations (representing the main aircrafts) of landing gears are represent by a full scale simulation vehicle. This one is able to represent the effects on pavement of an aircraft wide body. Therefore, all procedures have a constant part (to understand the dynamics of the pavement) and a specific part (to underline the influence of the changing parameter of the load).

III.1.2 Simulation vehicle

The simulation vehicle (Figure III-1) is a self powered one. Its speed is 2 km/h for the quasi-static test and 5 km/h during the fatigue test. The direction control is able to maintain a straight trajectory during 160 meters +/- 1 cm (lateral deviation). The translation can maintain the speed on a 1% uphill slope. The configuration changes from one aircraft to another has to be done very quickly.

Figure III-1 : Simulation vehicle.

The maximum mass of the simulation vehicle is 613 T. The different configurations with an identical load per wheel can vary from 12 wheels to 22 wheels. To obtain these different configurations, the simulation vehicle is equipped with four wheels or six wheels bogie, as shown in Figure III-2. The base and the track are the two parameters permitting to achieve an aircraft landing gear configuration.

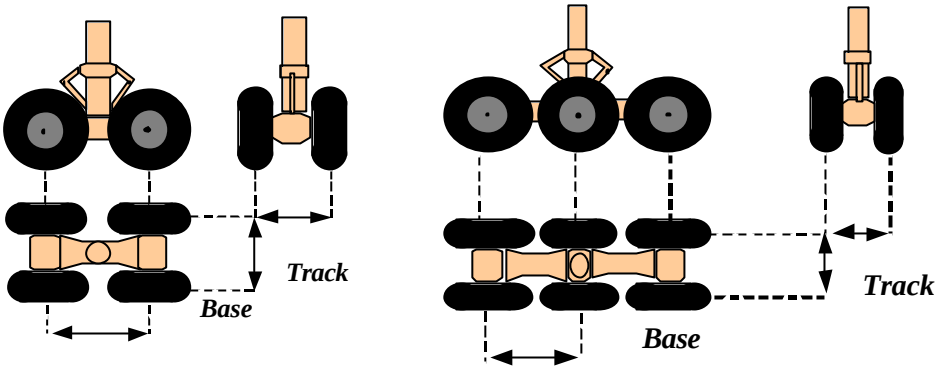

Figure III-2 : Four wheels & six wheels bogie.

Whatever the configuration, two steering wheels are installed in front of the vehicle. Their low load (13 T) induces no effect on the measurement. All tyres are the same as the ones used for the A340, i.e. 1400 mm diameter and 530 mm wide (tyres 1400x530R23 PR36). Tyre inflation pressure is adjusted to produce the same contact surface of the operational case.

III.1.3 Configurations G0, G1 & G2 – tracks, load & base effect

III.1.3.1 Configuration G0

Configuration G0 corresponds only to a preparation of the structure for running or installation of slabs.

The aim of the G0 configuration is to obtain the opening of the joints of the concrete surface course (preconditioning configuration). G0 corresponds to overruns with bogie B747-400 (4-wheels module) loaded by 20 metric tons per wheel, hauled by the Service truck of STBA (Figure III-3) or by overruns of the Service truck of STBA alone (7 metric tons per wheel on rear axle).

Figure III-3 : B747-400 bogie hauled by the Service truck of STBA.

Two trajectories are defined (Figure III-4):

- Trajectory 1 passes on either side of the instrumented strip,
- Trajectory 2 passes on both sides of the instrumented strip.

These trajectories are made over the complete length of the test zone and the return maneuvers are made on storage zones. Configuration G0 runs alternatively between trajectory 1 and trajectory 2 at a mean speed of 50 km/h and with an acquisition frequency of 50 Hz.
Note that on account of the two slab sizes (5 m and 7 m 50), G0 is offset to run at 50 cm from the joint when approaching the 5 x 5 m slab zone.

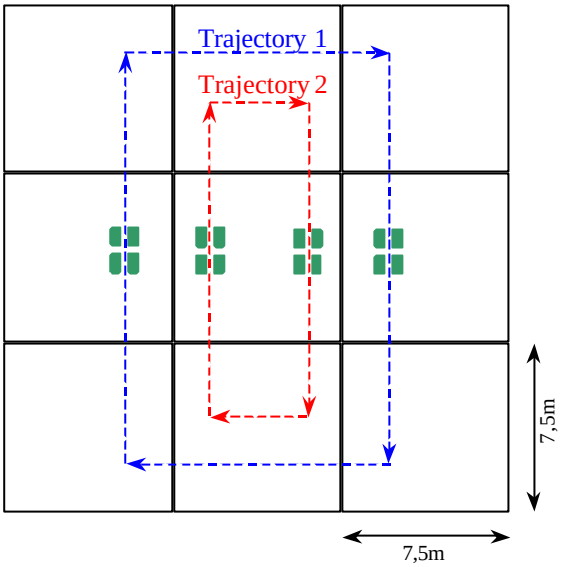

Figure III-4 : G0 trajectories.

III.1.3.2 Configuration G1

Configuration G1 tests the effects of track and load. It corresponds to the 2 wheels module M2 (Figure III-5) hauled by the Service truck of STBA. It is decomposed into 5 sub-configurations as described Table III-1.

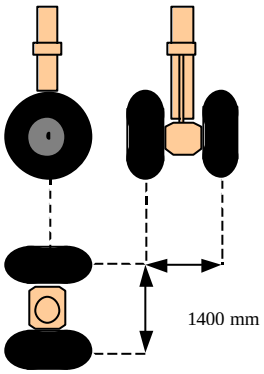

Figure III-5 : 2 wheels module M2.

Table III-1 : Configuration G1 family.

Family	Configuration	Number of bogies	Number of wheels	Track (cm)	Base (cm)	W/wheel (tons)	Pnz B1 (bars)
G1	G1_1	1	2	**140**	0	**20**	10.3
G1	G1_2SG	1	2	**140**	0	**25**	12.9
G1	G1_2	1	2	**140**	0	**25**	12.9
G1	G1_3	1	2	**140**	0	**30**	15.4
G1	G1_4	1	2	**130**	0	**25**	12.9
G1	G1_5	1	2	**150**	0	**25**	12.9

III.1.3.3 Configuration G2

The aim of the configuration G2 is to test the load and base effects of these types of bogies. It corresponds to the case where the simulator is equipped with a four wheels bogie and a six wheels bogie (Figure III-6).

Figure III-6 : Configuration G2.

The two modules are spaced of 10 meters to prevent all bogie-bogie interactions on a given slab. For each bogie, we have 6 sub-configurations:

Table III-2 : Configuration G2 family.

Family	Configuration	Number of bogies	Number of wheels	Track (cm)	Base (cm)	W/wheel (tons)	Pnz B1 (bars)
G2	G2_1	2	4/6	140	170	20	10.3
G2	G2_2	2	4/6	140	170	25	12.9
G2	G2_31	2	4/6	140	170	30	15.4
G2	G2_32	2	4/6	140	170	28	14.7
G2	G2_4	2	4/6	140	160	25	12.9
G2	G2_5	2	4/6	140	180	25	12.9

Note : The modules considered in the following are strictly the same as the mentioned aircraft bogies. The per wheel load corresponds to the aircraft load at MTOW with maximum rearward CG.

III.1.4 Configuration G8 – Boeing 777-300 ER / A340-600 WLG

Configuration G8 is the first aircraft configuration (1/2 B777-300ER / 1/2 A340-600) shown Figure III-7. In reality, it corresponds to a specific case of configuration G2. The simulator is equipped with the A340-600 four wheels bogie (wing landing gear) and the B777-300ER six wheels bogie (Figure III-8). The modules were geometrically the same as the aircraft bogies.
The two modules are distant from 10 meters to prevent all bogie-bogie interactions on a given slab. Whilst meeting the targets fixed for G2 (load and base effect on four and six wheels bogie), we obtain here bogie data for these two aircrafts in real in-service conditions (track, base, load, tyre tracks and thermal gradient). The procedure was done once for the 4-wheels bogie and repeated once for the 6-wheels bogie.

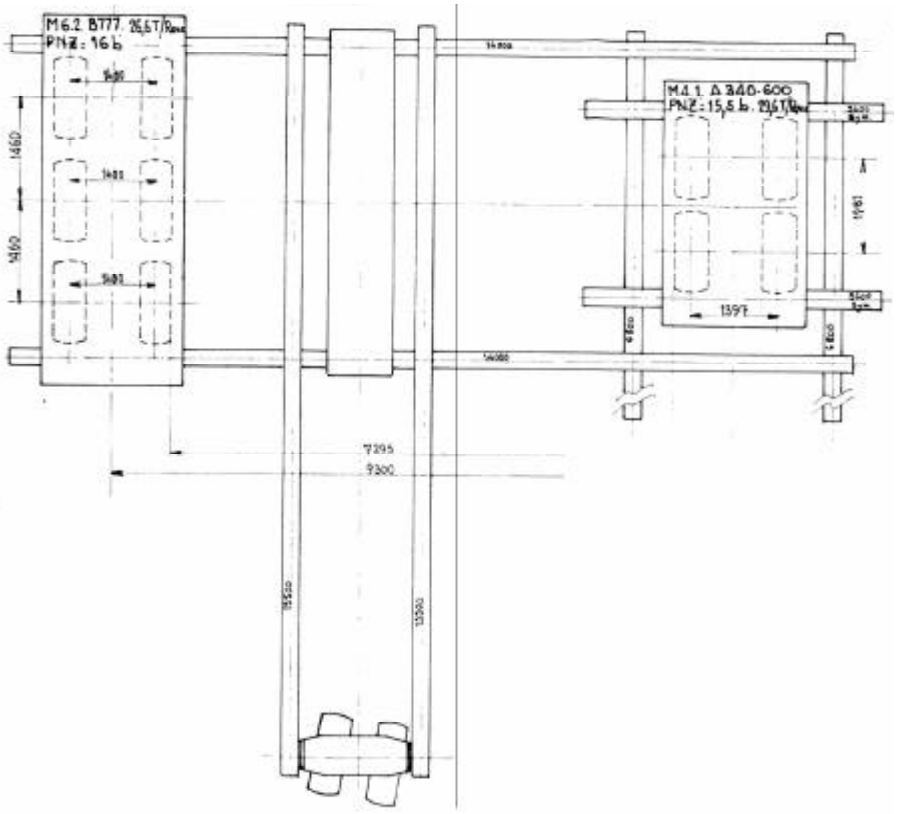

Figure III-7 : Configuration G8.

Figure III-8 : Details of the B777 six wheels bogie.

III.1.5 Configuration G4 – A340-600 : bogie interaction

Configuration G4 has to test the stresses due to bogie interaction. The simulator is equipped with the A340-600 centreline landing gear and a wing landing gear (Figures III-9 & III-10). The complete A340-600 landing gear can be taken into account by adding the second wing landing gear thanks to the Service truck of STBA. The procedure is thus completed by purely static acquisition by loading the slabs successively by two modules (simulator: wing landing gear - centreline landing gear) then three modules (simulator + truck: wing landing gear - centreline landing + wing landing gear). The interactions are measurable for a given gradient.

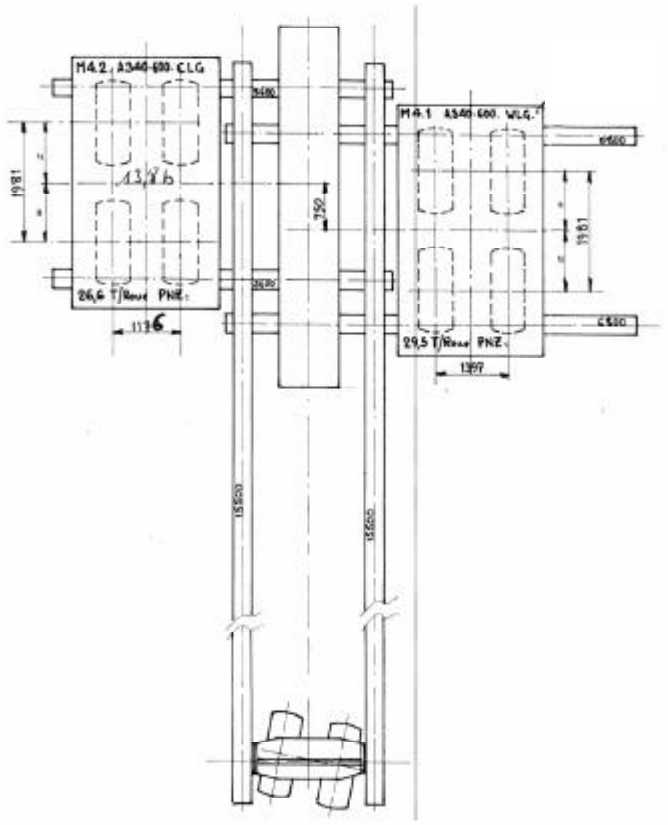

Figure III-9 : Configuration G4.

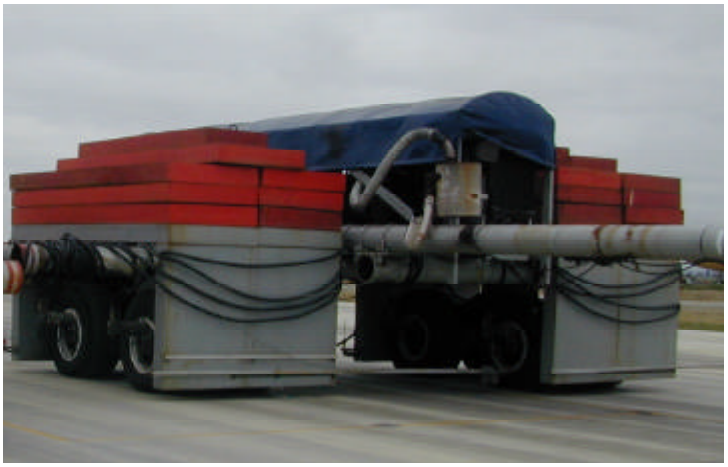

Figure III-10 : Details of the configuration G4.

III.1.6 Configurations G5, G6 & G7 – A380 test procedure

Configurations G5/G6/G7 correspond respectively to A380- 800/800F/Ultimate. They give aircraft data and enhance the bogie interaction effects.

Configurations G5/G6 correspond to three quarters of the A380-800/800F main landing gear (simulator equipped with an wing landing gear and fuselage landing gears, Figures III-11 & III-12). Configuration G7 (Figure III-13, III-14 & III-15) corresponds to configuration G6 with an added centerline landing gear (two wheels) between the fuselage landing gears. These configurations provide us with aircraft data for the various A380 versions.

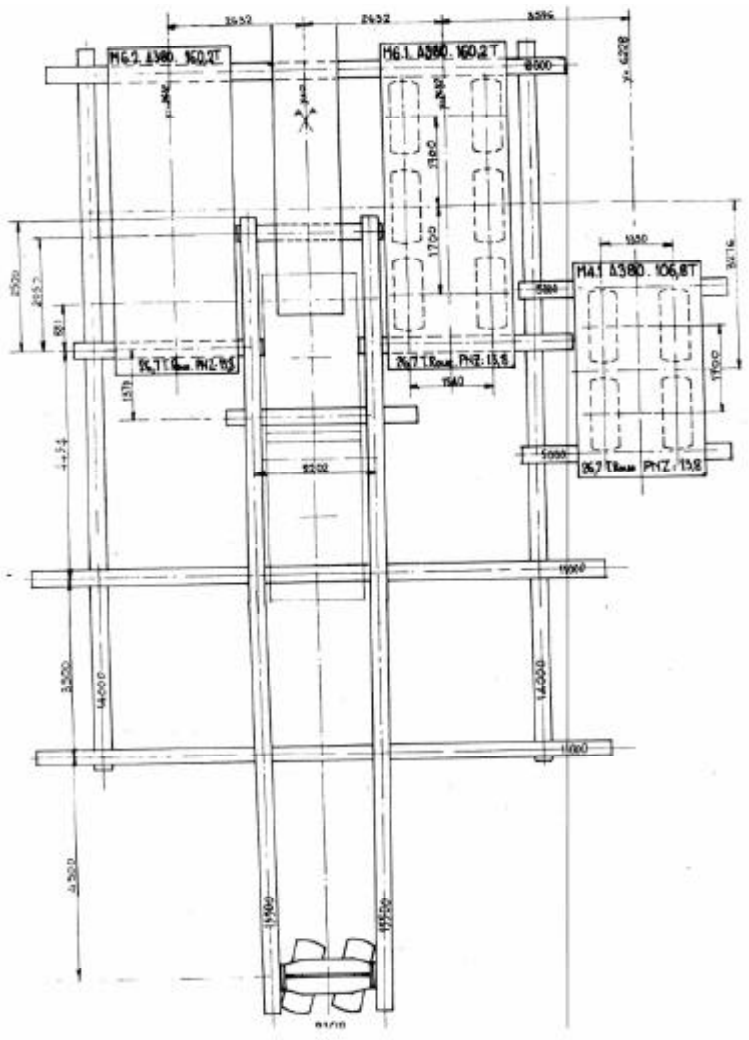

Figure III-11 : Configuration G5.

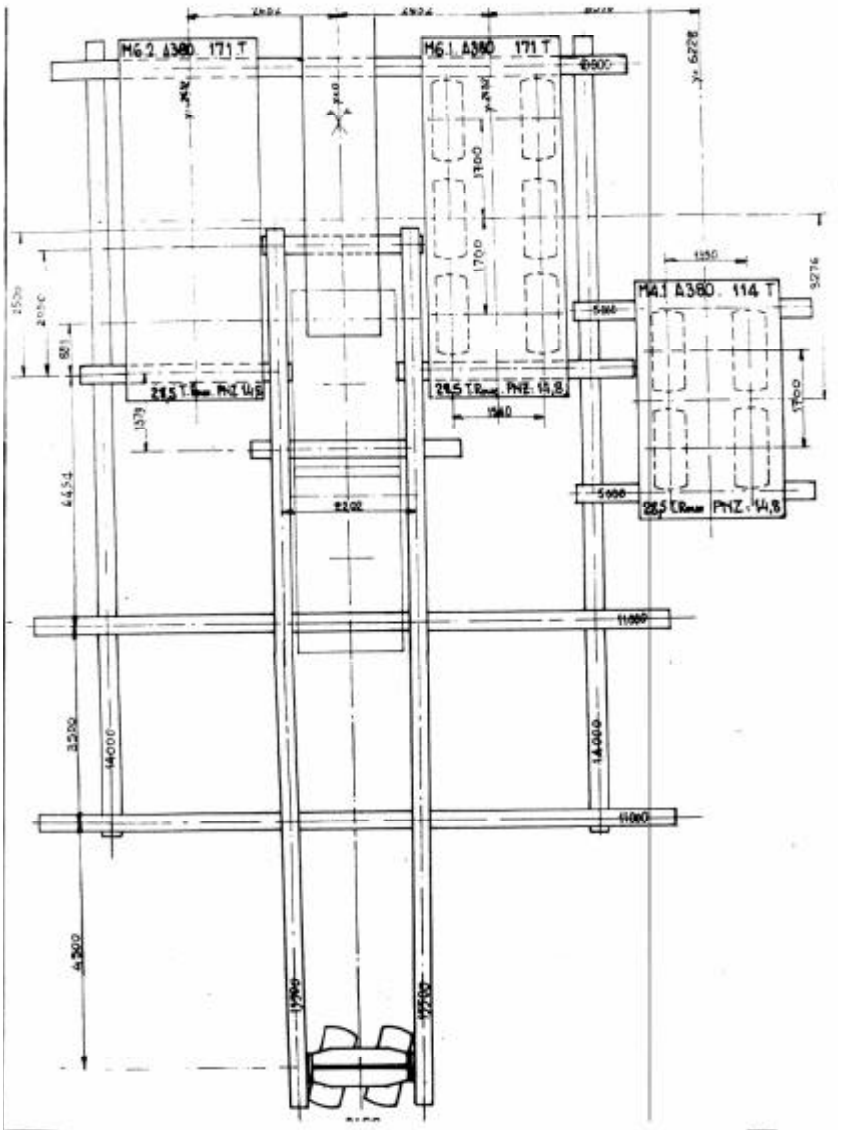

Figure III-12 : Configuration G6.

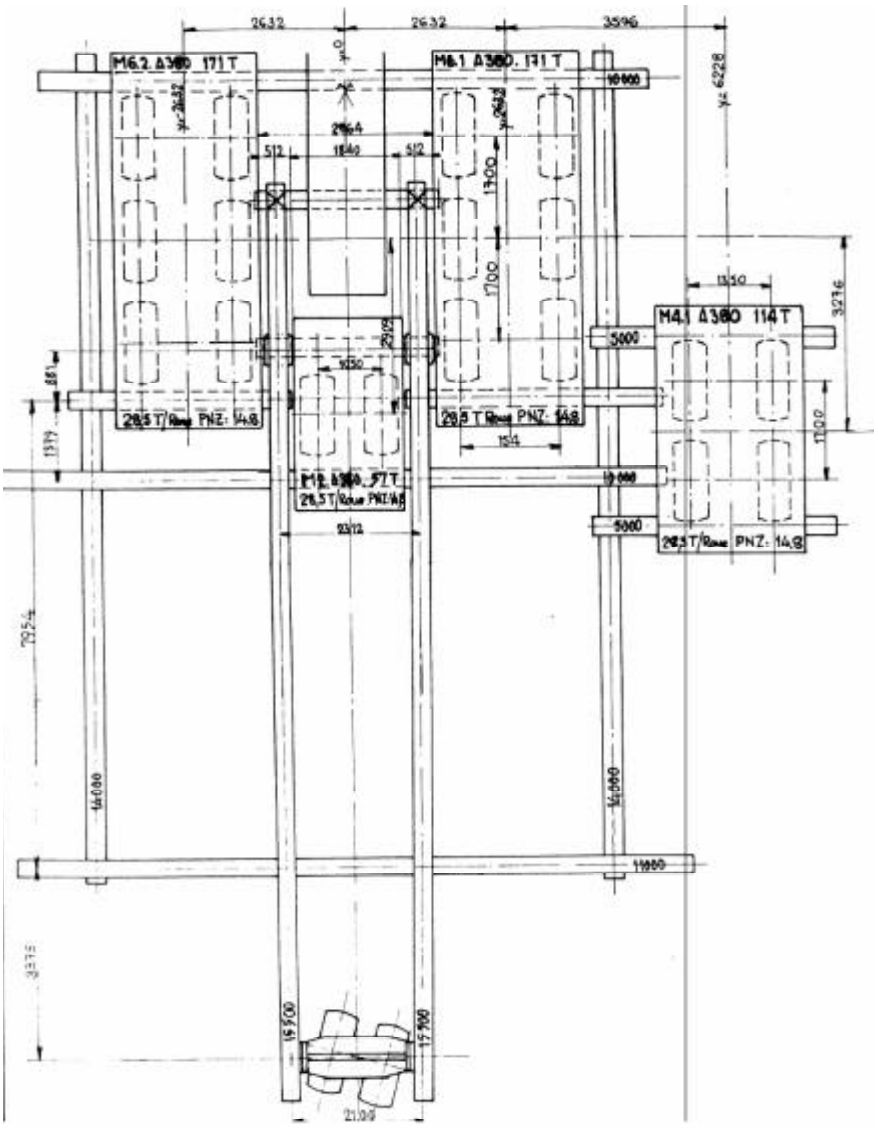

Figure III-13 : Configuration G7.

Figure III-14 : Photo of configuration G7.

III.1.7 Configuration G9 – Mac Douglas 11

Configuration G9 corresponds to the main landing gears of the Mac Douglas 11 (Figure III-16 & III-17).

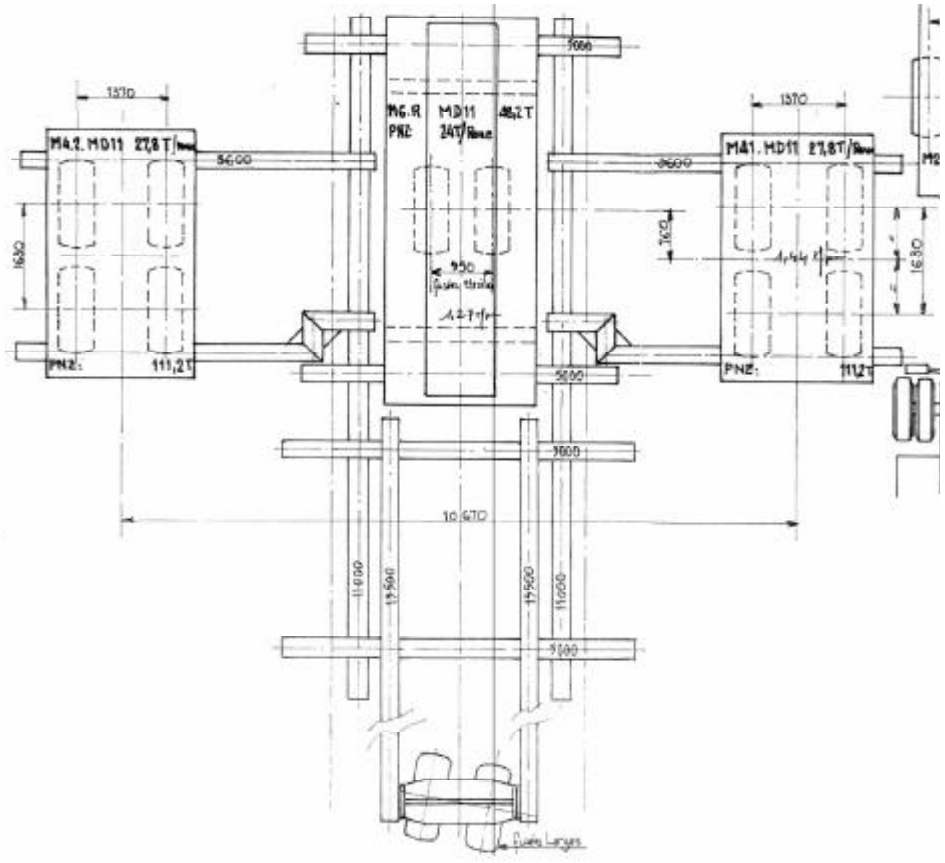

Figure III-15 : Configuration G9.

Figure III-16 : Photo of configuration G9.

III.1.8 Configuration G10 –Boeing 747-400

Configuration G10 corresponds to the main landing gears of the B747-400 (Figure III-18).

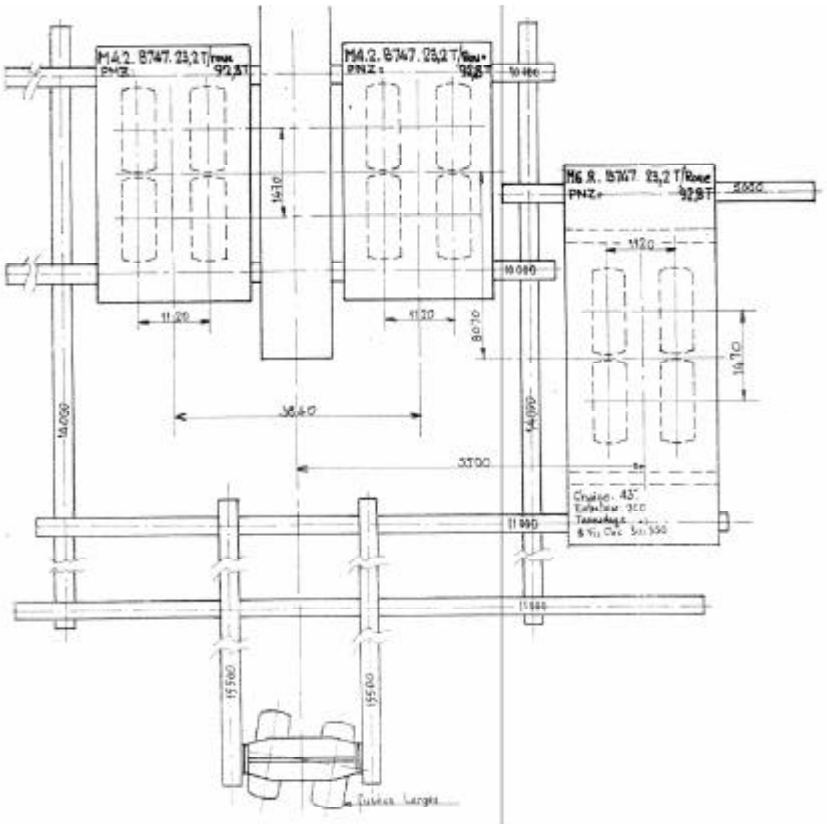

Figure III-17 : Configuration G10.

III.2 Main trajectories

The various configurations range from the single tandem to the aircraft configuration using up to four bogies. The position of the simulator is identified in relation to the leftmost bogie axle centreline. The position of the other bogies is deduced from the abscissa of the trajectory and the distance between bogies.

Thus, the trajectories can be defined by an abscissa Y in relation to the free edge of the runway or in relation to the reference joint (cf. Figures I-14 & I-15).

Some of these abscissas Y are constant and represent an axle-reference joint distance irrespective of the bogie track configuration.

The other trajectories identify a specific position of the tyres in relation to the reference joint (external tyre tracks of the tyre tangent to the joint, etc.). The abscissas of these trajectories vary according to the track of the modules.

III.2.1 Overrun direction

Before defining the different trajectories used during the static tests, it is important to notice the overrun direction on the runway (Figure III-18).

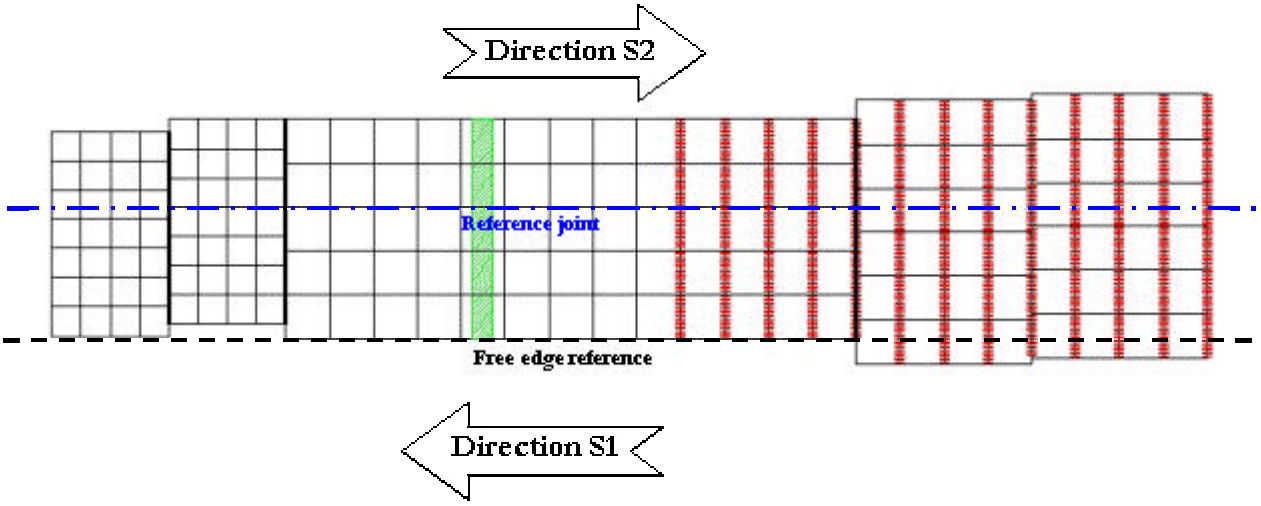

Figure III-18 : Overrun direction.

III.2.2 Trajectory T_0

The trajectory T_0 (Figure III-19) is defined by the outer edge of right tyre tangent to reference joint (complete module outside of instrumented slab).

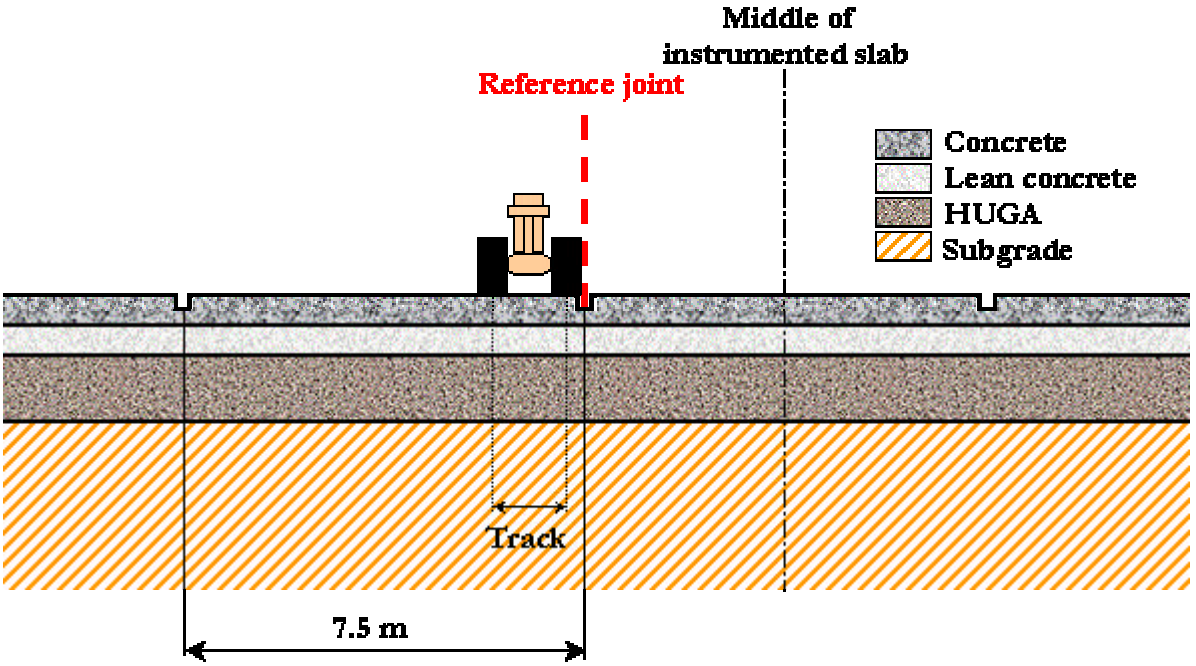

Figure III-19 : Trajectory T_0.

III.2.3 Trajectory T_1

The trajectory T_1 (Figure III-20) is defined by the inner edge of right tyre tangent to reference joint.

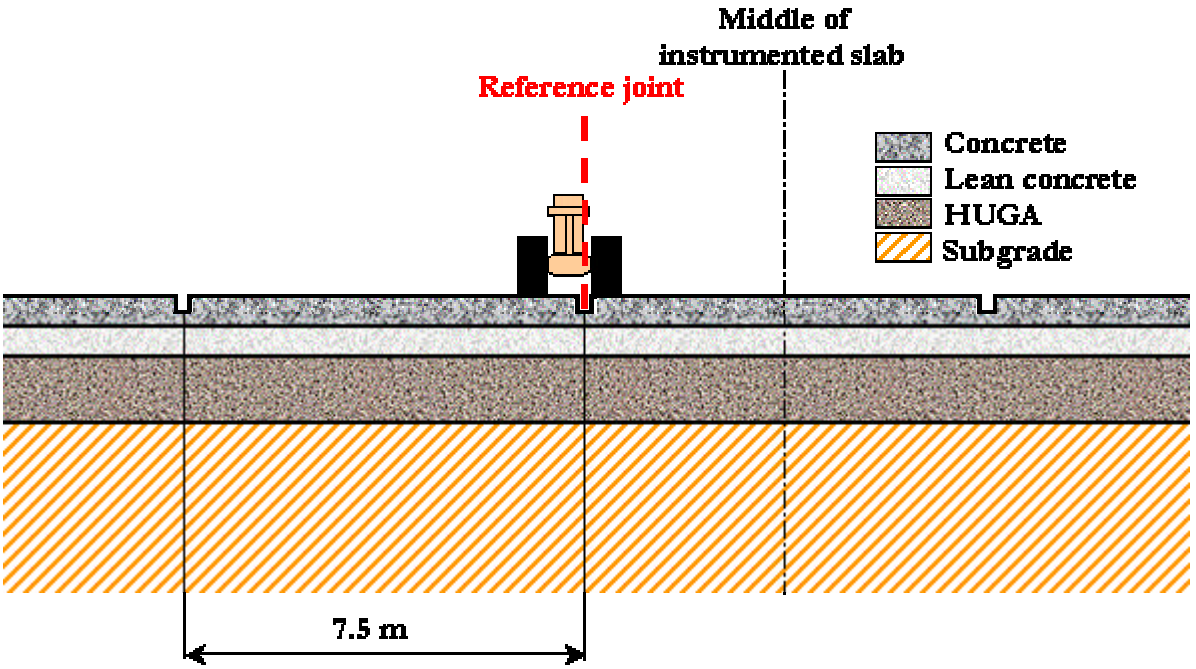

Figure III-20 : Trajectory T_1.

III.2.4 Trajectory T_2

The trajectory T_2 (Figure III-21) is the one with bogie centred on either side of reference joint (half module on instrumented slab).

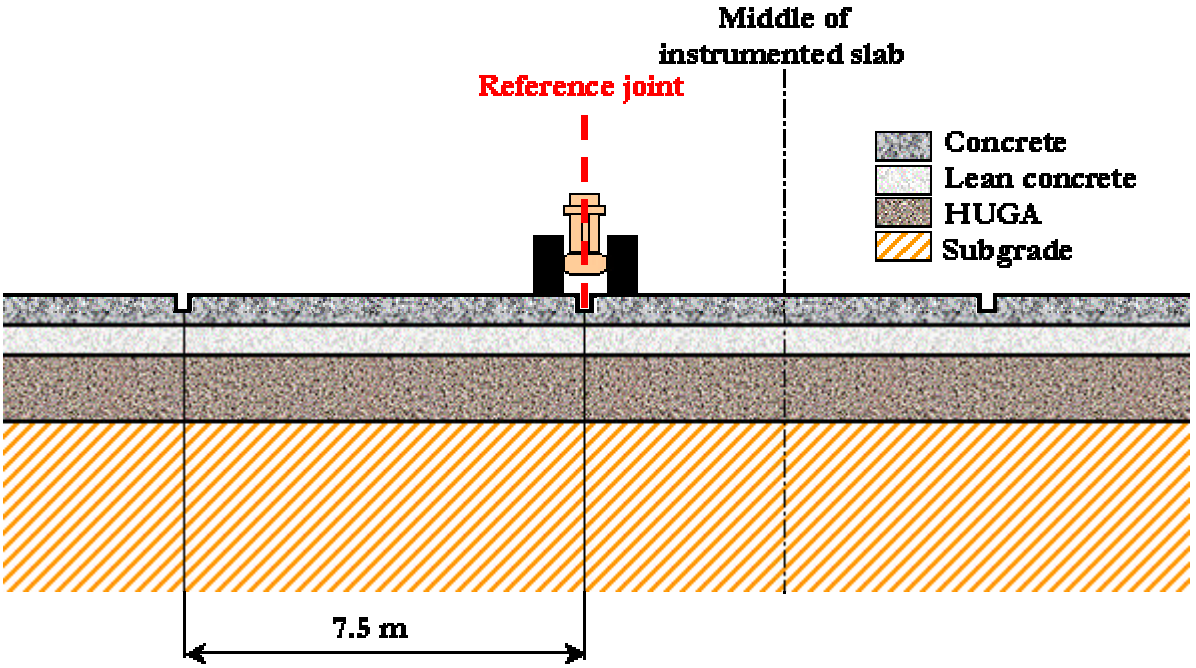

Figure III-21 : Trajectory T_2.

III.2.5 Trajectory T_3

The trajectory T_3 (Figure III-22) is defined by the outer edge of left tyre tangent to reference joint (module entirely on instrumented slab).

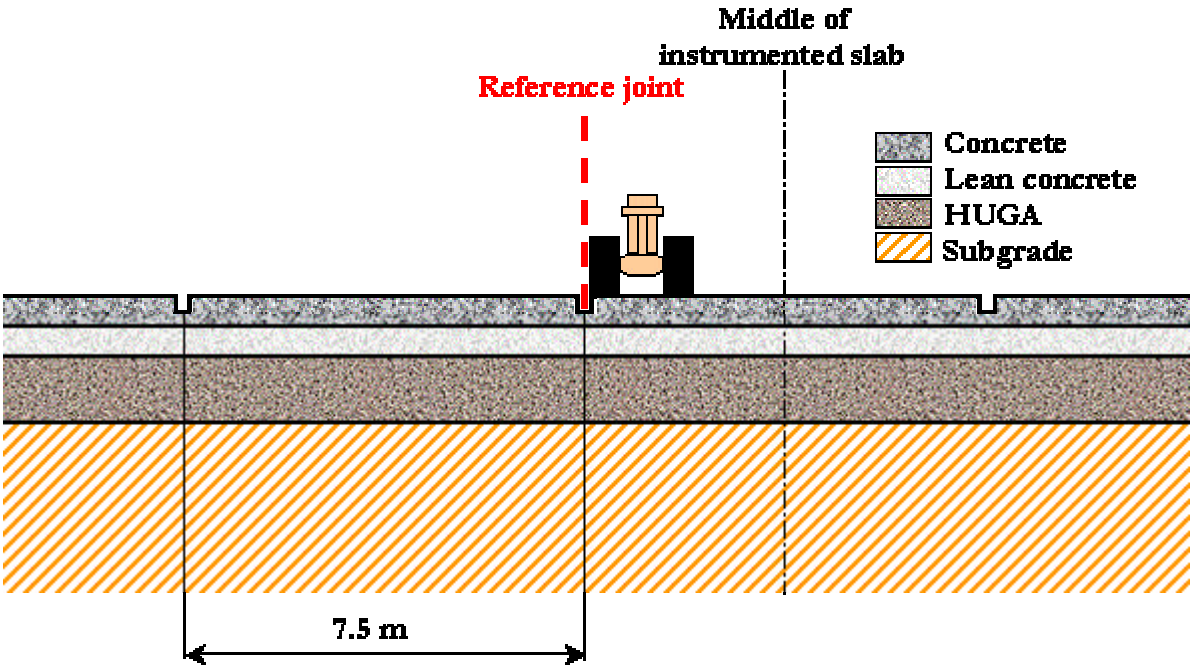

Figure III-22 : Trajectory T_3.

III.2.6 Trajectory T_4

The trajectory T_4 (Figure III-23) is characterized by an 1.55 m offset from reference joint (a strain gauge in vertical alignment).

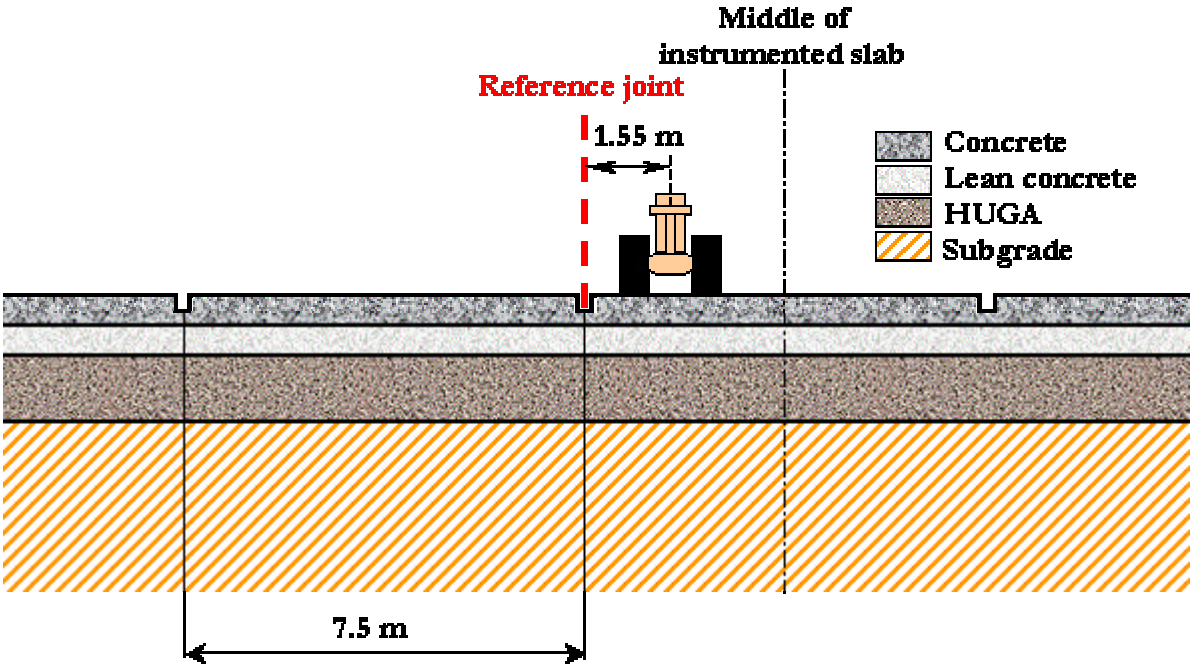

Figure III-23 : Trajectory T_4.

III.2.7 Trajectory T_5

The trajectory T_5 (Figure III-24) is defined by an 2.50 m offset from reference joint.

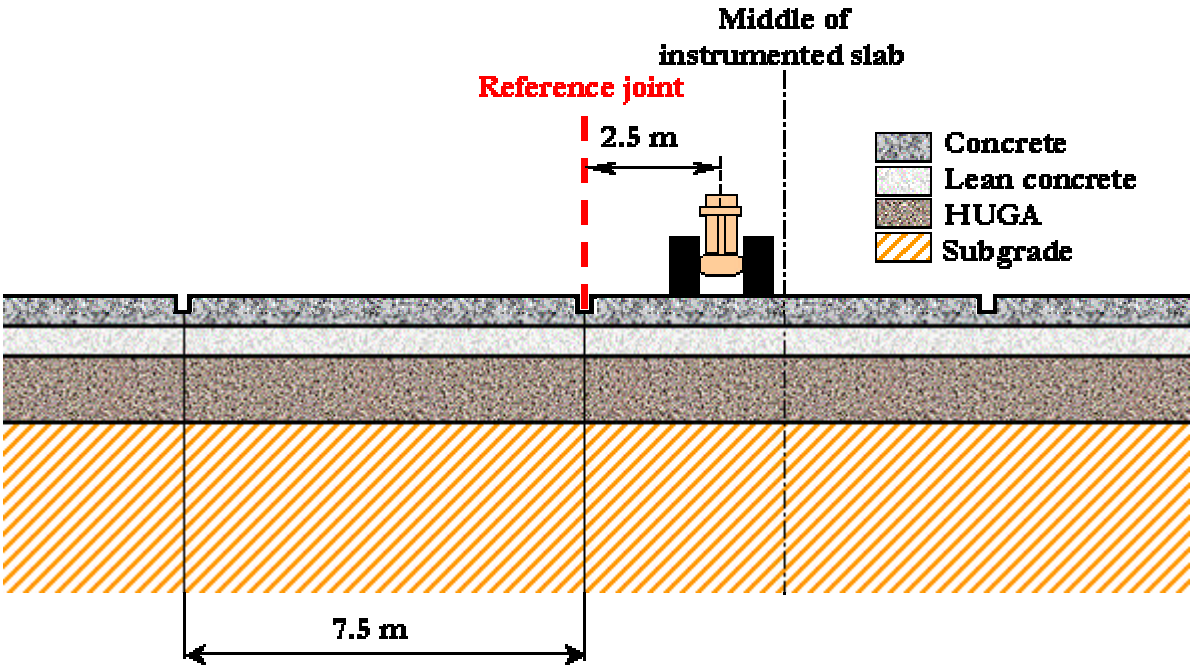

Figure III-24 : Trajectory T_5.

III.2.8 Trajectory T_6

The trajectory T_6 (Figure III-25) is defined by an 3.75 m offset from reference joint for 7.5 x 7.5 slabs or at 2.5 m from reference joint for 5 x 5 slabs (centre of slab). On 5 m slabs, T6 trajectory is the same than the T5 trajectory.

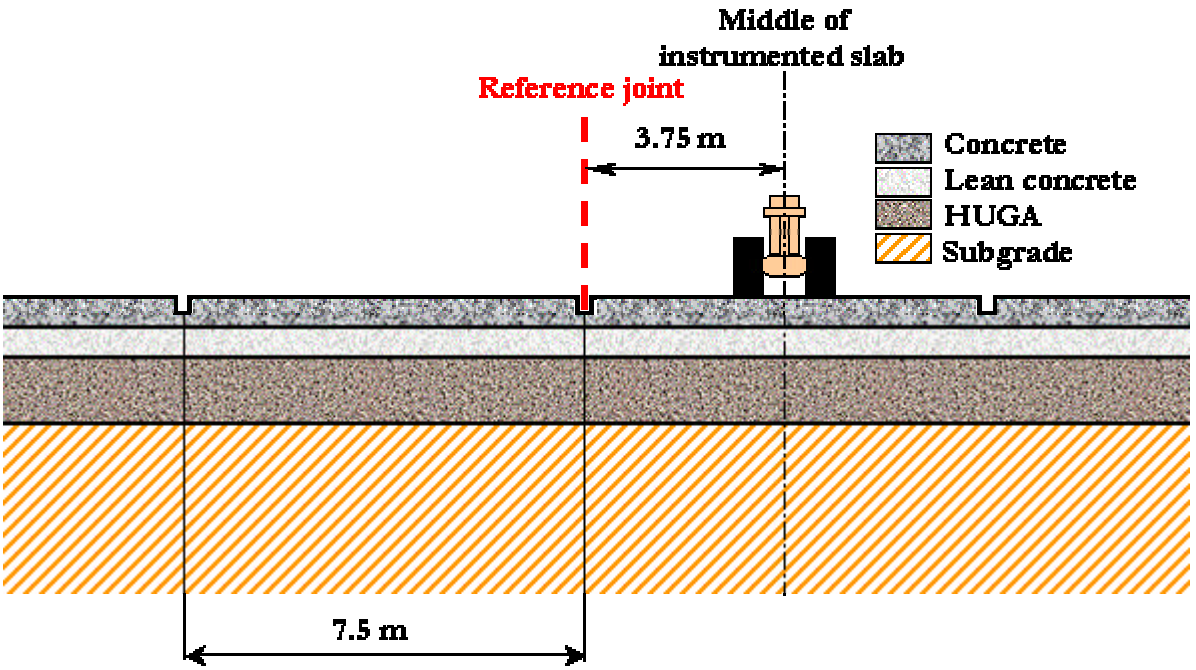

Figure III-25 : Trajectory T_6.

III.3 Typical configuration test sequence

Firstly, a reference load is used before all tested configuration. This permits to constitute a data base to evaluate thermal or structural effects with a well known procedure. This stage is very important: for further numerical modelling correlation.
The reference load is a two wheels bogie, without shock absorbers, loaded by 25 metric tons per wheel (internal pressure 1.29 MPa), with a 1400 mm track. It corresponds to configuration G1_2 hauled by the Service truck of STBA of the STBA.
Note that the use of the two wheels module with a different track or load during sub-configurations G1 does not allow to use the reference tandem for configurations G1_1, G1_3, G1_4 and G1_5.
Since configuration G2, and whatever trajectories or configurations used, the test procedure is the same, as to know:

- Overrun on T3 called "structure setting" in direction S1 (without acquisition),
- Return at 547 cm from free edge reference,
- Second overrun on T3 in direction S1 (without acquisition),
- Return at 547 cm from free edge reference,
- Overrun at T6 in direction S1.

The tests are then performed by the configuration (simulator or hauled 4 wheels module). At the end of the day, the reference module makes an overrun on T3 and on T6 and returns to 547 cm from free edge reference. These procedure is also used after each interruption of more than one hour (scheduled or unwanted interruptions). The subjacent aim is the pre-conditioning of the structure before loading with a more complex configuration.

III.4 Complementary tests

Several additional tests to improve the understanding of specific points are conducted at the end of the static campaign. Static results are analysed during the campaign and so a certain number of additional tests are conducted after the start of the fatigue campaign. These tests use the reference module and several modules extracted from the fatigue configuration. The aim of the tests is to complete the recorded data. The additional tests consist in:

- Evaluating the behaviour of a slab under a purely static load, including slab loading/unloading transition (the purely static acquisitions done during the campaign does not take this phenomenon into account),
- Acquiring measurements during a day with a very high thermal gradient variation by inserting a four wheels module and a six wheels module on trajectories T3 and T6.

Other very specific procedures are tested for different configurations. Further details will be developed in the results part.

IV. EXPERIMENTAL RESULTS

IV.1 Quasi-static campaign _ Main experimental results

As explained in the previous section, the runway hold 184 gauges and sensors located on 4 slabs. Up to 2550 acquisitions of the whole instruments have been done during the quasi-static campaign. The total volume of the collected data is nearing 24 Go. A specific software has been developed under OS-Solaris 6.2 (Unix system) in order to facilitate both storage and analysis of the measured signals. It allows:

- ✓ the automatic connexion with the temperature records (1 measure every 15 minutes since November 2001)
- ✓ an accelerated access to the signals and their automatic treatment, analysis and visualization, including statistical routines
- ✓ compatibility with Windows standards

IV.1.1 Thermal effects influencing measurements

On account of the importance of the temperature on slabs movements, gauges installed during the Airbus rigid PEP permit to monitor profile temperature in the pavement and so the strains induced. Experimental data are detailed in the present part.

IV.1.1.1 Unloaded slab

The aim of this part is to underline the temperature effect on rigid pavements. It is well known that concrete slabs behaviour is highly influenced by internal temperature field. This produces positive curvature, known as curling phenomenon or negative curvature, warping phenomenon. The monitoring of the instrumented slabs permit to show that temperature induces significant strain, even on an unloaded slab, as shown below. This is an important finding that could have serious implications in rigid pavement design.
The present results begin the 10th of July 2002, 13h00 and finish the 17th of July 2002, 8h09. An acquisition is realised every 5 minutes.
In order to illustrate these purposes, 4 gauges on slab 93 have been selected as shown Figure IV-1. The gauges 93-191 and 93-291 quantify longitudinal strain near the center of the slab, whereas gauges 93-192 and 93-292 quantify transversal ones. Remind that the gauges are 38 cm under the slab surface.

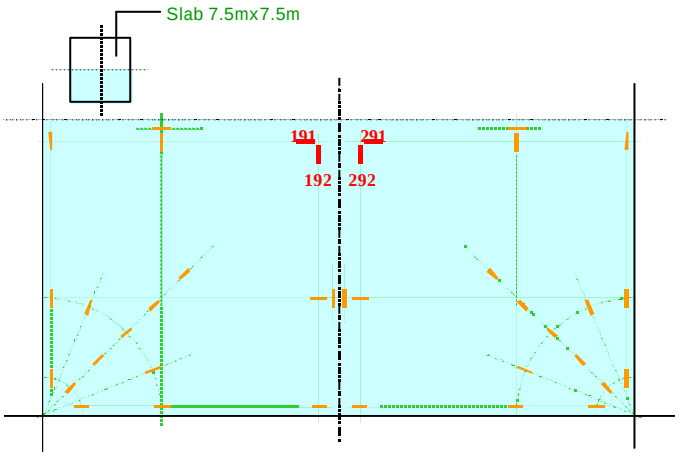

Figure IV-1 : Gauges 93-191, 93192, 93-291 & 93-292.

IV.1.1.1.1 Time evolution

This part present the evolution of the longitudinal and transversal strains during the acquisition. The only load effect on the slab 93 is the daily thermal variations during 6 days. The graphic shows the dependence of the slab deformations to these variations. The symmetric gauges follow the same trends. The strain band reach 40 µdef, which is comparable to a strain due to an aircraft.

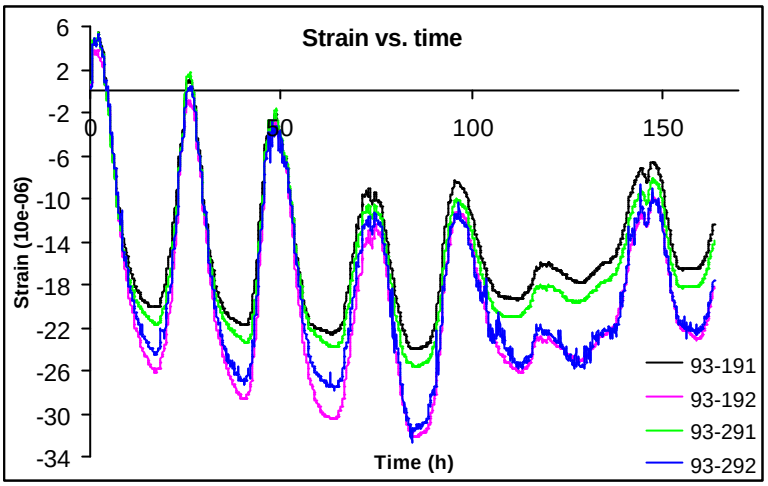

Figure IV-2 : Time evolution of strains.

IV.1.1.1.2 Characterization of a temperature profile

In order to characterize the behaviour of a concrete slab under thermal loading, we use two criteria. They permit to simply quantify the warping effect due to a temperature profile. It is important to underline that the temperature profile over the slab thickness determine the slab movements, and so can induce modifications of slabs supports conditions. Figure IV-3 illustrate a temperature profile over the slab thickness.

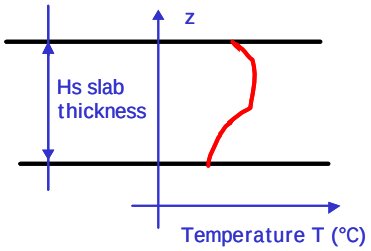

Figure IV-3 : Profile temperature over the slab thickness.

In the case of highly non-linear temperature distribution in the slab thickness, a bending moment and so self equilibrium stresses occur. Stresses level can be the same than the ones of an aircraft landing gear loading. So we define the mean temperature which represents a descriptive parameter. It is define as follows :

$$T_m = \frac{\int_{-Hs/2}^{Hs/2} T(z)dz}{Hs}$$

For a given temperature profile, we define the equivalent thermal gradient, which induces the same bending moment than the real profile. So we have :

$$GradTeq = \frac{12\int_{-Hs/2}^{Hs/2}(T(z)-T_m)}{Hs^3}$$

Note that only the strains are concerned by the equivalency, not the stresses.

IV.1.1.1.3 Relevance of mean temperature and equivalent thermal gradient

The problem is to know if the mean temperature and the equivalent thermal gradient allow a realistic description of the slab external environment. Here we show two tables concerning different cases with very near mean temperature and the equivalent thermal gradient. Note that the measured strains are of the same order, which permit to underline the perspicacity of the two previous criteria.

Table IV-1 : Thermal situations comparisons for positive GradTeq.

Tm = 5 to 6 °C GradTeq = 0.05 to 0.01 °C/cm

	Slab n°		93	93	93	45	45	68	68	108	108
	Gauge n°		162	262	113	162	113	162	113	162	113
Static test	23/01/2002	13H09	25	21	27	31	31	31	35	25	43
	23/01/2002	13H14	28	22	29	33	32	31	35	27	46
	23/01/2002	15H24	31	25	32	33	30	34	39	27	40
	24/01/2002	12H54	31	24	32	34	30	32	37	28	39
	24/01/2002	15H13	31	25	34	34	29	34	37	28	39
	29/01/2002	12H50	33	26	33	33	29	36	39	31	43
Fatigue test	23/01/2003	12H17	41	33		40	26	39			45
	03/02/2003	12H02	43	34		44	26	43			57

Table IV-2 : Thermal situations comparisons for negative GradTeq

Tm = 13 to 14 °C GradTeq = -0.15 to -0.1 °C/cm

	Slab n°		93	93	93	45	45	68	68	108	108
	Gauge n°		162	262	113	162	113	162	113	162	113
Static test	21/03/2002	07H31	29	34	31	46	16	45	31	45	45
	23/03/2002	09H16	28	32	30	45	13	43	30	44	44
	02/04/2002	07H35	26	29	28	45	12	43	26	44	47
Fatigue test	27/03/2003	04H31	34	39	0	37	23	45	0	0	65
	27/03/2003	04H38	35	41	0	37	24	45	0	0	69
	28/03/2003	06H40	36	45	0	37	28	43	0	0	86

IV.1.1.1.4 Strain vs. mean temperature

Let now show the variations of the longitudinal gauges 93-191 & 93-291 and transversal ones 93-192 & 93-292 according to the mean temperature defined as above.

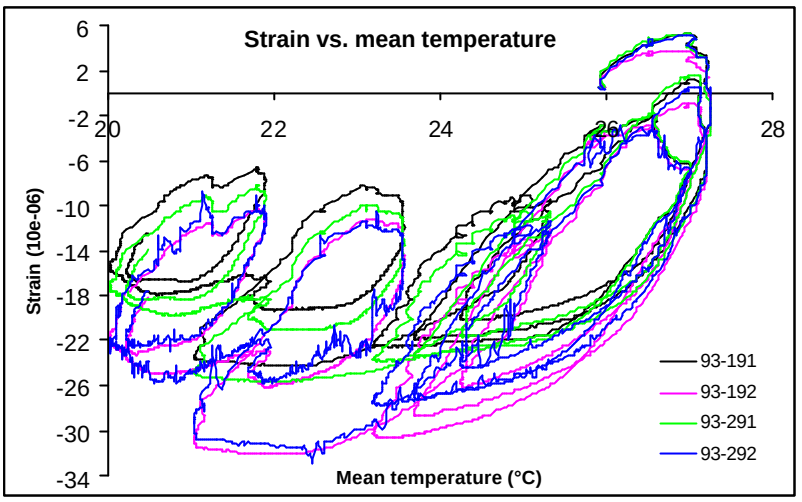

Figure IV-4 : Strains according to mean temperature.

We can note three curls due to mean temperature very disparate. The curves present an important hysteresis which underline a different behaviour during ascending and descending temperature. This phenomenon can be attribute to 2 principle factors, the material calorific capacity and the possibility for a same mean temperature to correspond to different temperature profile across the pavement. So this criteria is not enough to characterize a thermal situation.

IV.1.1.1.5 Strain vs. equivalent thermal gradient

The Figure IV-5 shows the longitudinal and transversal center strains of slab 93 according to the equivalent thermal gradient. The hysteresis phenomenon looks better during the ascending and descending gradient phases. The equivalent gradient criteria seems to be a sensitive criteria to describe temperature variation over the slab thickness.

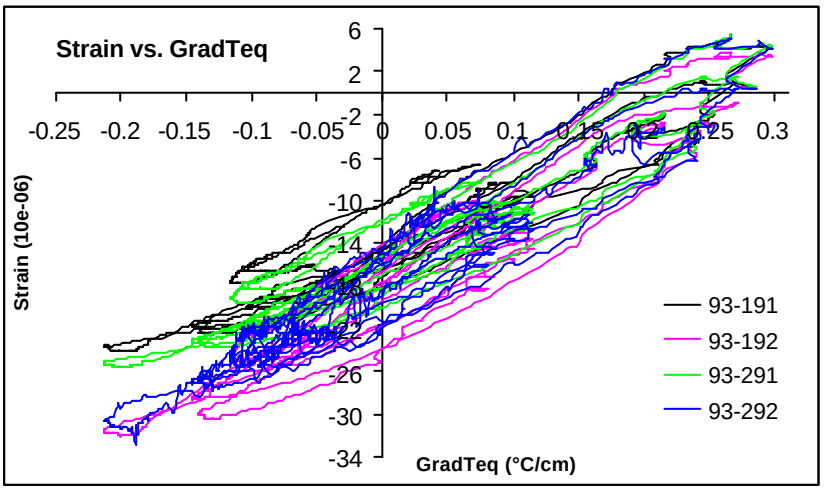

Figure IV-5 : Strains according to equivalent thermal gradient.

IV.1.1.2 Loaded slab

The presented results show the evolution of longitudinal and transversal strains (gauges 93-191, 93-192, 93-291 & 93-292) in a concrete slab with both loading of temperature and configuration G1-2. The presented results begin the 15th of March 2002, 9h10 and finish the 18th of March

2002, 7h20. An acquisition is realised every 4 minutes. The load is placed in the middle of the slab 93 the 15th of March 2002, 10h15, as shown Figure IV-6. Then we follow the evolution of the strains due to the thermal environment with a pre-stressed static load.

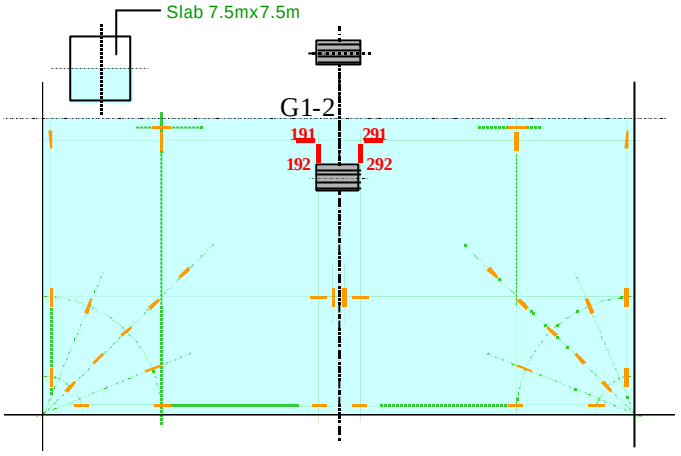

Figure IV-6 : Gauges 93-191, 93192, 93-291, 93-292 & module G1-2.

IV.1.1.2.1 Time evolution

As previously, we expose the time variations of the strains due to the thermal conditions and the static load G1-2. The instant we placed the module G1-2 in the middle of slab 93 is represented by the red dotted circle. The application of G1-2 increase the longitudinal strain of 8 µ-strains and the transversal one of 6 µ-strains. Thereafter, and because of the thermal conditions, the longitudinal strain reach –20 µ-strains and the transversal 26.8. We could see a good correlation between two symmetric gauges. The strains variations after the placing of G1-2 are due to thermal variations, and so underline the thermal effects on a concrete slab.

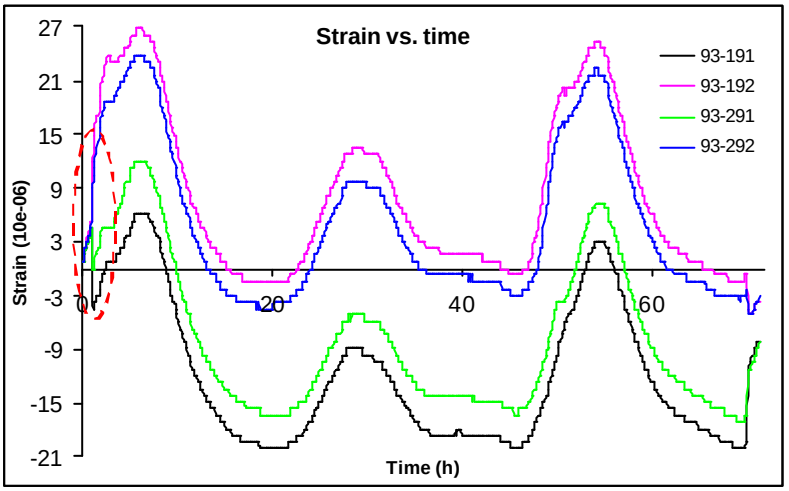

Figure IV-7 : Time evolution of strains with G1-2.

IV.1.1.2.2 Strain vs. mean temperature

Here we find a large hysteresis. Two symmetric gauges follow the same tendency.

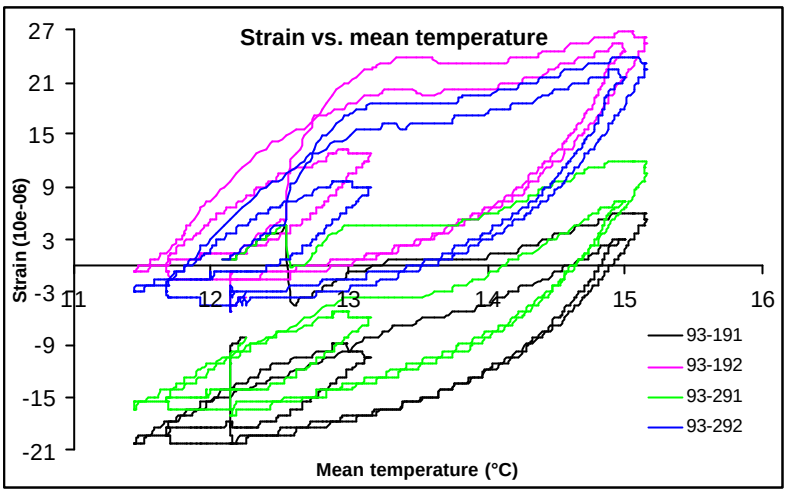

Figure IV-8 : Strains according to mean temperature with G1-2.

IV.1.1.2.3 Strain vs. equivalent thermal gradient

As the equivalent thermal gradient seems to be the best criteria to describe the slab movements due to thermal effects, let's see the Figure IV-9.

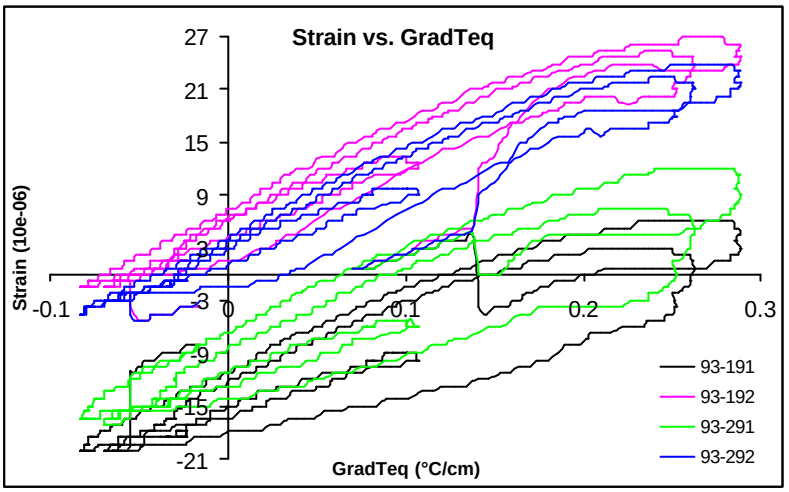

Figure IV-9 : Strains according to equivalent thermal gradient with G1-2.

These results underline the effects of thermal conditions on the concrete pavement. The strains vary with an amplitude of 30 to 40 µ-strains for the presented conditions. So we could think that this phenomenon could be majored for other periods. This permit to conclude that the cumulative effects of both temperature and wheels loading could be very damageable for the pavement.

IV.1.22 wheels configurations

The 2 wheels configurations include the configurations G1-1 to G1-5. The parameters are the load and the track (cf. Table III-1).

The following tables present characteristics results obtained on the four instrumented slabs for the previous configurations.

IV.1.2.1 Example of a 2 wheels bogie characteristic signals

The following figures illustrate the set of signals obtained for all gauges monitoring slab 45. The configuration used is the reference one G1-2, 2 wheels tracked by the STBA truck, trajectory T6, direction S2, as shown in the following scheme. The loading is 25 tons per wheel.

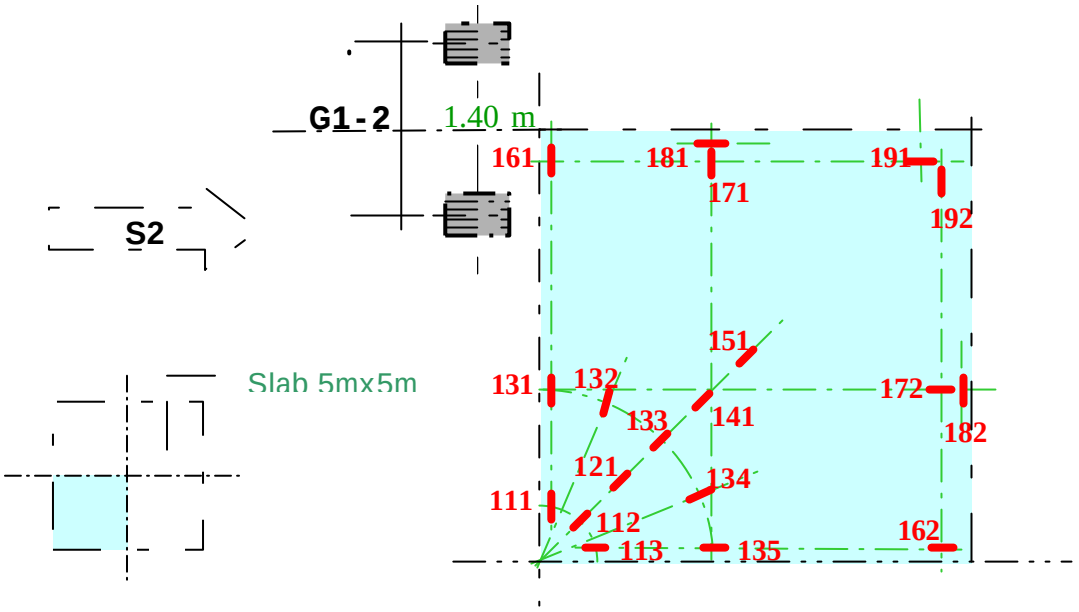

Figure IV-10 : Simulation vehicle _ config. G1-2 2 wheels / Gauges on slab 45 / Trajectory T6.

The presented signals have been obtained the 11th of February 2002, 14h32, in the following conditions :

- ✓ Medium temperature : 10.04 °C
- ✓ Equivalent gradient in the slab : 0.193 °C/cm

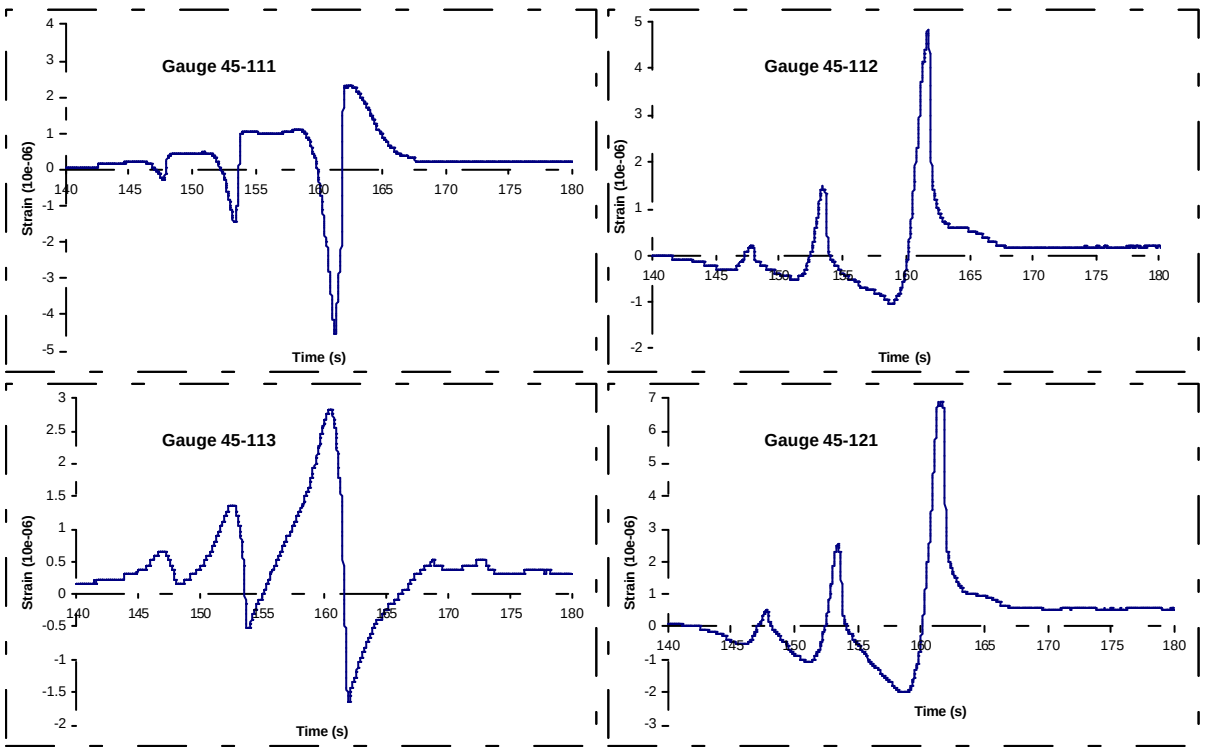

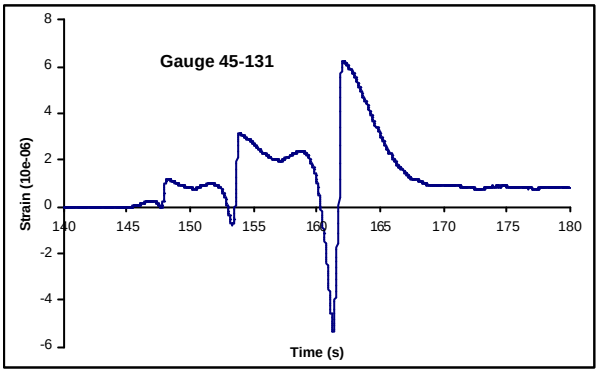
Gauge 45-131
Strain (10e-06)
Time (s)

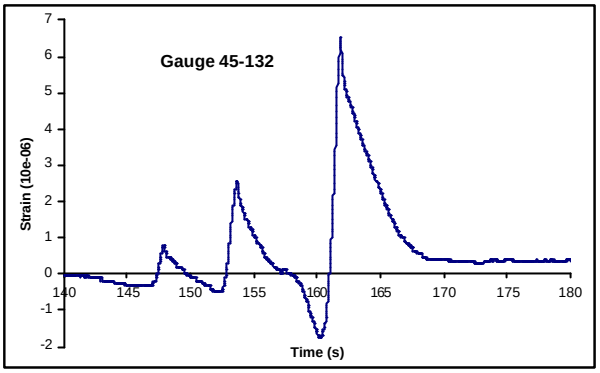
Gauge 45-132
Strain (10e-06)
Time (s)

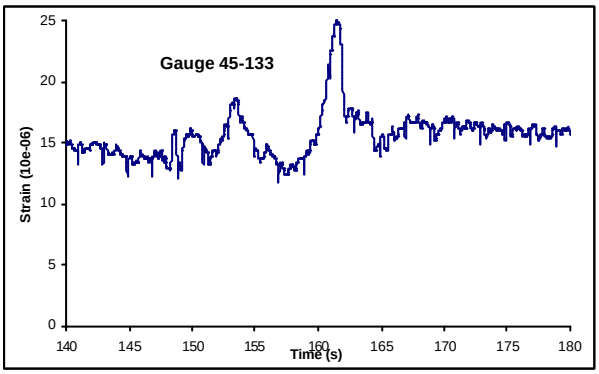
Gauge 45-133
Strain (10e-06)
Time (s)

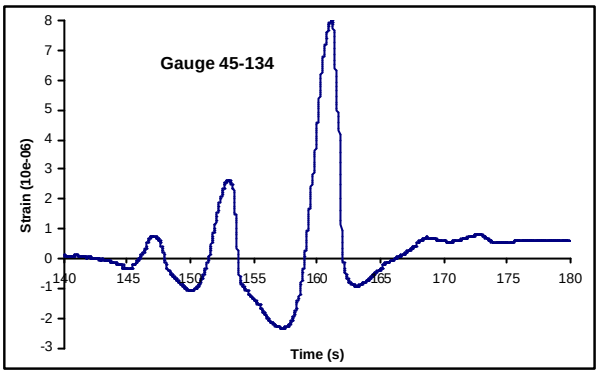
Gauge 45-134
Strain (10e-06)
Time (s)

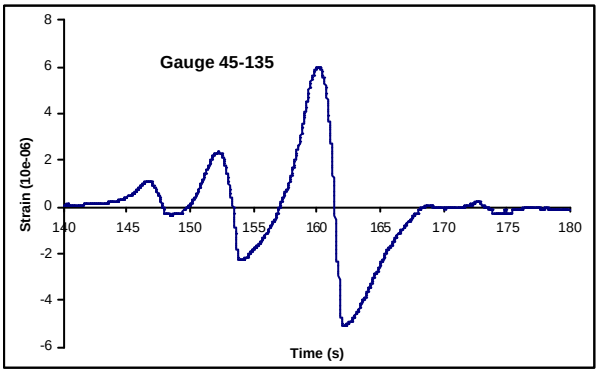
Gauge 45-135
Strain (10e-06)
Time (s)

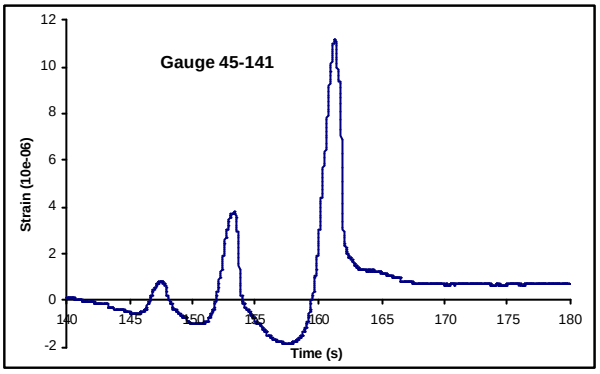
Gauge 45-141
Strain (10e-06)
Time (s)

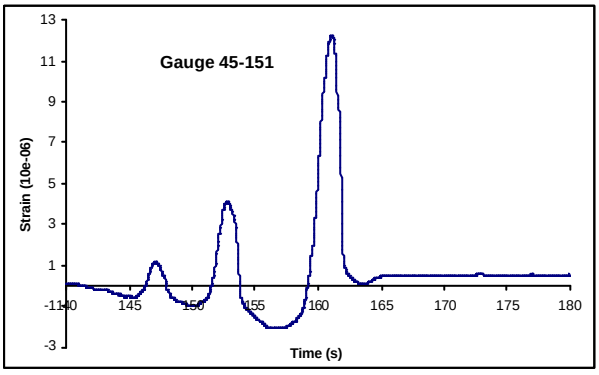
Gauge 45-151
Strain (10e-06)
Time (s)

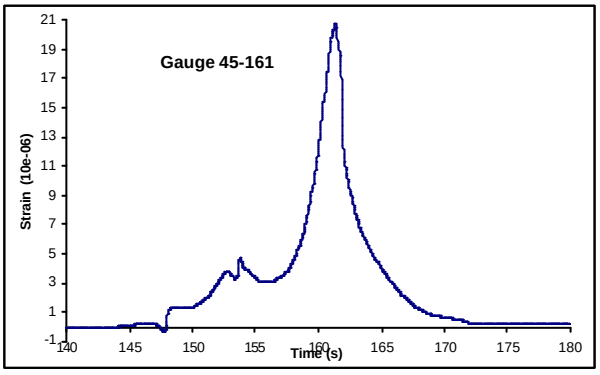
Gauge 45-161
Strain (10e-06)
Time (s)

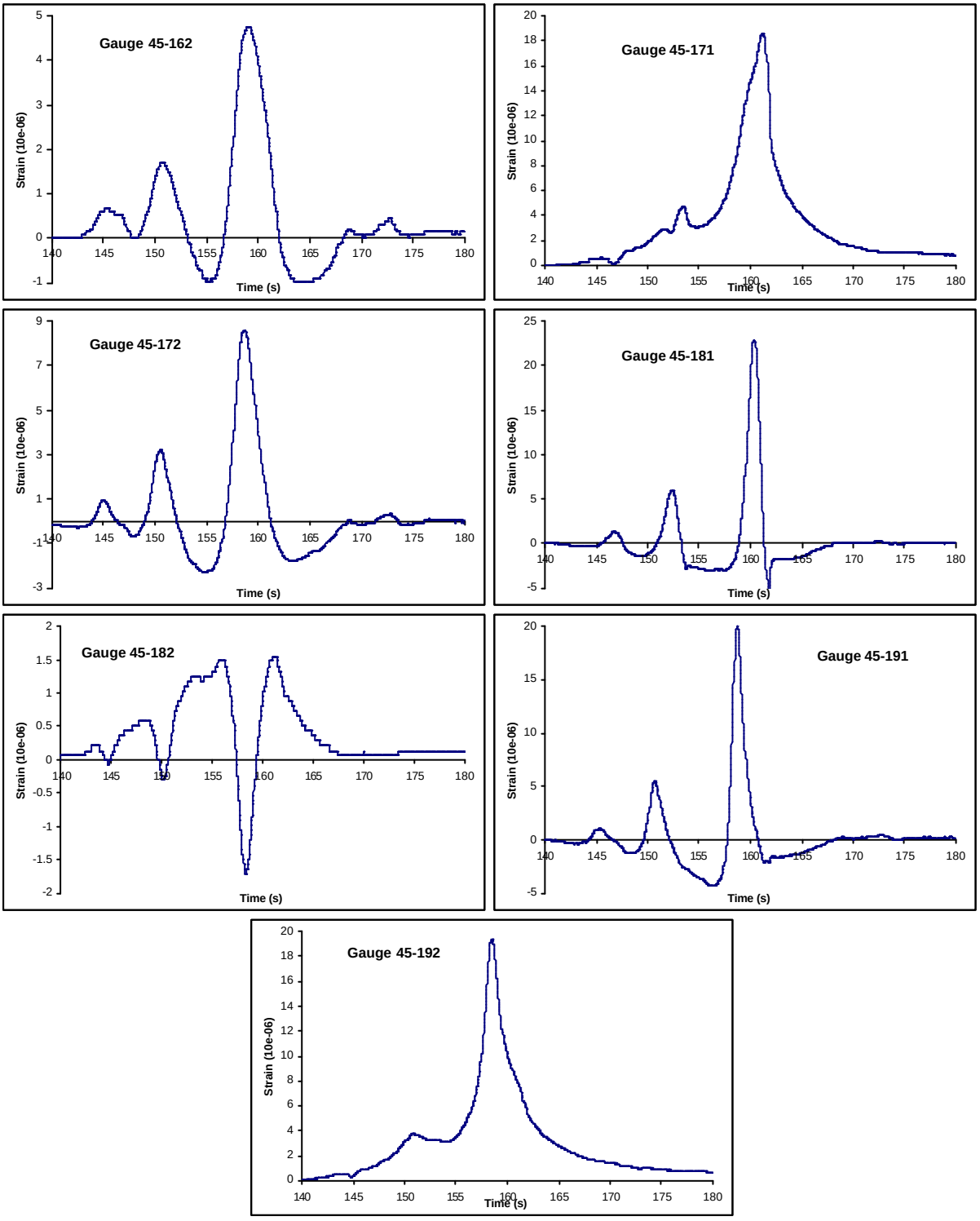

Figure IV-11 : Gauges signals on slab 45 _ config. G1-2 T6.

The maximum strain is reached gauge 181, in the middle of the quarter of the slab, with a value of 22.9 µ-strains for this run. Note that the passage of the truck pulling the load is visible on the signals. The Figure IV-2 shows the distribution of strain value obtained for the gauge 45-181 according respectively to the medium temperature level and the equivalent temperature gradient in the slab 45.

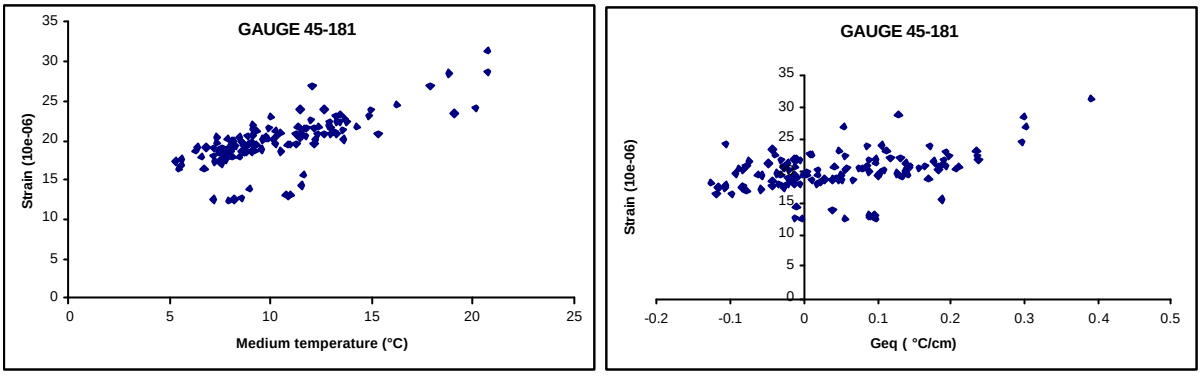

Figure IV-12 : Values distribution of gauge 45-181_config. G1-2 T6.

IV.1.2.2 Principles results

This part concerns the main results obtain for the 2 wheels configurations on the four instrumented slabs. The following tables gather the maximum strain measured on a slab for a given configuration. Note that we precise the number of the gauge which permit to know where the maximum strain is localized. The thermal condition are therefore precise so as to relativize certain results, as evocated previously.

IV.1.2.2.1 Slab 45

Table IV-3 : Configuration G1 – slab 45.

	slab 45 (th=37cm, soil 2, no dowels, 5mx5m)			
	εmax	gauge	qm °C	Geq °C/cm
G1-1	w. track = 1.40 m, 20 tons/wheel			
	43	135	-1.0	-0.10
G1-2	w. track = 1.40 m, 25 tons/wheel			
	47	135	2.5	-0.11
G1-3	w. track = 1.40 m, 30 tons/wheel			
	54	135	3.9	0.0
G1-4	w. track = 1.30 m, 25 tons/wheel			
	46	135	6.7	-0.02
G1-5	2 wheels, w. track = 1.50 m, 25 tons/wheel			
	45	135	2.4	-0.15

IV.1.2.2.2 Slab 68

Table IV-4 : Configuration G1 – slab 68.

	slab 68 (th=37cm, soil 2, not dowelled)			
	εmax	gauge	qm °C	Geq °C/cm
G1-1	w. track = 1.40 m, 20 tons/wheel			
	22	135	-1.0	-0.10
G1-2	w. track = 1.40 m, 25 tons/wheel			
	37	113	5.2	0.11
G1-3	w. track = 1.40 m, 30 tons/wheel			
	45	135 & 162	3.9	0.00
G1-4	w. track = 1.30 m, 25 tons/wheel			
	42	113	6.7	-0.02
G1-5	2 wheels, w. track = 1.50 m, 25 tons/wheel			
	37	113	/	/

IV.1.2.2.3 Slab 93

Table IV-5 : Configuration G1 – slab 93.

	slab 93 (th=42cm, soil 1, not dowelled)			
	εmax	gauge	qm °C	Geq °C/cm
G1-1	w. track = 1.40 m, 20 tons/wheel			
	23	161	-0.9	-0.08
G1-2	w. track = 1.40 m, 25 tons/wheel			
	34	135	4.4	-0.05
G1-3	w. track = 1.40 m, 30 tons/wheel			
	39	135	3.9	0.00
G1-4	w. track = 1.30 m, 25 tons/wheel			
	36	135	7.5	0.09
G1-5	w. track = 1.50 m, 25 tons/wheel			
	34	135	2.4	0.15

IV.1.2.2.4 Slab 108

Table IV-6 : Configuration G1 – slab 108.

	slab 108 (th=31cm, soil 1, dowelled)			
	εmax	gauge	qm °C	Geq °C/cm
G1-1	w. track = 1.40 m, 20 tons/wheel			
	32	113	-1.0	-0.10
G1-2	w. track = 1.40 m, 25 tons/wheel			
	48	113	2.5	-0.12
G1-3	w. track = 1.40 m, 30 tons/wheel			
	58	111	3.6	-0.04
G1-4	w. track = 1.30 m, 25 tons/wheel			
	50	135	6.7	-0.01
G1-5	2 wheels, w. track = 1.50 m, 25 tons/wheel			
	54	135	2.4	-0.15

IV.1.2.3 Conclusions

The aim of the G1 configuration was to evaluate the variations effects of load and track. The previous results permit to conclude that, logically, when the load increase, the strain increase too. Concerning the track effects, the configurations G1-2, G1-4 and G1-5 are compared. It shows that G1-2 and G1-4 give similar results whereas G1-5, with a greater track, raise the longitudinal strain of about 10%. Note that the results for G1-2 and G1-5 have been obtained for quite the same mean temperature and thermal equivalent gradient. So as a conclusion, we can say that the track have an impact on pavement that can not be neglected.

IV.1.34 wheels and 6 wheels bogies

The 4 wheels and 6 wheels bogies configurations concern the configurations G2-1 to G2-5. The present part exhibits the main results obtained for the different configurations on the four instrumented slabs. The first paragraph is devoted to a non-exhaustive presentation of characteristics signals obtained during a test run, the following items concern recapitulative tables of the maximum strain measured for a slab during the tests sequences.

IV.1.3.1 Example of a 4 wheels bogie characteristic signals

4 wheels bogie illustrate the set of signals obtained for all gauges monitoring slab 68. The configuration used is the G2-3 4 wheels, trajectory T3, direction S1, as shown in the following scheme. The loading is 30 tons per wheel.

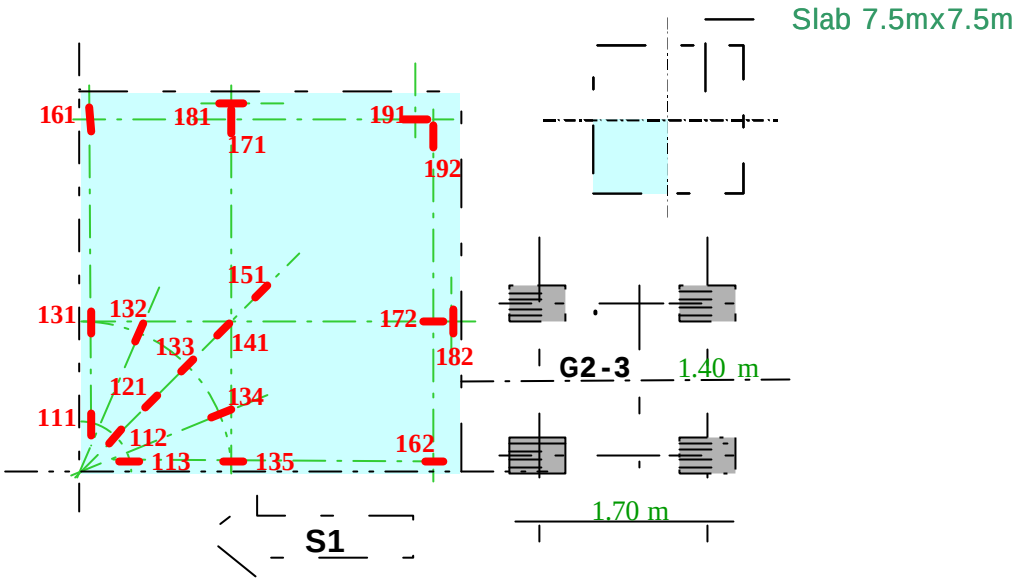

Figure IV-13 : Simulation vehicle _ config. G2-3 4 wheels / Gauges on slab 68 / Trajectory T3.

The presented signals have been obtained the 12th of February 2002, 8h36, in the following conditions :

- ✓ Medium temperature : 7.29 °C
- ✓ Equivalent gradient in the slab : -0.097 °C/cm

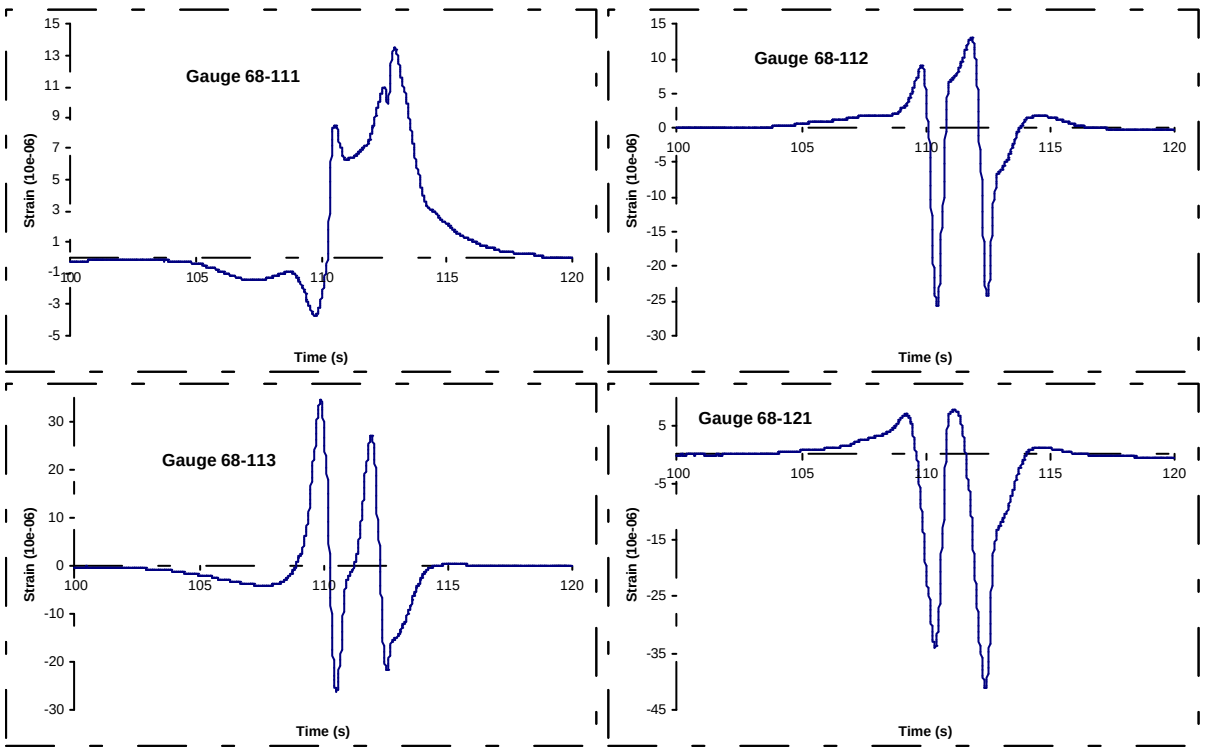

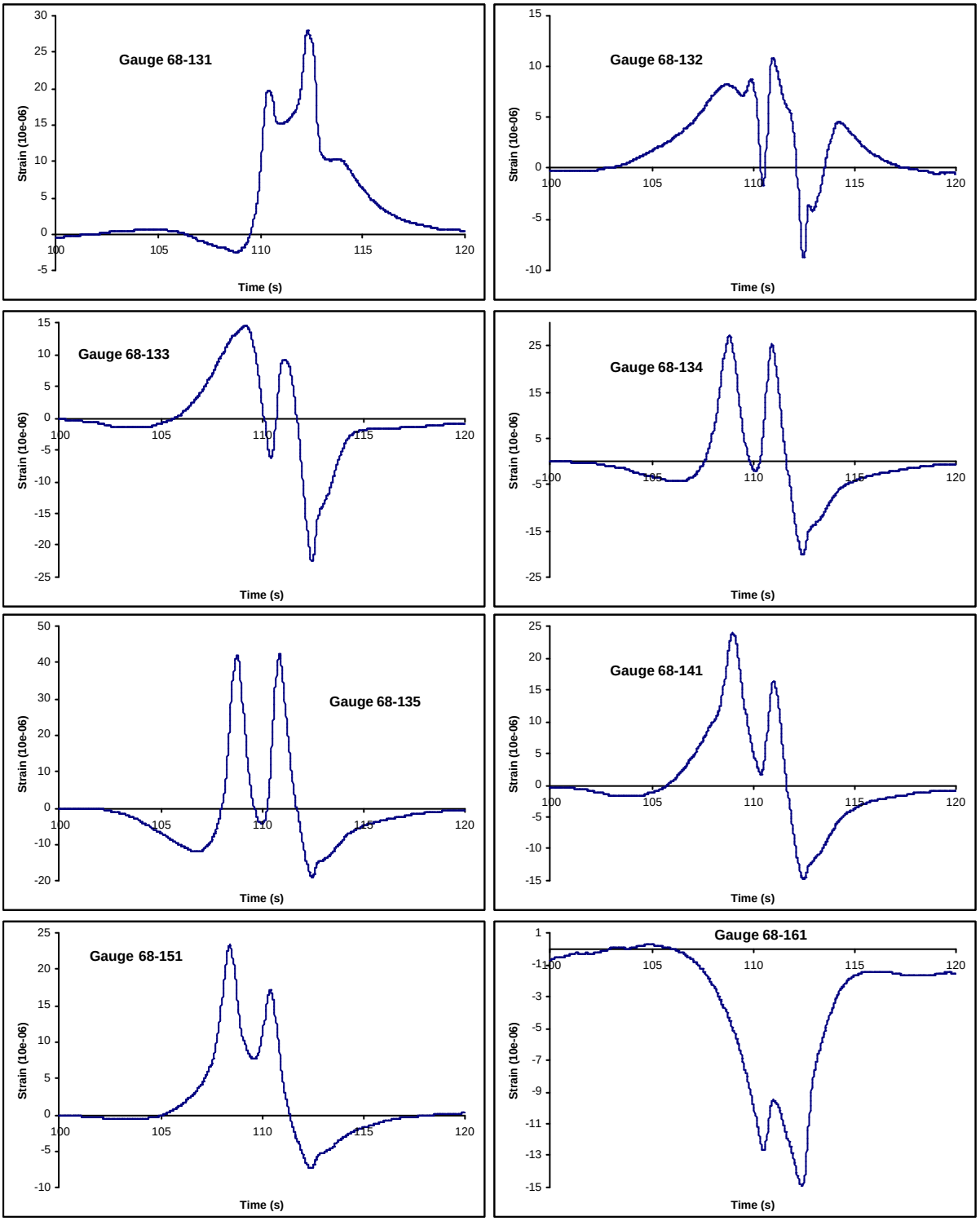
Gauge 68-131
Strain (10e-06)
Time (s)
Gauge 68-132
Strain (10e-06)
Time (s)
Gauge 68-133
Strain (10e-06)
Time (s)
Gauge 68-134
Strain (10e-06)
Time (s)
Gauge 68-135
Strain (10e-06)
Time (s)
Gauge 68-141
Strain (10e-06)
Time (s)
Gauge 68-151
Strain (10e-06)
Time (s)
Gauge 68-161
Strain (10e-06)
Time (s)

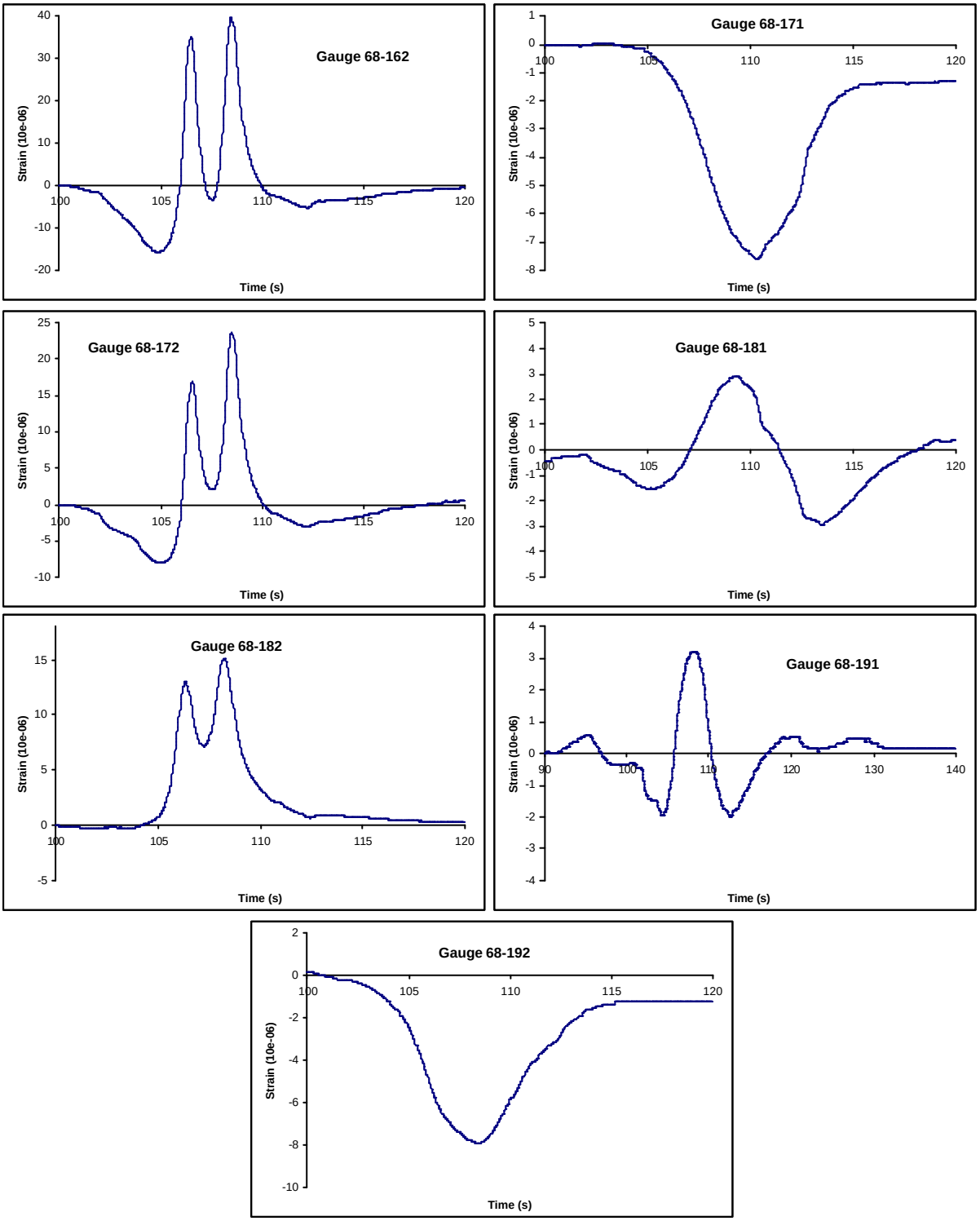

Figure IV-14 : Gauges signals on slab 68 _ config. G2-3 4 wheels.

The maximum strain is reached gauge 135, in the middle of the quarter of the slab, with a value of 42.4 µ-strains for this run. The longitudinal signals strains (gauges 113, 135, 162) show two peaks, characteristic of a 4 wheels bogie.

IV.1.3.2 Example of a 6 wheels bogie characteristic signals

Let show the set of signals obtained for all gauges monitoring slab 108. The configuration used is the G2-3 6 wheels, trajectory T1, direction S1, as shown in the following scheme. The loading is 30 tons per wheel.

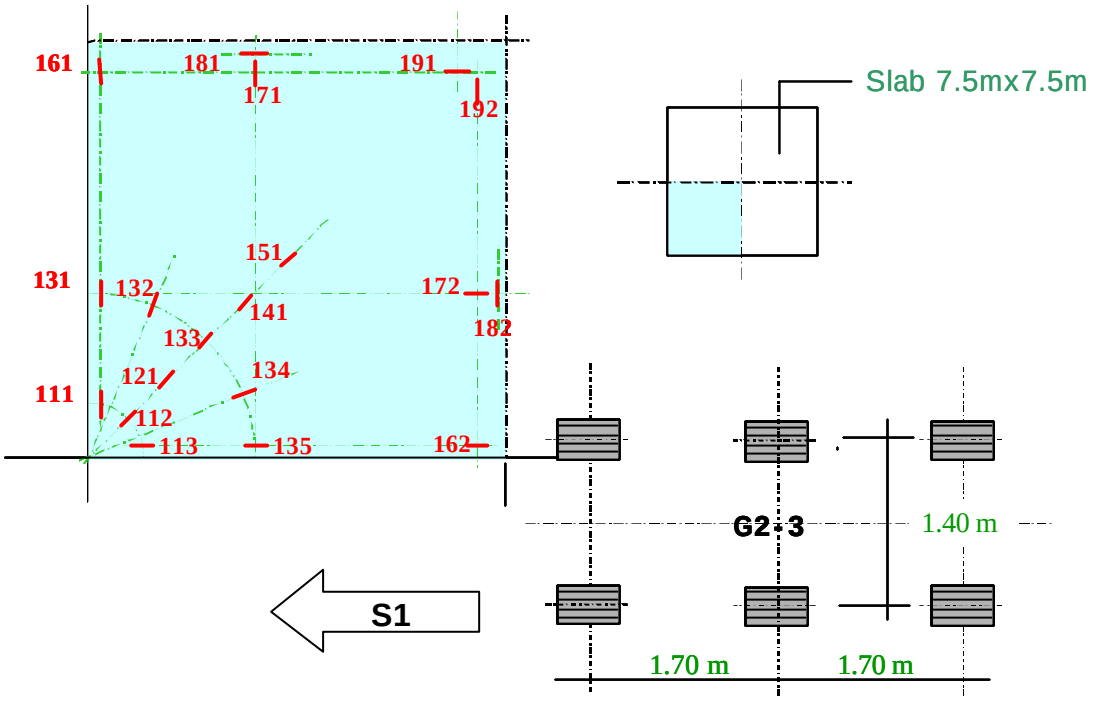

Figure IV-15 : Simulation vehicle _ config. G2-3 6 wheels / Gauges on slab 108 / Trajectory T1.

The presented signals have been obtained the 12th of February 2002, 15h32, in the following conditions :

- ✓ Medium temperature : 10.1 °C
- ✓ Equivalent gradient in the slab : 0.19 °C/cm

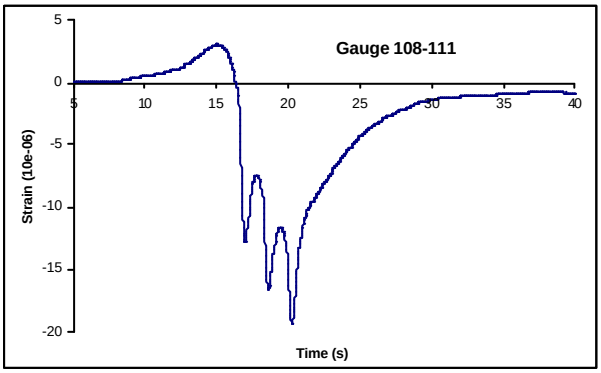

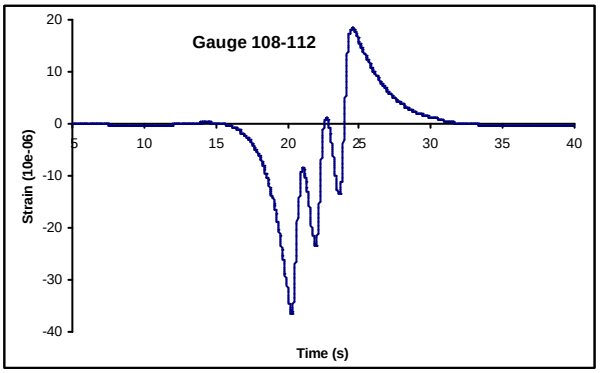

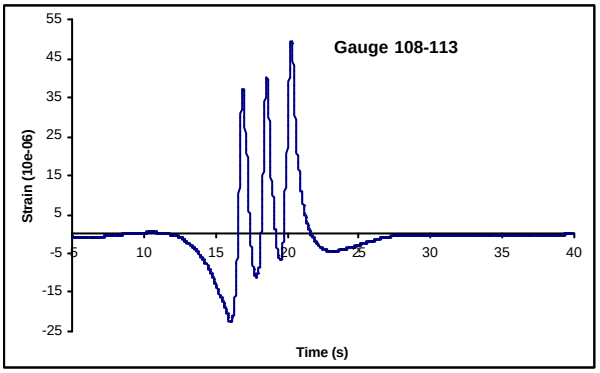
Gauge 108-113
Strain (10e-06)
Time (s)

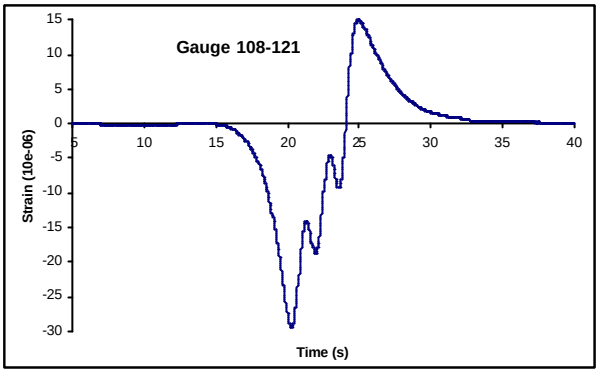
Gauge 108-121
Strain (10e-06)
Time (s)

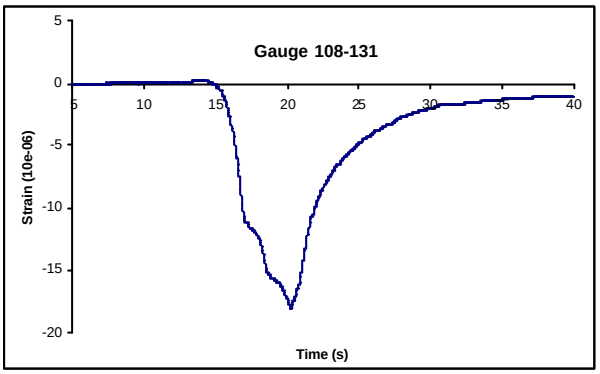
Gauge 108-131
Strain (10e-06)
Time (s)

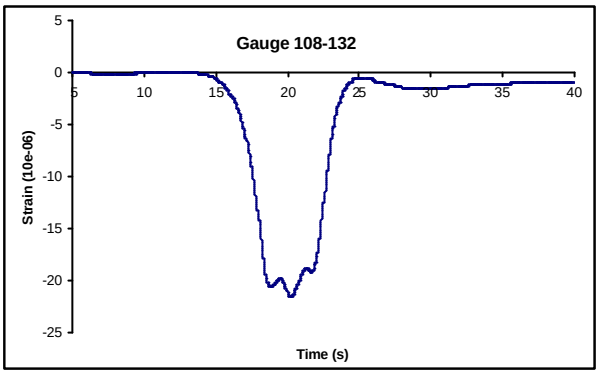
Gauge 108-132
Strain (10e-06)
Time (s)

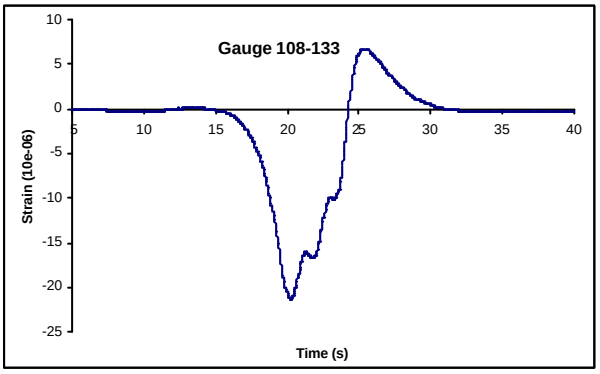
Gauge 108-133
Strain (10e-06)
Time (s)

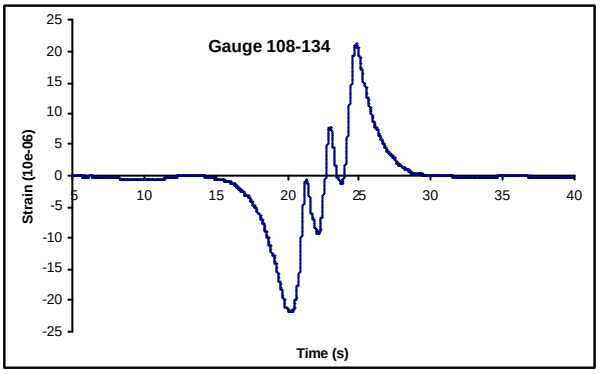
Gauge 108-134
Strain (10e-06)
Time (s)

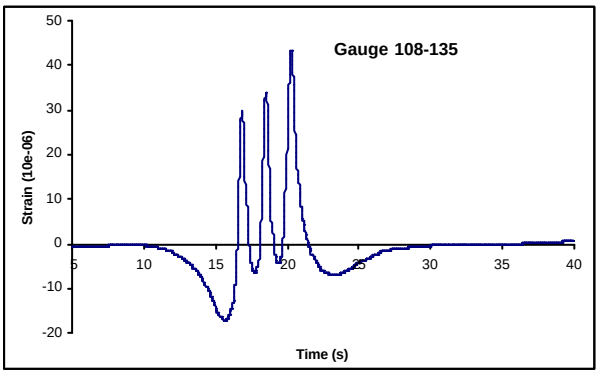
Gauge 108-135
Strain (10e-06)
Time (s)

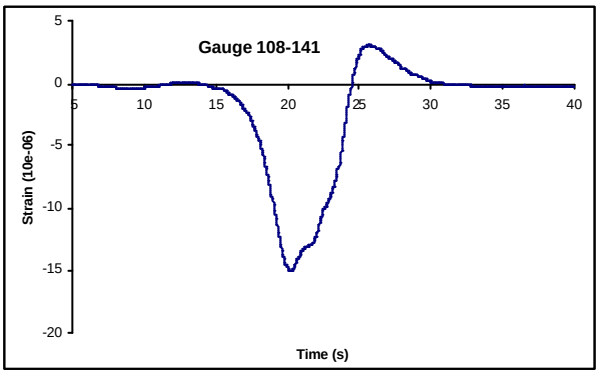
Gauge 108-141
Strain (10e-06)
Time (s)

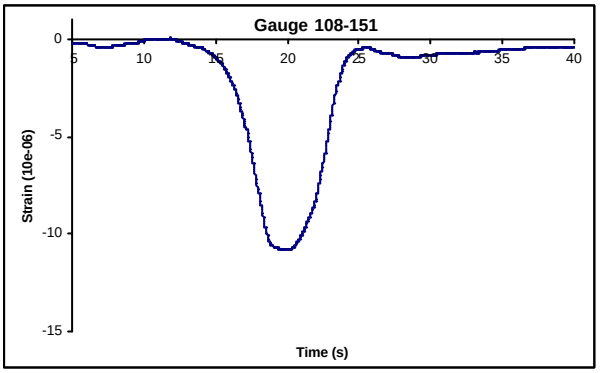
Gauge 108-151
Strain (10e-06)
Time (s)

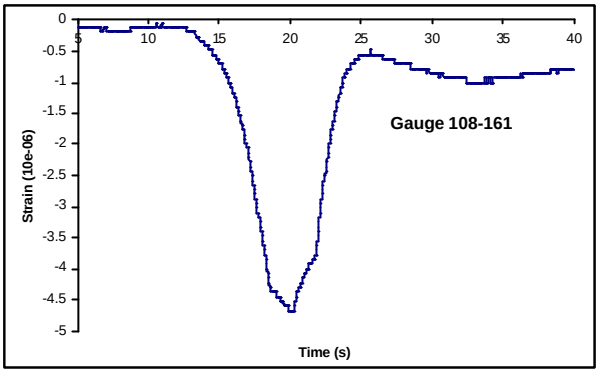
Gauge 108-161
Strain (10e-06)
Time (s)

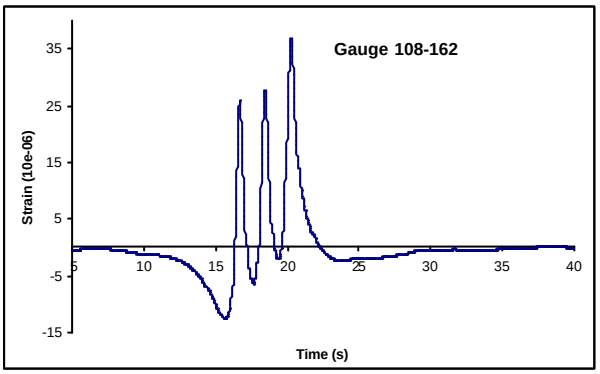
Gauge 108-162
Strain (10e-06)
Time (s)

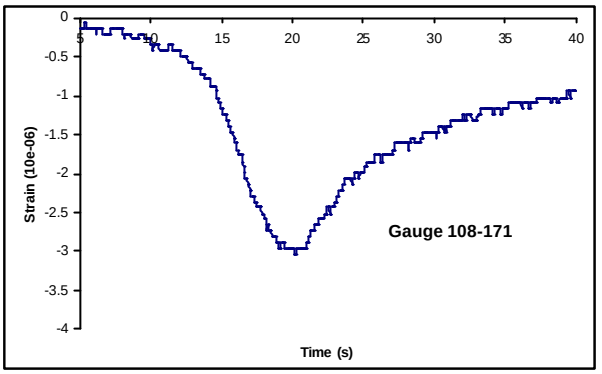
Gauge 108-171
Strain (10e-06)
Time (s)

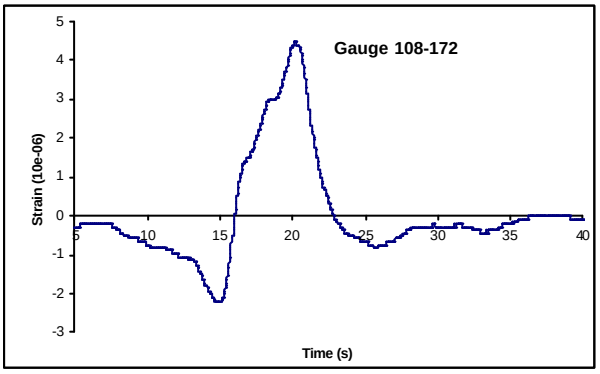
Gauge 108-172
Strain (10e-06)
Time (s)

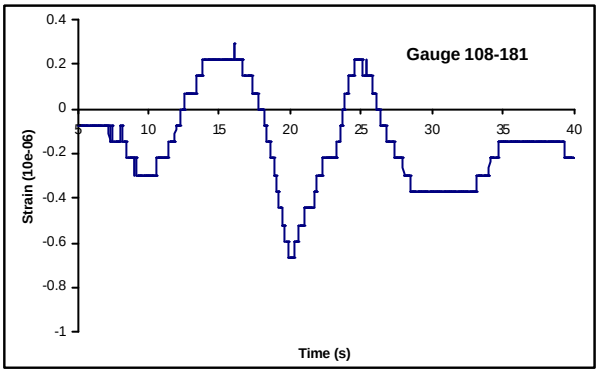
Gauge 108-181
Strain (10e-06)
Time (s)

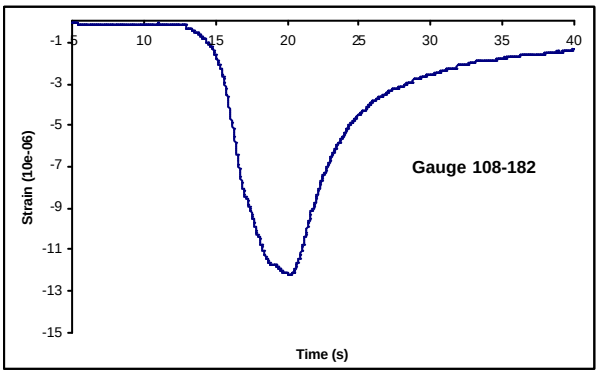
Gauge 108-182
Strain (10e-06)
Time (s)

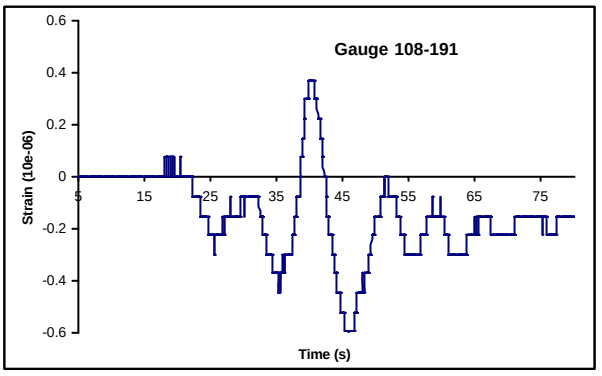
Gauge 108-191
Strain (10e-06)
Time (s)

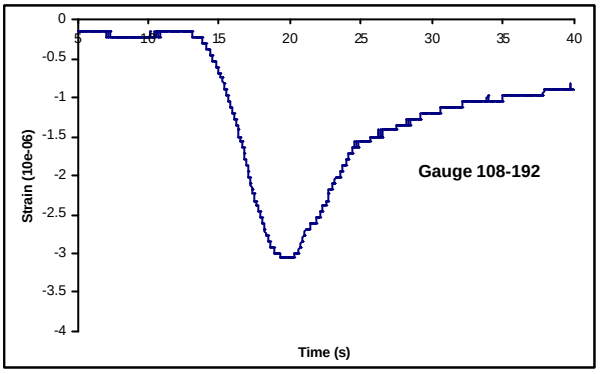

Figure IV-16 : Gauges signals on slab 108 _ config. G2-3 6 wheels.

The maximum strain is reached gauge 113, near the corner, with a value of 49.3 µ-strains for this run. The longitudinal signals strains (gauges 113, 135, 162) show three peaks, characteristic of a 6 wheels bogie.

IV.1.3.3 Main results

This part concerns the main results obtained for the G2 configurations, comprising a 4 wheels bogie and a 6 wheels bogie, running on the 4 instrumented slabs. The variables are here the load and the base. The following tables gather the maximum strain measured on a slab for a given configuration. We precise the number of the gauge which permit to know where the maximum strain is localized. The thermal conditions are therefore specified.

IV.1.3.3.1 Slab 45

Table IV-7 : Configuration G2 – slab 45.

		slab 45 (th=37cm, soil 2, no dowels, 5mx5m)			
		εmax	gauge	qm °C	Geq °C/cm
G2-1	**track = 1.40m, base = 1.70m, 20 tons/wheel**				
	4 wheels	35	135	7.1	0.06
	6 wheels	36	131	8.7	0.19
G2-2	**track = 1.40m, base = 1.70m, 25 tons/wheel**				
	4 wheels	46	131	9.1	0.04
	6 wheels	48	131	8.3	0.08
G2-3	**track = 1.40m, base = 1.70m, 30 tons/wheel**				
	4 wheels	57	131	9.6	0.17
	6 wheels	58	131	9.7	0.20
G2-4	**track = 1.40m, base = 1.60m, 25 tons/wheel**				
	4 wheels	46	131	6.1	0.03
	6 wheels	50	131	8	0.04
G2-5	**track = 1.40m, base = 1.80m, 25 tons/wheel**				
	4 wheels	50	131	10.1	0.09
	6 wheels	/	/	/	/

IV.1.3.3.2 Slab 68

Table IV-8 : Configuration G2 – slab 68.

		slab 68 (th=37cm, soil 2, no dowels)			
		εmax	gauge	qm °C	Geq °C/cm
G2-1	**track = 1.40m, base = 1.70m, 20 tons/wheel**				
	4 wheels	32	135	5.6	-0.07
	6 wheels	29	162	5.3	-0.08
G2-2	**track = 1.40m, base = 1.70m, 25 tons/wheel**				
	4 wheels	-39	112	7.9	0.02
	6 wheels	-37	112	9.2	0.04
G2-3	**track = 1.40m, base = 1.70m, 30 tons/wheel**				
	4 wheels	-60	121	7.9	-0.05
	6 wheels	52	161	7.8	-0.02
G2-4	**track = 1.40m, base = 1.60m, 25 tons/wheel**				
	4 wheels	-47	112	5.7	-0.03
	6 wheels	43	161	7.9	0.04
G2-5	**track = 1.40m, base = 1.80m, 25 tons/wheel**				
	4 wheels	-42	112	9.2	0.02
	6 wheels	33	135	10.9	0.09

IV.1.3.3.3 Slab 93

Table IV-9 : Configuration G2 – slab 93.

		slab 93 (th=42cm, soil 1, not dowelled)			
		εmax	gauge	qm °C	Geq °C/cm
G2-1	**track = 1.40m, base = 1.70m, 20 tons/wheel**				
	4 wheels	32	135	6.4	0.03
	6 wheels	31	161	7.5	0.123
G2-2	**track = 1.40m, base = 1.70m, 25 tons/wheel**				
	4 wheels	32	135	7.1	-0.12
	6 wheels	42	161	8.2	0.08
G2-3	**track = 1.40m, base = 1.70m, 30 tons/wheel**				
	4 wheels	-43	212	7.8	-0.06
	6 wheels	59	161	7.9	-0.01
G2-4	**track = 1.40m, base = 1.60m, 25 tons/wheel**				
	4 wheels	44	161	6.0	0.00
	6 wheels	48	161	7.9	0.04
G2-5	**track = 1.40m, base = 1.80m, 25 tons/wheel**				
	4 wheels	44	161	8.2	0.02
	6 wheels	38	131	11.7	0.17

IV.1.3.3.4 Slab 108

Table IV-10 : Configuration G2 – slab 108.

		slab 108 (th=31cm, soil 1, dowelled)			
		εmax	gauge	qm °C	Geq °C/cm
G2-1	**track = 1.40m, base = 1.70m, 20 tons/wheel**				
	4 wheels	48	135	5.7	-0.06
	6 wheels	43	135	5.3	-0.08
G2-2	**track = 1.40m, base = 1.70m, 25 tons/wheel**				
	4 wheels	63	111	7.1	-0.12
	6 wheels	60	111	9.3	0.03
G2-3	**track = 1.40m, base = 1.70m, 30 tons/wheel**				
	4 wheels	84	111	7.4	-0.08
	6 wheels	67	111	9.7	0.20
G2-4	**track = 1.40m, base = 1.60m, 25 tons/wheel**				
	4 wheels	64	111	6.1	0.03
	6 wheels	58	111	8.0	0.15
G2-5	**track = 1.40m, base = 1.80m, 25 tons/wheel**				
	4 wheels	56	111	10.1	0.09
	6 wheels	48	131	11.8	0.18

IV.1.3.4 Conclusions

The previous results show that logically, comparing the configuration G2-1, G2-2 and G2-3, the strains increase with the applied load. The maximum strains are mainly obtained on gauges 135 and 161, that means longitudinal strains along the longitudinal joint of the slab. The results concerning the slab 68 are difficult to interpret because a singular behaviour near the corner (gauges 112 & 121). The base effect isn't underline on slab 45, in particular by taking into account the thermal effects that modified significantly the strains. The slab 108 shows maximum strain level obtained transversally (gauge 111), that forbidden to see any base effect. Generally, the base effect is more sensitive on 6 wheels bogie, a longer base inducing lower longitudinal strains.

IV.1.4Aircraft configurations

The 4 wheels and 6 wheels bogies configurations concern the configurations G5 to G10.
The following paragraphs present characteristics results obtained on the four instrumented slabs for the previous configurations. First let show characteristic signals obtained for the two real aircraft configuration tested, it means the A380-800F and the B747-400. Then tables resume, for each slab, the maximum strain measured for a configuration on a trajectory.

IV.1.4.1 Example of an A380-800F characteristic signals

Let show the set of signals obtained for all gauges monitoring slab 93 (2 quarters instrumented). The configuration used is the G6 composed of a 4 wheels bogie for the wing landing gear (WLG) and a 6 wheels for the body landing gear (BLG), trajectory T3, direction S1, as shown in the following scheme. The loading is 28.5 tons per wheel. The passages are decomposed for having a gear (BLG or WLG) running on trajectory T3. Let show the signals.

IV.1.4.1.1 A380-800F BLG signals

The configuration used is G6, corresponding to the A380-800F. The signals presented correspond to the 4 wheels BLG running on T3 trajectory, direction S2, as shown in the following scheme. The loading is 28.5 tons per wheel.

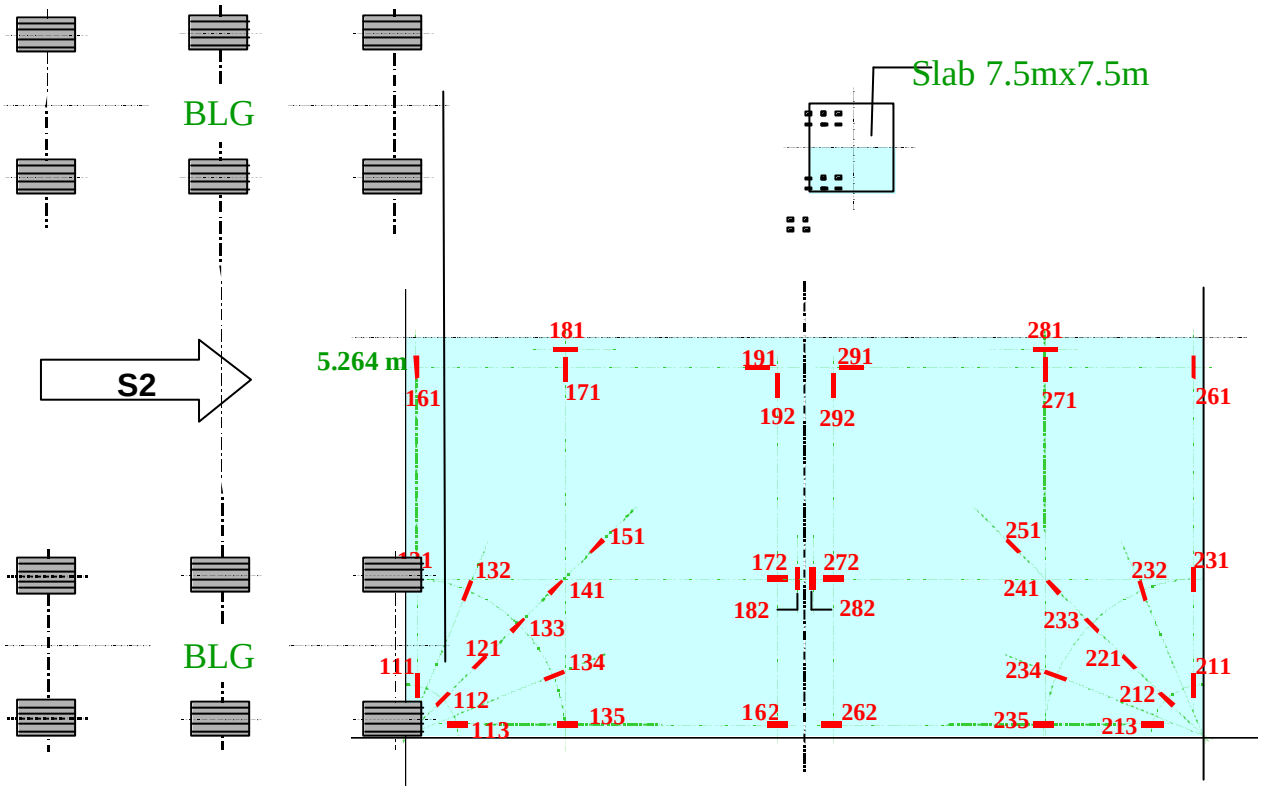

Figure IV-17 : Simulation vehicle _ config. G6-BLG / Gauges on slab 93 / Trajectory T3.

The presented signals have been obtained the 10th of April 2002, 12h25, in the following conditions :

- ✓ Medium temperature : 13 °C
- ✓ Equivalent gradient in the slab : 0.111 °C/cm

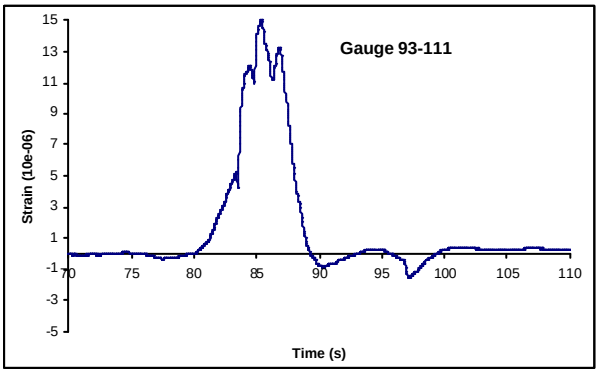

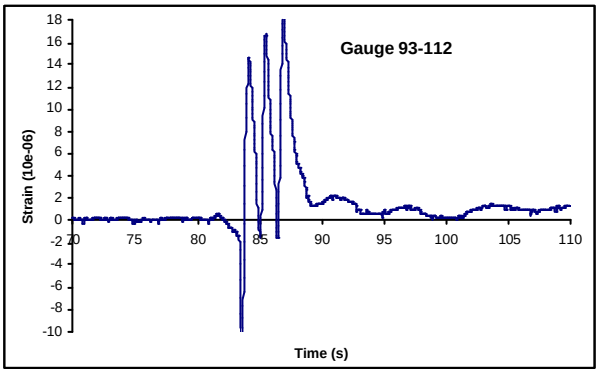

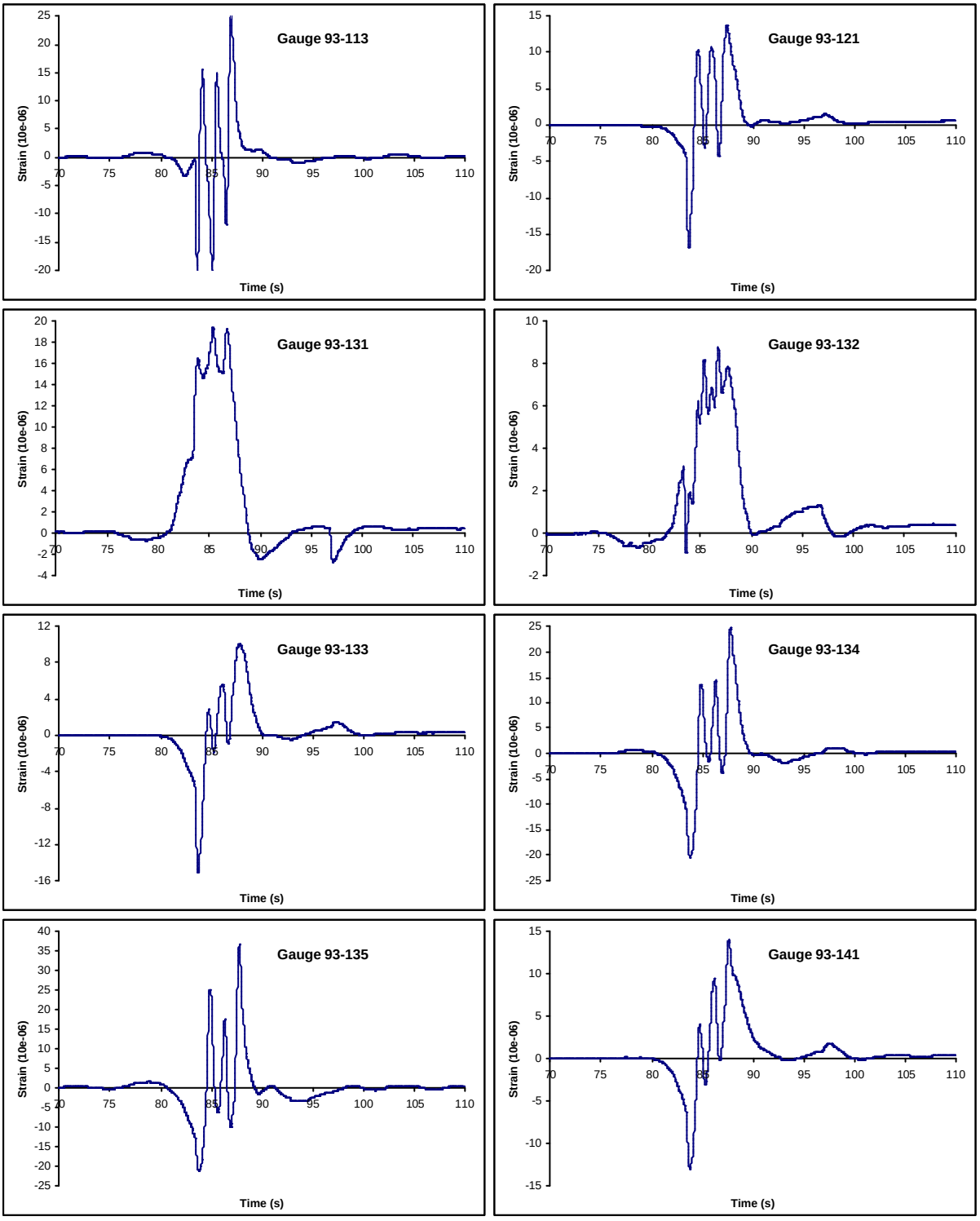
Gauge 93-113
Strain (10e-06)
Time (s)
Gauge 93-121
Strain (10e-06)
Time (s)
Gauge 93-131
Strain (10e-06)
Time (s)
Gauge 93-132
Strain (10e-06)
Time (s)
Gauge 93-133
Strain (10e-06)
Time (s)
Gauge 93-134
Strain (10e-06)
Time (s)
Gauge 93-135
Strain (10e-06)
Time (s)
Gauge 93-141
Strain (10e-06)
Time (s)

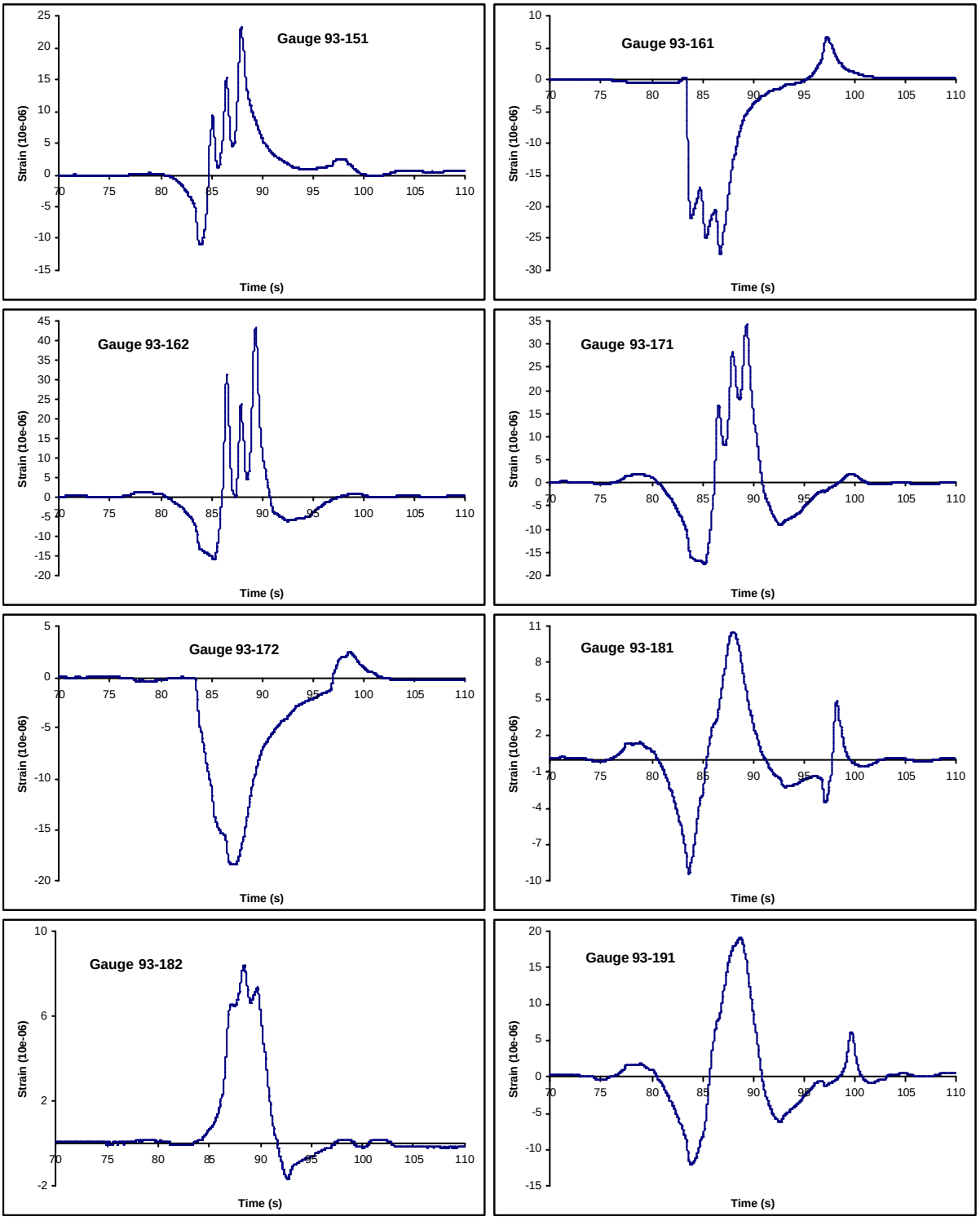
Gauge 93-151
Gauge 93-161
Gauge 93-162
Gauge 93-171
Gauge 93-172
Gauge 93-181
Gauge 93-182
Gauge 93-191
Strain (10e-06)
Time (s)

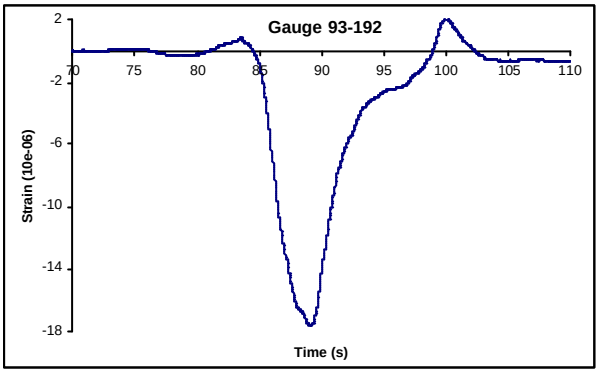
Gauge 93-192
Strain (10e-06)
Time (s)

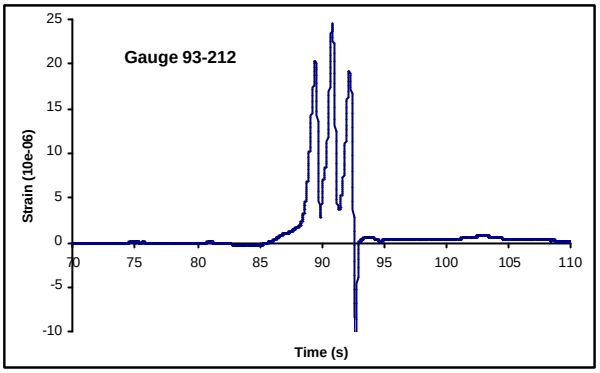
Gauge 93-212
Strain (10e-06)
Time (s)

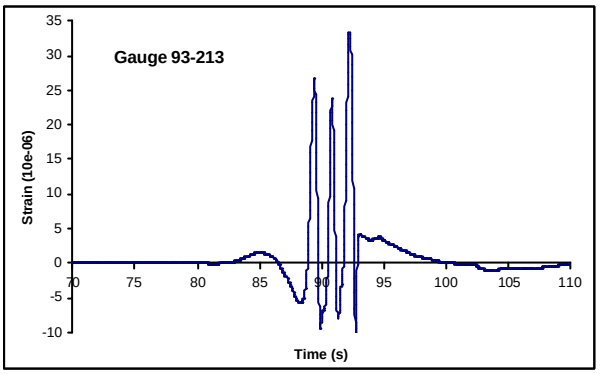
Gauge 93-213
Strain (10e-06)
Time (s)

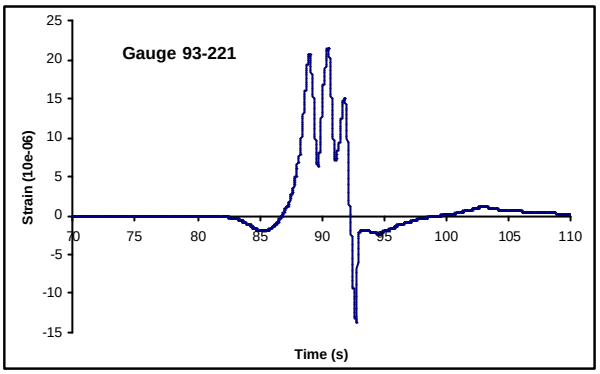
Gauge 93-221
Strain (10e-06)
Time (s)

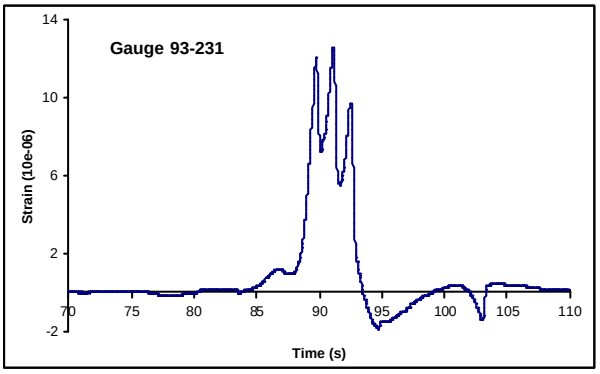
Gauge 93-231
Strain (10e-06)
Time (s)

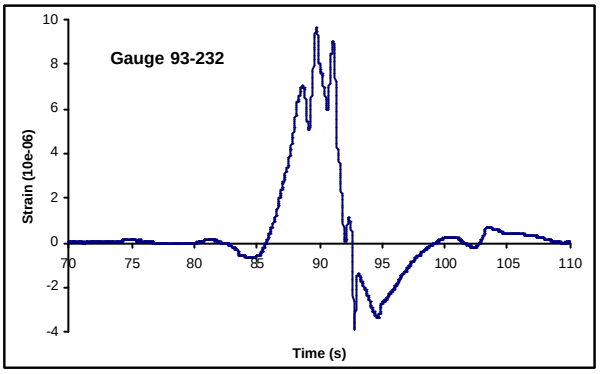
Gauge 93-232
Strain (10e-06)
Time (s)

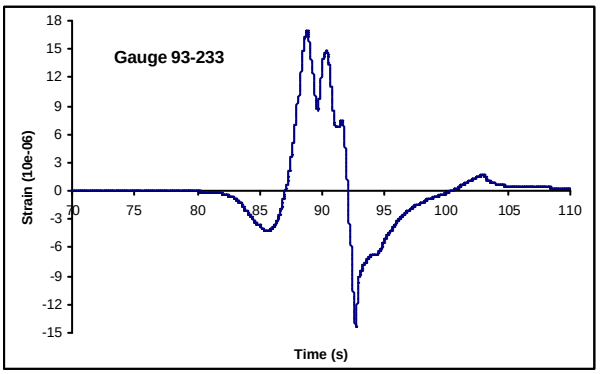
Gauge 93-233
Strain (10e-06)
Time (s)

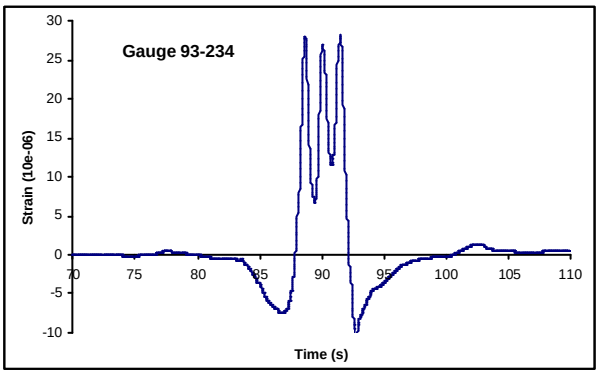
Gauge 93-234
Strain (10e-06)
Time (s)

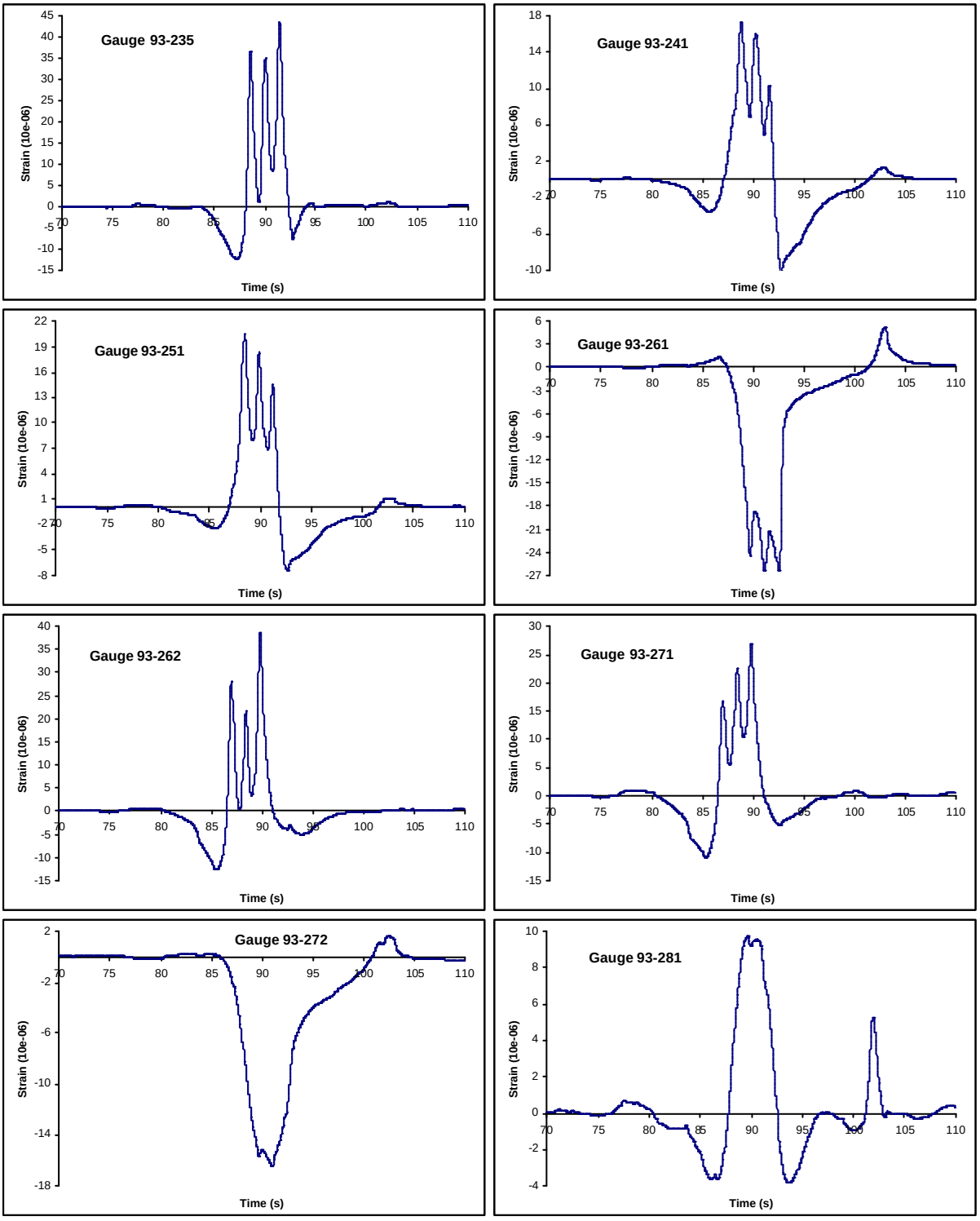
Gauge 93-235
Strain (10e-06)
Time (s)
Gauge 93-241
Strain (10e-06)
Time (s)
Gauge 93-251
Strain (10e-06)
Time (s)
Gauge 93-261
Strain (10e-06)
Time (s)
Gauge 93-262
Strain (10e-06)
Time (s)
Gauge 93-271
Strain (10e-06)
Time (s)
Gauge 93-272
Strain (10e-06)
Time (s)
Gauge 93-281
Strain (10e-06)
Time (s)

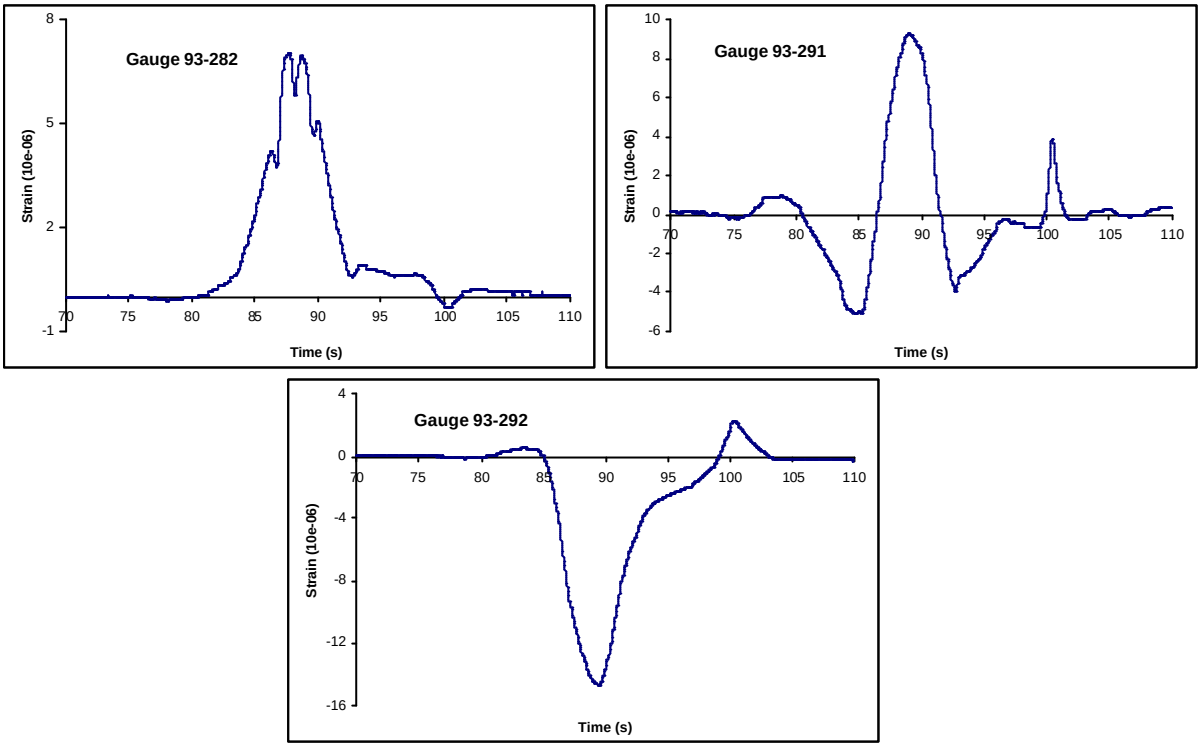

Figure IV-18 : Gauges signals on slab 93 _ config. G6 BLG T3.

IV.1.4.1.2 A380-800F WLG signals

The configuration used is G6, corresponding to the A380-800F. The signals presented correspond to a 6 wheels WLG running on T3 trajectory, direction S2, as shown in the Figure IV-9. The loading is 28.5 tons per wheel.

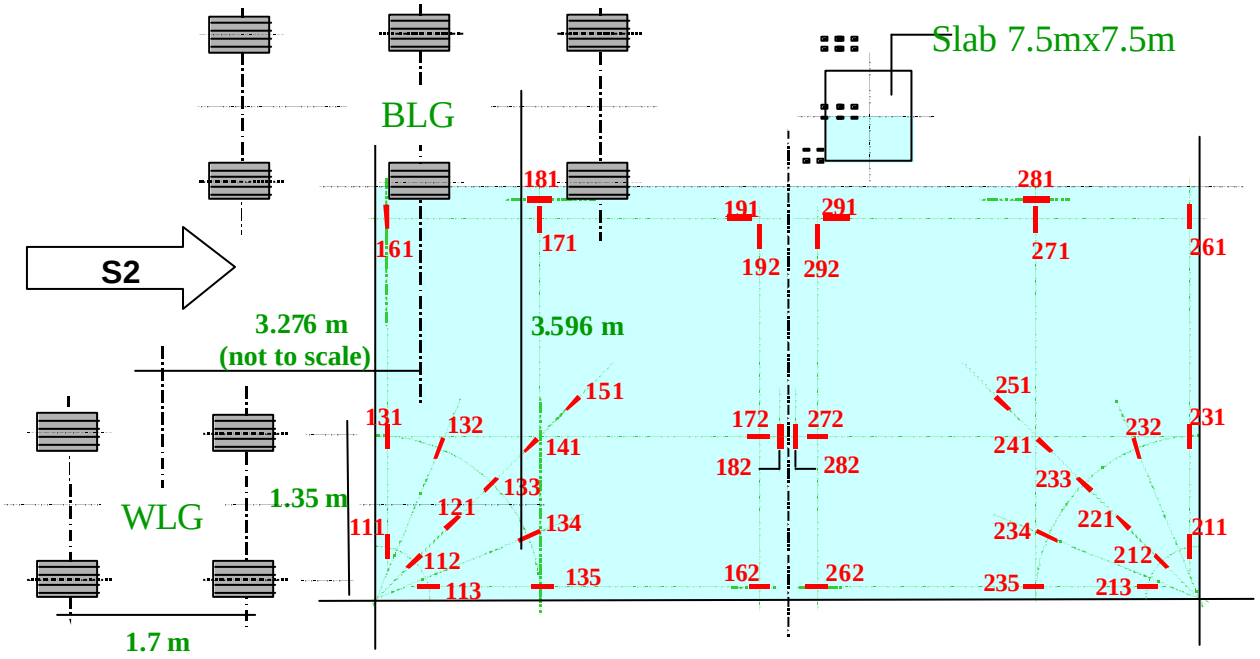

Figure IV-19 : Simulation vehicle _ config. G6-WLG / Gauges on slab 93 / Trajectory T3.

The presented signals have been obtained the 9th of April 2002, 12h28, in the following conditions :

- ✓ Medium temperature : 12.98 °C
- ✓ Equivalent gradient in the slab : 0.057 °C/cm

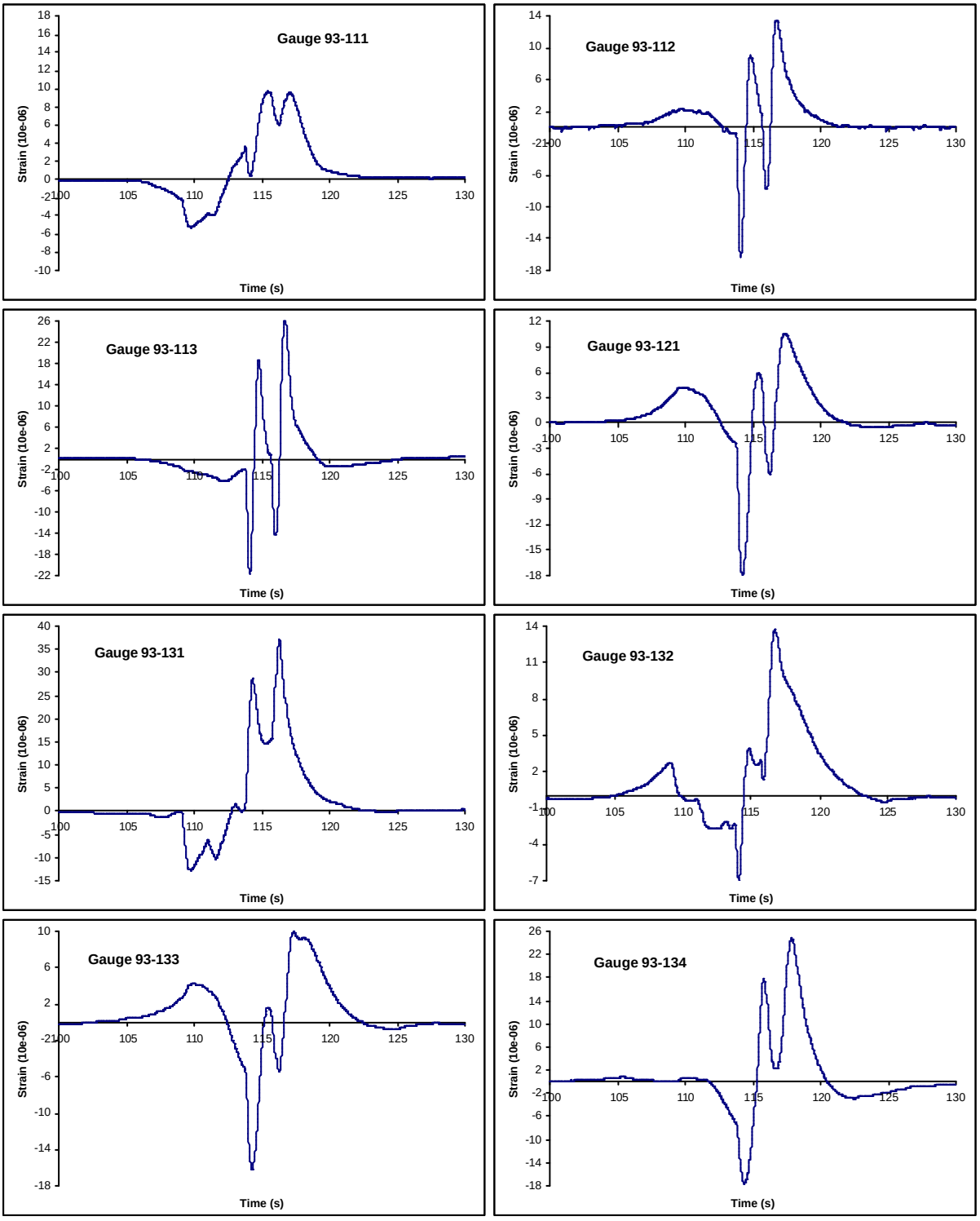

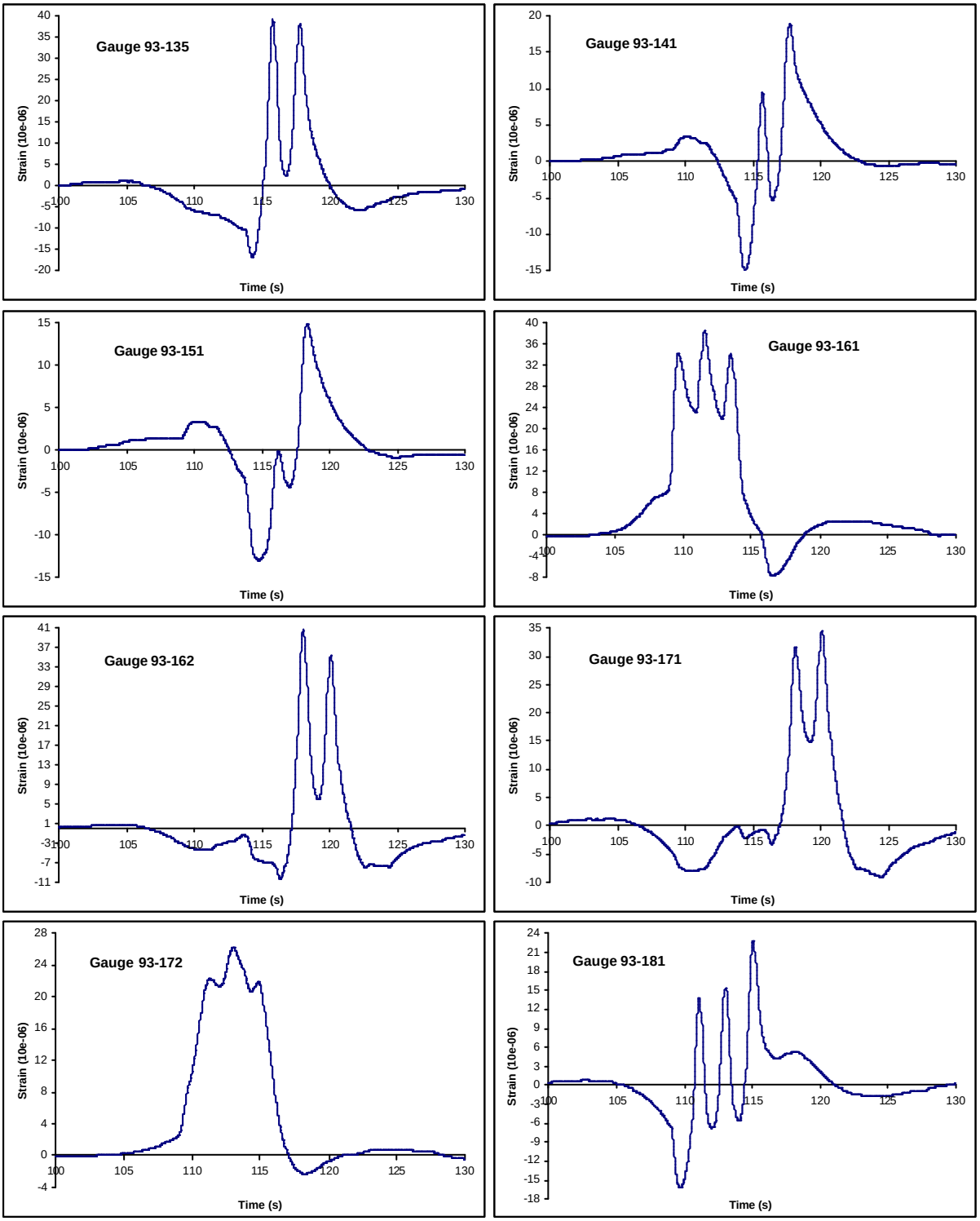
Gauge 93-135
Strain (10e-06)
Time (s)
Gauge 93-141
Strain (10e-06)
Time (s)
Gauge 93-151
Strain (10e-06)
Time (s)
Gauge 93-161
Strain (10e-06)
Time (s)
Gauge 93-162
Strain (10e-06)
Time (s)
Gauge 93-171
Strain (10e-06)
Time (s)
Gauge 93-172
Strain (10e-06)
Time (s)
Gauge 93-181
Strain (10e-06)
Time (s)

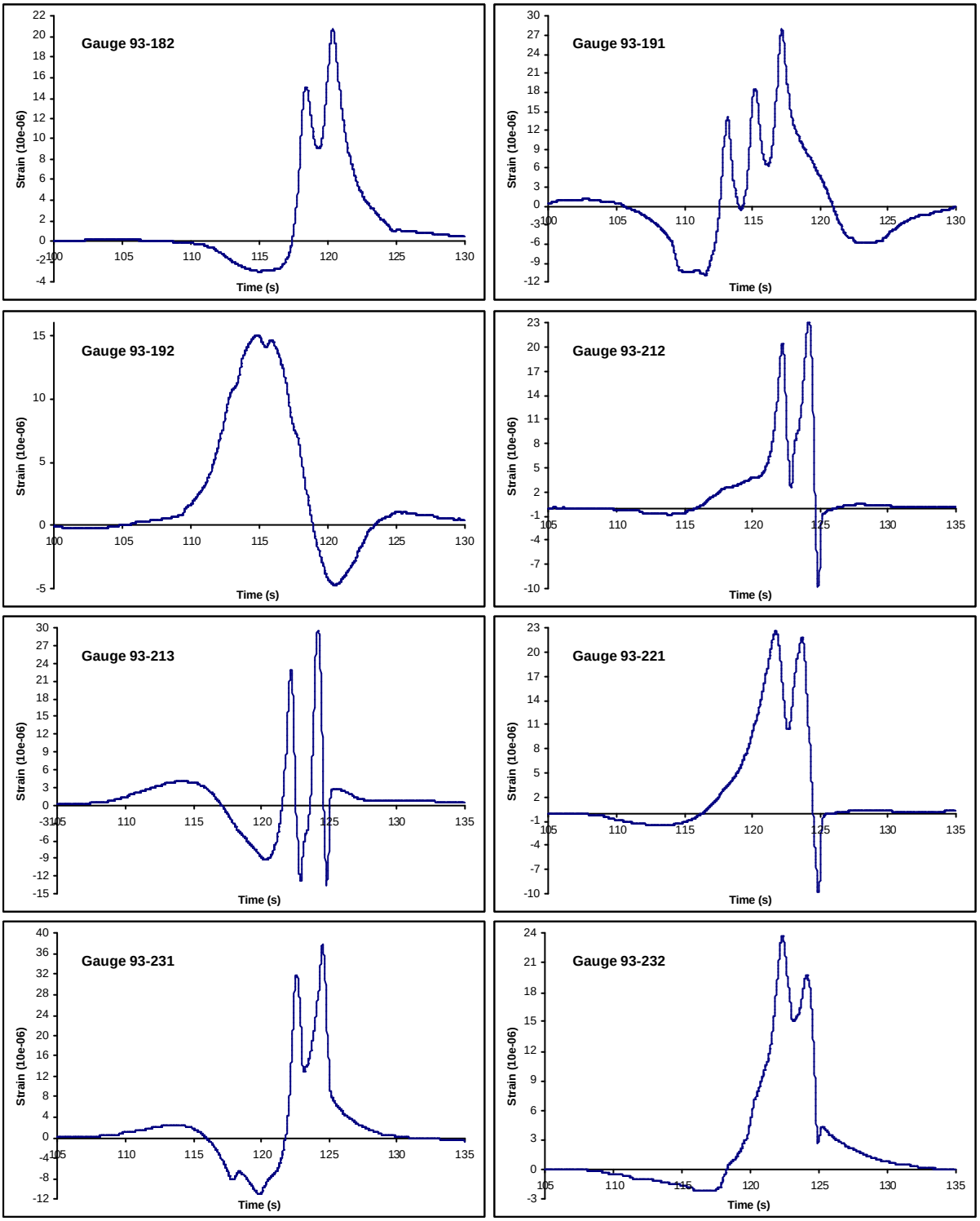
Gauge 93-182
Gauge 93-191
Gauge 93-192
Gauge 93-212
Gauge 93-213
Gauge 93-221
Gauge 93-231
Gauge 93-232
Strain (10e-06)
Time (s)

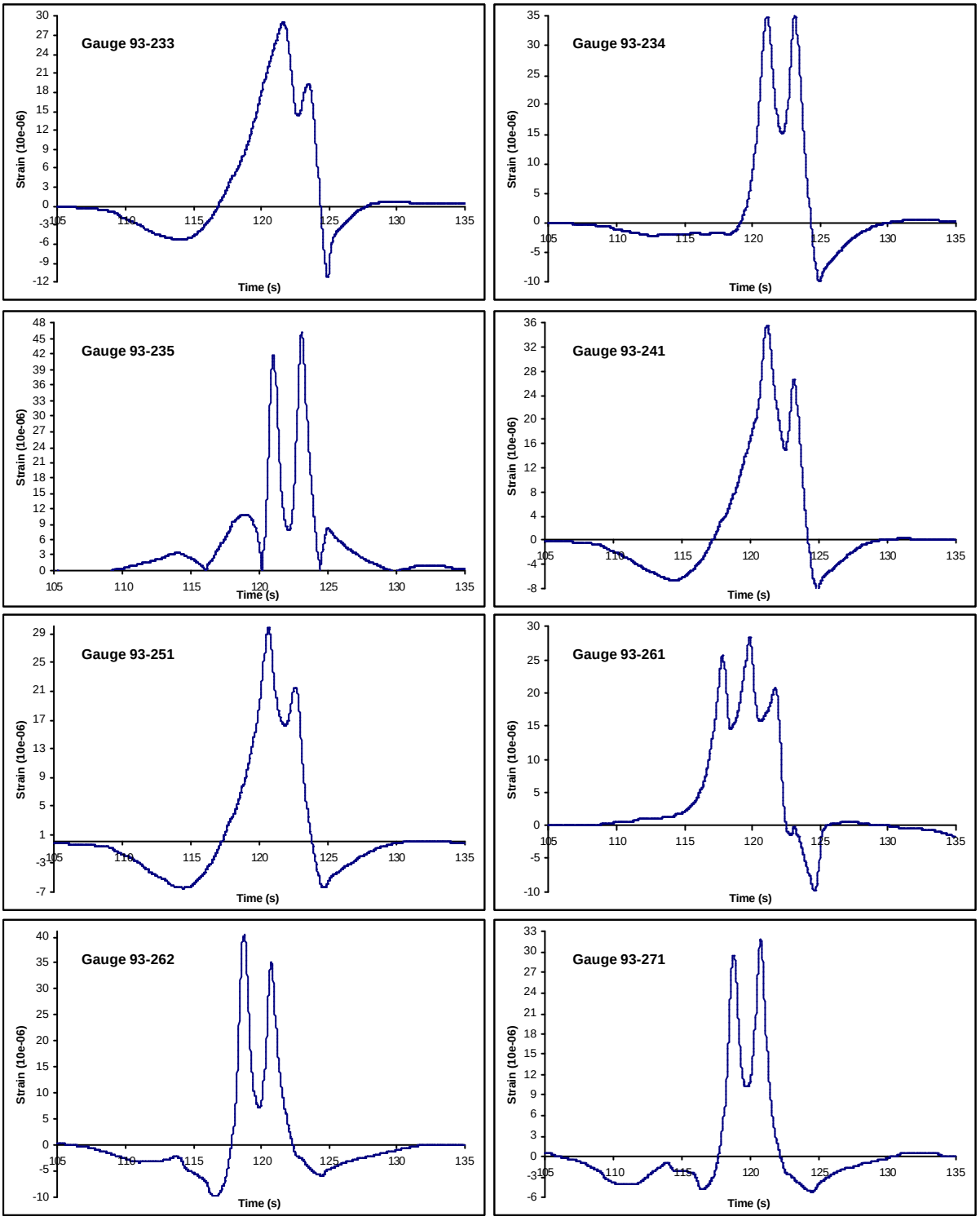
Gauge 93-233
Strain (10e-06)
Time (s)
Gauge 93-234
Strain (10e-06)
Time (s)
Gauge 93-235
Strain (10e-06)
Time (s)
Gauge 93-241
Strain (10e-06)
Time (s)
Gauge 93-251
Strain (10e-06)
Time (s)
Gauge 93-261
Strain (10e-06)
Time (s)
Gauge 93-262
Strain (10e-06)
Time (s)
Gauge 93-271
Strain (10e-06)
Time (s)

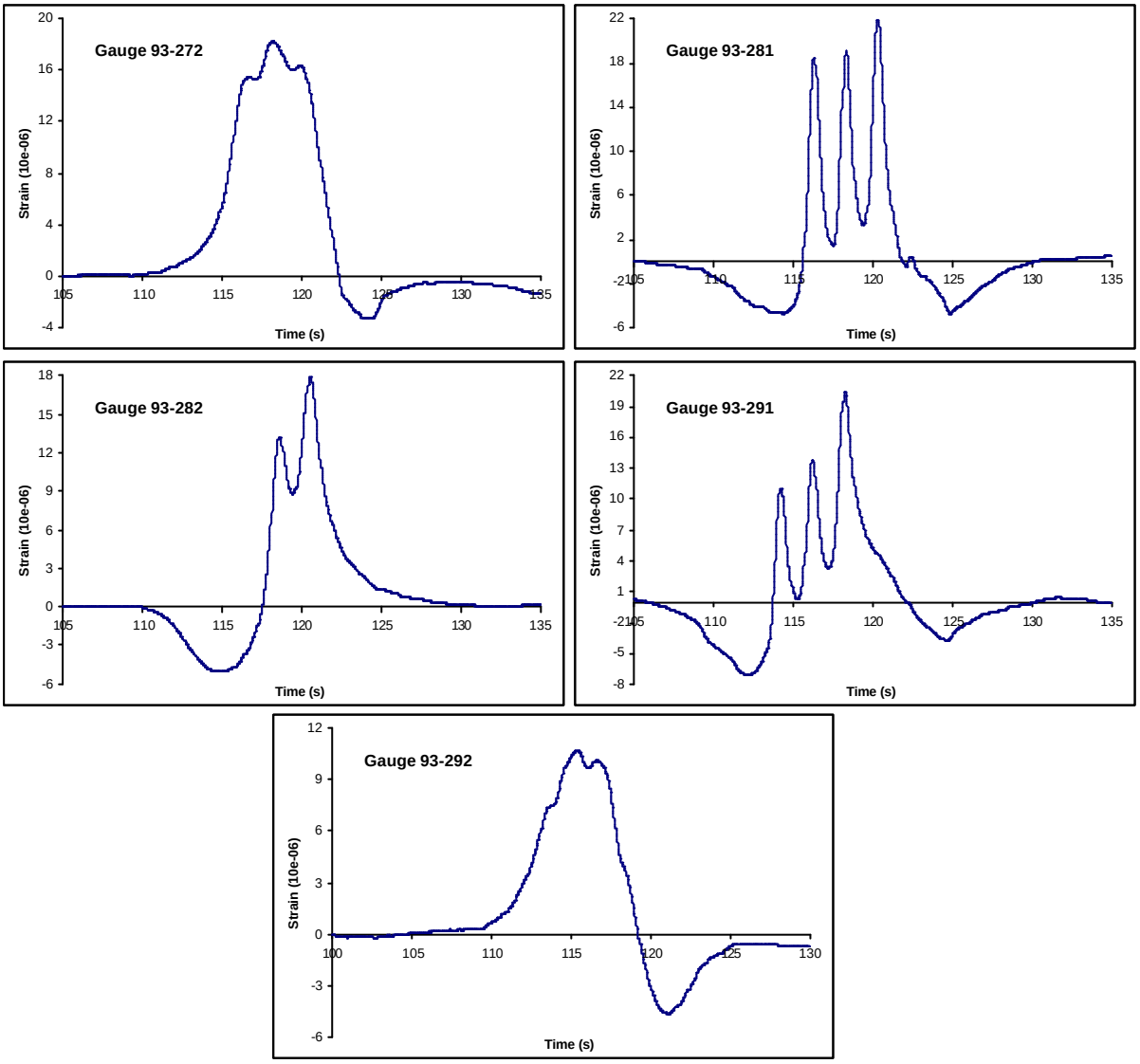

Figure IV-20 : Gauges signals on slab 93 _ config. G6 WLG T3.

IV.1.4.2 Example of a B747-400 characteristic signals

IV.1.4.2.1 B747-400 BLG signals

The configuration used is G10, corresponding to the B747-400. The signals presented correspond to a 4 wheels BLG running on T3 trajectory, direction S1, as shown in Figure IV-11. The loading is 23.2 tons per wheel.

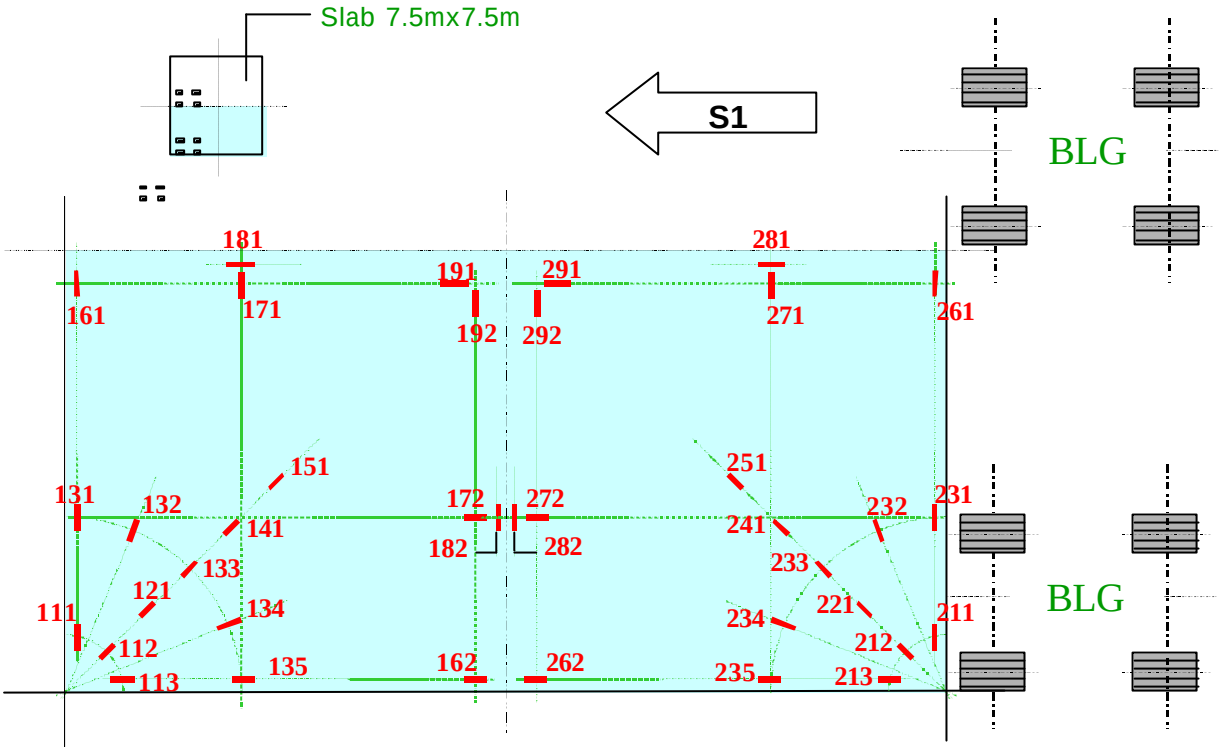

Figure IV-21 : Simulation vehicle _ config. G10-BLG / Gauges on slab 93 / Trajectory T3.

The presented signals have been obtained the 23th of September 2002, 13h48, in the following conditions :

- ✓ Medium temperature : 20.84 °C
- ✓ Equivalent gradient in the slab : 0.115 °C/cm

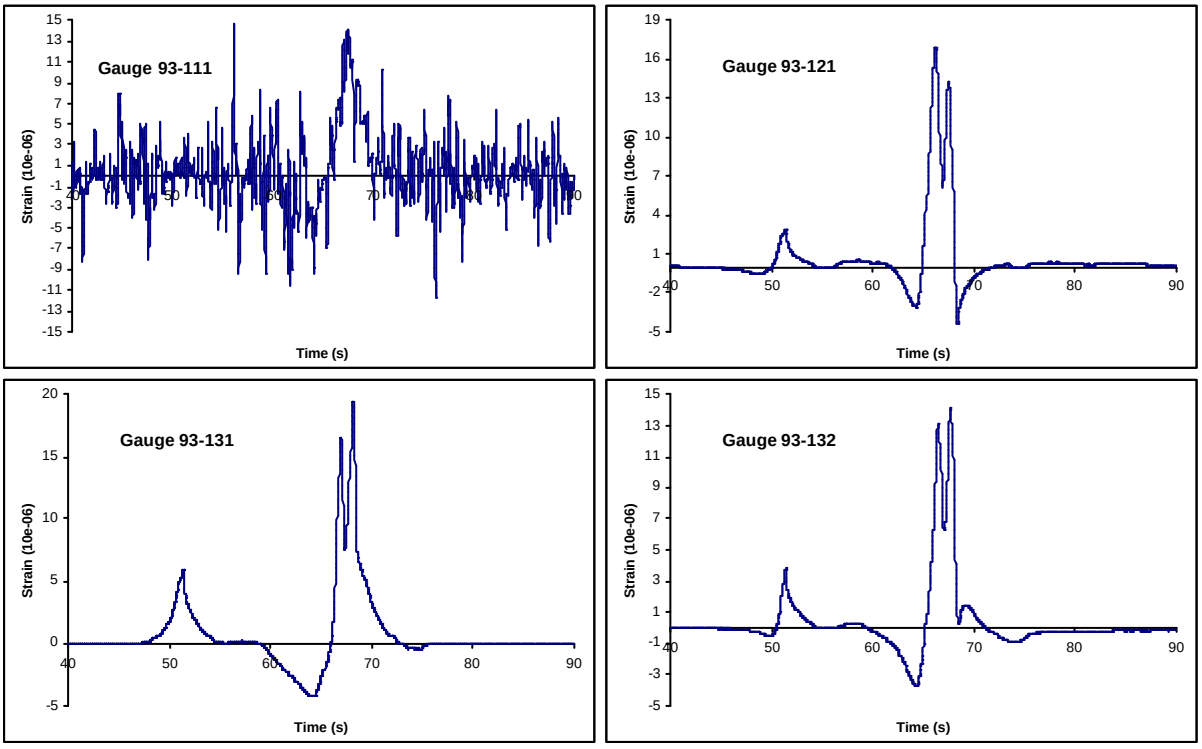

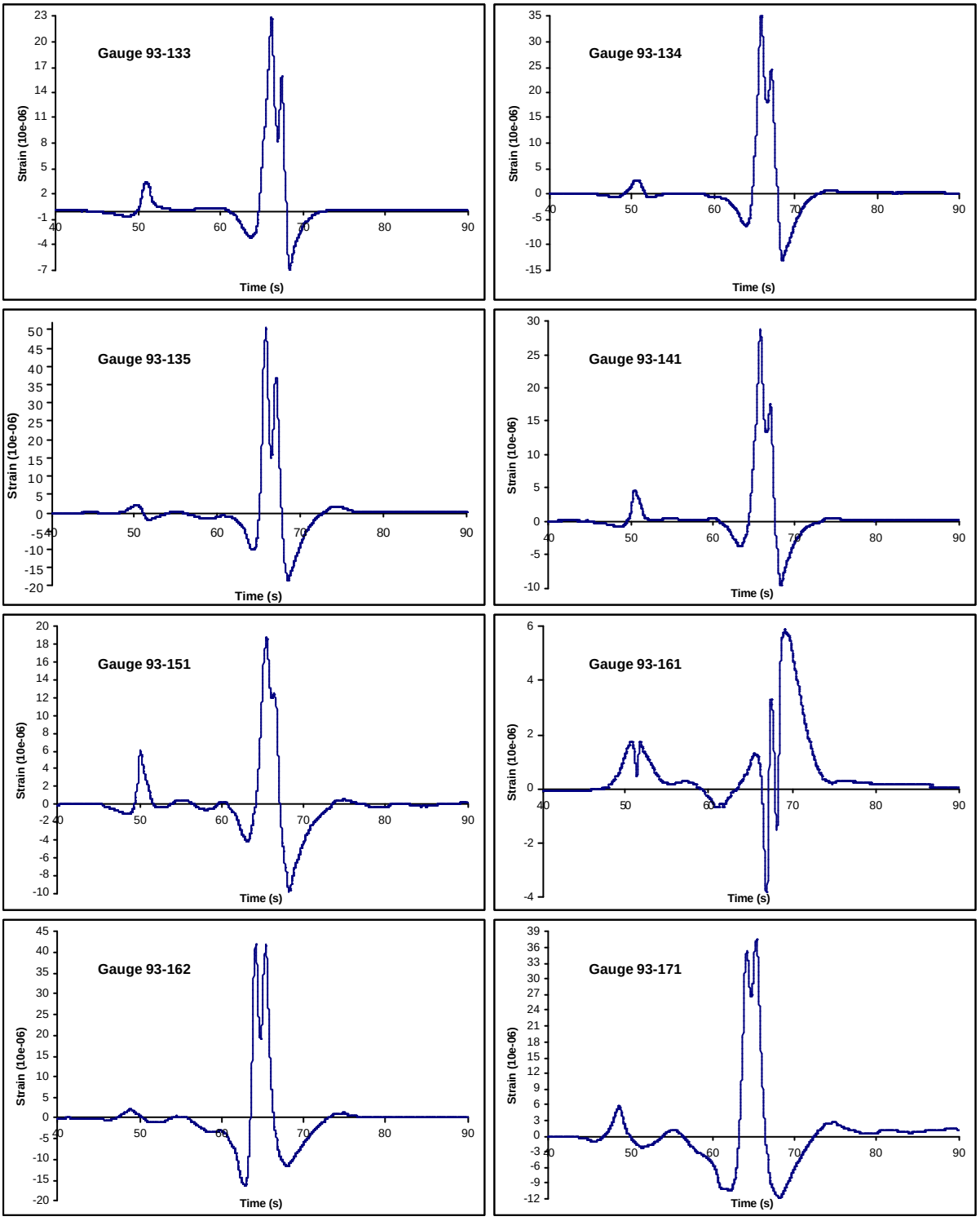
Gauge 93-133
Strain (10e-06)
Time (s)
Gauge 93-134
Strain (10e-06)
Time (s)
Gauge 93-135
Strain (10e-06)
Time (s)
Gauge 93-141
Strain (10e-06)
Time (s)
Gauge 93-151
Strain (10e-06)
Time (s)
Gauge 93-161
Strain (10e-06)
Time (s)
Gauge 93-162
Strain (10e-06)
Time (s)
Gauge 93-171
Strain (10e-06)
Time (s)

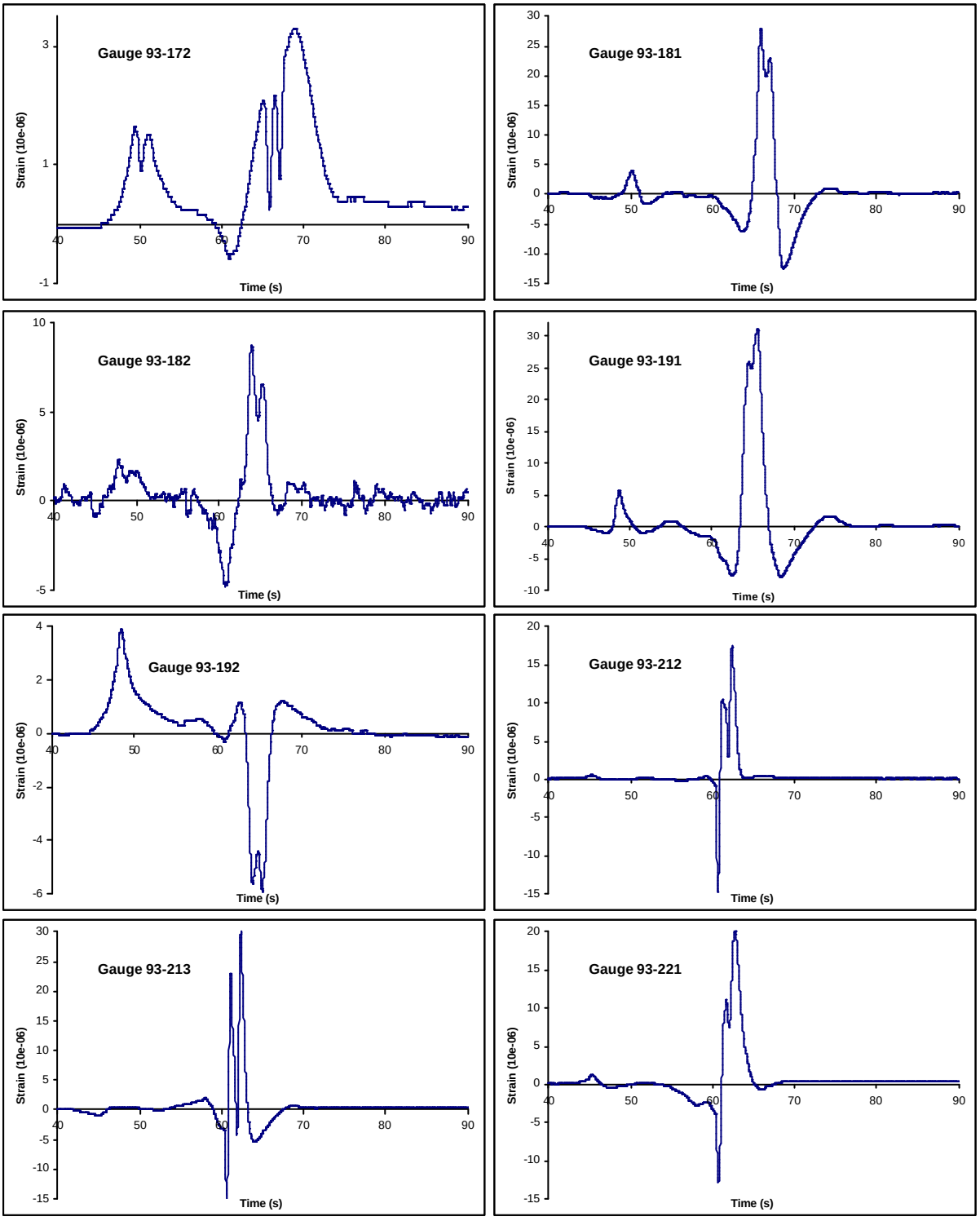
Gauge 93-172
Strain (10e-06)
Time (s)
Gauge 93-181
Strain (10e-06)
Time (s)
Gauge 93-182
Strain (10e-06)
Time (s)
Gauge 93-191
Strain (10e-06)
Time (s)
Gauge 93-192
Strain (10e-06)
Time (s)
Gauge 93-212
Strain (10e-06)
Time (s)
Gauge 93-213
Strain (10e-06)
Time (s)
Gauge 93-221
Strain (10e-06)
Time (s)

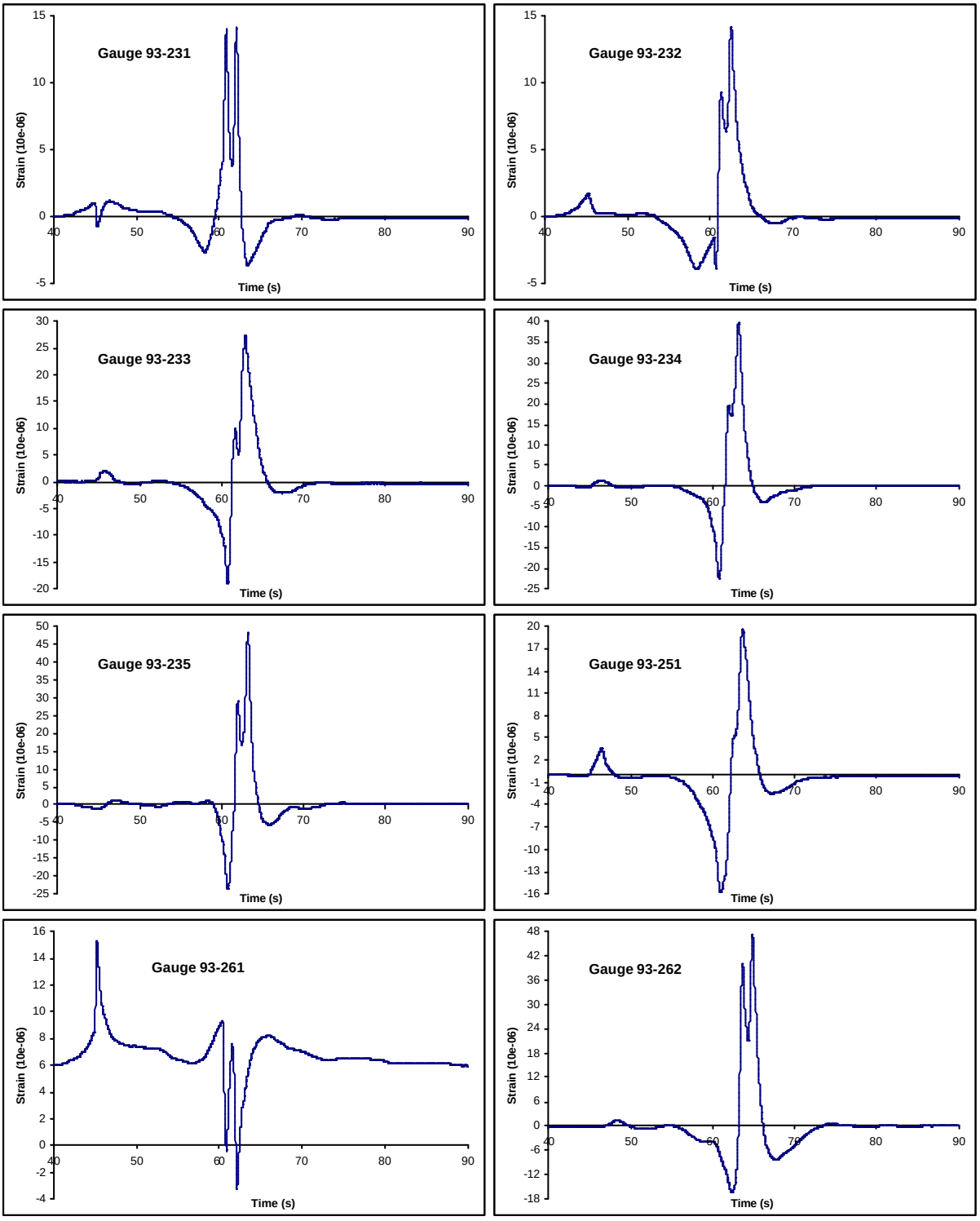
Gauge 93-231
Strain (10e-06)
Time (s)
Gauge 93-232
Strain (10e-06)
Time (s)
Gauge 93-233
Strain (10e-06)
Time (s)
Gauge 93-234
Strain (10e-06)
Time (s)
Gauge 93-235
Strain (10e-06)
Time (s)
Gauge 93-251
Strain (10e-06)
Time (s)
Gauge 93-261
Strain (10e-06)
Time (s)
Gauge 93-262
Strain (10e-06)
Time (s)

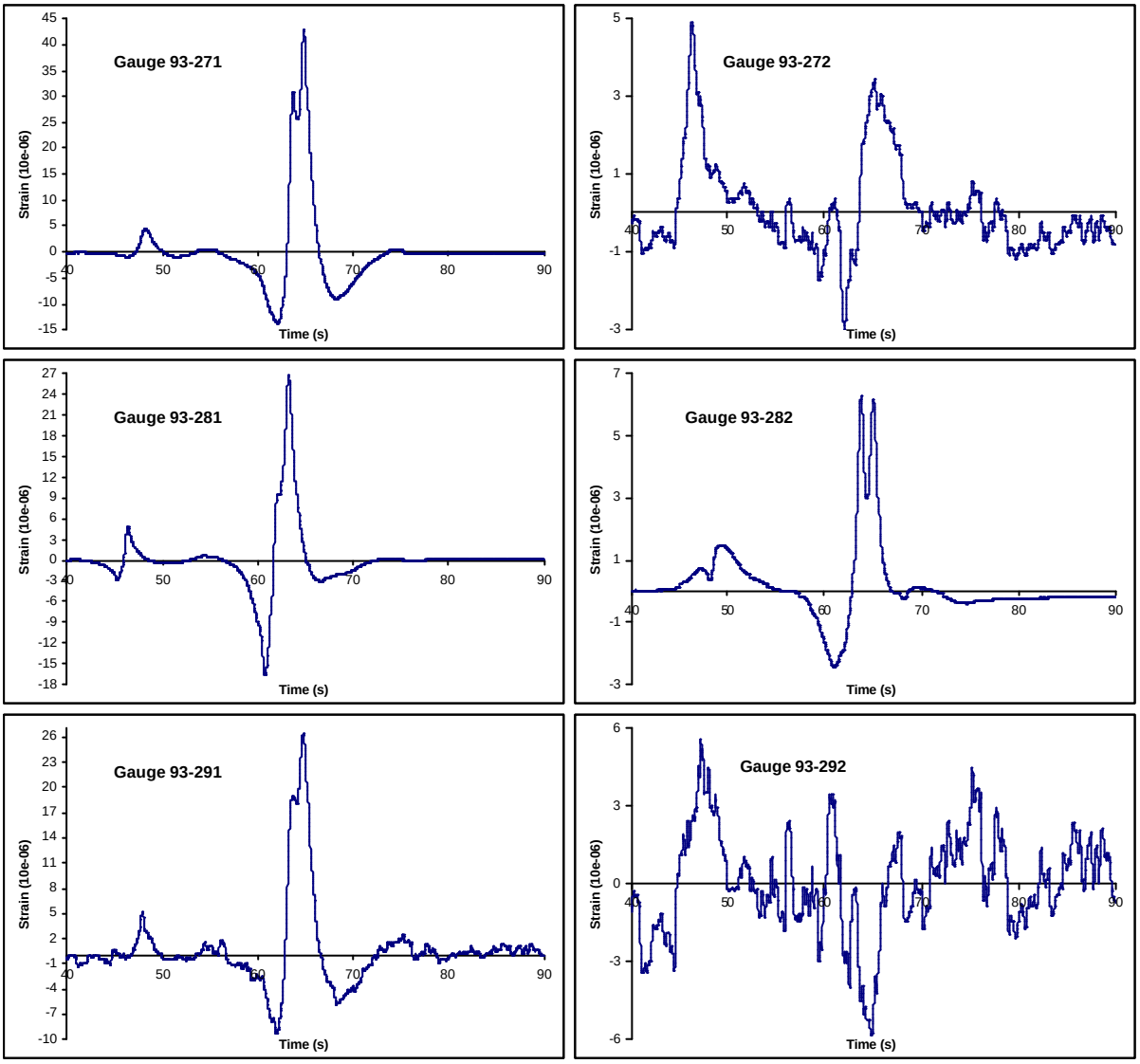

Figure IV-22 : Gauges signals on slab 93 _ config. G10 BLG T3.

IV.1.4.2.2 B747-400 WLG signals

The configuration used is G10, corresponding to the B747-400. The signals presented correspond to a 4 wheels WLG running on T3 trajectory, direction S2, as shown in Figure IV-13. The loading is 23.2 tons per wheel.

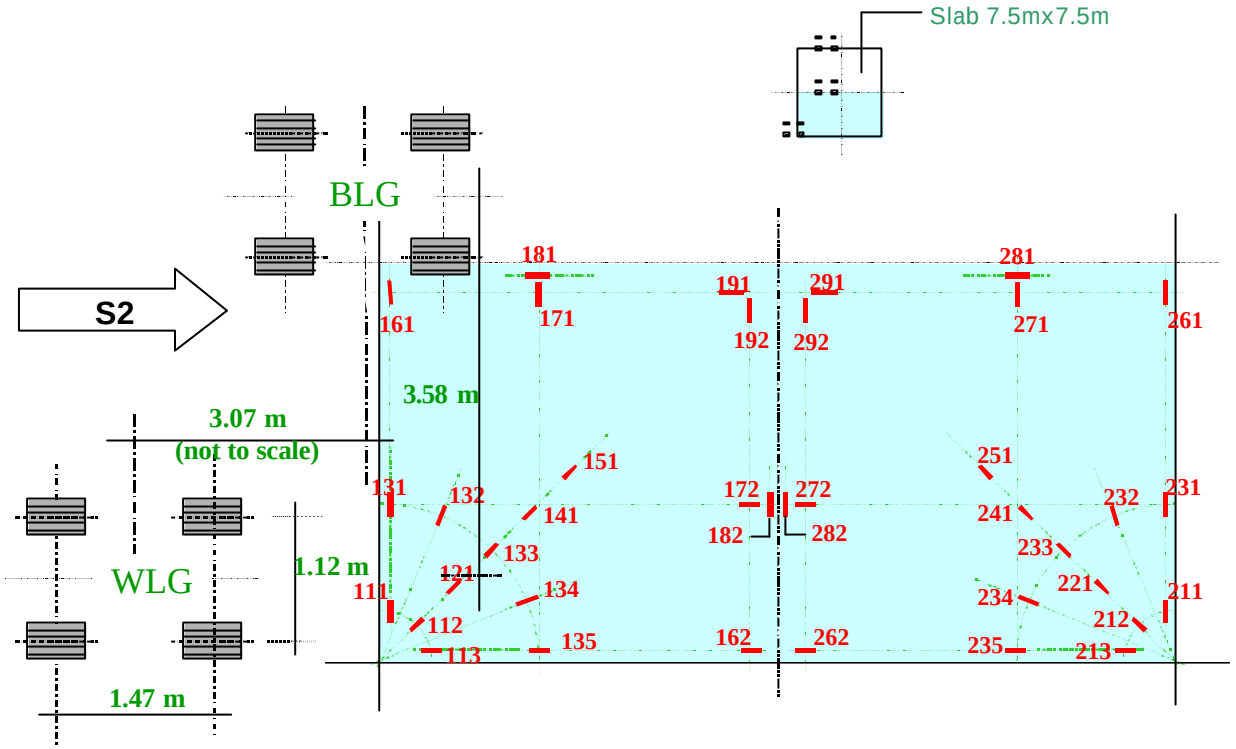

Figure IV-23 : Simulation vehicle _ config. G10-WLG / Gauges on slab 93 / Trajectory T3.

The presented signals have been obtained the 23th of September 2002, 9h06, in the following conditions :

- ✓ Medium temperature : 18.87 °C
- ✓ Equivalent gradient in the slab : -0.072 °C/cm

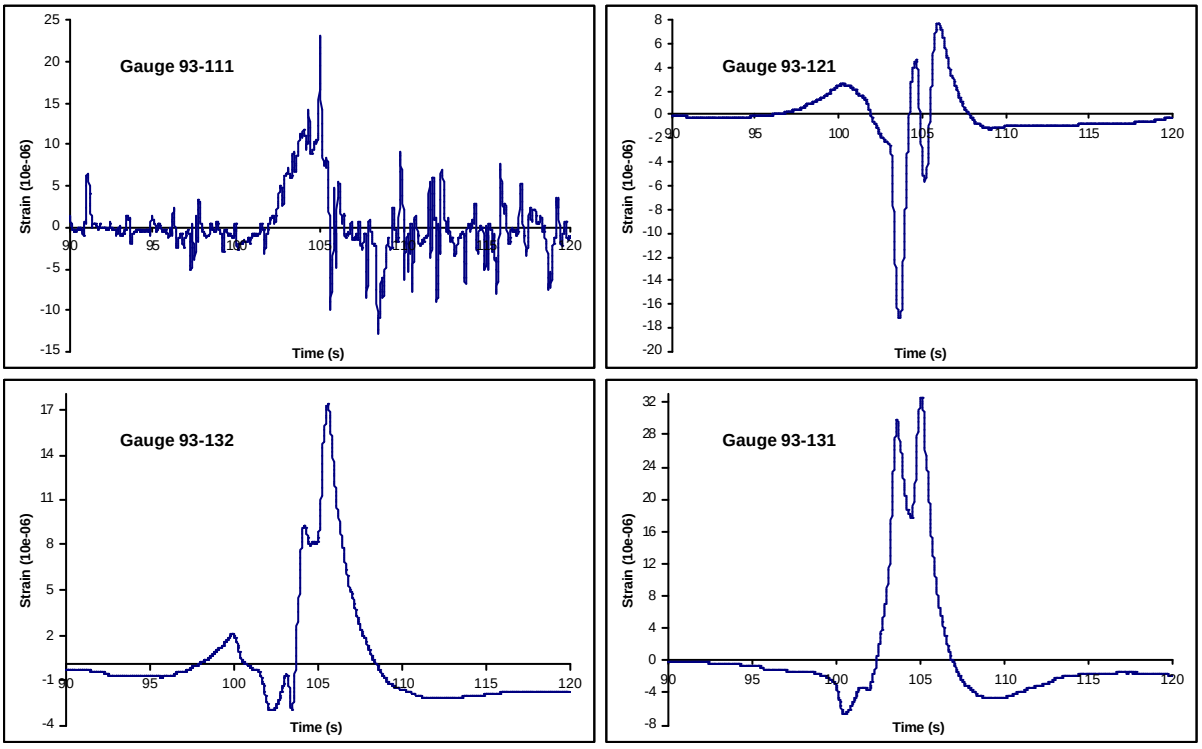

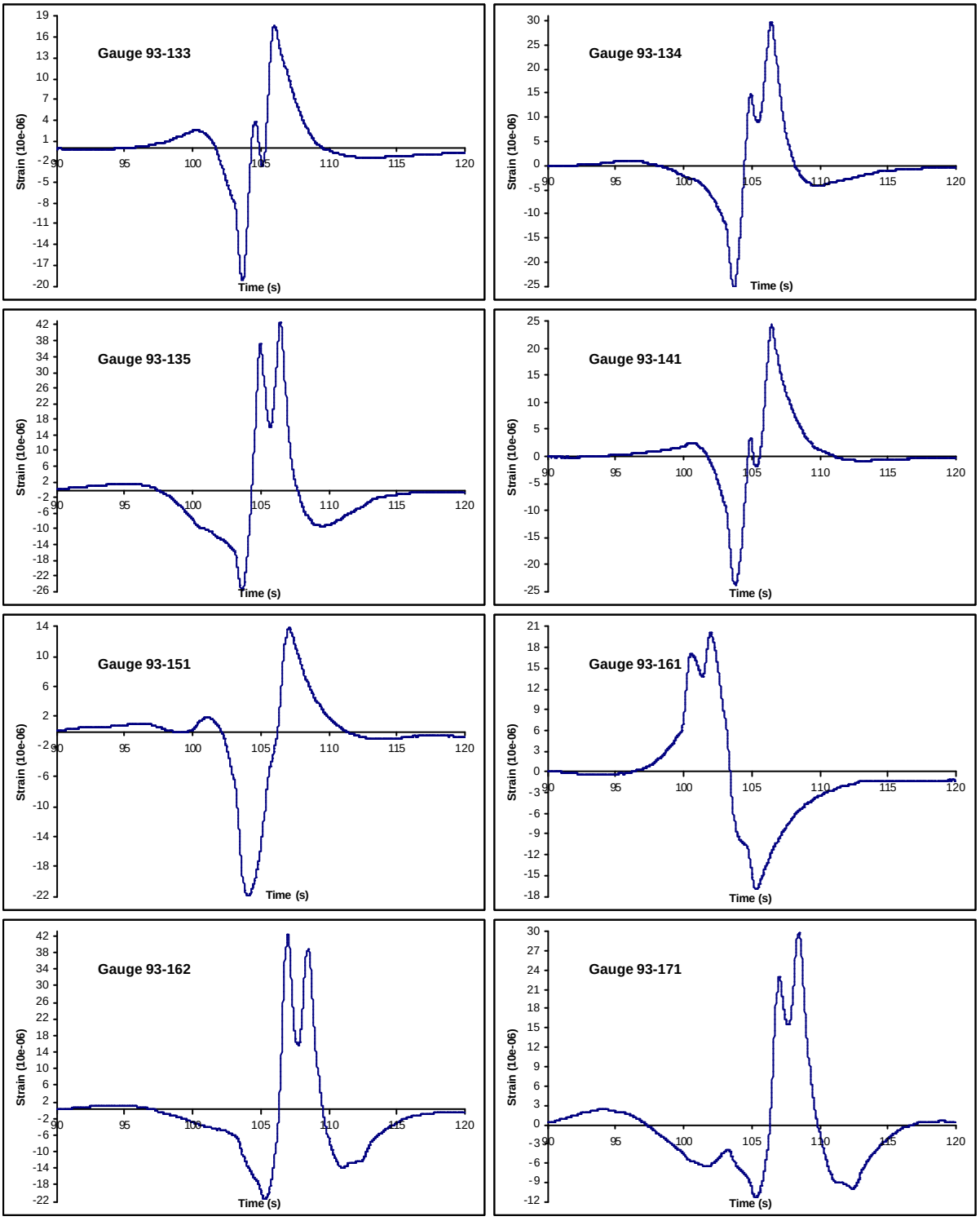
Gauge 93-133
Gauge 93-134
Gauge 93-135
Gauge 93-141
Gauge 93-151
Gauge 93-161
Gauge 93-162
Gauge 93-171
Strain (10e-06)
Time (s)

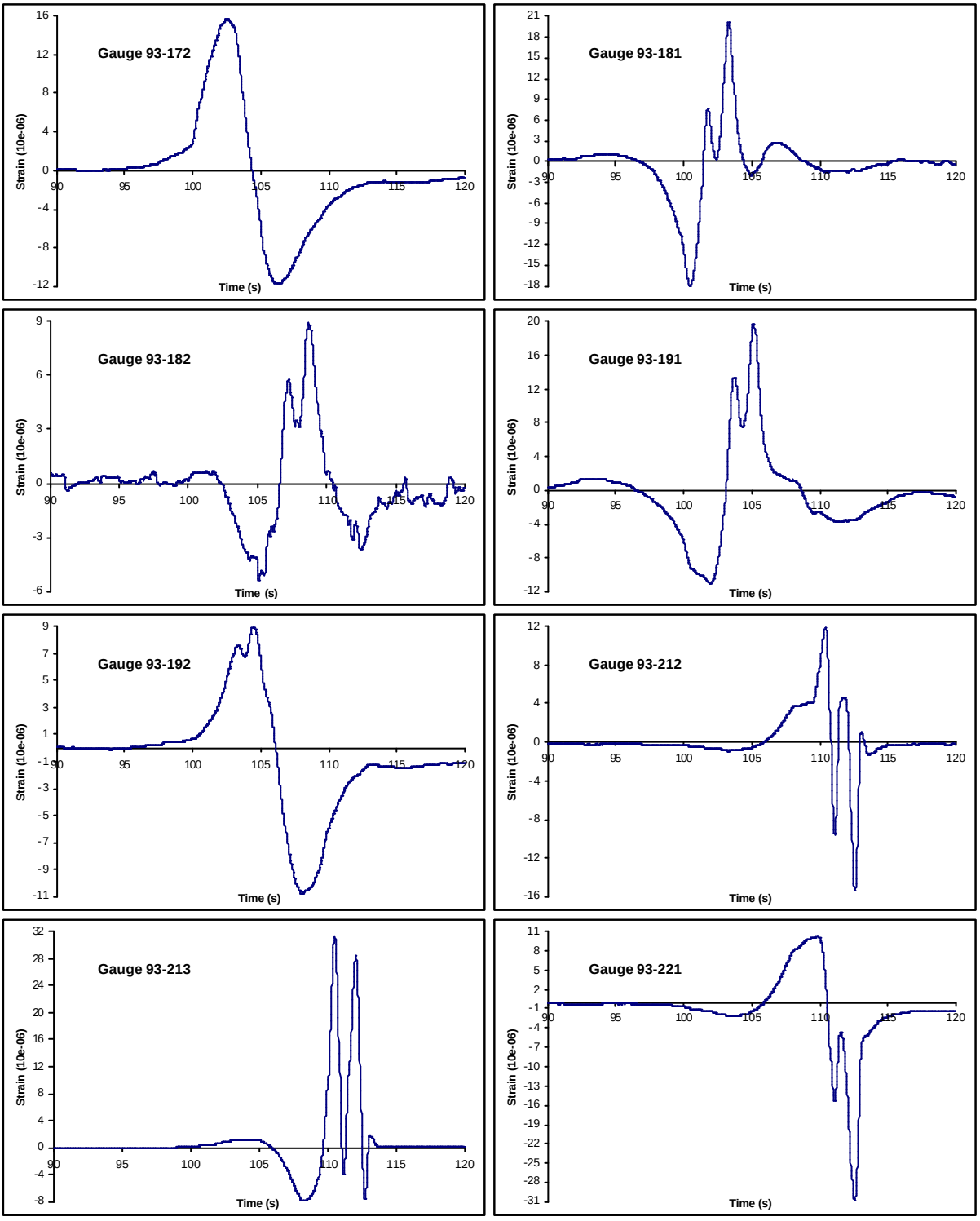
Gauge 93-172
Strain (10e-06)
Time (s)
Gauge 93-181
Strain (10e-06)
Time (s)
Gauge 93-182
Strain (10e-06)
Time (s)
Gauge 93-191
Strain (10e-06)
Time (s)
Gauge 93-192
Strain (10e-06)
Time (s)
Gauge 93-212
Strain (10e-06)
Time (s)
Gauge 93-213
Strain (10e-06)
Time (s)
Gauge 93-221
Strain (10e-06)
Time (s)

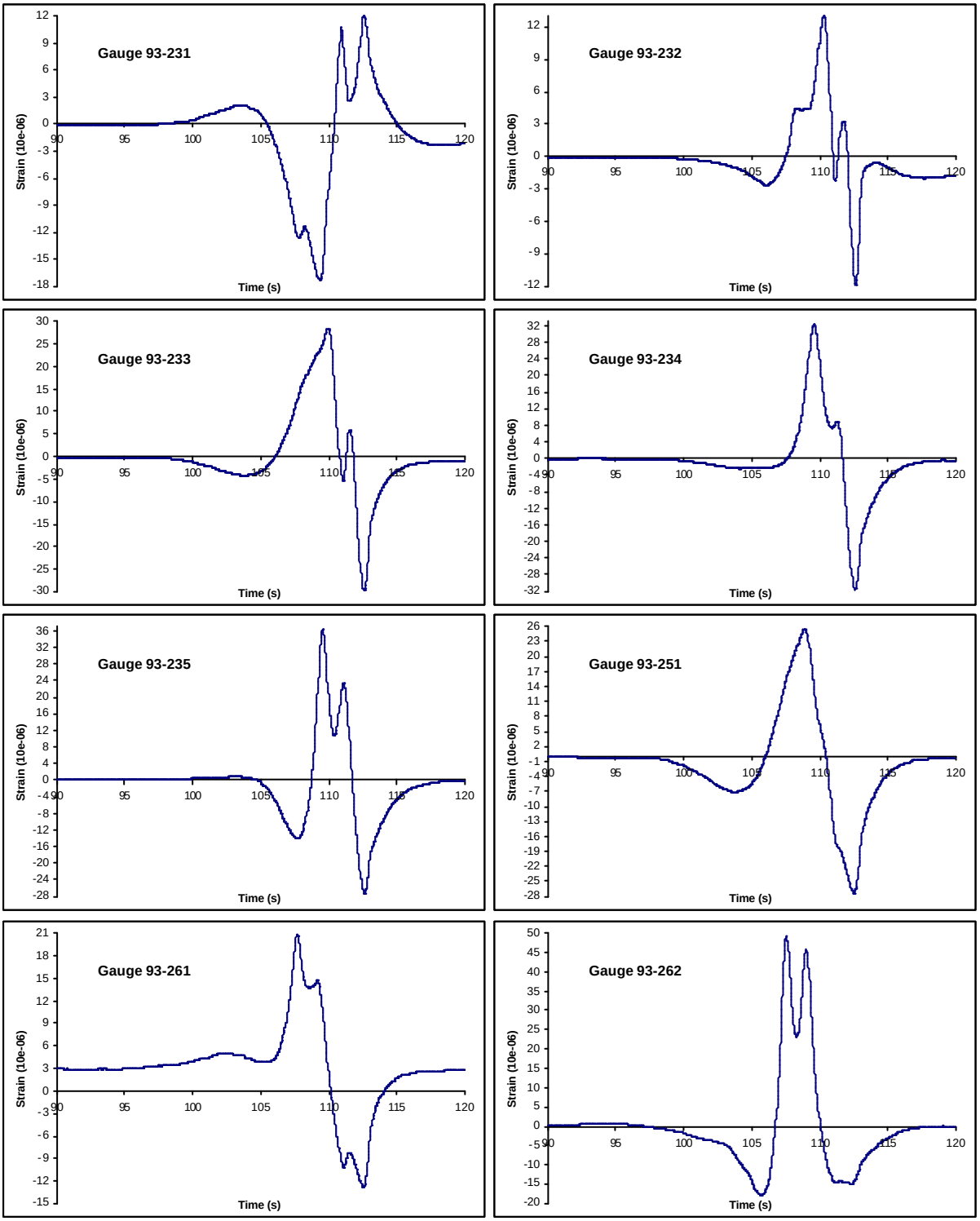
Gauge 93-231
Gauge 93-232
Gauge 93-233
Gauge 93-234
Gauge 93-235
Gauge 93-251
Gauge 93-261
Gauge 93-262
Strain (10e-06)
Time (s)

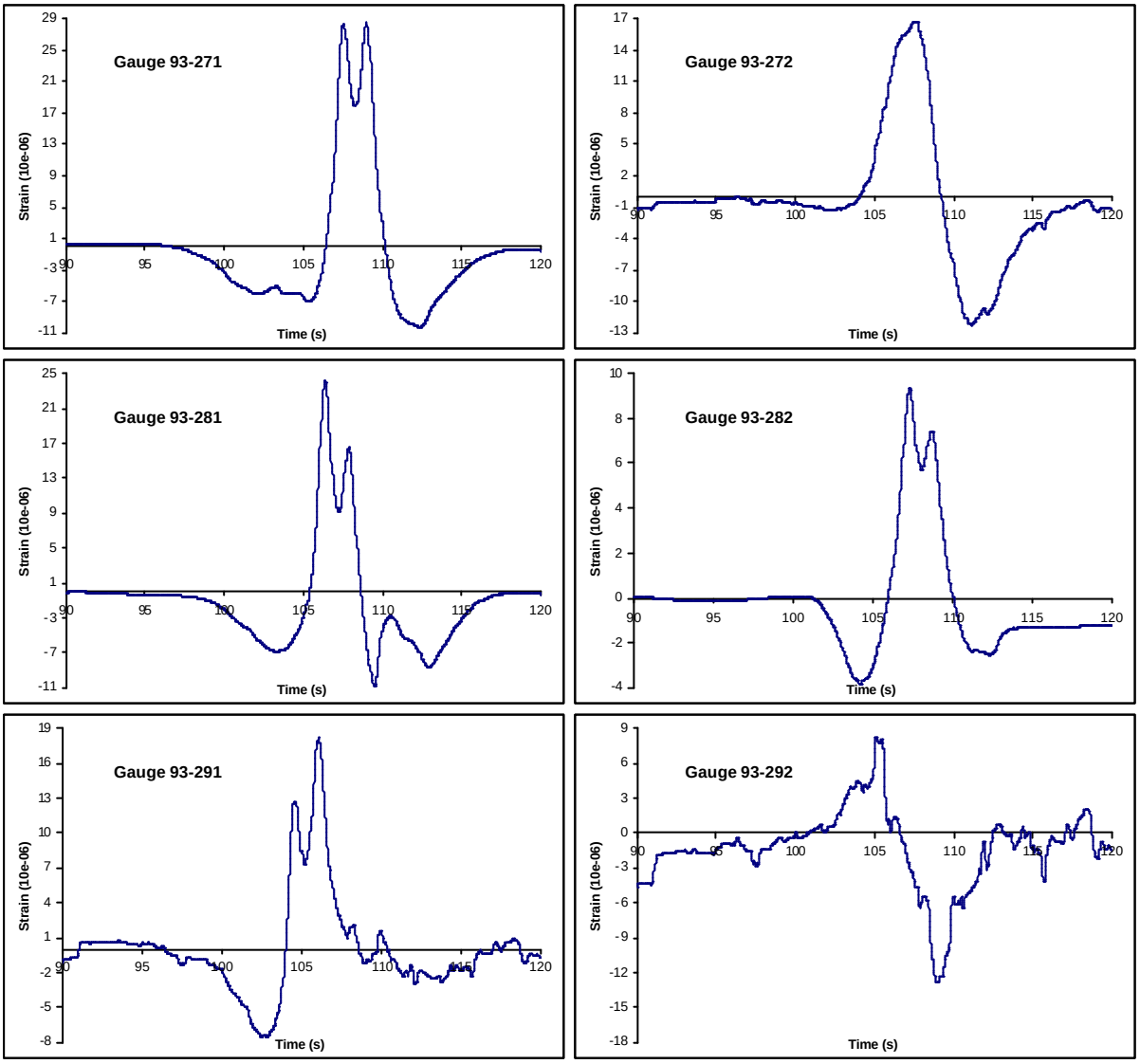

Figure IV-24 : Gauges signals on slab 93 _ config. G10 WLG T3.

IV.1.4.2.3 Comparison for the presented signals

The following table show the maximum strain obtained for each aircraft during the BLG & WLF running on T3. The maximum strain measured on T3 was systematically on longitudinal gauges, as shown below.

Table IV-11 : Comparisons A380-800F – B747-400.

	BLG		WLG	
	A380-800F	**B747-400**	**A380-800F**	**B747-400**
93-135 (e_{max} µ-strains)	36.5	50.5	39.1	42.8
93-235 (e_{max} µ-strains)	43.8	48.3	46.1	36.2
93-162 (e_{max} µ-strains)	43.7	42	40.7	42.2
93-262 (e_{max} µ-strains)	38.6	47.1	40.3	49.1

The strain levels remain the same order, but with higher values for the B747-400, which is less loaded. It becomes from a better distribution of the load on the pavement, due to optimised base and track dimensions of the landing gears.

IV.1.4.3 Main results

In this part, we focus on the main results obtained for the G5 to G10 configurations, that means real aircrafts comparisons. The following tables gather the maximum strain measured on an instrumented slab for a given configuration among all possible trajectories. We precise the number of the gauge which permit to know where the maximum strain is localized. The thermal conditions are therefore specified.

IV.1.4.3.1 Slab 45

Table IV-12 : Configurations G5 to G10 – slab 45.

			slab 45 (th=37cm, soil 2, no dowels, 5mx5m)			
			εmax	gauge	qm °C	Geq °C/cm
G5	**A380-800 26.7t/w**	WLG	60	135	20.8	0.12
		BLG	59	135	11.5	-0.01
G6	**A380-800F 28.5t/w**	WLG	48	135	11.3	-0.05
		BLG	57	135	12.2	-0.04
G7	**A380-900S 28.5t/w**	WLG	53	135	16.0	-0.08
		BLG	46	162	16.7	0.03
G8	**A340 & B777-300ER 26.6t/w**	A340	55	161	11.2	0.04
		B777	48	171	13.2	0.20
G9	**MD11 27.8t/w**	WLG	60	135	18.5	0.19
		CLG	87.8	135	16.3	-0.07
G10	**B747-400 23.2t/w**	WLG	54	135	18.9	-0.06
		BLG	52	135	16.6	-0.11

IV.1.4.3.2 Slab 68

Table IV-13 : Configurations G5 to G10 – slab 68.

			slab 68 (th=37cm, soil 2, no dowels)			
			εmax	gauge	qm °C	Geq °C/cm
G5	**A380-800 26.7t/w**	WLG	-51	121	13.6	0.00
		BLG	-33	121	20.2	0.03
G6	**A380-800F 28.5t/w**	WLG	-49	133	11.3	-0.05
		BLG	-50	121	12.2	-0.03
G7	**A380-900S 28.5t/w**	WLG	67	135	16	0.00
		BLG	59	135	20.0	0.04
G8	**A340 & B777-300ER 26.6t/w**	A340	-56	121	11.0	0.02
		B777	48	161	12.8	0.17
G9	**MD11 27.8t/w**	WLG	57	162	18.5	0.19
		CLG	71	162	17.5	0.11
G10	**B747-400 23.2t/w**	WLG	66	113	18.8	-0.08
		BLG	55	121	16.4	-0.2

IV.1.4.3.3 Slab 93

Table IV-14 : Configurations G5 to G10 – slab 93.

			slab 93 (th=42cm, soil 1, not dowelled)			
			εmax	gauge	qm °C	Geq °C/cm
G5	**A380-800 26.7t/w**	WLG	58	231	13.4	-0.03
		BLG	43	135	10.2	-0.07
G6	**A380-800F 28.5t/w**	WLG	53	131	11.3	-0.06
		BLG	56	161	13.2	0.05
G7	**A380-900S 28.5t/w**	WLG	57	131	15.7	0.01
		BLG	59	131	20.0	-0.03
G8	**A340 & B777-300ER 26.6t/w**	A340	58	161	11.5	0.05
		B777	54	161	12.9	0.18
G9	**MD11 27.8t/w**	WLG	-65	261	17.6	-0.10
		CLG	66	135	17.5	0.11
G10	**B747-400 23.2t/w**	WLG	60	131	18.7	-0.12
		BLG	56	135	16.5	-0.14

IV.1.4.3.4 Slab 108

Table IV-15 : Configurations G5 to G10 – slab 108.

			slab 108 (th=31cm, soil 1, dowelled			
			εmax	gauge	qm °C	Geq °C/cm
G5	**A380-800 26.7t/w**	WLG	76	135	11.7	-0.07
		BLG	74	135	10.4	-0.05
G6	**A380-800F 28.5t/w**	WLG	-49	133	11.3	-0.05
		BLG	69	111	12.8	0.11
G7	**A380-900S 28.5t/w**	WLG	83	111	15.9	0.06
		BLG	74	111	16.6	0.02
G8	**A340 & B777-300ER 26.6t/w**	A340	66	111	11.7	0.10
		B777	61	111	13.2	0.21
G9	**MD11 27.8t/w**	WLG	73	135	17.6	-0.08
		CLG	88	135	16.3	-0.07
G10	**B747-400 23.2t/w**	WLG	63	135	18.9	-0.06
		BLG	-38	121	16.5	-0.14

IV.1.4.4 Conclusions

Mainly the maximum strains are obtained for the longitudinal gauges close to the longitudinal joint. The study shows that the A380 is not more aggressive for the pavement than a B747, whatever the thermal conditions. The 2 wheels bogie added for the A380-900S permit to decrease the BLG strains.

IV.2 Fatigue tests

The fatigue tests on rigid pavement is the ultimate experimentation of the rigid phase and consists in comparing damage caused by heavy aircrafts such as the A380-800F and the B777-300ER on 4 different sections of the experimental runway. Tests are completed up to failure. This part describes the principles results obtained during the fatigue tests and a comparison of the two previous aircrafts aggressiveness to the pavement.
The fatigue campaign started the 10th December 2002 and ended on 11th September 2003 after 5,692 passages for the large 7.5 m x 7.5 m slabs and 10,054 passages for the short 5 m x 5 m slabs.

IV.2.1Recall of the runway characteristics

As detailed in the first part of the brochure, the experimental runway is built according to traditionally techniques used for cement concrete pavements and instrumented with the constraint of having representative sections of an operational pavement. The four sections characteristics are detailed Figure IV-25 and Table IV-16.

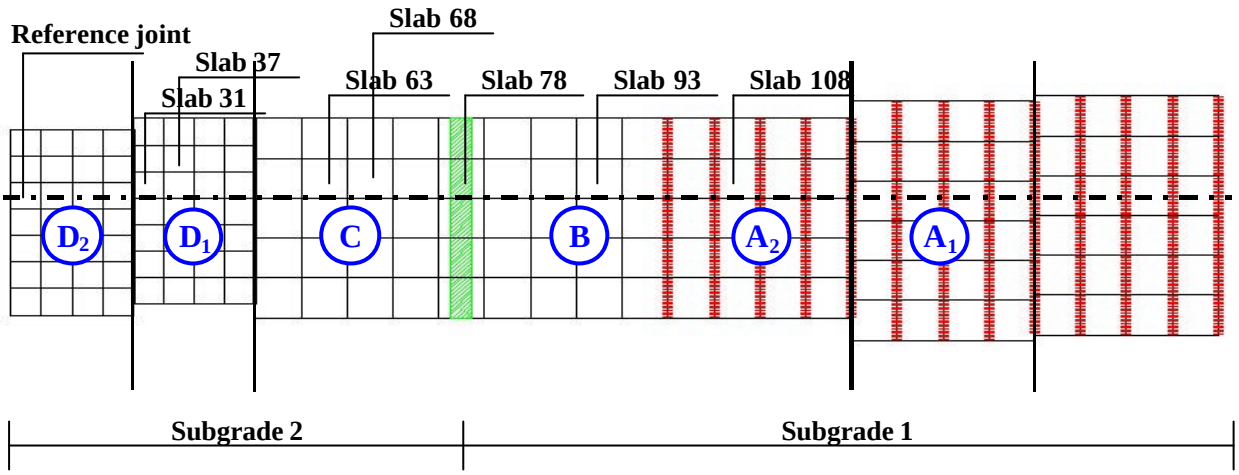

Figure IV-25 : Experimental runway.

Table IV-16 : Runway sections characteristics.

	Sections A_1 & A_2	Section **B**	Section **C**	Sections D_1 & D_2
joints	dowelled	un-dowelled		
Slab dimension	7.5 m x 7.5 m			5 m x 5 m
Concrete E = 35000 MPa	0.31 m	0.42 m	0.37 m	
Lean concrete E = 24000 MPa	0.15 m			
untreated graded aggregate (3-31.5 mm)	0.43 m		0.30 m	
Subgrade (Westergaard modulus)	Subgrade 1 - K_0 = 25 MN/m^3		Subgrade 2 - K_0 = 80 MN/m^3	

IV.2.2Simulation vehicle configuration and trajectory

A PEP facility is a full scale simulation vehicle, composed of four bogies, able to represent the effects on pavement of an aircraft wide body. Different configurations of landing gears representing the main aircrafts can simulated. During the fatigue test, the simulation vehicle (Figure IV-26) permits to reproduce simultaneously partial landing gears of the A380-800F and the B777-300ER. It is composed of three bogies of the A380-800F landing gear (one 4-wheels wing landing gear and the two 6-wheels body landing gear) and one bogie of the B777-300ER main landing gear (one 6 wheels wing landing gear) as shown in Figure IV-27.
The distance between the B777 bogie and the A380 is sufficiently large to avoid any interference between these two aircrafts. It is fixed at 7 meters.

Figure IV-26 : Fatigue simulation vehicle configuration.

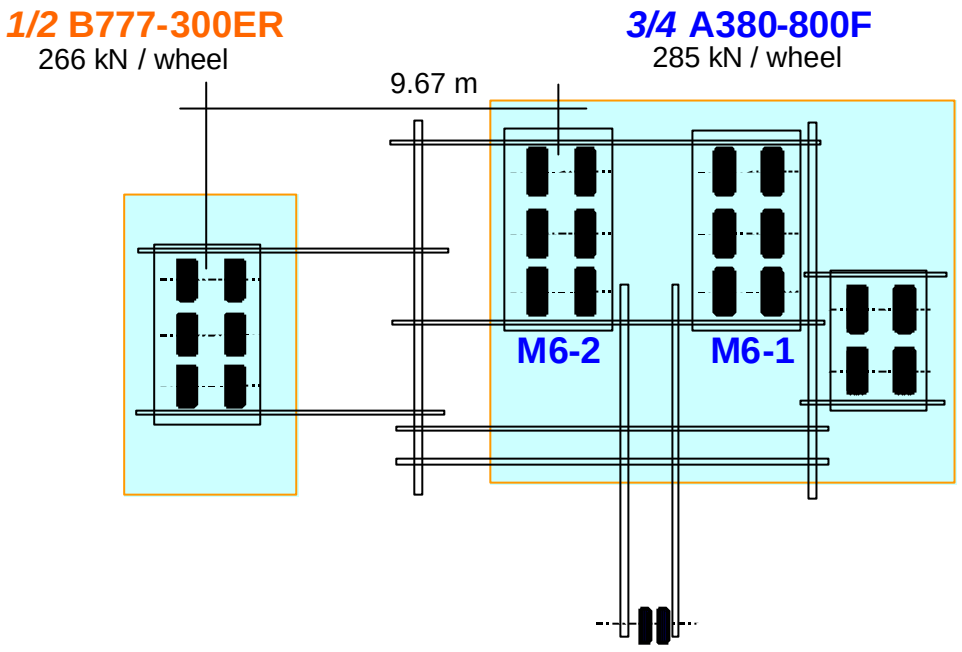

Figure IV-27 : Airplanes partial landing gears configuration.

Table IV-17 contains the geometrical characteristics of the simulation vehicle used for the fatigue test. The type of bogie and the load per wheel are also presented.

Table IV-17 : Simulation vehicle configuration characteristics.

Aircraft	Bogie type	Wheel track (m)	Wheel base (m)	Load per wheel (kN)
A380-800F	4 wheels	1.35	1.70	285
A380-800F (M6-1 & M6-2)	6 wheels	1.53/1.55/1.53	1.70	285
B777-300ER	6 wheels	1.40	1.46	266

The simulation vehicle drives along a straight line, so that the transversal position of the bogies on the slabs (distance to the longitudinal “reference” joint) is varying according to its longitudinal position on the runway. The runway is divided in straight sections, located by vertical bold dark lines, as shown in Figure IV-28. The central straight section is sub-divided into sub-sections (**A2**,

B & **C**) which characteristics are varying from one to another (slab size, subgrade or dowelling). Note the longitudinal "reference" joint and the location of the slabs number 31, 37, 63, 68, 78, 93 & 108 mentioned above.

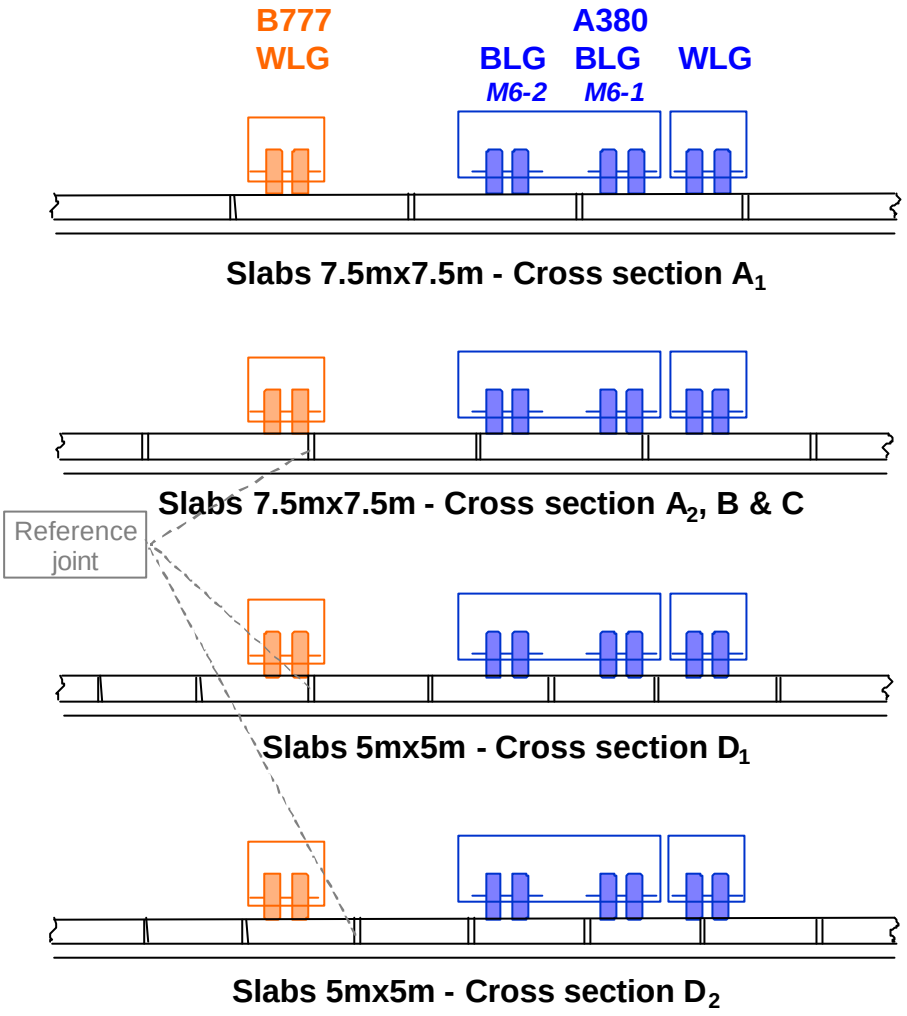

Figure IV-28 : Trajectories of the simulation vehicle.

IV.2.3Pavement condition follow up

Table IV-18 : Pavement condition follow-up.

Measurement	Tool	Modality
Cracks	Visual survey	2 times per a day
Service index determination	Visual survey	Every 1,000 passes
Topographical survey	Laser measurement over all pavement surface	Every 1,000 passes
Slab rocking	Displacement gauge	Only at 0 and 1,000 passes

The pavement integrity is evaluated by means of surface cracking, slab rocking measurements, pavement Service Index and topography survey. The procedure may differ from one parameter measured to another, so Table IV-18 resumes the pavement survey.

IV.2.4Slabs rocking measurements

A first criteria for estimating a structural pavement integrity is the slab rocking that occur with traffic. Slab rocking is measured until average temperature in slab was inferior or equal to 10°C. Above this temperature, we consider that slabs joints are closed and don't present any differential vertical displacement. Slab rocking was only measured before the start of fatigue campaign and after 1,000 passages. The measurement, using a LVDT sensor fixed on a mass, was done on the middle of a transversal joint as shown Figure IV-29.

Figure IV-29 : Slab rocking measurement device.

These measurements permit to underline that there is no evolution on doweled slabs at the opposite of non-doweled slabs. Figure IV-30 shows the slab rocking evolution for the two 6 wheels bogies of the A380 (M6-1 & M6-2) and for the 6 wheels bogie of the B777. The efficiency of the slab dowelling (sections A_2 & A_1) is clearly observed in these graphics, whereas the rocking is roughly homogeneous in the other sections. The last graphic presents a comparison of the slab rocking measured for the two aircrafts at 1,000 passages leading to the conclusion that both aircrafts induce the same order of slab rocking.

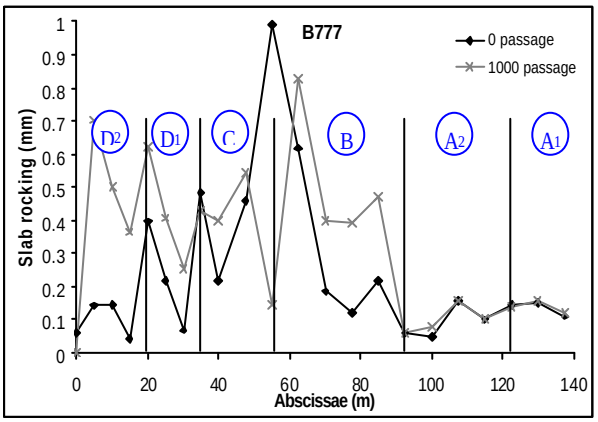

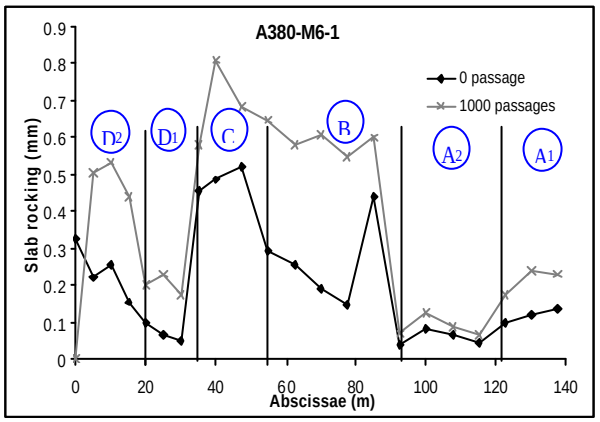

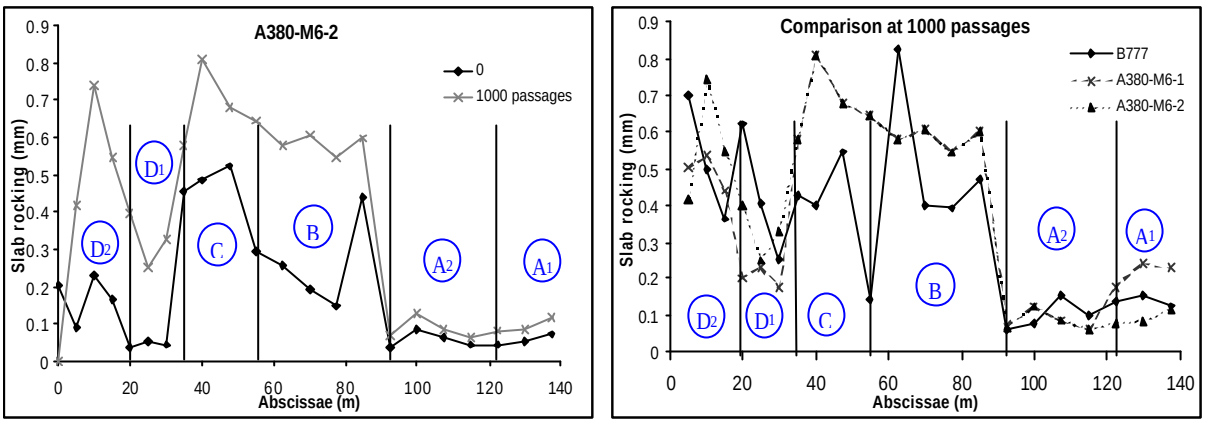

Figure IV-30 : Slab rocking measurements.

IV.2.5Cracks survey

Figure IV-31 : (a) Example of longitudinal crack – (b) Example of corner cracks.

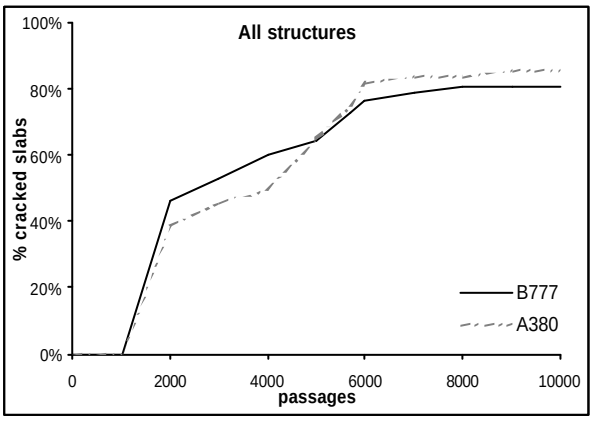

Figure IV-32 : % of cracked slabs.

Figure IV-31 shows an example of longitudinal and corner cracks. Figure IV-32 presents the proportion of cracked slabs (number of cracked slabs vs. number of circulated slabs extended to the complete configuration) according to the number of passages for the B777-300ER and the

A380-800F. For both airplanes, the slab cracking start after 1,000 passages and reach at least 81 % at the end of the test. Note that, as previously mentioned, only the 5 m x 5 m slabs are circulated between 5,692 and 10,054 passages. Globally, the two aircrafts have a similar effect on slabs degradation. The proportion of cracking slabs are very similar. It has been observed that slabs cracking are poorly correlated with cold temperature and pluviometry. The revelation of cracking at the surface is a particular phenomenon : infrequent instantaneous apparition, but frequently delayed apparition (after rest period – night or week end breaks).
Figure IV-33 details the cracks on the four different sections **A**, **B**, **C** & **D** of the runway. Note that the A380 seems to be more aggressive for short slabs. Concerning 7.5 m un-dowelled slabs on subgrade 1, the B777 cracks 100 % of the circulated slabs whereas the A380 levels off at 80 %. For this same subgrade, the B777 damages faster the runway than the A380.
As a conclusion, we can estimate that, on the same subgrade :

- ✓ 5 m x 5 m slabs have a incontestable better behaviour than 7.5 m x 7.5 m slabs
- ✓ Non-dowelled slabs (42 cm thick) have a better behaviour than dowelled ones (31 cm thick), which means that the thickness design has overestimated the dowelling effect
- ✓ The damage caused in pavement by the two aircrafts are very closed

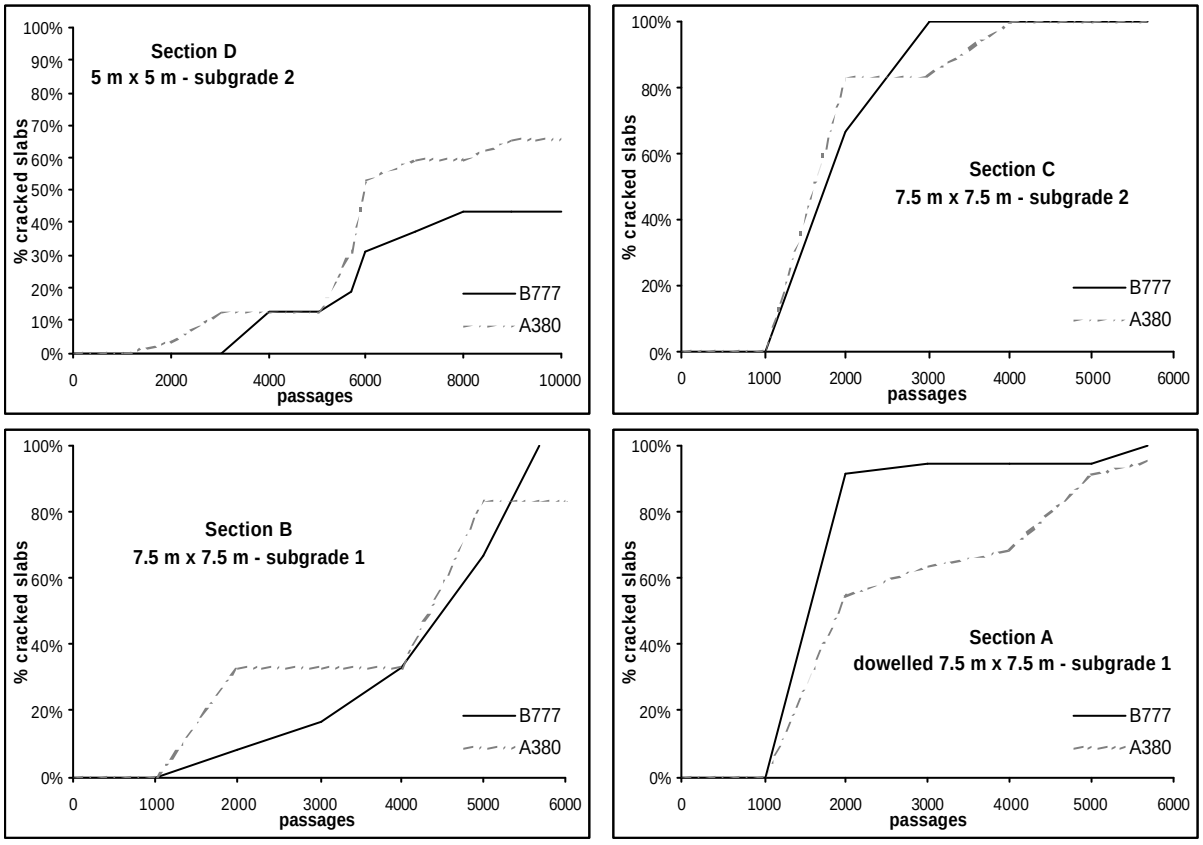

Figure IV-33 : % of cracked slabs according to the runway section.

The crack survey leads to calculate a Service Index value (the French PCI) using the "Service Index method". It permits to characterize the pavement integrity at a given time with a value comprise between 0 and 100 (IS = 100 i.e. no deterioration, IS = 10 i.e. runway should be closed).

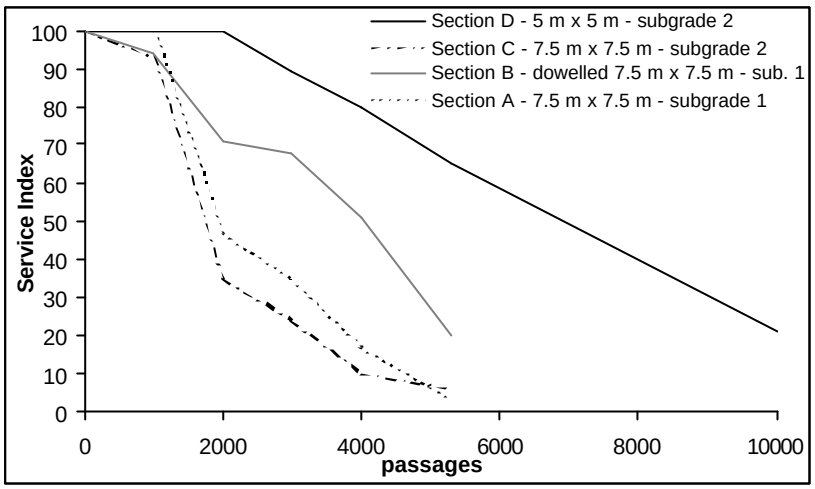

Figure IV-34 : Evolution of Service Index value.

The Service Index value is determined after a visual survey of superficial distresses (type of deterioration and level of gravity). Results are compiled by a software created by the STAC (French Civil Aviation Technical Department). Service index calculation is realized every 1,000 passages, until 5,000 passages, on each sections and also at 10,000 passages on 5 m x 5 m slabs. Figure IV-34 presents the evolution of the Service Index. This one confirm the better behaviour of the short slabs (5 m x 5 m). It also shows again that dowelling effect is over-estimated by the French design method. The service Index evolution for the sections **A** & **C** are very similar, meaning that the variations of bearing capacity of the subgrade are correctly estimated by the design.

IV.2.6Topographical survey

A topographical survey of the pavement surface is added to pavement deterioration survey. Nine points of control (one on each corner, one on the slab center and one on the middle of each joint) are measured for each slab. This control is realized at the beginning of fatigue campaign, then every 1,000 passages between 2,000 and 5,000 passages and finally after 10,000 passages. Vertical displacements are calculated in relative height in comparison with a fixed reference point out of the experimental runway. The topographical survey shows a general settling of the whole pavement during fatigue tests. The permanent vertical displacement due to B777 and A380-M6-2 are equivalent (Figure IV-35). The higher level concerning the A380-M6-1 may be explained by the proximity of the 4 wheels bogie that can induce interferences. This displacement is lower for the 5 m x 5 m slabs for all gear types.

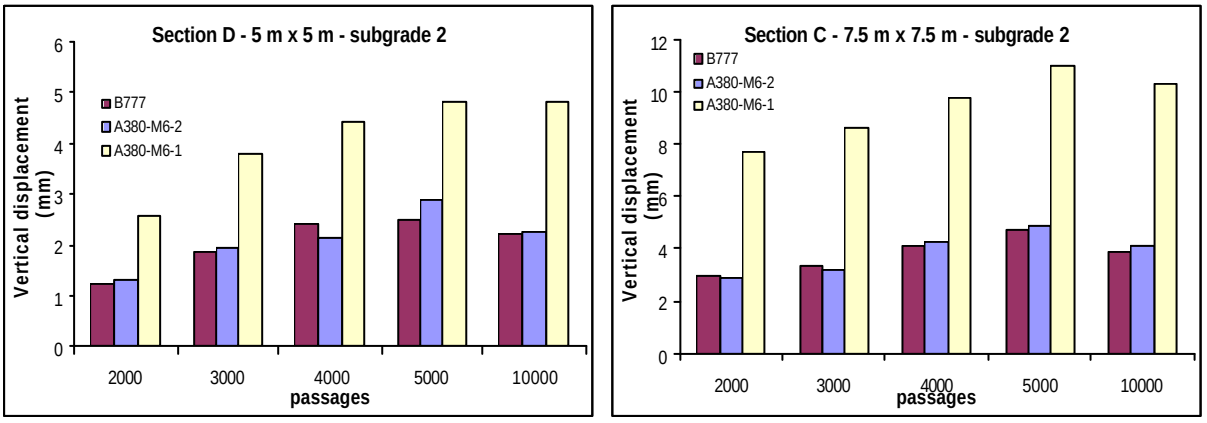

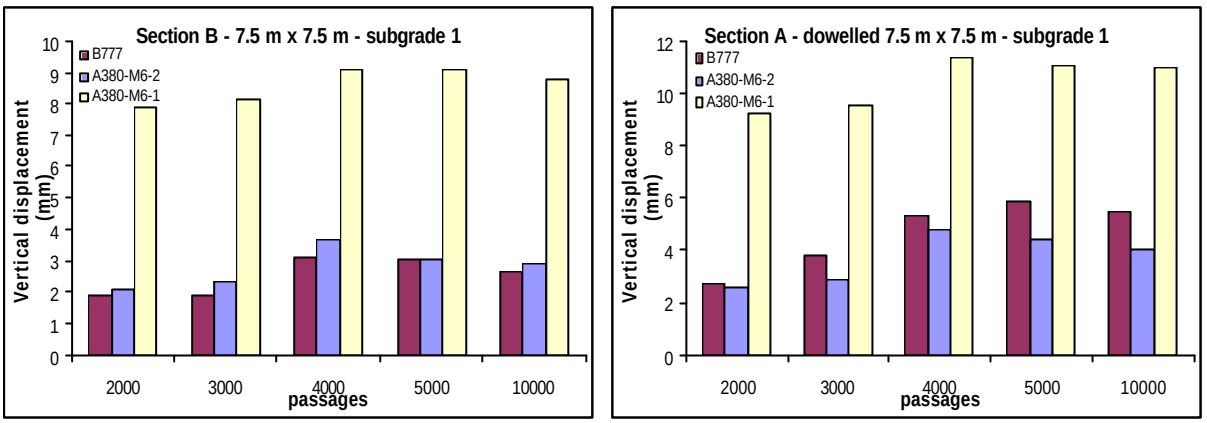

Figure IV-35 : Evolution of topography on bogie trajectory.

IV.2.7Post-auscultation

During the PEP, the development of cracks at the surface of the pavement is representative of damage observed on real concrete structures, which means that the traffic effects are correctly reproduced by the Airbus simulator. The cracks survey described above permits to observe both bottom to top and top to bottom cracks. Nevertheless, top to bottom cracking appears to be the most frequent, as detailed below.

IV.2.7.1 Core sampling

Core sampling has two principal aims :

- ✓ Checking the interface between the concrete slab and the lean concrete at different localization, more or less close to the center or to the border of the slabs
- ✓ Determination of the direction of propagation of cracks : top to bottom or bottom to top

23 boreholes have been realised all over the trafficked slabs, in order to characterize these two factors. Some boreholes are done across cracks visible at the surface, and other are done on safe zone. An example of core is presented. It shows two boreholes realised on slab 63, as shown Figure IV-36. A bounded interface and a crack along the concrete thickness are visible on Figure IV-37.

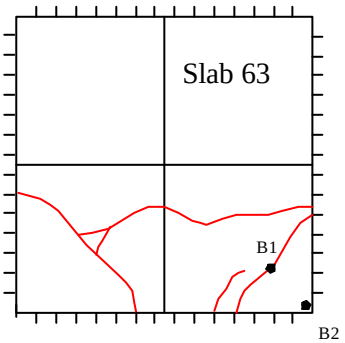

Figure IV-36 : Slab 63 – localization of the boreholes B1 & B2.

Figure IV-37 : Slab 63 – Core sampling.

All the cores permit to note the interface condition : on 23 cores, 15 were bounded and 8 sliding. Only 10 cores can be exploited for cracks propagation interpretation, the other 13 were realised on safe zone. Among the 10 cracked cores, 8 illustrate partial top to bottom cracks (Figure IV-38 for the slab 78), and the two last ones were full depth, as illustrated Figure IV-37. These results don't differentiate corner cracks or center cracks.

Figure IV-38 : Slab 78 – borehole b3 – Partial top to bottom crack.

IV.2.7.2 Splitting tensile strength tests

In order to find an explanation to the top to bottom cracking, it is decided to realise laboratory splitting tensile strength tests. These are realised on horizontal samples with a slenderness ratio equal to 1 for the slabs 108, 93 and 68 and 1.4 for the samples of the slabs 31 & 37 (2 samples for these slabs). The samples are taken on the wearing course and at the base of the cement concrete slab. The following table shows the results obtained for samples of the slabs 108, 93, 68, 37 & 31 (see Figure IV-25 for localization).

We can note a significant difference (on the order of 20 %) between the top and the bottom of the slabs. The bottom base is "harder" than the top. It may be due to the vibrators of the slip-form paver that are placed in the inferior part. A bigger desiccation of the concrete surface can induce a concrete with lower performance.

Table IV-19 : Splitting tensile strength tests results.

	Slab 108	Slab 93	Slab 68	Slab 37-1	Slab 37-2	Slab 31-1	Slab 31-2
Section	**A_2**	**B**	**C**	**D_1**	**D_1**	**D_1**	**D_1**
Top slab indirect tensile strength (Mpa)	3.64	4.06	3.85	4.28	4.46	4.59	4.78
Bottom slab indirect tensile strength (Mpa)	4.35	4.37	4.76	5.22	5.41	6.22	3.87
Difference (%)	19.51	7.63	23.64	21.96	21.3	35.51	-19.04

IV.2.7.3 Conclusions

In conclusion, we can estimate that the cumulative damage effects of A380-800F (MTOW 600 tons) and B777-300ER (MTOW 340 tons) are very close. The pavement auscultation permits to note that damage results mainly from top to bottom cracking (at corner, along central longitudinal slab axis, …). Bottom to top cracking appears to be less extended. This tendency has still to be evaluated and may be due to a difference between the wearing course and the slab base stiffness. It is also important to note that cracking affects trafficked as not trafficked slabs. On trafficked slabs, cracking is not systematically localized in or near the wheel paths. Concrete pavement functioning is strongly influenced by contact condition between slabs and their foundation. This contact condition depends on temperature condition, but also on the warping deformation due to initial concrete moisture heterogeneity. Globally, a better behavior of short slabs (5mx5m) is observed.

IV.3 Special tests

The special tests have been realised in order to explain or to underline certain specific phenomenon that occurred during the tests.

IV.3.1G6 – fatigue trajectory

Visual checks permit to observe a large number of longitudinal cracks over the A380 6 wheels bogie trajectory. It was decided to do a complementary test on instrumented slabs. Using the G6 configuration, the aim is here to highlight the strains that could explain the longitudinal cracks that occurred in the middle of many slabs. For practical reasons, the test occurs only on slabs 68 and 93. A 6 wheels bogie runs on trajectory T3 so that the second 6 wheels bogie is running on the same slab, as shown Figure IV-39 (Same thing for slab 68, with only a quarter instrumented). In order to take into account thermal effects, the running have been realised with negative (comprise between –0.2 and –0.1 °C/cm) and positive (comprise between 0.2 and 0.3 °C/cm) thermal equivalent gradient. The results presented below exhibit the maximum strain value measured on the gauges for a negative and a positive thermal equivalent gradient.

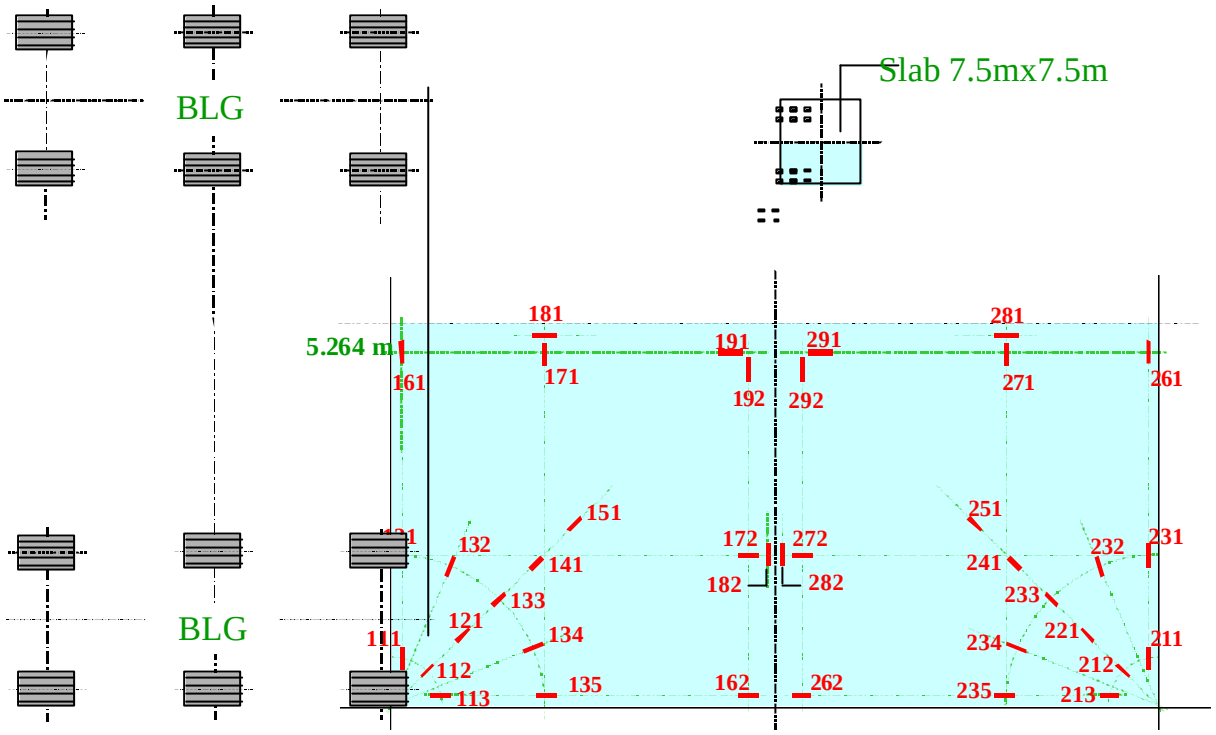

Figure IV-39 : Complementary test on slab 93 _ config. G6 trajectory T3.

IV.3.1.1 Slab 68

Table IV-20 : Complementary G6 test – slab 68.

	GradTeq = -0.134 °C / cm (le 11/04/2003 6h05)	**GradTeq = 0.235 °C / cm** (le 17/04/2003 10h41)
68-111 (e_{max} / µ-strains)	/	/
68-112 (e_{max} / µ-strains)	/	/
68-113 (e_{max} / µ-strains)	/	/
68-121 (e_{max} / µ-strains)	-20.86	-20.11
68-131 (e_{max} / µ-strains)	28.31	22.35
68-132 (e_{max} / µ-strains)	/	/
68-133 (e_{max} / µ-strains)	-11.92	-11.92
68-134 (e_{max} / µ-strains)	/	/
68-135 (e_{max} / µ-strains)	/	/
68-141 (e_{max} / µ-strains)	10.43	-10.43
68-151 (e_{max} / µ-strains)	-11.18	14.15
68-161 (e_{max} / µ-strains)	-38.74	-28.31
68-162 (e_{max} / µ-strains)	**46.94**	**47.68**
68-171 (e_{max} / µ-strains)	-24.58	-20.86
68-172 (e_{max} / µ-strains)	20.11	26.08
68-181 (e_{max} / µ-strains)	-10.43	10.43
68-182 (e_{max} / µ-strains)	-17.14	8.19
68-191 (e_{max} / µ-strains)	5.96	8.94
68-192 (e_{max} / µ-strains)	-16.39	-17.14

the maximum strains are measured on the gauge 68-162, that means a longitudinal strain along the joint of the slab (bold type). The maximum transversal strain (red type) is obtained on the gauge 68-161. This means that the surface of the slab support tensile strain, but the level reached can't explain a crack. Note that for this slab, the thermal conditions don't induce important modifications of the strains. This may be explained by good contact condition between the slab and the lean concrete.

IV.3.1.2 Slab 93

Table IV-21 : Complementary G6 test – slab 93.

	GradTeq = -0.134 °C/cm (le 11/04/2003 6h05)	**GradTeq = 0.235 °C/cm** (le 17/04/2003 10h41)
93-111 (e_{max} / µ-strains)	/	/
93-112 (e_{max} / µ-strains)	/	/
93-113 (e_{max} / µ-strains)	/	/
93-121 (e_{max} / µ-strains)	-37.25	-11.92
93-131 (e_{max} / µ-strains)	14.15	29.06
93-132 (e_{max} / µ-strains)	-10.43	11.18
93-133 (e_{max} / µ-strains)	-26.82	-8.94
93-134 (e_{max} / µ-strains)	-32.78	20.86
93-135 (e_{max} / µ-strains)	43.96	37.99
93-141 (e_{max} / µ-strains)	-21.6	17.14
93-151 (e_{max} / µ-strains)	17.14	20.86
93-161 (e_{max} / µ-strains)	-37.25	-24.58
93-162 (e_{max} / µ-strains)	**/**	**/**
93-171 (e_{max} / µ-strains)	28.31	35.01
93-172 (e_{max} / µ-strains)	/	/
93-181 (e_{max} / µ-strains)	-20.86	-18.62
93-182 (e_{max} / µ-strains)	-5.96	11.92
93-191 (e_{max} / µ-strains)	15.64	22.35
93-192 (e_{max} / µ-strains)	-20.86	-17.14
93-211 (e_{max} / µ-strains)	/	/
93-212 (e_{max} / µ-strains)	-40.23	-29.06
93-213 (e_{max} / µ-strains)	31.29	-23.09
93-221 (e_{max} / µ-strains)	-68.54	-33.53
93-231 (e_{max} / µ-strains)	-8.94	23.09
93-232 (e_{max} / µ-strains)	-36.5	-11.92
93-233 (e_{max} / µ-strains)	-65.56	-29.06
93-234 (e_{max} / µ-strains)	**-66.31**	**-29.06**
93-235 (e_{max} / µ-strains)	-51.4	32.78
93-241 (e_{max} / µ-strains)	/	/
93-251 (e_{max} / µ-strains)	-40.23	19.37
93-261 (e_{max} / µ-strains)	-62.58	-32.03
93-262 (e_{max} / µ-strains)	43.96	37.25
93-271 (e_{max} / µ-strains)	23.09	29.8
93-272 (e_{max} / µ-strains)	-30.55	-18.62
93-281 (e_{max} / µ-strains)	-8.94	8.94
93-282 (e_{max} / µ-strains)	-5.96	9.69
93-291 (e_{max} / µ-strains)	7.45	10.43
93-292 (e_{max} / µ-strains)	-17.88	-14.9

The maximum strain is here measured on the gauge 93-234, in the corner of the slab as shown in the previous table in bold type. The tensile strain obtained on the slab surface is quite high. Note the influence of the thermal conditions that decrease the strain of more than 50 % in that case. More generally, the slab 93 is sensitive to thermal variations as shown by the differences between the two columns of Table IV-21. The transversal strain measured on the gauge 93-261 with a negative equivalent thermal gradient reach a comparable level as the one obtained for the gauge 93-234. So the tensile strain induced in the surface can be aggressive for the structure. This is here the association of a moving load and thermal condition that produce such an effect.

IV.3.2G4 completed : full A340-600 landing gear

This parts deals with bogie interaction. The complete A340-600 landing gear is reconstitute using a supplementary 4 wheels bogie. The simulator is equipped with the A340-600 centreline and wing landing gears. The second wing landing gear is added thanks to the STAB truck so as to reconstitute the full A340-600 landing gear. Purely static acquisitions are carried out. The slab is firstly loaded by the two modules of the simulator and secondly by the second WLG. The acquisition differences between the two loading permit to measure the bogie interaction for a given thermal situation.

IV.4 General conclusions

It is not easy to conclude concerning a so complex study comprising so many parameters. However, we try to derive strong conclusions from the experimental data collected during the rigid PEP.

Firstly, the possibilities of harmonization of the experimental results are limited because of the complexity of a highly three-dimensional and not linear problem.

To contradict generally accepted ideas, the 6 wheel-bogie may not be the most severe configuration, as shown by measurements underlining the distribution of internal stresses in the slab.

Unfortunately, the experimental strain distribution does not reflect the usual “Corner cracking” at top of the slab.

The effect of dowelled seems to be overestimated in the initial design.

An important place will be necessary given to the numerical modelling in order to optimize the benefits of the PEP.

So, concrete pavement behaviour is really complex !

V. NUMERICAL MODELLING

The numerical modelling of the PEP concrete pavement presented in this technical report mainly focuses on two following topics:

- Validation and calibration of a three-dimensional finite element model for simulating the concrete slabs subjected both to thermal loading and traffic loading. The FEM software Cesar-LCPC has been selected for that purpose.
- Numerical simulation of the fatigue test in order to explain the mechanism of the damage that has been observed.

A more extensive numerical analysis of the whole experimental results obtained during the Rigid PEP has also been carried out. It particularly concerns the simulation with Cesar-LCPC of the three bogies configurations (2, 4 & 6 wheels) and the seven real aircraft landing gears that have been tested. Since these different static tests have not been realized with similar climatic condition, as it as been pointed out above, the experimental results cannot be directly translated into neither the comparison of the aggressiveness of the tested configurations, nor the explicit effects of the loading parameters such as wheel-track, base track, weight per wheel, etc… For that reason, the recourse to numerical modelling is necessary in order to reach these results, which rank among the objectives of the PEP. This extensive numerical analysis is not presented in this report, but will be a part of a coming technical annex, which will be issued from the PEP team.

V.1 Pavement model assumptions

V.1.1 Kinematical hypothesis

The model used for finite element analysis is three-dimensional, each layer of the structure being discretized with hexahedral isoparametric elements with 20 nodes. All the materials are considered in the modelling as linear-elastic. The possibility for the slab to separate from its lean concrete foundation, due to temperature curling, is taken into account. This is made by integrating between slab and foundation, special hexahedral contact elements with 16 nodes, fitted with their own contact law. Cesar-LCPC leads to the determination of the contact area between slab and foundation in addition to stresses, strains and displacements in the structure.

V.1.2 Mechanical characteristics

The mechanical characteristics of the different layers are obtained by adjustments between experimental and numerical results, mainly for what concerns longitudinal, transversal strains and deflections. The values of Young modulus resulting from these adjustments are then compared with the ones issued from tests realized on the runway or on samples in laboratory. Table V-1 presented the values obtained for the different materials:

Table V-1 : Elastic parameters of materials for then FEM calculations

	Young Modulus	Poisson coefficient
Slab PCC	40 000 MPa	0.25

Lean concrete	23 100 MPa	0.25
UGM untreated graded materials	150 MPa	0.35
Subgrade	50 MPa	0.35

The coefficient of thermal contraction-expansion used for the concrete is a=10e-06 /°C.

Figure V-.1 presents an example of the modelized pavement structure, with simplifications due to the 2 plane-symmetries. Only one slab is represented on this example, whereas more completed calculations, including up to nine slabs, has also been realized.

Figure V-1 : Slab n°93, one slab model

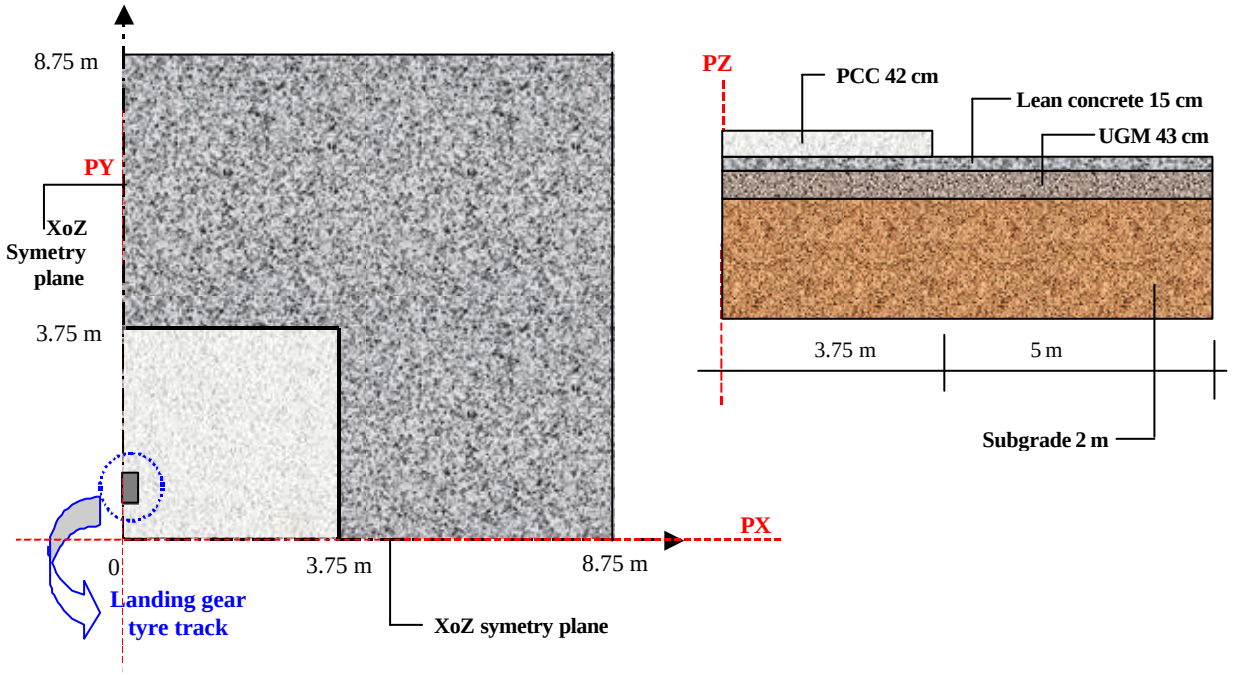

Figure V-2 shows an example of the non-deformed mesh and an example of the deformation of the one slab model, loaded by a positive gradient temperature profile without bogie load. In this example the mesh contains 7 339 nodes, 1 530 hexahedral elements and 120 contacts elements.

Figure V-2 : View of the 3D mesh and calculated deformation, one slab model

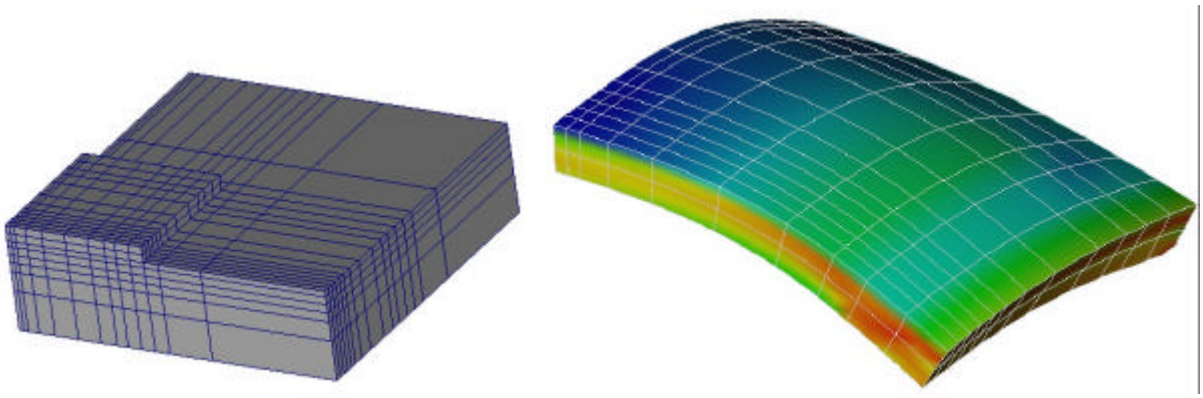

Figure V-3 shows two examples of the deformed mesh resulting from the 9-slabs model.

Figure V-3 : View of the 9-slabs model – Deformation calculated for positive and negative thermal gradient temperature profile

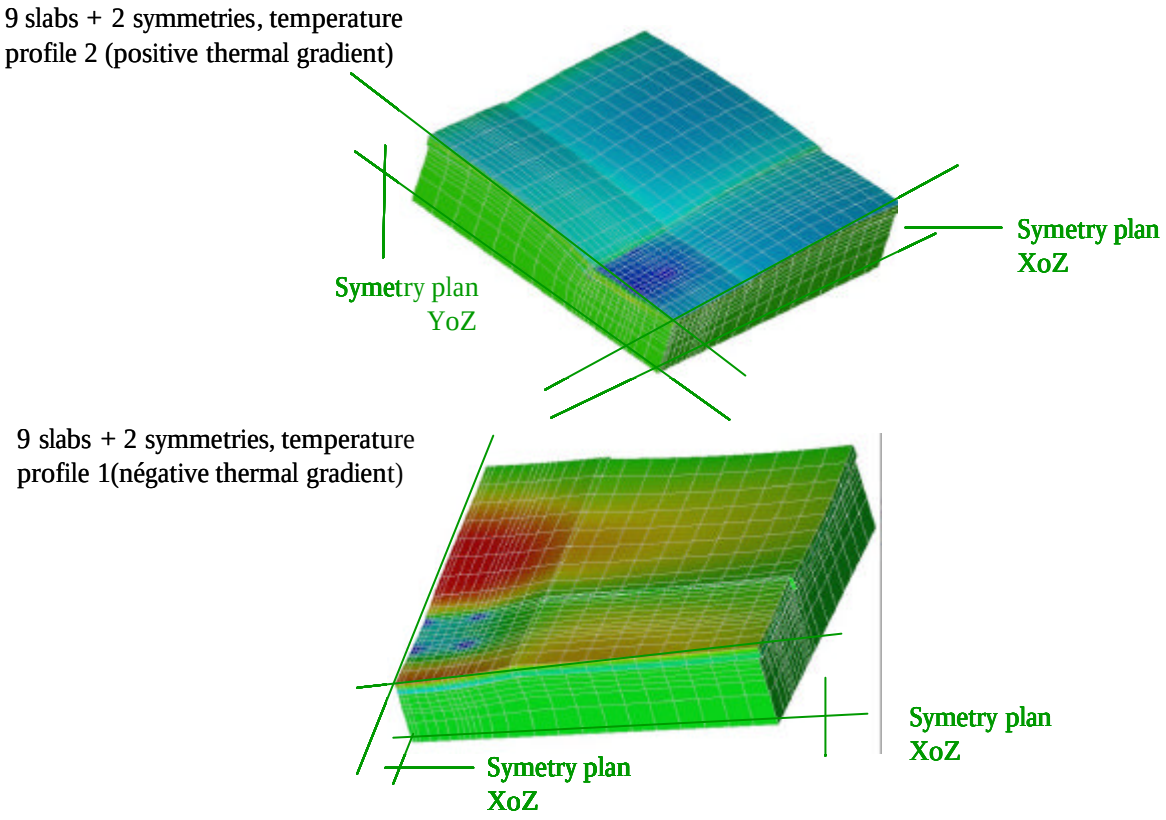

V.2 Assessment of the 3D FEM model

V.2.1 Main modelling options

For the 3D FEM calculations presented in this report, the choice of the parameters and the main modelling options such as the number of modelled slabs and joint transfer simulation are issued from adjustments between measurement and numerical results for the slab n° 93 (not dowelled slab 7.5mx7.5 m on subgrade n°1, 42 cm thick). Finally the main characteristics of the model are as follows:

- Material parameters: cf. table V-1
- Number of slabs:
  - Corner loading (2 bogies M6-1 and M6-2 of the A380): 6 slabs;

- Corner loading (1 bogies of the A380 or the B777): 4 slabs;
- Load at the middle of longitudinal joint (2 bogies M6-1 and M6-2 of the A380): 2 slabs;
- Load at the middle of longitudinal joint (1 bogies of the A380 or B777): 2 slabs;
- Load (bogie) at the middle of transversal joint: 2 slabs;
- Load at the center of the slab: 1 slab.

- Load transfer modelling:
  - Longitudinal joint: assimilated to a perfect hinge (total transfer of the shearing stress)
  - Transversal joint (slab n°93): opening 1mm (no load transfer)
- Bogie load simulation: uniform vertical static pressure applied on a rectangular contact area, 50 cm (longitudinal edge) x 38 cm (transversal edge).
- Thermal condition: temperatures in concrete (slabs and foundation layer) are reproduced by the vertical measured profile, extended to each point in the horizontal plane.
- Interface condition between the slabs and the lean concrete foundation layer: The successive attempts of adjustment between the measurement and calculation results have led to the following interface modelling: it is assumed to be perfectly sliding on strip 0.75 m wide around the periphery of the slab. On the opposite, the central surface ,6 m x 6 m square, is assumed to be perfectly bonded (full adhesion between slabs and lean concrete layer). This modelling of the interface results from the iterative adjustment procedure, and is also in good accordance with the observation done on the core samples after the end of the fatigue test (cf. IV.2.7.1).

V.2.2 Examples of validation calculations

The level of adjustment between the experimental and the numerical results is illustrated for the slab n°93, considering two different thermal conditions shown in Table V-2. These temperature profiles, named profile T1 and profile T2, were measured in April 2003. They have been selected for the model validation, because they are respectively representative of the temperature distributions showing the minimal negative thermal gradient (profile T1), and the maximal positive thermal gradient (profile T2), for which deflexion and strains measurement created by the reference load G1-2 are available.

Table V-2 : Example of temperature profiles for the model validation

Depth of the temperature sensor	Profile T1 - 06h20 11 April 2003 Equivalent linear gradient -0.133 °C/cm	Profile T2 - 10h40 17 April 2003 Equivalent linear gradient : -+0.233 °C/cm
0	9.9 0C	29.3 °C
3 cm	10.3 °C	25.6 °C
6 cm	10.9 °C	22.3 °C
11 cm	11.9 °C	19.4 °C
16 cm	12.6 °C	17.3 °C
21 cm	13.4 °C	16.5 °C
26 cm	14.0 °C	16.2 °C
31 cm	14.6 °C	16.2 °C

36 cm	14.9 °C	16.2 °C
37 cm	15.0 °C	16.1 °C
41 cm	15.2 °C	16.1 °C
42 cm	15.2 °C	16.1 °C
46 cm	15.4 °C	16.0 °C
51 cm	15.4 °C	16.0 °C

Tables V-3 presents an example of comparison between the strain measurement and the numerical results, in the case of thermal loading alone (temperature profile n°2, no bogie running on the pavement). The strain values shown in table V-3 are relative strain values corresponding to the fluctuation of the strain measurement between 10h40 (profile 2 time) and 08h25 which is the time corresponding to an appreciatively uniform vertical temperature profile in the slabs. A satisfactory correlation between experimental measures and calculated results is obtained. It observed that for this type of loading (no bogie load), the four gauges n°191, 291, 192 and 292 should ideally deliver the same measured strain, because they are located at the centre of a square slab. The observed fluctuations (17 to 23 µstrains) are indicative of the accuracy of the measure.

Table V-3 : Example of adjustment between measurement and numerical results, slab n°93, temperature profile n°2

Strain gauge n°	Experimental values (µstrains)	Numerical results (µstrains)	Relative difference
191	17	18	7%
291	19		-5%
192	23		24%
292	22		-19%

Table V-4 presents a comparison between the FEM numerical results and the experimental values in the case of loading by the reference load G1-2, for the positive non-linear temperature profile. The 2 wheels of the reference bogie G1-2 bogie are loaded at 25 kN, the contact pressure on pavement is 1.29 Mpa, and the track is 1.4 m. The measured and the numerical strains shown in this example are the relative value corresponding to the effects of the bogie. The results present a satisfactory concordance with a maximum relative gap between numerical and experimental of 21 %, in spite of the simplification hypothesis comprised in the model.

Table V-4 : Example of adjustment between measurement and numerical results, slab n°93, temperature profile n°2 and reference load G1-2

Strain gauge n°	Experimental values (µstrains)	Numerical results (µstrains)	Relative difference
191	18	15	-21%
291	13		9%
192	10	12	11%
292	11		4%

V.3 Application of the 3D FEM model to the fatigue test

V.3.1 Data for the FEM calculations

Numerical simulations of the fatigue campaign have been performed for slab n°93, for the following loading conditions and interface hypothesis:

- Temperature condition. Three conditions have been considered:
  - Vertical profile T1 (negative gradient);
  - Vertical profile T2 (positive gradient);
  - Uniform vertical thermal distribution in concrete.

Figure V-4 : Positions of the isolated bogie and the 2-bogies load considered by the FEM calculations of the fatigue test

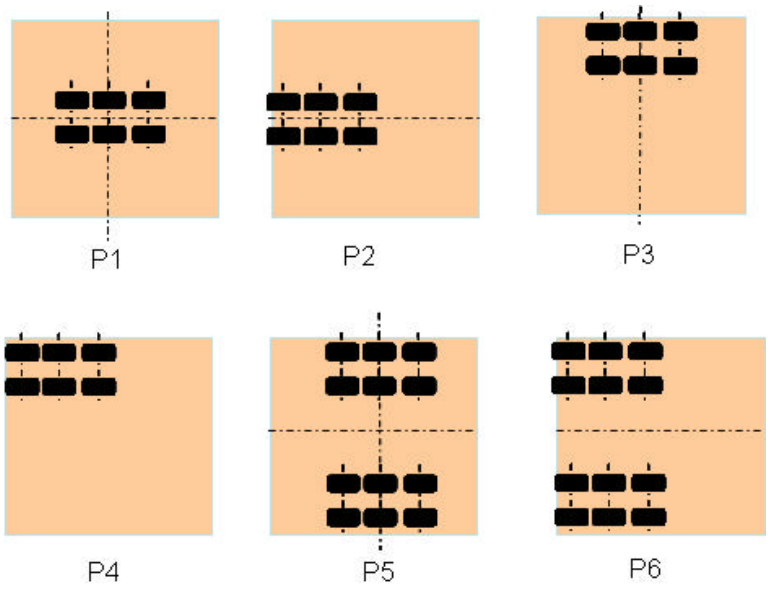

P1: Isolated bogie at the center of the slab (A380 and B777)

P2: Isolated bogie at the middle of the transversal joint, tangent to the joint (A380 and B777)

P3: Isolated bogie at the middle of the longitudinal joint, tangent to the joint (A380 and B777)

P4: Isolated bogie at the corner of the slab (A380 and B777)

P5: 2-bogie load centred on the slab (A380)

P6: 2-bogie load tangent to the transversal joint (A380)

- Interface between the slabs and the lean concrete foundation layer. Two bounding conditions have been considered:

- Semi-bounded interface described above (cf. V.2.1). It comprises the central square area 6m x 6m perfectly bonded, and the surrounding area assumed to be completely sliding (no interface shear stresses);
- Sliding interface condition over the whole contact area between the slab and the foundation layer. This second interface condition has not been identified on the PEP rigid pavement. However it has been considered because the completely sliding condition is normally representative of in service highly trafficked pavement.

- Bogie configuration. Three load configurations, comprising the A380 and the B777 6-wheels bogie used for the fatigue test, have been taken into account:
  - The isolated 6-wheel A380-800F bogie: 28.5 tons per wheel, contact pressure 1.49 MPa, wheel-track 1.54 m and wheel base 1.70 m;
  - The two 6-wheel A380-800F bogies with the same characteristics as above, distance 5.26 m from axe to axe;
  - The isolated 6-wheel B777-300ER bogie: 26.6 tons per wheel, contact pressure 1.50 MPa, wheel-track 1.40 m and wheel base 1.45 m.

- Load positioning at the surface of the pavement. The 3D FEM calculations have been performed for 4 different positioning of the isolated 6-wheel bogie of the A380 and the B777. For the two 6-wheel bogies load, two additional positioning have been considered. These different load positions are shown in figure V-4. They have been selected because they correspond to the load positions for which maximal tensile stresses in concrete may normally occur, depending on the pavement structure and geometry, the soil bearing capacity, the load characteristics, the thermal loading, etc.

V.3.2 Results of FEM calculations : tensile stresses in the slabs

Tables V-5 and V-6 present a part of the results of the FEM modelling, for the different calculation cases listed above. For each case, the maximal computed tensile stress in the loaded concrete slab is shown, with indication about its direction and its location. The following notations are used:

T :	transversal stress
L :	longitudinal stress
D :	diagonal stress
Bottom :	stress located at the bottom of the slab
Top :	stress located at the top of the slab
Center :	stress located at the center of the slab

Unit for stress value : MPa

It has to be pointed out that the stress indicated in tables V-5 and V-6 represent absolute value, incorporating the effects of :

- The bogie load;
- The weight of the slab;

- The internal temperature in concrete. In case of linear vertical temperature profile, thermal stresses are nil. In case of non-linear profile, auto-equilibrium stresses, which may be not negligible at all, are generated in the slab.

Table V-5 : FEM modelling of the fatigue test, calculated stresses (MPa) – part 1

Load position : P1 – center of the slab					
A380 – One 6-wheel bogie			B777 – One 6-wheel bogie		
Interface condition : semi-bonded					
Temperature : T1	Temperature : T2	Temperature : Uniform	Temperature : T1	Temperature : T2	Temperature : uniform
1.29	3.41	1.61	**1.35**	**3.67**	**1.69**
T-bottom	T-bottom	T-bottom	T-bottom	T-bottom	T-bottom
Center	Center	Center	Center	Center	Center
Interface condition : completely sliding					
Temperature : T1	Temperature : T2	Temperature : Uniform	Temperature : T1	Temperature : T2	Temperature : uniform
2.12	4.49	3.79	2.21	4.71	4.05
T-bottom	T-bottom	T-bottom	T-bottom	T-bottom	T-bottom
Center	Center	Center	Center	Center	Center

Load position : P2 – tangent to transversal joint at its middle					
A380 – One 6-wheel bogie			B777 – One 6-wheel bogie		
Interface condition : semi-bonded					
Temperature : T1	Temperature : T2	Temperature : uniform	Temperature : T1	Temperature : T2	Temperature : uniform
3.08	3.95	3.44	**3.23**	**4.19**	**3.61**
T-bottom	T-bottom	T-bottom	T-bottom	T-bottom	T-bottom
Middle TJ	Middle TJ	Middle TJ	Middle TJ	Middle TJ	Middle TJ
Interface condition : completely sliding					
Temperature : T1	Temperature : T2	Temperature : uniform	Temperature : T1	Temperature : T2	Temperature : uniform
4.53	5.65	4.97	**4.65**	**5.68**	**5.02**
T-bottom	T-bottom	T-bottom	T-bottom	T-bottom	T-bottom
Middle TJ	Middle TJ	Middle TJ	Middle TJ	Middle TJ	Middle TJ

Load position : P3– tangent to longitudinal joint at its middle					
A380 – One 6-wheel bogie			B777 – One 6-wheel bogie		
Interface condition : semi-bonded					
Temperature : T1	Temperature : T2	Temperature : uniform	Temperature : T1	Temperature : T2	Temperature : uniform
2.48	3.42	2.83	**2.92**	**3.80**	**3.28**
L-bottom	L-bottom	L-bottom	L-bottom	L-bottom	L-bottom
Middle LJ	Middle LJ	Middle LJ	Middle LJ	Middle LJ	Middle LJ
Interface condition : completely sliding					
Temperature : T1	Temperature : T2	Temperature : uniform	Temperature : T1	Temperature : T2	Temperature : Uniform
3.37	4.61	3.86	**4.42**	**5.56**	**4.89**
L-bottom	L-bottom	L-bottom	L-bottom	L-bottom	L-bottom
Middle LJ	Middle LJ	Middle LJ	Middle LJ	Middle LJ	Middle LJ

Table V-6 : FEM modelling of the fatigue test, calculated stresses (MPa) – part 2

Load position : P4 – corner loading

A380 – One 6-wheel bogie			B777 – One 6-wheel bogie		
Interface condition : semi-bonded					
Temperature : T1	Temperature : T2	Temperature : uniform	Temperature : T1	Temperature : T2	Temperature : uniform
4.63	6.17	6.00	**4.90**	**6.51**	**6.25**
D-bottom	D-bottom	D-bottom	D-bottom	D-bottom	D-bottom
Corner	Corner	Corner	Corner	Corner	Corner
Interface condition : completely sliding					
Temperature : T1	Temperature : T2	Temperature : uniform	Temperature : T1	Temperature : T2	Temperature : uniform
4.88	6.55	6.12	**5.02**	**6.73**	**6.26**
D-bottom	D-bottom	D-bottom	D-bottom	D-bottom	D-bottom
Corner	Corner	Corner	Corner	Corner	Corner

Load position : P5 – 2 bogies tangent to the longitudinal joints at middle

A380 – Two 6-wheel bogies loading			B777 – Two 6-wheel bogies loading		
Interface condition : semi-bonded					
Temperature : T1	Temperature : T2	Temperature : uniform	Temperature : T1	Temperature : T2	Temperature : uniform
5.35	2.87	2.87			
T-top	L-bottom	L-bottom			
Center	Middle LJ	Middle LJ			
Interface condition : completely sliding					
Temperature : T1	Temperature : T2	Temperature : uniform	Temperature : T1	Temperature : T2	Temperature : uniform
5.77	3.90	3.90			
T-top	L-bottom	L-bottom			
Center	Middle LJ	Middle LJ			

Load position : P6– 2 bogies at the corners of the slab

A380 – Two 6-wheel bogies loading			B777 – Two 6-wheel bogies loading		
Interface condition : semi-bonded					
Temperature : T1	Temperature : T2	Temperature : uniform	Temperature : T1	Temperature : T2	Temperature : uniform
5.47	**7.43**	6.05			
D-bottom	D-bottom	D-bottom			
Corner	Corner	Corner			
Interface condition : completely sliding					
Temperature : T1	Temperature : T2	Temperature : uniform	Temperature : T1	Temperature : T2	Temperature : uniform
5.16	**7.40**	5.56			
D-bottom	D-bottom	D-bottom			
Corner	Corner	Corner			

The main following facts about the aggressiveness of the two tested configurations can be already deduced from these results, which will be detailed in a complementary technical annex.

- Effects of the A380 and B777 6-wheel isolated bogie. The tensile stresses induced in the concrete slabs by these two bogies are very close. The B777 6-wheel bogie generally induces slightly higher tensile stresses that the isolated 6-wheel bogie of the A380. This is the consequence of more compact geometry (wheel base and track) of the B777. The direct effect of the broader geometry of the A380 bogie is to compensate the heavier load applied to its A380 (+1.9 tons per wheel more than the B777 bogie).

- Among the four simulated locations of the load at the surface of the pavement, the corner loading produces the maximum tensile stress. Two points has to be emphasized:

  - These maximum stress values are reached at the bottom of the slab, whereas the corner maximum stresses are often observed at the top of the slab according to various numerical approaches. The type of loads modelized for this study (3 axles) and their large geometry, as the relatively low bearing capacity of the support, probably contribute to this permutation.
  - The level of the tensile stresses obtained (6.7 MPa for the B777, 6.6 MPa for the A380) is really high in comparison with the bending tensile strength of the concrete (class BC6, strength 6 MPa according to laboratory tests). This probably explain the fast development of cracking that has been observed during the PEP fatigue test.

- Effects of the two 6-wheel bogies of the A380. For the trajectory selected for the FEM calculations (running of the two boogies along the two opposite longitudinal joints of the slab), high tensile stresses are obtained at the top of the slab in its middle (5.35 to 5.77 MPa). The generalized longitudinal median crack (top to bottom) observed at the surface of the slabs trafficked by the two A380 bogies during the fatigue campaign has to be related to these results.
- The very high stresses developed at the bottom of the slab in the corner (up to 7.4 MPa) also may explain the frequent corner cracks in case of slab trafficked by the two A380 bogies along longitudinal joints.
  We have to underline that the main important position such as the edge, the centre of the slab with one or two gear loading allow typical slab behaviour representative of the operational aircraft movement, excepted the figures P6 because whatever a 45 or 60 meters runway width, with 7.5 m² slab, the runway center line is generally a longitudinal joint.
- Obviously, we assume that A380-800 (pax version at 560 tons) will produce stress value significantly lower than the heavier freighter version but it was necessary to select the most aggressive version in order to take into account the A380-800 weight potential increase. The A380-800 model will be modelized in the version-2 of this technical report as well as the other wide bodies aircraft such as B747-400, A340-500/-600, MD-11 and B777-300.

ANNEXE 1

French method for dimensioning rigid aeronautical pavements

Like the flexible pavements (see previous brochure), the calculation load is determined for each aircraft. It depends on the total weight of the aircraft, the distribution of the weights on the main landing gear and a weighting coefficient dependent upon the considered areas.

As reference design traffic is 10 movements per day, we convert the design-critical traffic (N movements per day at weighted load P) to an equivalent traffic (10 movements per day at equivalent load P') by formula: $P' = P \times (1.2 - 0.2 \cdot Log(N))$.

The second input parameter of the method is the subgrade. It is characterised by its Westergaard modulus K_0, expressed in MN/m^3, determined by plate tests.

This modulus is then corrected according to the equivalent foundation course thickness thanks to the graph below. The equivalent thickness is the sum of the real thicknesses weighted by the material equivalence coefficient of the layer concerned (see flexible PEP brochure). We obtain the corrected modulus K_C.

Practices concerning the lower foundations have constantly changed. The aeronautical runways of the NATO bases constructed by the Americans in France after the 2nd World War generally had no foundation at all, the slab resting directly on the base ground, or at best, on a capping layer. Foundations of natural aggregates then treated aggregates with hydraulic binders appeared gradually. The current trend is to recommend no-erodible foundations in order to avoid pumping and steps in the slabs. In practice, a lean concrete or porous concrete slab is placed between the surface slab and the granular subbase (possibly treated elsewhere).

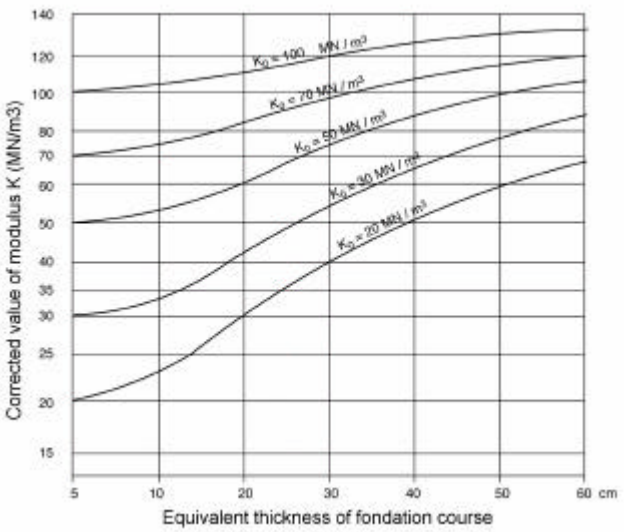

The concrete specified for French aeronautical pavements is BC6, that is with a minimum bending tensile strength on fracture of the concrete measured at 90 days of 6 MPa (equivalent to a characteristic strength determined by splitting tests of around 3 to 3.33 MPa).
The allowable bending tensile stress σ_a of concrete is given by:

$$s_a = \frac{f_t}{SF}$$

where *SF*: safety factor, *SF* = 1.8 for good load transfers (dowelled slabs)
SF = 2.6 for poor load transfers (undowelled slabs)

The thickness of the concrete slab is then read directly on graphs plotted for each aircraft according to the Portland Cement Association (PCA) method.

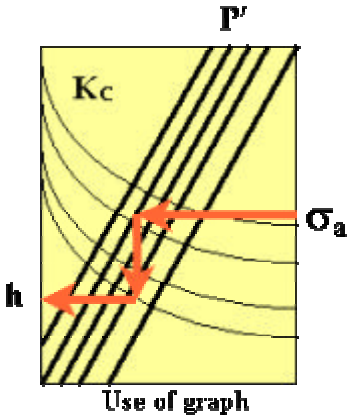

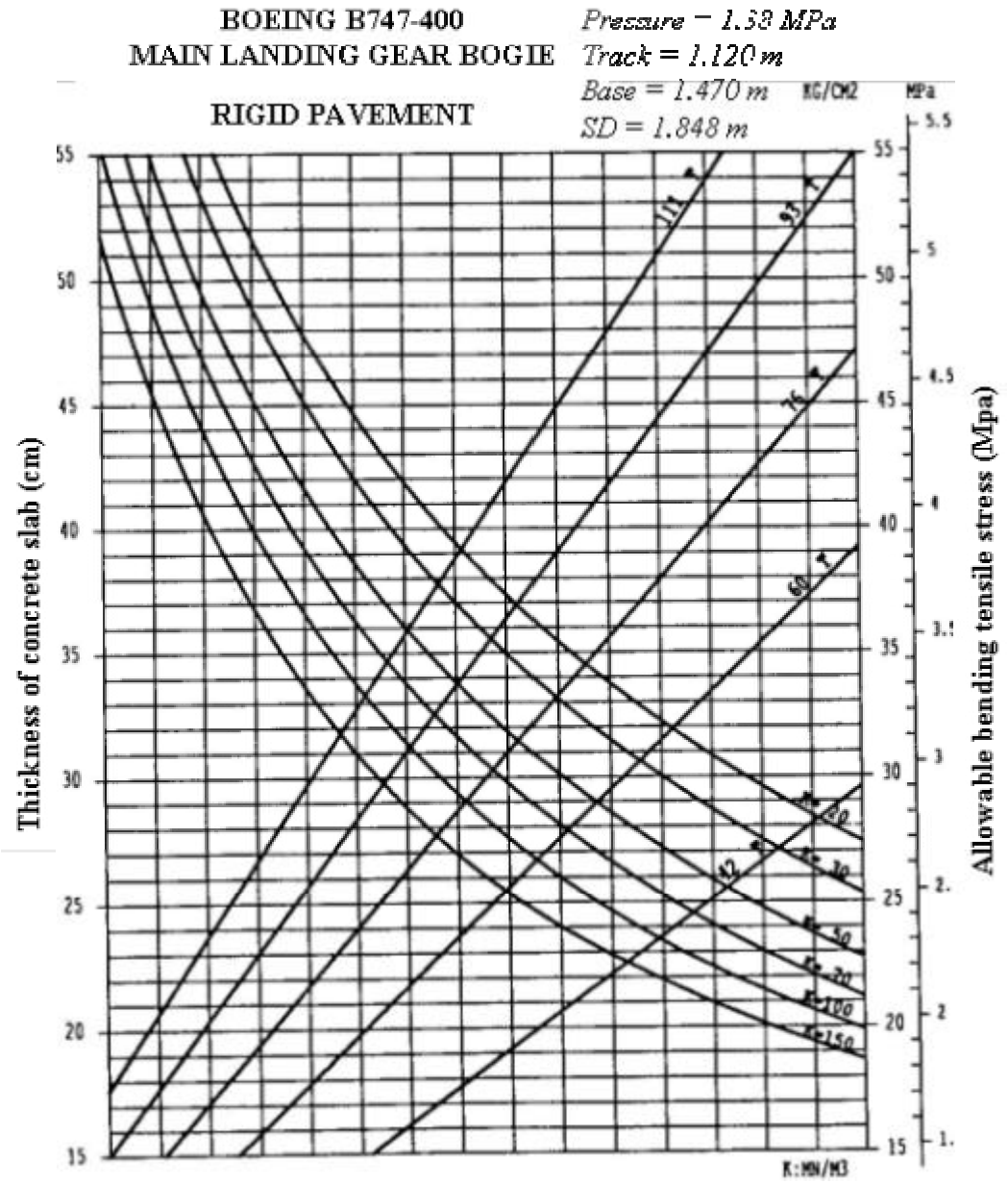

The coefficient K_C is also used to characterize the class of the pavement in the sense used in the ACN / PCN method:

Class A	**$K_C > 120$ MN / m^3**
Class B	**120 MN / m^3 > K_C > 60 MN / m^3**
Class C	**60 MN / m^3 > K_C > 25 MN / m^3**
Class D	**25 MN / m^3 > K_C**

ANNEXE 2

Historic of the tested configurations

The static campaign starts on 14 December 2001 and ends on 07 October 2002. Eleven different configurations are tested using the simulator. Additional static tests are performed during the fatigue campaign (especially in March 2003).

Date	14/12/01	19/12/01– 17/01/02	22/01 – 26/02/02	11/03 – 14/03/02	21/03 – 25/03/02
Tested configuration	G0	G1	G2	G8	G4

Date	03/04 – 08/04/02	09/04 – 12/04/02	22/04 – 25/04/02	23/09 – 25/09/02	3/10 – 07/10/02
Tested configuration	G5	G6	G7	G10	G9

ANNEXE 3

Summary of the tested configurations

Aircraft	Family	Configuration	Number of bogies	Bogie B1							Bogie B2							Bogie B3							Bogie B4						
				YY (cm)	N (wheels)	Track (cm)	Base(cm)	W/Wheel (tons)	Pns (bars)	YY (cm)	N (wheels)	Track (cm)	Base (cm)	W/wheel (tons)	Pns (bars)	YY (cm)	N (wheels)	Track (cm)	Base (cm)	W/wheel (tons)	Pns (bars)	YY (cm)	N (wheels)	Track (cm)	Base (cm)	W/wheel (tons)	Pns (bars)					
	G1	G1_1	1	0	2	140	0	20	10.3																						
	G1	G1_2SG	1	0	2	140	0	25	12.9																						
	G1	G1_2	1	0	2	140	0	30	15.4																						
	G1	G1_3	1	0	2	140	0	25	12.9																						
	G1	G1_4	1	0	2	130	0	25	12.9																						
	G1	G1_5	1	0	2	150	0	25	12.9																						
	G2	G2_1	2	0	4	140	170	20	10.3	1030	6	140	170	20	10.3																
	G2	G2_2	2	0	4	140	170	25	12.9	930	6	140	170	25	12.9																
	G2	G2_3_1	2	0	4	140	170	30	15.4	930	6	140	170	30	15.4																
	G2	G2_3_2	2	0	4	140	170	28	14.7	930	6	140	170	28	14.7																
	G2	G2_4	2	0	4	140	160	25	12.9	930	6	140	160	25	12.9																
	G2	G2_5	2	0	4	140	180	25	12.9	930	6	140	180	25	12.9																
A340-600	G4	G4	2	0	4	140	199	29.6	15.5	534	4	117	199	26.6	13.8																
A380-800	G5	G5	3	0	4	135	170	26.7	13.8	359	6	154	170	26.7	13.8	886	6	154	170	26.7	13.8										
A360-800F	G6	G6	3	0	4	135	170	28.5	14.8	359	6	154	170	28.5	14.8	886	6	154	170	28.5	14.8										
A380-900S	G7	G7	4	0	4	135	170	28.5	14.8	359	6	154	170	28.5	14.8	622	2	105	0	28.5	14.8	886	6	154	170	28.5	14.8				
A340 & B777-300ER	G8	G8	2	0	4	140	199	26.6	13.7	930	6	140	146	26.6	16																
MD-11	G9	G9	3	0	4	137	163	27.8	14.4	533.5	2	96.1	0	24	12.7	1067	4	137	163	27.8	14.4										
B747-400	G10	G10	3	0	4	112	147	23.2	8.8	358	4	112	147	23.2	8.8	743	4	112	147	23.2	8.8										
A380-800 / B777-300ER	CF1	CF1	4	0	4	135	170	26.7	14.1	359	6	154	170	26.7	14.1	886	6	154	170	26.7	14.1	1853	6	140	146	26.6	16.4				
A380-800F / B777-300ER	CF2	CF2	4	0	4	135	170	28.5	16	359	6	154	170	28.5	16	886	6	154	170	28.5	16	1853	6	140	146	26.6	16.4				

ANNEXE 4

Service Index Method

With service index method, we can characterize the pavement condition at a given time. Service index is a value between 0 and 100 (IS= 100 → no deterioration, IS=10 → runway should be closed). The service index value is determined after a visual survey of superficial distresses (type of deterioration and level of gravity). Results are compiled by a software created by the STBA.

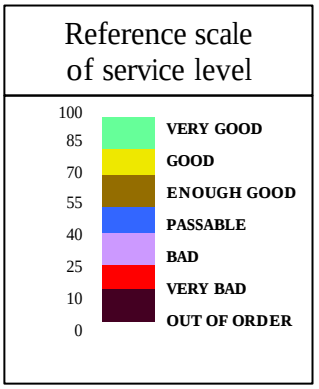

Fig. Distresses book of the STBA / DCIA – reference scale of service level.

To make the visual survey, you need the deterioration book written in 1984. Into it you can find all types of structure classified in two families : flexible pavement and rigid pavement. Each distress is illustrated and analyzed (cause and consequences).
On a rigid pavement, survey are made on each slab and distresses are characterized by their sort (10 different types) and their level of gravity (light, medium or high).

Calculation procedure
In the method, each doublet (type of distress, level of gravity) is converted in a numeric value meaning the influence of this distress on pavement quality. It is called “deducted value” (VD).
Deducted value is expressed like a malus applied on service level of pavement, taken by definition equal to 100 for a new pavement.

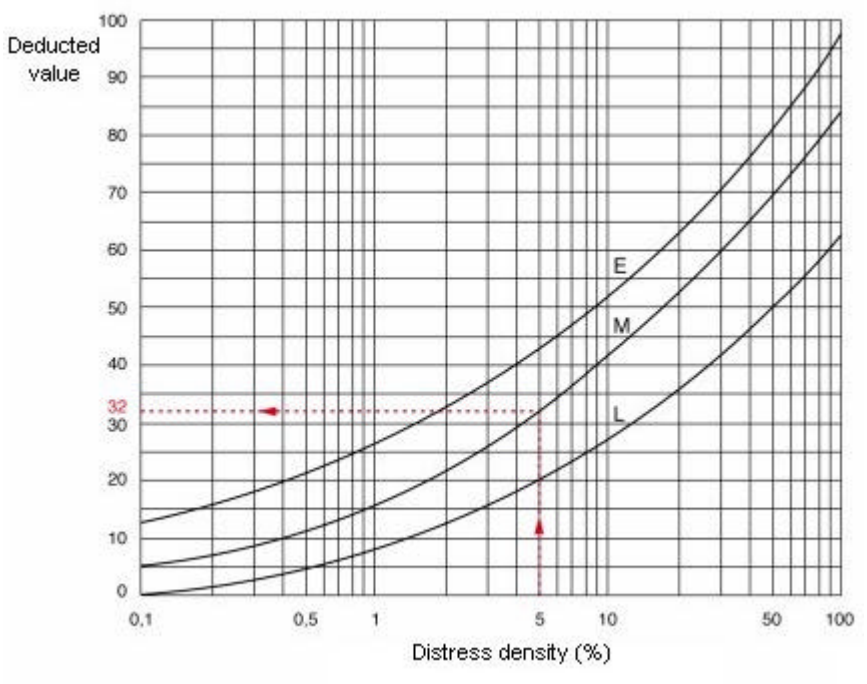

Fig. Example of deducted values curves

Sum of deducted value of each noticed distress is calculated on each inspected mesh. It's the total deducted value (VDT).
With total deducted value, using a new abacus, is determined a corrected deducted value (VDC) taking in account of significant distresses number (deducted value superior to 5). The ponderation of total deducted value relativize deterioration process of runway according to observed distress number.
Service index value is now defined by the formula : IS = 100 – Corrected deducted value.

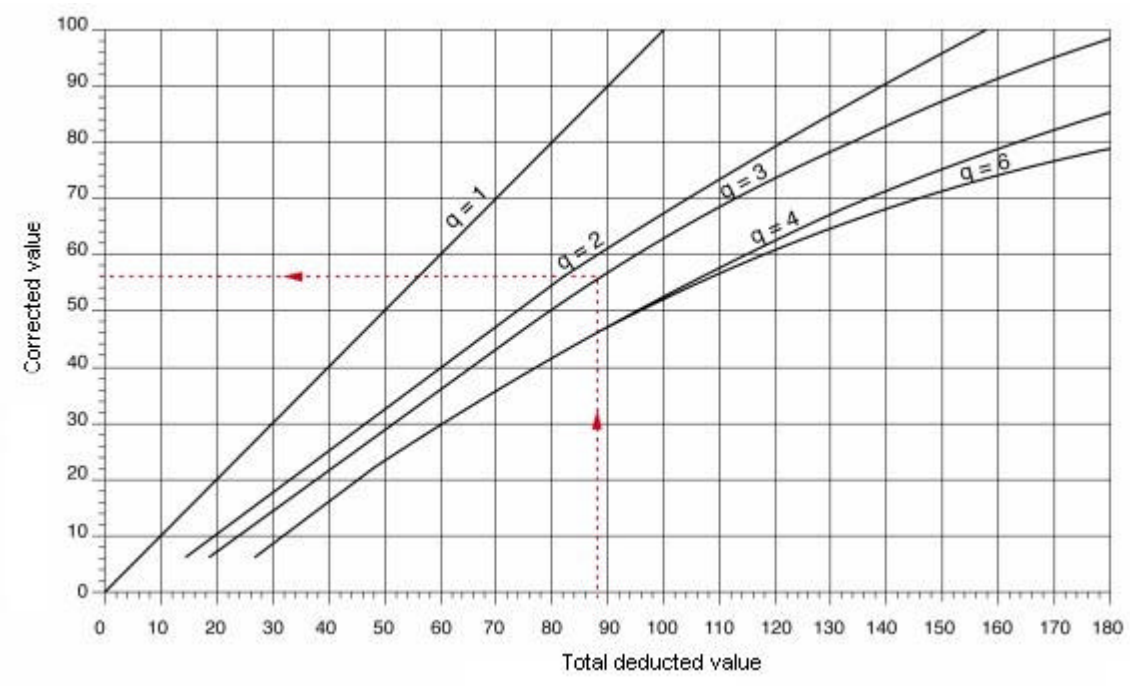

Fig. Abacus for correction of total deducted value (q is number of observed distress on mesh)

Abacus and software have been made from relationship between estimated deterioration states and observations on runway surface.

Noticed distresses :

	Structural distresses	Surface distresses
Rigid pavement	crack block crack corner crack pumping stairs	spalling scaling crazing deteriorated punctual repair joint default rubber deposit

ANNEXE 5

Historic of the pluviometry

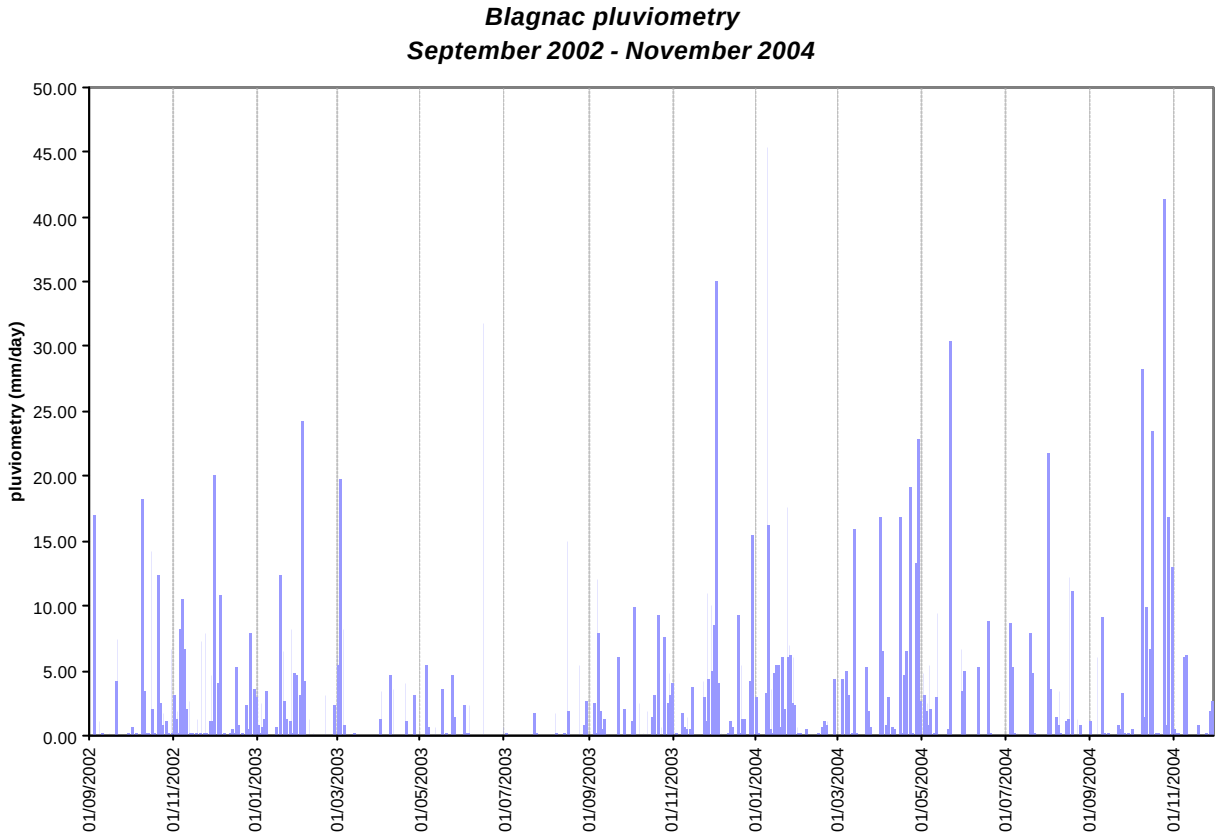

ANNEXE 6

P.E.P VEHICULE SIMULATOR

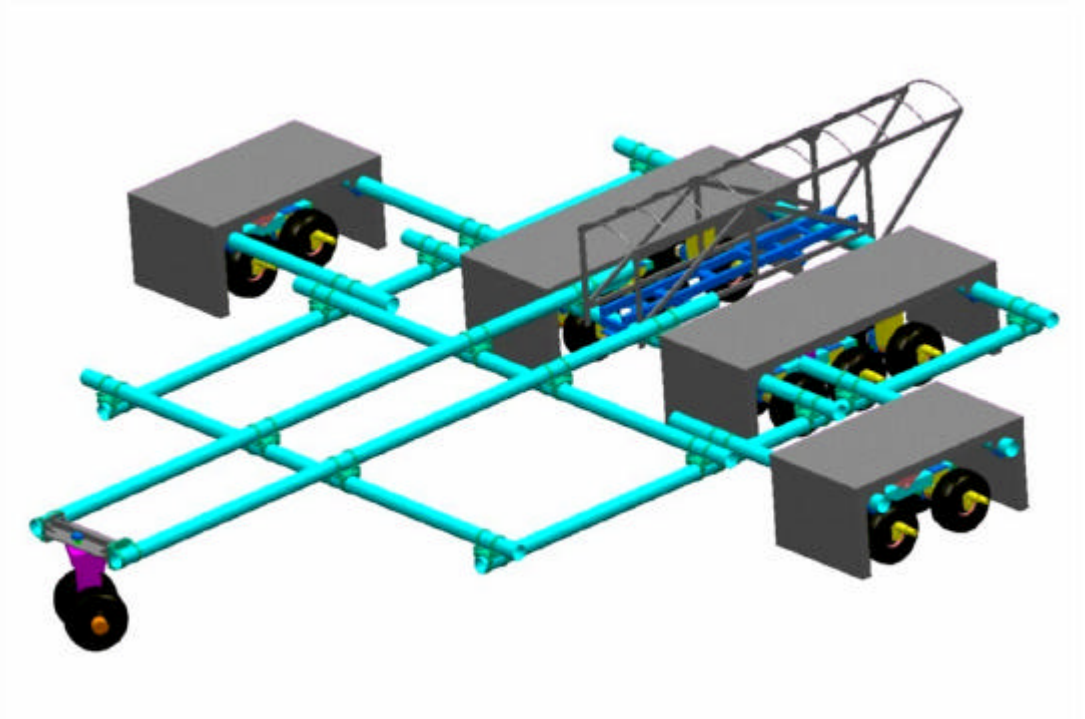

Modularity

The maximum mass of the simulation vehicle was 631T.
The different configurations with an identical load through each wheel are the followings:

- being 22 wheels with 2 steering wheels
- being 20 wheels with 2 steering wheels
- being 16 wheels with 2 steering wheels
- being 12 wheels with 2 steering wheels

The steering axle installed in front of the vehicle with a low load has not effect on the measure (13T).

Configurations with different loads by wheel are possible:
4 (114T) – 6 (143T) – 6 (172T) – 4 (93T) for example

Moreover, 2 modules are used to calibrate the measure equipment:
One with 2 or 6 wheels capability
One with 2 wheels capability only

These modules for calibration are not motorized (it must be towed).

Modules

The modules were made with 3 steel plates 220mm thickness. One of these plates constituted the horizontal tray, and the two other are assembled to the extremities of the tray.
The bearing subassembly was fixed under the tray.
The axles were articulated one time in case of 4 wheels module, or two times in case of 6 wheels module.
Each axle was cross-articulated.
This mounting was used to ensure that the system was isostatic and the load distribution by wheel for a module was identical.

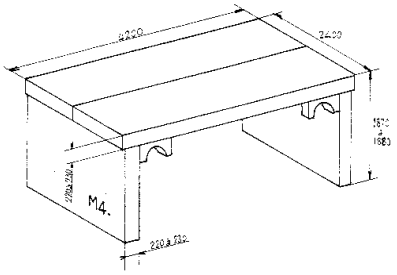

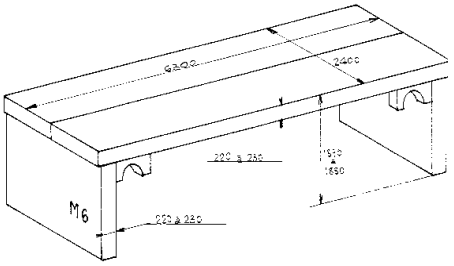

All modules can be configured :
Width between bogies
Width of the axles

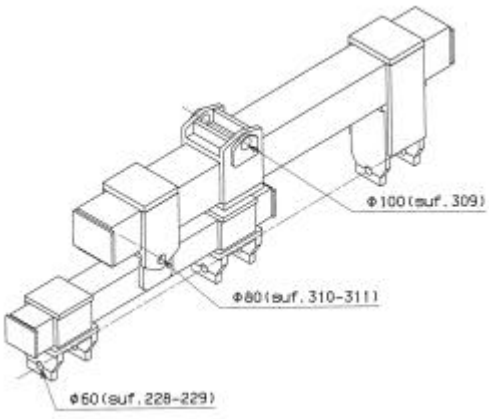

A reference module(as twin) had to be passed on flexible pavement before every simulator configuration, for the instrumentation calibration.(cf. § II-2-3)

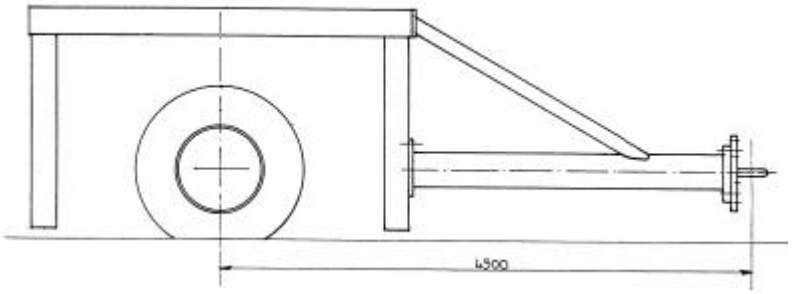

Wheels

The wheels were the same of the A340. The external sizes of the wheels are 1400mm for the diameter, and 530mm wide.
The rims were standards, but no nuts were used for fixing bolts. The screws fixed a crown with internal gears for the driving.

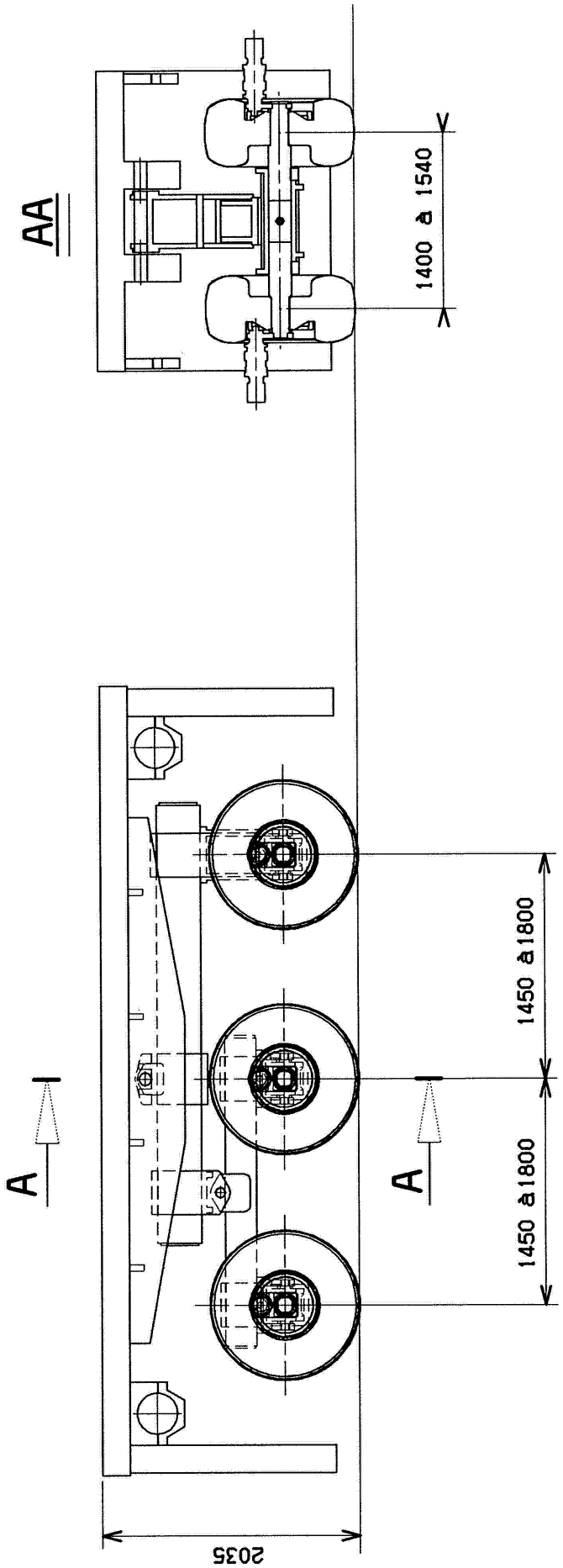

6 WHEEL BOGIE

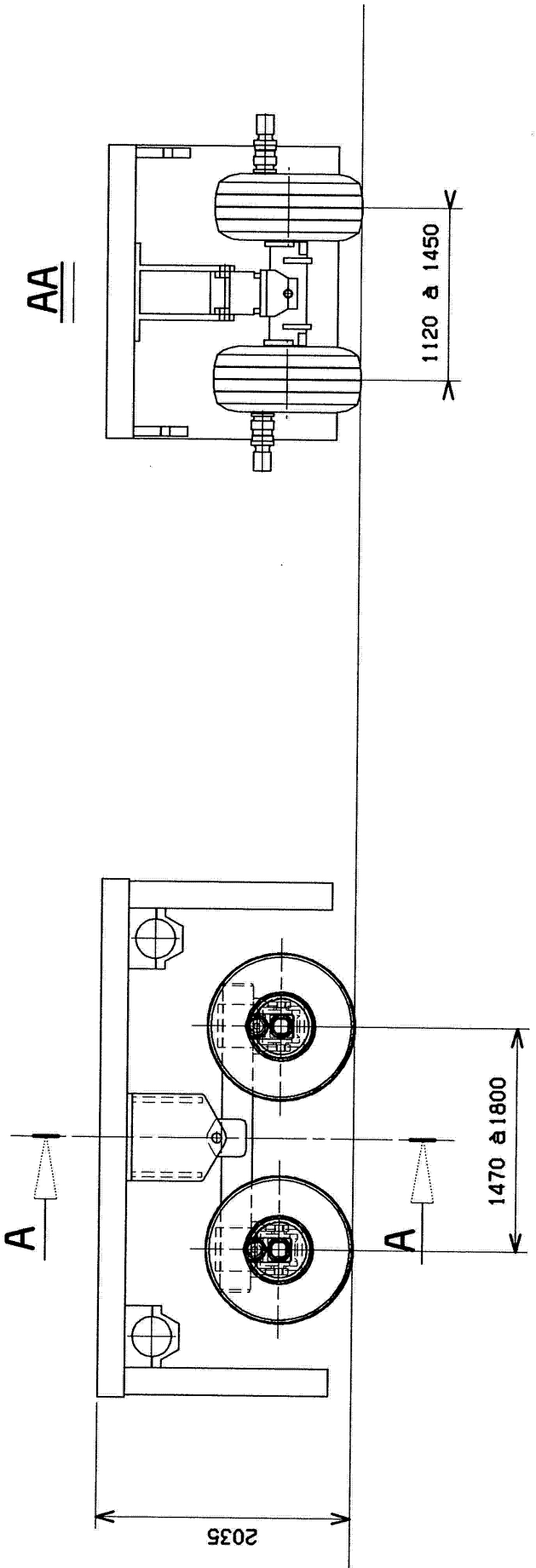

4 WHEEL BOGIE

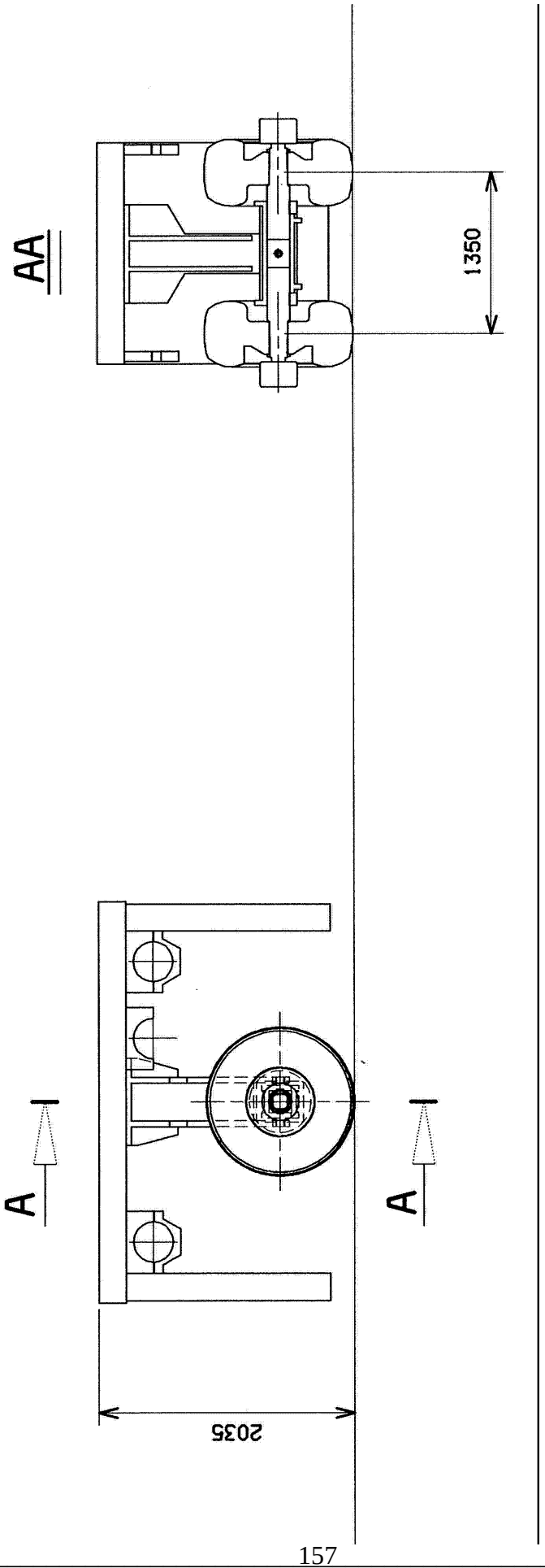
AA
1350
A
A
2035
TANDEM

Load variation

On the top of the tray, there are 4 indexes to assure the positioning and to keep the pigs.
These pigs are made with steel (E24) plates 220mm thickness, and the dimensions are the same of the module tray.

Loads

6 wheels module	57.5T empty	16 pigs 13T each
4 wheels module	38.5T empty	16 pigs 8.7T each
2 wheels module	23T empty	12 pigs 5T each
Hydraulic generation	2.5T	10 pigs 2T each
		10 pigs 1T each

Vehicle assembly

The modules are assembled by a tubular structure. This structure has a low rigidity in the vertical plan in order to avoid interaction between modules.
These tubes are 232mm internal diameter. They are fixed with simple collars under the tray of the modules.
Collars with orthogonal axis do the tube links. This disposal can position the modules, from the hydraulic generation and the steering axle.
For example, the simulation vehicle can have 21m length, 20m large and 3.4m height.

Load on the subgrade

The simulation vehicle have only one type of tire, consequently the load on the subgrade for different tires is based on the tire sprocket.
Consequently, the inflation pressure was varied to change the equivalent surface for a load.

Vehicle power train

Gas oil motor RVI250KW at 2300t/mn

In the front of the vehicle: A constant flow pump 20cm3/T tarred 220 bars for directional control.
At the back of the vehicle: a distribution box to drive the motive pumps.

Hydraulic circuit

Direction:
The pump is equipped with a filter on the aspiring circuit, and a filter on the pressure circuit. The pump discharges into a manual distributor on the control board; this distributor controls the hydraulic jack of which the 2 chambers have the same section.
A back filter completes the installation.

Translation:
2 adjustable flow pumps with manual control installed on the control board; they were open circuit mounted.
These pumps discharged through a pressure filter in the bored blocs. They 22-gear motor with brake for the wheels.

Filters:
Aspiring pressure and backs.

Cooling:
Electric drive for each pump.

Specifications:

Feed tank	600 liters
Pump	89cm3 – 350b pressure
Motor	25cm3 – 350b pressure
Pinion-Crown ratio	1/8, 61
Drive ratio	1/5, 77

Speed variation:
Two possibilities can be used:
Action on the speed of the heat motor (the maximum torque is about 1250T/mm)
Action on the flow of the pumps with the manual control
With 20 driving wheels, the theoretical speed is 2,9km/h (drag 26T)
With 12 driving wheels, the theoretical speed is 4,9km/h (drag 15T)

Speed control:
An encoder, fixed on a referential wheel, transmits the speed on a dial on the control panel.

Direction – Trajectory

The steering axle is installed at 19m forward the rear module.
The jack is applying 15T pressure.
The axle is assembled on a directing crown with external gears. This gear controls the angular position of the axle by means of an encoder with display on the control panel.

The trajectory is ensure like followed:

On the subgrade a continuous line is plotted on all the length of the runway; the large of this line is 3 to 5 cm.
2 cameras are installed on 2 graduated gauges.
One of the gauges is in the front of the vehicle, the other is at the back. The operator has 2 screens on the control panel; he steers the vehicle following the line in the axis of the screen. The gradation of the gauges is used to change the trajectory with regard to the axis of the runway.

Acclivity

The vehicle has not enough power to standing start on an acclivity more than 1%. On the other hand, when moving, the vehicle can step over the runway deformations.

Control panel

The whole commands and control systems of the vehicle are available on the control panel.
The functions are followings:
Power source operating
Translation
Direction
Safety equipment.

engine operating

Revolution
Timer
Gas oil gauge
Oil temperature of the engine indicator
Water temperature light
Oil pressure of the engine light
Battery load light
Ignition key
Starter button

Translation

Speed indicator (km/h)
Digital display for the HP pressure circuit left pump
Digital display for the HP pressure circuit right pump
Two controls levers for the pumps dipping
One button to power on the aero-cooling
One button to power on the flashes
A digital display for the oil temperature circuit.

Direction

Left and right control lever
Screen display of the front camera

Screen display of the back camera
Digital display for the angular position

Safety and control equipment

11 clogging indicators (hydraulic filters)
1 emergency stop with key and bracelet for the operator
1 emergency stop
1 disconnecting switch
1 power on light
1 green light “power on permit”
1 red light “hydraulic oil level circuit”
1 light “emergency stop is on”
1 push button to power on the electrical box.

Configuration modification

General case

Use jacks to put the module horizontally on its skirts (First one side then clamp, then the second side).
When all modules are clamped at the same height, lock the crossbar.
The lock system is composed:
1 fixed part with 2% allowance on the 2 sides
1 mobile part with only one allowance (4 to 5mm) on one side.
The module always on the slips installed the pigs in accordance with the configuration.
With jacks, side by side, remove a part of wedges. Be careful, the module does not sloped.
When the module is on the wheels, keep the wedges on the 4 angles
Link by tubes the vehicle
With jacks, wheel by wheel, axle by axle, remove the mobile part of the crossbar locked system.
The vehicle can now move.

axle Width modification

A lifting jack is used under the axle and the width can be chosen.
For this operation it is not necessary to lift the module. The axles are articulated and only one jack is enough.

Width between bogie modification

For this operation, the pigs must be removed and the module lifted.
During the fatigue testing, we have continuous modifications. A crane is installed near the runway.

Landing gears position modification

For this operation a crane is also required, and the overhaul of the link tubes is necessary.

Vehicle design

The design is very simple because the vehicle is very rustic.
Only one design modification was made: a platform was added with seat driving capability. It is necessary during the fatigue tests (5000 continuous ways are required).
The welded structure of the vehicle is less machining.
The components of the translation and the direction come from the trade and very used for the earth working vehicles.

recycling materials

The vehicle can be recycling up to 95%.